SYNTHESIS AND BIOLOGICAL EVALUATION OF SELECTED PENTACYCLIC TRITERPENOID HYBRID DERIVATIVES

By

Wasiu Olalekan, Afolabi

Thesis submitted in fulfilment of the requirements for the degree

Doctor of Philosophy: Chemistry

In the Faculty of Applied Sciences

At the Cape Peninsula University of Technology

Supervisor: Prof Ahmed Mohammed

Co-supervisor: Prof Francis Shode

Bellville

July 2019

DECLARATION

I, Wasiu Olalekan Afolabi, declare that the contents of this thesis represent my own unaided work, and that the thesis has not previously been submitted for academic examination towards any qualification. Furthermore, it represents my own opinions and not necessarily those of the Cape Peninsula University of Technology.

Signed _____ Date _____

ABSTRACT

Natural products have continuously generated significant therapeutic agents and often provide substantial guide to the development of new lead formulations. Among these compounds are the pentacyclic triterpenes (PTs) of the types: betulinic acid (BA), oleanolic acid (OA), and ursolic acid (UA) that possess bioactive and several anti-infective properties.

The development of conjugate hybrid-type formulations consisting of PTs without introduction of additional structural linkers was carried out. PTs (BA, OA, UA, MA), and a flavonoid compound, 6-methyltectochrysin were extracted from plant sources including *Tectona grandis, Syzygium aromaticum, Mimusops caffra, Lavandula angustifolia* and *Melaleuca salicina* using standard methods. The starting materials were characterized using spectroscopic methods. The hybrid-type derivatives were prepared following C3 and/or C28 derivatization of the PT compounds, and the formation of PT- acid chlorides intermediates for coupling to yield C28 – C3 PT–PT hybrids, C28 – C28 PT–PT hybrids, flavonoid– PT derivatives and calixarene–PT conjugated derivatives.

The antioxidant and antimicrobial potentials of the derivatives were assessed. Preliminary *in-vitro* investigation showed that the hybrid combinations differed in the levels of anti-oxidative activities relative to parent PTs. MA, OA-MA mixture, flavonoid crude extract and calix[4]arene were generally more active than the hybrids, but are less potent relative to ascorbic acid positive control, except for MA. The compounds were tested against multi-drug resistant strains (MDRS) of three gram-positive (*Bacillus cereus, Staphylococcus aureus*, and *Enterococcus faecalis*) and three gram-negative bacteria (*Escherichia coli, Klebsiella pneumoniae*, and *Pseudomonas aeruginosa*). The hybrid derivatives containing PT–PT ester type conjugate hybrids showed antimicrobial activity (>70% inhibition) against resistant strains of *B. cereus* at a dosage of 55 µg/mL. The antimicrobial activities were low against the gram negative strains and generally inactive against the gram positive *S. aureus*. The synergistic effect was observed for the activities of crude extract of *L. petersonii*, which was found to be more bioactive than the purified flavonoid. The flavonoid-PT conjugates were found to be inactive antimicrobials.

The significance of derivatization of PTs and the potential to explore new hybrids of known parent bioactive compounds is an ongoing study focused on finding modifications to improve alternative therapeutic formulations from natural sources. The exploration directly coupled conjugated hybrids without additional linkers may be further explored.

Keywords

Pentacyclic triterpenes; Triterpene hybrid conjugates; Antioxidant activity; Antimicrobial agents; Oleanolic acid; Betulinic acid; Ursolic acid; 6-methyltectochrysin.

ACKNOWLEDGEMENTS

I wish to express my gratitude to:

- Almighty Allah, the Most Beneficent and Merciful, for the Grace to undertake this study.

- My supervisor, Professor Ahmed Mohammed for swift supervisory intervention, contribution and assistance. I am particularly grateful to my co-supervisor and the initiator of this project, Professor Francis Shode for his mentorship and coordination.

- The technical staff of Analytical Chemistry laboratory, CPUT, especially Ms Zandile Mthembu and Gillian Fennesy-Yon for technical support.

- The head of Oxidative Stress Research Institute, CPUT, Professor J. Marnewick; and the laboratory manager, Mr Fanie Rautenbach for assisting with biological assays.

- Prof Edith Antunes at the NMR spectroscopy laboratory, University of the Western Cape, and Dr Brand at the NMR unit, Central Analytical Facilities, Stellenbosch University, for assisting with spectroscopic analysis.

- The entire staff of Chemistry department, CPUT. Special thanks to Mrs Dawn Petersen, Mr Rafeeq Adams, Mr Solomon, Mrs Le Reoux, Dr Francois Wewers, and Mrs Shaheeda Adonis.

- The Cape Peninsula University of Technology, for granting University Research fund. Opinions expressed in this thesis and the conclusions arrived at, are those of the author, and not necessarily to be attributed to the Cape Peninsula University of Technology.

- My residence manager, Mrs Sharon Du Plesis, and her family for the support and hospitality throughout my programme at CPUT.

- My parents, Mr Ishaq Afolabi and Mrs Ramat Afolabi, and my siblings, Abdul'Azeez, Aminat, Nusroh, and Lateefah for their unwavering family support.

- The families of Dr Hussein Okoro, Dr AMO Abdul Raheem, and Professor FA Adekola, for their sustained support.

- My colleagues, Mr Omoniyi Oluseyi, Ms Toyin Udje, and Mr Omar Badegi. Special thanks to Nkululeko Zenzele Ndlovu, for the love and support. Finally, I am grateful to the members of Cape Town Dua group and all friends who might have contributed indirectly to the success of this work.

DEDICATION

To the glory of Allah (SWT)

TABLE OF CONTENTS

LIST OF FIGURES

LIST OF TABLES

APPENDICES

GLOSSARY

Terms		Definitions
^{13}C NMR	:	Carbon-13 Nuclear Magnetic Resonance
^{1}H NMR	:	Hydrogen (proton)-1 Nuclear Magnetic Resonance
AA	:	Ascorbic Acid
ABTS+	:	[2, 2′-azino-bis (3-ethylbenzothiazoline-6-sulfonic acid)] cation
AAPH	:	2,2′-azobis (2-amidino-propane) dihydrochloride
BA	:	Betulinic acid
BAA	:	3-*O*-Acetylbetulinic acid
CC	:	Column Chromatography
$CDCl_3$	:	Deuterated chloroform
DMAP	:	4-(Dimethylamino)pyridine
DMSO	:	Dimethyl sulfoxide
DMSO-d_6	:	Deuterated dimethyl sulfoxide
FRAP	:	Ferric Reducing Antioxidant Power
FTIR	:	Fourier Transform Infrared spectroscopy
HPLC	:	High Performance Liquid Chromatography
MA	:	Maslinic acid
MDRS	:	Multi-drug resistant strain
NMR	:	Nuclear Magnetic Resonance
OA	:	Oleanolic acid
OAA	:	3-*O*-Acetyloleanolic acid
ORAC	:	Oxygen Radical Absorbance Capacity
PTs	:	Pentacyclic triterpenes
TEA	:	Triethylamine
TEAC	:	Trolox Equivalent Antioxidant Activity
TLC	:	Thin Layer Chromatography
UA	:	Ursolic acid
UAA	:	3-*O*-Acetylursolic acid
UV-Vis	:	Ultraviolet-Visible Spectroscopy

CHAPTER ONE
INTRODUCTION

1.0 Chapter Introduction

The introductory chapter provides a general overview of the research project. This chapter gives a concise background of the research, rationale for the study, aims and objectives, the significance, and the major research questions relevant to this study.

1.1 Research Background

Pentacyclic triterpenes (PTs) of the general types (i) lupane **(1),** (ii) oleanane **(2),** and (iii) ursane **(3)** constitute a large class of natural products widespread in the plant kingdom (Thimmappa et al. 2014). Several analogues of these compounds have a wide range of biological activities including antimicrobial, anticancer, anti-inflammatory, anti-malarial, anti-HIV, anti-obesity, anti-diabetic, and anti-sickling, to mention a few (Vazquez et al. 2012).

In the past two decades, extensive research has been carried out on selected members of these sub-groups of PTs including betulinic acid **(4),** oleanolic acid **(5),** and ursolic acid **(6)** leading to generation of remarkable information on their therapeutic properties (Liu, 1995; Kowalski, 2007; Bhatia & Sekhon, 2015). To date, these compounds continue to provide useful frameworks and templates in the development of potentially bioactive lead compounds.

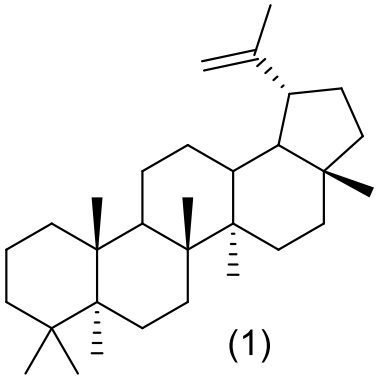

(1)

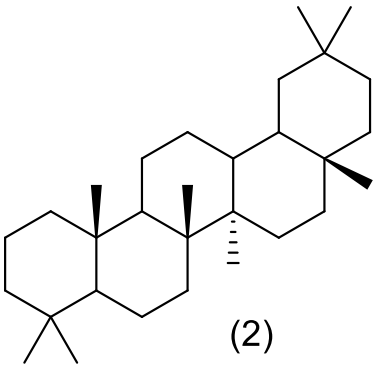

(2)

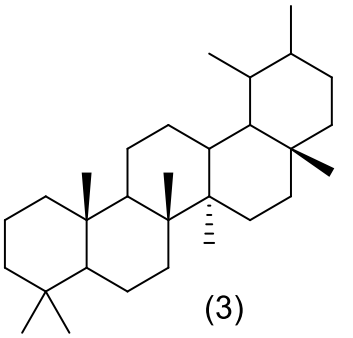

(3)

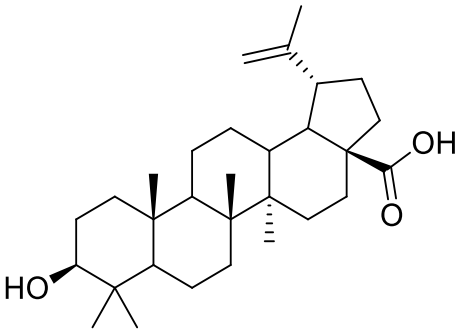

(4)

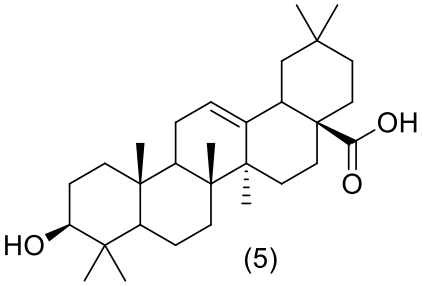

(5)

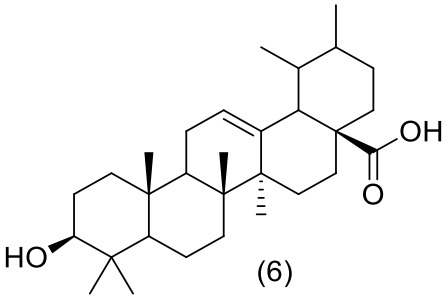

(6)

Natural products possess potent bioactivity and selectivity, resulting from evolution and natural selection. Often times, known bioactive natural compounds serve as useful starting materials for developing new bioactive candidates, which complement the efforts of combinatorial drug discovery methods (Paterson & Anderson, 2005). Among the known natural products, the bioactivities and the therapeutic potential of PTs have been reported severally over the past few decades (Patocka, 2003; Wang et al. 2019). However, new applications continue to emerge, thus indicating the vast unexplored gaps that still exist to date for PT-based compounds (JC Furtado, et al. 2017; Manayi et al. 2018; Sharma et al. 2018).

An important rationale for investigating new, potentially therapeutic formulations relates to the increasing prevalence of drug resistance microorganisms. Although the occurrence of drug resistance poses health risks to humans, there has been several successful countermeasures through the development of promising formulations evident from multidisciplinary research works that produced lead compounds in different stages of trials (Hughes & Karlen, 2014).

The development of new therapeutic formulations often involves chemical modifications to starting compounds and then an assessment of changes in bioactivity, which may be linked to the structural changes, followed by efficacy tests, stability tests, toxicity assays, and others.

A semi-synthesis approach or derivatization of PTs may lead to improved pharmacological profile, bioavailability and aqueous solubility (Herrera et al., 2006; JC Furtado et al., 2017) to suit various chemical drug needs in the food, pharmaceutical and cosmeceutical applications.

1.2 Justification for the Research

Natural product chemistry often provides new therapeutic leads (Koparde et al. 2019). The approach of natural products is suitable to complement alternative drug discovery methods (Butler, 2004) especially in resource constrained regions where application of high-throughput screening for combinatorial drug discovery is limited.

PTs possess potent biological activities (Vázquez et al., 2012), and are reported to cause minimal side effects (Saratha et al., 2011) since the compounds are often devoid of prominent toxicity (Jager et al., 2009). Chemical modifications can yield significant improvement. A 'simple' acetylation of salicylic acid (**26**) by targeting the phenolic hydroxyl group of salicylic acid with acetic anhydride produced acetylsalicylic acid (aspirin (**27**)), a product renowned for the analgesic, antipyretic and anti-inflammatory activities, which has also been used in the management of heart diseases (Zhou et al., 2014).

The discovery of therapeutic derivatives may involve the testing of several chemical compound combinations to form synthetic hybrid molecules with an aim to find new derivatives showing improved properties. Ackermann et al. (2017) investigated potentially therapeutic hybrid formulations by attempting to couple betulinic acid (**4**) to the known pharmacologically active compound, artesunic acid (**28**), which is generally used as an antimalarial drug (Ellis et al. 2009). The resulting product (artesunic acid-betulinic acid hybrid) was found to be more effective in the termination of tumoral cells than single treatment regimens with either betulinic acid (**4**) or artesunic acid (**28**) alone. This gave an earlier indication of the potential of hybrid combinations, and the development of hypothesis to investigate other PT-based combinations that have not been previously reported in the literature to the best of our knowledge.

The design and preparation of potential derivatives often take cues from guided structure-activity relationship studies focusing on compounds with known therapeutic properties. The outcome of such rapid investigations is limited by uncertainties. Chemical modification or synthetic derivatization of PTs based on known or guided structure-activity relationship is often adopted to develop new therapeutic compounds.

The wealth of information on the biological activities of pentacyclic triterpenes, flavonoids, and other saponins had established the potency of these compounds when tested alone in different assays. Other approach will involve the assessment of conjugated hybrids and product combinations. The formation of hybrid bridges to link identified compounds with other multimember ring ones often takes cue from nature. The roots and/or rhizomes of Glycyrrhiza species has been reported to contain potent pharmacological compounds (Qingying & Ye, 2009). The authors identified glycerrhizic acid (**29**) as a bioactive constituent of the plant. The structure of the product shows conjugation hybrid formation with the C3 of the parent oleanane-type compound. It is noteworthy that such combinations may lead to an improved synergistic activity, or an overall reduction in parent bioactivities.

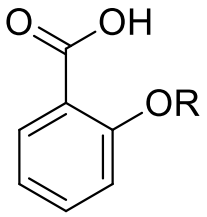

(26) R = H
(27) R = $COCH_3$

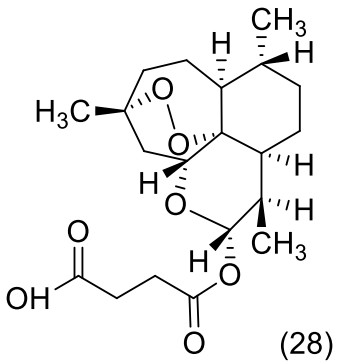

(28)

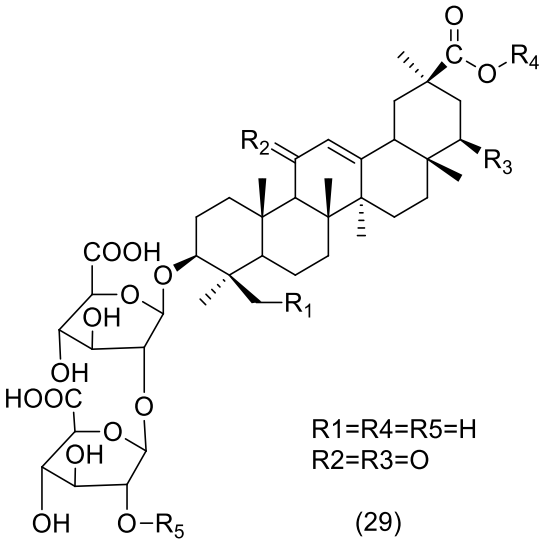

R1=R4=R5=H
R2=R3=O

(29)

1.3 Research Problem Statement

Several instances have shown that natural products possess significant bioactivity in the parent natural form, however, such level of activities are often below desired threshold. One of the gaps, therefore, lies in the need for partial modifications of the parent compounds. The proposal entails exploratory studies to assess the synergistic effects of bringing together two different compounds to form new derivatives, and incorporating the bioactivities of phenolic compounds and pentacyclic triterpenes into a single compound, which could either enhance or depress known activities expressed by the starting materials. The idea from this area of research, as well as several other studies create added knowledge and supports the concerted global effort in the search of new products or processes that may yield new lead compounds.

1.4 Aim and Objectives of the Research

This work sought out to prepare analogues of the main PT scaffolds of **(4) (5) (6)**, and to assess alterations in their bioactivity due to such modifications. The end goal would focus on the investigation of variations in the anti-oxidative properties exhibited by these compounds, as well as the activities against some drug resistant microbial strains. The broad objective was to attempt coupling of pentacyclic triterpenes to form series of hybrid conjugated compounds. The specific objectives include:

1. To extract and isolate betulinic acid (**4**), oleanolic acid (**5**) and ursolic acid (**6**) from selected different plants based on ethnobotanical literature
Expected outcome: (i) Confirmed botanical sources of PTs from South African plants, (ii) crude quantities of BA (**4**), OA (**5**), and UA (**6**).

2. To purify and characterize the crude BA (**4**), OA (**5**), UA (**6**), and any other isolated products or starting materials using available analytical techniques.
Expected outcome: Confirmation of identity of the isolated compounds.

3. To prepare derivatives of BA (**4**), OA (**5**), and UA (**6**) analogues discussed in Chapter 3.
Expected outcome: The conjugate hybrid compounds listed in Chapter 3.

4. To evaluate/investigate the antioxidative and antimicrobial properties of the pentacyclic triterpenes (**4**, **5**, **6**) and the synthesized derivatives.
Expected outcome: Data on the effects of derivatization on the bioassays and recommendations for further exploration.

1.5 Research Questions

This proposal will attempt to screen the following questions:

1. Were the PTs of interest isolated from the target medicinal plants? In what yields? Are there any observable trends relative to existing knowledge found in literature?
2. Was a general synthetic route applicable to prepare derivatives of betulinic acid (**4**), oleanolic acid (**5**), and ursolic acid (**6**)? What are the synthesis challenges and difficulties?
3. Are there any variations in the efficiency and bioactive potency of the PTs and their derivatives?

1.6 Hypothesis/Assumptions

The PTs, (**4**), (**5**), and (**6**) are known biologically active molecules that can be isolated from locally available medicinal plants. Since these PTs possess active functional groups in their structures capable of coupling with other compounds, preliminary investigation supports the potential to prepare these hybrid derivatives that are to be assessed comparatively. Chemical modifications of the PTs may improve or suppress the levels of parent biological activities, but the results and information provided would supplement the list of derivatives being screened for potential lead agent properties.

1.7 Significance of Study

PTs are known to exhibit pharmacological properties and provide useful information in formulations of new therapeutics. Relevant studies continue to assess the beneficiation of natural products with an aim of improving the bioactive properties. The socio-economic impact concerns value addition to African medicinal plants, and support to the knowledge creation process for the management of burden African diseases which are often neglected or deemed diseases of the poor.

1.8 Delineation

This study focused on the extraction of PTs and flavonoid from some medicinal plant species originating from South Africa or elsewhere. The work was delineated to the synthesis of some selected hybrid derivatives resulting from combination of the starting materials, followed by antioxidative and antimicrobial assays of the products. Spectroscopic FTIR and 1D ^{1}H NMR results were obtained in the preliminary studies for rapid screening and analysis of several compounds being generated. This study included some information on the characterization of derivatives obtained but not to a full extensive nature that would suffice to claiming exact structural elucidation, although, probable structures were proposed. The scope of the work covered *in vitro* assays and does not involve *in-vivo* studies.

1.9 Expected Research Output

- It was expected that synthetic derivatives of PTs (BA (**4**), OA (**5**), and UA (**6**)) would be produced using laboratory methods.
- Publications in accredited scientific journals.
- It was hoped that some of the results could provide preliminary information on some relevant products that could be further pursued for technical development and commercial value.
- A PhD thesis, which reports the methods and major findings of the research.

1.10 Thesis Outline

This thesis has been structured to a Six Chapter report. Each chapter contains an introduction and precise chapter summary. The chapters and their contents are as follows:

Chapter One, being the introductory chapter gives an insight into the rationale for the project, the focus of work undertaken and foreknowledge on structure of this thesis.

Chapter Two reports on the knowledge acquired or compiled from existing literature which are deemed relevant to this study.

Chapter Three covers the research methodology, including the extraction methods and design of related organic synthesis work.

Chapter Four provides results and discussions on the extraction, isolation and characterisation of target (natural) compounds, and the synthesis of derivatives, and characterisation of the synthesised compounds.

Chapter Five provides results and discussions on anti-oxidative assays and anti-microbial activities of isolated PTs and synthesised derivatives.

Chapter Six concludes this thesis with summary and recommendations.

Reference section contains all the reference works consulted in this work, while the **Appendix section** provides reference to additional relevant data.

1.11 Chapter Summary

An overview of this research work and a foreknowledge of the field of study, including justifications for embarking on the study was provided. The background highlighted the aims, objectives and motivation for the project as it relates to natural products, synthesis of derivatives and the need for continual efforts to find new drug leads. The preface to the thesis structure was outlined. The next chapter reports on the review of relevant literature, and how this study fits and complements the existing body of knowledge in the field.

CHAPTER TWO
LITERATURE REVIEW

2.0 Chapter Introduction

This section provides a review of prior research work that has been carried out on the selected triterpene scaffolds. The chapter gives a background on natural products and discusses the classifications and important pharmacological applications of triterpenes. The review of literature focused on sources, isolation and biological properties of pentacyclic triterpenes.

2.1 Background on Natural Products

Since ancient times, natural products from plants, as well as from animals, marine and microorganisms have been used in the treatment of several human diseases with high rate of success and efficiency. The plant kingdom is highly diversified and consists of numerous natural products. These natural products possess important therapeutic properties, serving as the basis and leading source of novel bioactive compounds, ranging from those with simple structures, (for example, salicylic acid (**26**), to the ones with complex stereochemistry (for example, vancomycin (**30**)) (Guo, 2017). About 50% of new drugs were first sourced from natural products (Newman & Cragg, 2016) and have been greatly explored for their potent anti-infective activities. The significant interest and emphasis on natural products can be linked, in part, to the renowned tolerance, biological safety and quality of compounds derived from these sources. Natural products are considered safer and more environmentally friendly, and more importantly, the compounds from natural product origin can co-exist with target sites in biological systems (Rainsford et al., 2015).

Other fields of research also contribute towards generation of new bioactive agents. For instance, high throughput screening (Wegner et al., 2016), precision medicine and sequencing (Vicini et al., 2016), computational functional group mapping (Guvench, 2016), reverse ethnopharmacology (Leonti et al., 2017), among many others, are widely employed as guide in drug discovery. However, the approach of natural product is often preferred to these alternative methods and routes because alternative systems often involve extensive computations, longer time and several other considerations including cost, and lack of urgency to combat emerging drug resistant viruses and bacteria.

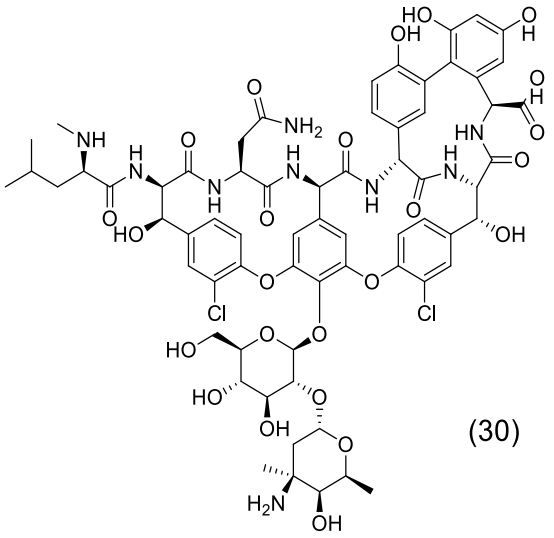

(30)

To date, phytochemical screening and immediate bioassay evaluation of natural products is a faster approach which has contributed immensely to discovery of new drugs and essential food supplements. Although the infinite potential of plants to be used as keystone in treatment of ailments cannot be overemphasized, the main concern is the sourcing of useful plants and effective isolation and identification of active components.

Many developing countries still depend mainly on traditional drug preparations from plants for the purposes of primary health care. The medicinal practices of ancient times have been the basis of modern medicine and will remain as one major source of future medicines. The Ayurvedic and Chinese traditional medicine systems of India and China respectively, have been well established. Unfortunately, despite been regarded as one of the oldest form of folk medicine, African medicine is still an under-developed system of medicine. There are recent developments on this subject, most especially, it is now possible to conduct valuable research and achieve excellent results in Africa due to improved knowledge and availability of modern instruments for separation, isolation and identification of targeted compounds.

In recent times, the increase in cases of oxidative stress diseases, and prevalence of pathogenic bacteria and other microorganisms such as drug-resistant strains of *Mycobacterium tuberculosis,* methicillin resistant *Staphylococcus aureus*, to mention a few, pose a major problem to public health worldwide. The prevalence of drug resistant pathogens has been linked to human habit of overuse and misuse of antibiotics (Yong et al., 2009). The potential of usage of most old antibiotic drugs is less likely nowadays, since they are becoming less efficient or showing no activity (Li & Ma, 2015). Pentacyclic triterpenes are among the top promising natural products with potential applications as agents for many diseases such as antioxidative, antimicrobial, anti-inflammatory and anticancer drugs.

2.2 Pentacyclic triterpenes

Pentacyclic triterpenes are widely distributed in nature, and often found in fruits, vegetables, leaves, tree bark and roots of several medicinal plant species in the form of natural products (Laszczyk, 2009). These natural products may have complex and diversified structures. The isolation and identification of these compounds and the successful application to build frameworks in drug discovery can be attributed to improved modernized techniques for separation and structural elucidation (Al Qaraghuli et al., 2017). Extensive research over the last few decades have utilized analytical advancements to identify several natural products including PTs that would otherwise remain unknown, many of which now provide essential health benefits for humans and useful to manage diseases (Halabalaki, et al., 2014).

2.2.1 General classification of pentacyclic triterpenes

Triterpenes are ubiquitous class of natural non-steroidal compounds that are obtainable from plants and marine organisms. These compounds possess six isoprene units with basic molecular formula $C_{30}H_{48}$. Triterpenoids are synthesized naturally in plants via cyclization of squalene and can be found in their free form (sapogenins) or bound to glycosides (saponins) and comprises of different types of compounds that can be grouped based on their skeletal features. Triterpenes are divided into acyclic, mono-, bi-, tri-, tetra- and pentacyclic classes of triterpenes. The tetracyclic and pentacyclic triterpenes are the most studied groups (Sheng & Sun, 2011). This research focuses on pentacyclic triterpenes (PTs), with emphasis on betulinic acid (**4**) (lupane), oleanolic acid (**5**) (oleanane) and ursolic acid (**6**) (ursane) scaffolds (See Chapter 1).

2.2.2 Betulinic acid

Betulinic acid (3β-hydroxy-lup-20(29)-en-28-oic acid) (BA) **(4)** is ubiquitous and a very biologically active molecule in the *Betulaceae* family (genus *Betula*) in plant kingdom. Natural occurring sources of BA **(4)** include *Betula pubescens*, *Betula alba, Betula platyphylla*, and *Romarinus officinalis* (MR de Melo et al., 2014; Pai & Joshi, 2014) to mention just a few plants.

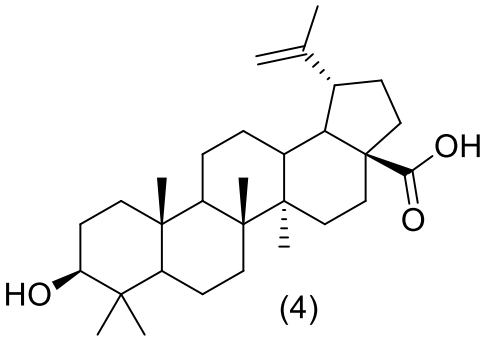

(4)

Naturally occurring lupane-type triterpenoids have been of great interest in the research community for their biological properties, especially the antitumor properties. This class of compounds are referred as mitocanes (mitochondria targeting chemical substances). Many studies have explored the anticancer and antiviral potential of BA (**4**) and its derivatives following the first discovery of the potent anticancer activity in 1995 when it was found that BA (**4**) induced cell apoptosis and at a clinical concentration of ED_{50} 1.1 – 4.8 µg/ mL (Spivak et al., 2017).

The reduction product of BA (**4**), betulin (3*β*-lup-20(29)-ene-3, 28-diol) **(7)** was first detected from the bark of *Betula alba* in 1788, however, it took more than a century later before the first natural form of BA was isolated and reported as an unknown compound from extracts of *Gratiola officinalis* in 1902 (Krasutsky, 2006). BA (**4**) was properly identified in 1939 (Robertson et al., 1939). BA (**4**) can be obtained from natural sources and can be synthesized in the laboratory. The synthetic preparation of BA (**4**) can be achieved from betulin (**7**), which serves as abundant starting material that can be obtained from plants in relatively higher yields. Several studies on synthesis of BA (**4**) became available in 2003, with most of the synthetic work using betulin (**7**) as the starting precursor. A convenient method for synthesis of BA (**4**) from betulin (**7)** is a two-step preparation involving Jones oxidation of C3 and C28 hydroxyl groups of betulin (**7**), followed by reduction of the intermediate by sodium borohydride **(Scheme 2.1)**.

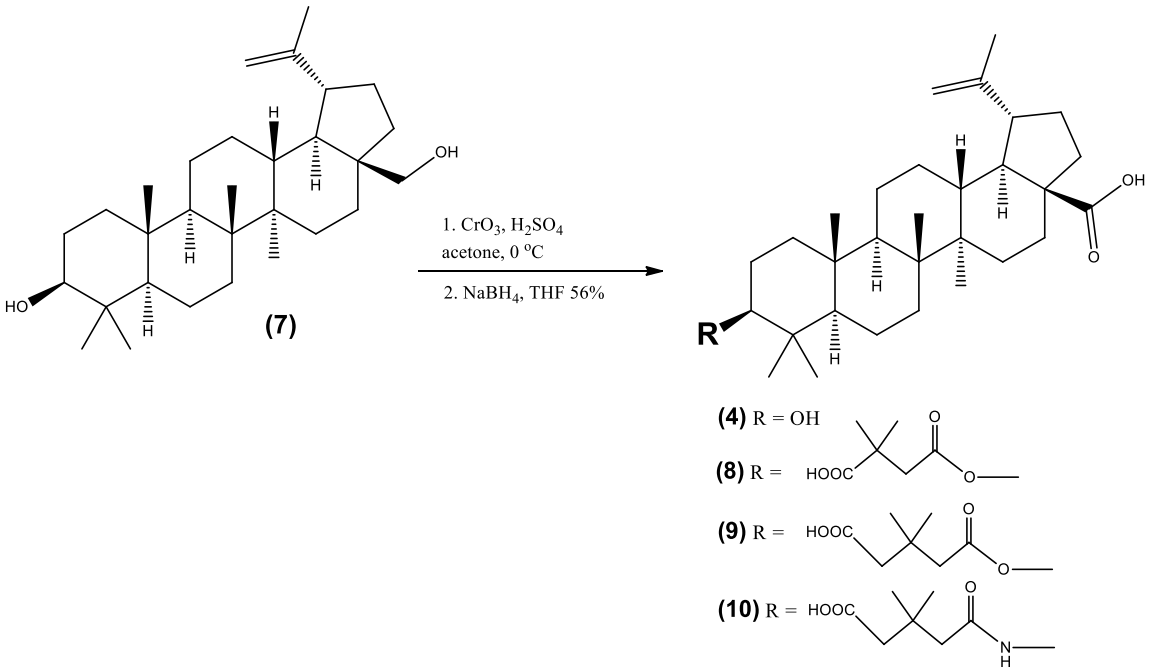

Scheme 2.1: Semi-Synthesis of betulinic acid (**4**) and some known derivatives (**8** – **10**) of betulinic acid (**4**) from betulin (**7**).

The total synthesis of pentacyclic triterpenes such as BA (**4**) has been widely researched since the 1960s. However, the syntheses of these compounds are greatly limited by several reaction steps, very low overall yield, expensive protocols, formation of mixture of epimers, and challenge of stereochemical resolutions (Chen et al., 2009).

There is great difficulty in total synthesis of PTs, especially in the construction of the pentacyclic framework in enantiomeric form. Thus, it is more economical and time efficient to extract these bioactive molecules from natural sources, and subsequently undertake semi-synthesis to improve their pharmacological properties.

BA (**4**) is a white crystalline powder found to be slightly soluble in water; moderately soluble in petroleum ether, dimethylformamide, benzene, methanol, ethyl acetate, chloroform and ether; and highly soluble in pyridine and acetic acid and can be purified by crystallization in methanol (Joshi et al., 2013).

BA (**4**) exhibits anti-cancer (Rufino-Palomares, et al., 2015), anti-HIV (Bori, et al., 2012), anti-malarial (Ziegler, et al., 2004), anti-inflammatory (del Carmen Recio et al., 1995), and other bioactivities. BA (**4**) has been proven to be a selective inhibitor of human melanoma that functions by induction of apoptosis (Pisha et al., 1995). BA (**4**) is also a potent anti-HIV agent, and can protect the cells of human immunological system and inhibit maturation of the virus (Kanamoto, 2001; Reutrakul, 2010).

Derivatization of BA (**4**) has been shown to significantly improve the biological properties of the compound. For instance, the semi-synthesis studies carried out on BA (**4**) by Kashiwada et al. (1996) and Hashimoto et al. (1997) focused on functionalization of C-3 position to synthesize 3-*O*-(3', 3' –dimethyl)-succinyl-betulinic acid (**8**). The chemical modification step involved substitution of acyl groups to replace the hydroxyl functionality at C3 of BA (**4**) by treating BA (**4**) with dimethyl succinic anhydride in pyridine. The product was found to be a more potent anti-HIV derivative with an EC_{50} < 0.00035 µM, whereas parent BA (**4**) showed an EC_{50} value of 1.4 µM.

The progressive effect of derivatization was reflected in the hydrogenation of BA (**4**) which produced dihydrobetulinic acid with an EC_{50} value of 0.9 µM against multiplication of HIV-type 1 in lymphocytic cells (Kashiwada et al., 1996).

Based on structure-activity relationship, 3',3'–dimethylglutaryl betulinic acid (**9**) was synthesized and found to inhibit the life cycle development of infected HIV cells with promising efficiency (EC_{50} = 0.0023 µM). The observed potent anti-HIV activity was linked to the presence of the ester group at C3 of PTs in these derivatives. The attempted replacement of the ester group with other groups such as amido group (for example, 3-alkylamido-3deoxy-betulinic acid) **(10)** resulted in decreased potency and formed compounds that became inactive against HIV virus (Kashiwada, et al., 2000).

2.2.3 Oleanolic acid

Oleanolic acid (3β-hydroxyolean-12-en-28-oic acid) (OA) (**5**) is a non-toxic natural triterpenoid possessing anti-inflammatory, antitumor, antiviral, hepatoprotective, anticancer and antihyperlipidemic activities (Pollier & Goossens, 2012). OA (**5**) is widely distributed in plant kingdom and can be found in food, medicinal herbs, and nutritional supplements. While OA (**5**) can be obtained from *Oleaceae* plants, *Syzygium* spp, amongst others. It has been shown that the olive plant (*Olea europaea)* is the major commercial source of OA (**5**) (Sporn et al., 2011). Naturally, OA (**5**) exists in the free acid form or aglycones of triterpenoid saponins and often co-exists with its isomer, ursolic acid (3β-hydroxyurs-12-en-28-oic acid) (UA) (**6**). Both isomers (OA (**5**) and UA (**6**) possess several similar pharmacological properties (Liu, 1995). After extraction and isolation, OA (**5**) is a white powder, which can be crystallized using methanol.

In nature, OA (**5**) forms physical barrier against fungal attacks in plants and is found as epicuticular waxes to prevent water loss. In addition, glycoconjugated OA (**5**) compounds serve as a defence or as allelopathic agents in plants (Szakiel et al., 2005).

By 1995, OA (**5**) was only isolated from 120 plant species (Wang & Jang, 1992; Liu 1995) and over the last decade, OA (**5**) has been isolated from more than 1620 medicinal and food plants species (Fukushima et al., 2011).

A cost-effective method in the synthesis of OA (**5**) is via the technique of heterologous biosynthesis or synthetic biology involving expression of plant biosynthetic genes in heterologous hosts, such as *Escherichia coli* or yeast (Pollier et al., 2011; Zhang et al., 2011). Heterologous biosynthesis of OA (**5**) has already been achieved by co-expression of genome of a model legume, *Medicago truncatula* (Fukushima et al., 2011).

The natural biosynthesis of OA (**5**) via folding and cyclization of squalene, forming oleanyl cation intermediate is illustrated in Scheme 2.2 (Babalola & Shode, 2013).

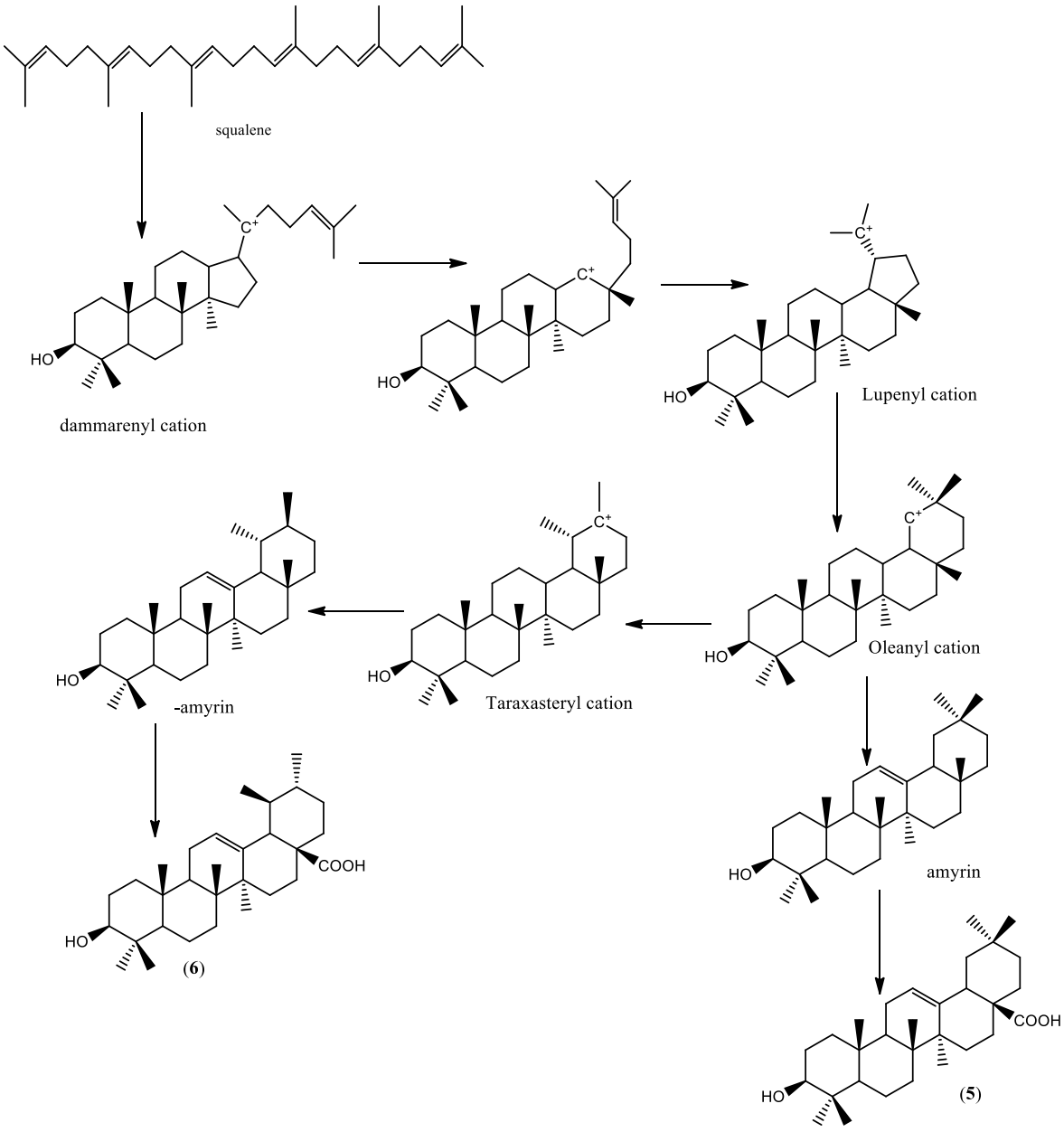

Scheme 2.2: Biosynthesis of oleanolic acid (**5**) and ursolic acid (**6**)

OA (**5**) is considered as an important starting material for synthesis of another highly potent bioactive compound, maslinic acid (MA) (**11**) (Qui et al., 2009). Recently, an effective and convenient four step procedures for the synthesis of maslinic acid (**11**) from oleanolic acid (**5**) was published by Sommerwerk and Csuk (2014). The protocol involves oxidation of C3 hydroxyl group of OA (**5**), then, bromination of the oxidized product to form mixture of bromides, followed by reduction with sodium borohydride at 0 ^{o}C and 60 ^{o}C, respectively.

Pure MA (**11**) was obtained after recrystallization from ethyl acetate with an overall yield of 41.2% (Scheme 2.3).

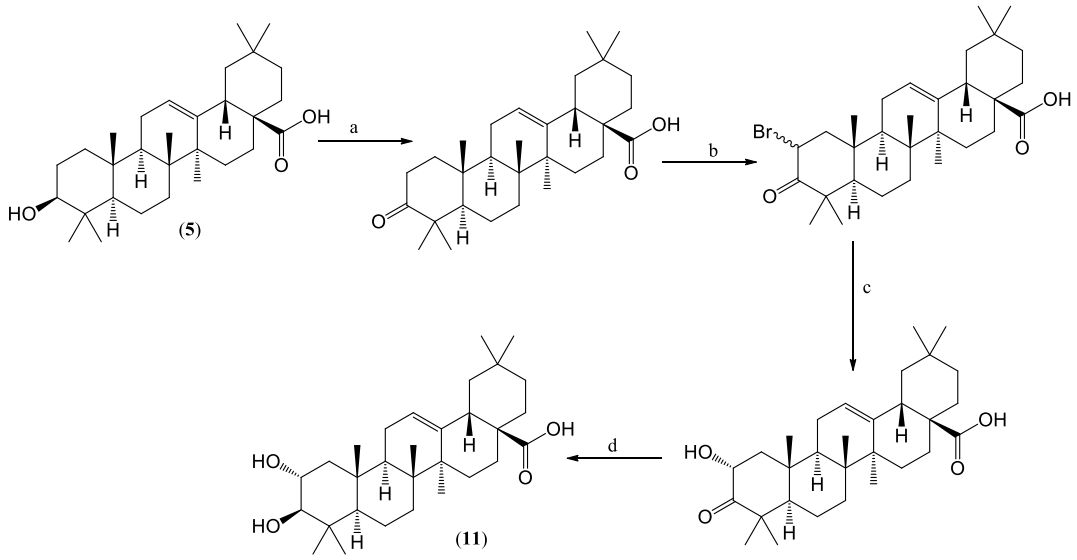

Scheme 2.3: Synthesis of MA (**11**) from OA (**5**). (a) CrO_3/H_2SO_4, silica gel, 0 ^{o}C (b) pyridinium tribromide, acetic acid, 25 °C, 3h (c) NaOH, DMF, 0 °C, 30 min (d) $NaBH_4$, 0 °C, 1 h, then acetone/H_2SO_4, 30 min, 0 °C

Rali et al. (2016) prepared several derivatives of OA (**5**), and focused on the active C3 and C28 positions to introduce acetyl, trifluoroacetyl and/or methyloxy- functionalities. The derivatives bearing trifluoroacetyl group at the C3 were prepared by blocking the C28 position (methylation using iodomethane) and subsequent treatment with dimethylformamide, to yield products that showed significant antinociceptive and anti-inflammatory biological properties.

2.2.4 Ursolic acid

Ursolic acid (3β-hydroxyurs-12-en-28-oic acid) (UA) (**6**) is an ursane-type triterpene found in many plants including *Mentha peperita L., Lavandula augustifolia, Thymus vulgaris, Ocimum sanctum* and many others. UA (**6**) is found naturally in free acid form or as aglycone precursor for triterpenoid saponins which contain linkage with one or more sugar moieties (Szakiel et al.,

2005). Depending on the source, UA (**6**) may occur as a white, light green, or yellow solid. The biosynthesis of UA via cyclization of squalene is shown in Scheme 2.2.

UA (**6**) has anti-inflammatory, anti-oxidative and anti-tumoral properties. UA (**6**) and its isomer, OA (**5**) have been isolated from ethanolic extracts of *Wrightia tomentosa* leaves and were reported to inhibit advancement of tumor cells (Chakravarti et al., 2012). The authors reported that UA (**6**) and OA (**5**) inhibit cell proliferation in two breast cancer cells (MCF-7 and MDA-MB-231) at inhibitory concentration (IC_{50}) of 7.5 µM and 7.0 µM, respectively. These triterpenes target cancerous cells and show no inhibitory activity in HEK-293 non-cancer cells. The anti-inflammatory activity of the extracts of *Salvia officinalis L*. leaves has also been linked to UA (**6**) constituent of the plant, with a reported activity that was twice as potent as control anti-inflammatory drug, indomethacin (Zupancic, 2001). Other important biological activities including trypanocidal properties have been attributed to UA (**6**) constituent of plants (Abe et al., 2002).

In a recent structure-activity-based synthesis of UA (**6**) analogues, Wu et al. (2017) simultaneously modified the C2 and C3 positions of UA (**6**) to synthesize novel ligands suitable as inhibitors of α-glucosidase – an important process in management of *Diabetes mellitus*. Synthesis procedure to prepare acyl bearing moieties at C3 or C2 involved esterification using N, N-dimethyl-4-aminopyridine, or by two-step procedure involving jones oxidation and Claisen Schmidt condensation.

2.3 Extraction of pentacyclic triterpenes

Pentacyclic triterpenes are found in various plant materials such as leaves, wood, bark, roots and fruits. It is a common practice to dry and grind materials prior to extraction procedures. Extraction of pentacyclic triterpenes can be carried out with organic solvents including alcohols, chloroform, dichloromethane, acetone, or hexane. Moreover, hydrophilic solvents are often used in the extraction of natural products because water-based solvent can penetrate cell tissue, causing the tissues to swell, thereby improving extraction yield.

Isolation of pentacyclic triterpenes from natural sources involves three major steps: (i) extraction using suitable organic solvent, (ii) separation using fractional solubility (crystallization) or column chromatographic technique, and (iii) purification by recrystallization or repeated chromatography. Solvent-solute levels of interactions differs, and the use of different solvents could lead to varied extraction efficiencies. In an attempt to assess such possibility, a comparison was made between the yields obtained when UA (**6**) was extracted from the same plant source in two different studies. Rao et al. (1966) isolated UA (**6**) from the alcoholic extract of *Diospyros melanoxylon* leaves and reported a yield of 0.24%; however,

isolation of UA (**6**) from the leaves of the same plant using ethyl acetate produced a yield of 0.56% (Mallavadhani et al., 2001), twice the yield obtained when the extraction was done with alcohol in earlier studies. Although the nature or type of solvent might have played a role in the observed varied yields, it is nonetheless sufficient to base the claims on the type of solvent alone since other factors such as method of extraction (conventional maceration, or soxhlet extraction vs advanced methods such as ultrasound-assisted or supercritical fluid extraction), or concentration of solvent might also contribute to such discrepancies in yields (Azwanida, 2015).

2.4 Bioactivity of pentacyclic triterpenes and their derivatives

There has been tremendous interest in recent years in the chemistry and pharmacological properties of PTs. An increasing number of plants containing PTs have demonstrated wide spectrum of biological activity (Pai & Joshi, 2014). Pentacyclic triterpenes, especially the lupane-, oleanane-, and ursane- types are secondary metabolites exhibiting promising chemotherapeutic potentials. These PTs are antioxidative, antiviral, antidiabetic, anti-HIV, and several other biological properties (Xu et al., 1996; Szakiel et al., 2012; Khwaza et al., 2018).

Pentacyclic triterpenes and their derivatives have also found applications in nutraceuticals. PTs can be found in different food substances and may be isolated and produced in form of pills, powders, tinctures for safe use to improve human wellness. For instance, corosolic acid (2-hydroxy-ursolic acid) from the extracts of *Lagerstroemia speciosa L.* (Banaba) is a food supplement that could be administered in prevention and/or management of diabetes (Stohs et al., 2012). Similarly, the cholesterol lowering effects of dichloromethane extracts of *Crataegus pinnatifida* (Hawthorn) on intestinal acylCoA:cholesterol acyltransferase (ACAT) activity was attributed to the presence of OA (**5**) and UA (**6**) in the extracts (Lin et al. 2011). This positive inhibitory activity shows potential application of PTs as beneficial food additives.

Although pentacyclic triterpenes are naturally potent bioactive molecules, the most significant problem is limited availability, and affordability. However, exploration of African plants can provide affordable and more viable source of these safe bioactive molecules.

Another emerging application of natural products is their use in functional foods. These are foods and beverages proven scientifically to possess specific health promoting properties. There is increasing preference by consumers in opting for natural food additives over conventional synthetic preservatives due to perceived lower risks. Naturally occurring antimicrobial agents are now utilized in food industries. For example, alcoholic extract of *Ocimum basilicum* (basil) has been found to be a good natural antibiotic and preservative agent for agro-foods (Nazzaro et al., 2013). The antimicrobial, antibacterial and antifungal potential of PTs can thus be exploited for applications in food sector.

The lupane **(1)**, oleanane **(2)** and ursane **(3)**-type triterpenoids are significant and potent bioactive agents. They occur as secondary metabolites and are formed through complex metabolic processes in different parts of plants. Lupane-type triterpenoids possess antiviral, antifungal and antiparasitic properties. This class of compounds also inhibits progression of neurodegenerative disorders such as those related to loss of memory and cognitive ability (found in Alzheimer's disease patients). The disorder is due to low levels of acetylcholine (a neurotransmitter found in the brain). The low amount of this neurotransmitter is caused by secretion of two enzymes in the brain: acetylcholinesterase and butyrylcholinesterase. Both enzymes catalyze hydrolysis and metabolic degradation of acetylcholine, respectively. However, a study by Castro and coworkers (2014) investigated a treatment for the disease using derivatives synthesized from lupane. The authors found out that some derivatives of naturally occurring calenduladiol, particularly the semi-synthesized 3,16,30-trioxolup-20(29)-ene (IC50 = 21.5 µM) can suppress production of acetylcholinesterase and butyrylcholinesterase, thus offering a promising treatment for alzheimer's disease.

Some plant species may contain either one or combination of BA (**4**), OA (**5**) and UA (**6**). This may result in combined synergistic healing effect, or otherwise be a limiting influence to the overall activity obtainable from the target PTs. For instance, the phytochemical screening work done by Tezuka and co-workers (2000) confirmed the presence of BA (**4**), OA (**5**) and UA (**6**) in *Orthosiphon stamineus.* Traditionally, the leaves of the plant are used in local medicine by the Indonesian people to treat rheumatism, diabetes, eruptive fever, influenza, hepatitis and hypertension, although, the observable therapeutic effects were not linked directly to a specific PT (Tezuka et al., 2000). Hossain and Ismail (2013) isolated triterpenes from methanolic extract of the plants' leaves and reportedly found seven triterpenoids including BA (**4**), OA (**5**) and UA (**6**). It is noteworthy that the authors also found the plant to contain derivatives of BA (**4**), OA (**5**) and UA (**6**) in the forms of 2*α*-hydroxybetulinic acid **(12)**, maslinic acid **(11)** and corosolic acid **(13)**, respectively.

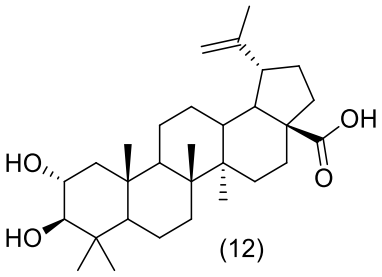

(12)

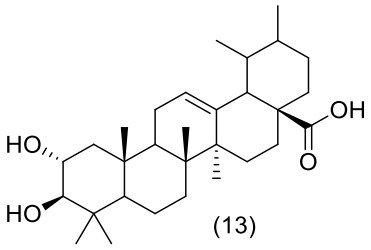

(13)

Although parent pentacyclic triterpenes are found to possess some degree of bioactive properties, other studies have shown that a remarkable increase in potency can be achieved after derivatization (Yu et al., 2006; Zhou, et al., 2017). Semi-synthesis as a chemical modification approach therefore, can be followed to prepare PT derivatives exhibiting lower toxicity, improved solubility and increased level of bioactivity (Sultana & Ata, 2008). Semi-synthetic derivatives of natural products often exhibit higher activity at lower concentrations relative to parent compounds obtained directly from plants (Isah et al., 2016). Hence, the advancements in analytical techniques, and continuous exploration of new products, in combination with ancient therapeutic knowledge and skills provide better information on the significance of, and ways of improving profiles of natural products in drug discovery.

The synthetic derivatives of PTs reflect effect of functionalization of parent compounds, thereby illustrating how the addition of, or substituting constituent elements by targeting C3, C17, C28 and/or other active positions in the rings of the PTs can significantly alter biological properties of compounds (Leal, 2012). Derivatives are also formed based on preference for multiple chirality, and the possibility to initiate ring opening, intra-ring functionalization or additional cyclization reactions (Jatczak, & Grynkiewicz, 2014).

The hydroxyl group (on ring A) of pentacyclic triterpenes has been identified to influence antibacterial activity. To determine the correlation between hydroxyl constituents and activity of PTs, Huang et al. (2015) investigated the variations in hydroxyl-group functionality on ring A of PTs and the direct effect on level of biological activity. The study revealed that an increase in the number of hydroxyl groups in ring A of pentacyclic triterpenes led to an increased antibacterial activity as reported for derivatives of UA (**6**) and OA (**5**). The derivatives were synthesized by protecting the C28 position (carboxyl group at ring E) of the pentacyclic triterpenes, thereby affording chemical modifications at C3. According to the researchers, the result of inhibitory studies on Gram-positive bacteria revealed that the derivatives of UA (**6**) and OA (**5**) possessing additional hydroxyl group at C1, C2, C3 and alkyl ester group at C17 were about three times more potent than positive controls. A contrasting effect was observed for other derivatives bearing oxygen functionality to replace the hydroxyl groups. The oxidation of the C3 hydroxyl group resulted in a decreased antibacterial activity Huang et al. (2015)

PTs can be derivatized to exploit the active sites on Ring A to synthesize products bearing multiple hydroxyl functionality on the ring A. Huang et al. (2015) synthesized some PT derivatives possessing multiple hydroxyl functional group on ring A. The significance of such polyhydroxyl-bearing compounds is abound in literature. For instance, MA (11) is a well-known antiproliferative agent (Juan et al., 2008), and an active inhibitor of serin-protease enzyme responsible for distribution of HIV within the human body (University of Granada, 2007), while corosolic acid (13) is a potent anti-inflammatory, antidiabetic, and antiproliferative agent.

There are limited reports on inhibitory activity of pentacyclic triterpenes on plant pathogenic bacteria, such as *Streptomyces scabies* and *Ralstonia solanacearum*. These bacteria grossly affect potato, tomato and banana crops leading to huge global economic losses and environmental problems (Bignell et al., 2010; Feng et al., 2013). The conventional methods of preventing these pathogens (chemical and biological controls) impacts the environment negatively (Fan et al., 2014). The potential of PTs can be explored in this area as well.

In another study, which compared the activity of oxidized forms of UA (**6**) and OA (**5**) with activity of parent UA (**6**) and OA (**5**) and acetylated derivatives. It was found that the introduction of carbonyl functionality at C3 position of a pentacyclic triterpene significantly increased the leukemia cell antiproliferation activities of the oxo- groups (IC_{50} = 18.6 µg/ mL) relative to the natural UA (**6**) and OA (**5**) (IC_{50} = 53.5 µg/ mL), and the acetylated derivative of (**6**) (IC_{50} = 37.9 µg/ mL) (Basir et al., 2014).

The potency of BA (**4**) has been significantly improved through semi-synthesis. These several chemical modifications have created novel compounds that are highly cytotoxic against target cells while being harmless against healthy cells. According to the work by Spivak et al (2013), the researchers synthesised conjugates of lupane triterpenoids by attaching a series of phosphonium substituents resulting in novel derivatives. The synthesized lupane-phosphonium conjugates were tested in both *in-vivo* and *in-vitro* against *Elrlich carcinoma* and *Mastocytoma* P-815 cell lines, respectively, with a reported activity in the order of 34 times more potent than naturally occurring BA (**4**). The increased cytotoxicity points to the potential of improving pharmacological activity through chemical modifications.

Derivatized compounds often exhibit varied activities against different diseases. Huang et al. (2015) reported improved activities after esterification of C17 position of pentacyclic triterpenes (OA (**5**) and UA (**6**)). Derivatives of OA (**5**) and UA (**6**) prepared by the researchers exhibited antibiotic activity of 4-fold more effective than control streptomycin and ampicillin drugs. The study also revealed that derivatives with short alkyl (methyl-, ethyl-, n-propyl-, and isopropyl-) ester groups possessed good inhibitory activity (>95%) against Gram positive bacteria than long alkyl and benzyl ester derivatives.

OA (**5**) also exhibits remarkable antitumor activities. The boronate derivatives of OA (**5**) presented a more enhanced biological activity according to studies by Moreira and coworkers (2013). The non-toxicity and potential of boron to form dative bonds with biological nucleophiles of enzymes was exploited. Due to presence of empty p-orbital, boron can also bond with hydroxyl groups of carbohydrates and nucleic acids. Oleanolic boronates were found to induce apoptosis and inhibit proteasomal activity on tumor cells (Moreira et al., 2013).

In the oleanane type pentacyclic triterpenoid, the boronate ester group was positioned at C3 via palladium-catalyzed cross coupling of bis(pinacolato)diboron with vinyl triflates in alkaline medium.

The low water solubility of triterpenes often limits their application. Improvement in solubility properties can be achieved using synthetic methods such as complex formation. Soica et al. (2008) synthesized cyclodextrin complexes of lupane-type tritertenoids (betulinic acid and betulin). The derivatization work resulted in formation of inclusion complexes between triterpenes and hydroxypropyl-γ-cyclodextrin (HPGCD), which were optimised by varying molecular ratio of the starting compounds. An increased and optimal solubility was observed in complex preparations involving molecular ratio of 1:2 (HPGCD: triterpene). It was further concluded that effective complexes were made through kneading process, when compared with other methods for complex formations. Other derivatives may involve converting the triterpene or drug moiety into a salt-derivative form to satisfy solubility considerations. This research work explored such salt-derivative formation for one of the derivatized compounds.

2.5 Antioxidants

Antioxidants are important substances that slows down or avoid oxidation of oxidable substrates. These compounds can inhibit or ensure elimination of oxidative stress and damages to cells or other molecules within the body of living hosts. Antioxidants are considered important nutraceuticals for their potential to guard the body against damages caused by free radicals and reactive oxygen species. The presence of reactive species is often linked to degenerative diseases in the body. Based on the mode of action, it became evident that antioxidants are significant to human health because they may lower oxygen levels, intercept singlet oxygen, scavenge radicals, and ensure degradation of primary compounds to non-reactive materials and the possibility of preventing some processes that involves removal of hydrogen from substances (Shahidi, 1997). Although living organisms have endogenous antioxidant defence systems, the mechanisms are insufficient in the complete prevention of free radical related damages.

Antioxidants prevent the onset of or reduce the further proliferation of oxidative stress related diseases. Oxidative stress results from imbalance between the production of reactive species and countering antioxidant defence network. Antioxidative compounds interact with or alter the breakdown of oxidable substances within the body (Halliwell, 2007). The oxidation of oxidable substrates is related to oxidative stress and/or damage and have been implicated in cellular damage and general susceptibility to diseases.

The direct consequence of excessive free radicals includes the onset of several diseases and tissue damage. Reactive species are involved in damage to tissues of heart, liver, brain, muscle skin, kidneys etc. (Yoshikawa et al., 2000). In recent times, efforts are being made to ensure diets contain antioxidants. These efforts are complemented by the application of antioxidants in the food industry (Halliwell et al., 1995). There is increasing knowledge on benefits of antioxidants leading to high demand for effective non-toxic naturally occurring products possessing antioxidant properties (Smina et al., 2011).

The food industry often utilizes food-grade antioxidants for two main purposes: (i) prevent reduction of quality of food products and (ii) to preserve the nutritional composition and value of food products (Halliwell et al., 1995). Living organisms rely on antioxidant defence mechanisms which are either produced within the body, for instance in the synthesis of superoxide dismutase, or obtainable externally from nutritive diets. External (exogeneous) source of antioxidants (vitamins A, C & E, carotenes, lycopene etc.) are mainly from plants, and just after the first successful extraction of ascorbic acid from plants (Szent-Gyorgyi, 1963), there have been many studies on antioxidants' potential of medicinal plants. Natural antioxidants such as phenols, polyphenols, vitamins, carotenes and carnosine are obtainable from plant sources (Caragay, 1992). The antioxidants are believed to serve as protection against tissue damage in plants, but in humans, dietary intake of antioxidants have several benefits including decline in proliferation of cardiovascular diseases, cancer, and aging (Aruoma, 1994).

Other forms of susceptible diseases that could result from reactive species are shown in Figure 2.1.

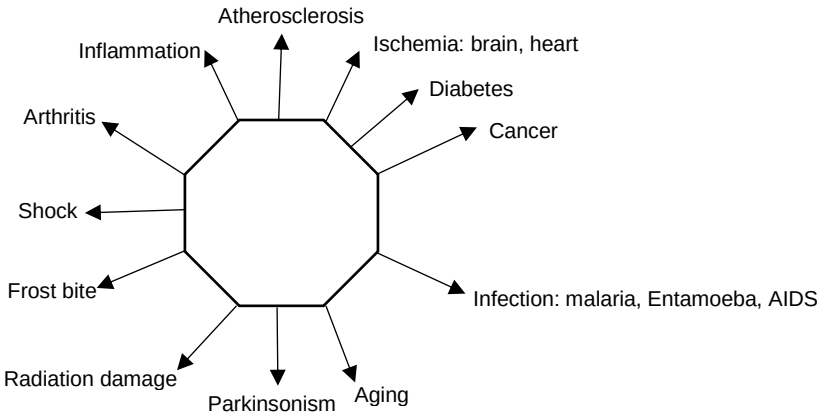

Figure 2.1: Diseases and damages caused by reactive oxygen species

(Source: Shahidi, 1997)

To discuss the benefits of triterpenes as valuable antioxidants, the work reported by Smina et al. (2011) and several other researchers have demonstrated the potential antioxidative activities of triterpenes. Triterpenes from *Ganoderma lucidum* showed no significant toxicity and are highly effective in lowering lipid peroxidation *in vivo,* and exhibited good ferric reducing activity (Smina et al., 2011). Montilla et al. (2003) explored the *in vivo* effect of triterpene on vulnerability of plasma to lipid peroxidation and reported that maslinic acid from olive pomace exhibited good antioxidative properties with a general conclusion on the applicability of triterpenes as excellent antioxidants. These characteristics of triterpenes to act as good scavengers of free radicals and improvement of body's antioxidative defences illustrate the potential of triterpenes as good antioxidants.

2.6 Antimicrobial agents

There has been an increase in antimicrobial resistance among the human microbial pathogens in the world. Although there is continuous effort to tackle the menace of microbial infections, the total number of new antimicrobial agents being introduced to the market declined over the past two decades (Moellering, 2011); however, there has been great interest and extensive research to find new leads. Conventional treatments have been shown to be less effective in managing microbial infections mainly due to increasing number drug resistance and multidrug resistance strains of these microorganisms which directly results from drug overdose, negligence and poor infection control practices (Rather et al., 2017). Efforts are being made to understand and provide effective response to multi-drug resistance microorganisms. For example, polyphenols are being widely studied in clinical treatment regime of these pathogens (Daglia, 2012).

Antimicrobial resistance directly frustrates the current efforts directed at management and treatment of ever-increasing number of infections caused by bacteria, viruses, fungi and parasites. Some of these microorganisms cause more disruptions than others, and according to global antimicrobial resistance surveillance conducted by world health organization (WHO, 2014), *Escherichia coli, Klebsiella pneumoniae, Staphylococcus aureus* and influenza are the most common bacteria and virus that cause infections and ill-health within communities and in clinics or hospitals.

The challenge of drug resistance strains of microorganisms has been around for several decades. In 1965, scientists in US (Boston) were the first to report drug resistance of *Streptococcus pneumoniae* to penicillin, and afterwards, the problem was observed in many other parts of the globe (Appelbaum, 1992). Cases of drug resistance have increased significantly. Recently, the span of research has been spread into understanding the behaviour and mechanisms of all forms of resistance bacteria.

Singh et al. (2017) provided insights on the mechanisms of antimicrobial resistance in bacterial biofilms on a molecular level and concluded with views that the problem of increased resistance to antibiotics (in this case by biofilm bacteria) there is enhanced outer membrane structure in the bacteria causing a reduced communication or limited diffusion of antimicrobial agent with the biofilm bacteria.

Antimicrobial activity of triterpenes and many natural products from medicinal plants have been studied against several microorganisms (Cowan, 1999). According to antimicrobial studies conducted by Paul et al. (2014), pentacyclic triterpenes from Cameroonian brown propolis have been shown to exhibit higher antimicrobial activity (MIC 0.1 – 0.2 mg/mL) than control standard drug, amoxicillin (0.4 mg/mL). Antimicrobial triterpenes from the stem bark extract of *Crossopteryx febriguga* also exhibited potent antimicrobial activity (MIC 8–64 µg/mL) which was at equal level, or higher than activity of standard drugs, chloramphenicol (MIC 16– 64 µg/mL) and nystatin (MIC 128–256 µg/mL) (Chouna et al., 2015), thus showing the potential of these classes of compounds as good lead for new antimicrobial agents.

Polyphenols are among interesting metabolites that have received increased attention due to their wide range and higher antimicrobial activity and because they can inhibit biofilm formation, lower adhesion of host ligands, and could neutralize bacterial toxins (Daglia, 2012). Polyphenolic compounds are now being applied as food preservatives (Ferrer-Gallego et al., 2017) due to increasing global appeal for substitution of synthetic preservatives in food. In this study, the bioactivity of pentacyclic triterpenes, their derivatives, as well as a flavonoid was assessed for potential nutraceutical application. The activity of derivatized calixarene and a named methylated flavone was also investigated, the flavone being extracted and isolation from a waste agro-material.

2.7 Analysis and identification of organic compounds

Thin layer chromatography (TLC) is an easy and fast approach for on-spot detection and to study profiles of plant extracts, and for partial identification of compounds (Haddad et al., 2008). TLC analysis is used in preliminary stages during extraction and isolation of compounds of interest.

The methods of Nuclear Magnetic Resonance (NMR) spectroscopy is important for identification and structural elucidation of pentacyclic triterpenes, and generally organic compounds. Pentacyclic triterpenes can be characterized with different 1D and 2D NMR methods such as ^{1}H- and ^{13}C-NMR, APT, DEPT, COSY, HMQC, HMBC and TOCSY (Pretsch et al. 2000; Kwan & Huang, 2008).

The quantitation of pentacyclic triterpenes in extracted plant samples is most commonly done with Gas chromatography (GC) and High-performance liquid chromatography (HPLC) techniques. Application of these techniques and the relevance to the chromatographic properties of triterpenes and sterols was investigated by Xu et al. (1988).

Other analytical techniques are the physical methods including measurement of optical rotation, melting point, UV-vis and Fourier transform infrared (FTIR) spectroscopy (Segneanu, et al. 2012; Braude & Nachod, 2013) and determination of solubility properties.

2.8 Statistical Analysis

Statistical significance was evaluated using one-way analysis of variance (ANOVA) by SPSS version 16 (SPSS Inc.).

2.9 Project Focus

Medicinal plants have been used in the treatment of all kinds of diseases for several thousands of years. To date, plants are still providing nutritional benefits and vast amount of information on potential drug compounds. However, there is an existing wide gap in the number of screened potential natural sources of bioactive compounds and a greater possibility of synthesizing useful derivatives. This study will attempt to contribute to the available wealth of information and research in the fields of natural product chemistry, organic synthesis and human health. The study compounds namely, betulinic acid, oleanolic acid, and ursolic acid and a flavonoid, 6-methyltectochrysin will be extracted from selected local medicinal plants. Several derivatives will be synthesized and assessed for biological activities.

2.10 Chapter Summary

This chapter provided relevant background on natural products with emphasis on classification of natural products, and further insight on triterpenes. The application of extracted metabolites in medicine to date have led to attribution of significant attention to the recognition of the importance of natural products in treatment of human pathogens. The literature review highlighted the known bioactivity of naturally occurring compounds and the improvement of pharmacological profile after chemical modifications. Advanced knowledge has proven that the technique of derivatization has yielded compounds that are several times more potent relative to starting materials, leading to the conclusion that significant research can be carried out with focus of exploring possibility of improving activity of triterpenes through synthetic modifications.

CHAPTER THREE
RESEARCH METHODOLOGY

3.1 Chapter Introduction

Pentacyclic triterpenes and one flavonoid were from plant samples. This chapter detailed the synthesis procedures for preparation of derivatives and the procedures for evaluation of the antioxidant and antimicrobial assays.

3.2 Chemicals

Solvents used for extraction, purification, synthesis and assays include ethyl acetate, n-hexane, methanol, ethanol, chloroform, pyridine, dichloromethane, acetic anhydride and acetone, sulphuric acid, glacial acetic acid, sodium carbonate, trifluoroacetic acid, hydrochloric acid, and tetrahydrofuran. These solvents were purchased from Merck (South Africa). Silica gel and TLC plates were purchased from Merck (South Africa). Other reagents including Ascorbic acid, meta-phosphoric acid (MPA), Trolox (6-Hydroxy-2,5,7,8-tetramethylchroman-2-carboxylic acid), gallic acid, fluorescein sodium salt, 2,2′-Azobis (2-amidino propane)dihydrochloride (AAPH), 2,4,6-tripyridyl-s-triazine (TPTZ), 2,2′-azinobis(3-ethyl-benzothiazoline-6-sulfonic acid) (ABTS), iron chloride hexahydrate ($FeCl_3.6H_2O$), chlorogenic acid, sodium acetate, Folin–Ciocalteau reagent, perchloric acid and potassium persulfate were obtained from Sigma-Aldrich (South Africa).

3.3 Thin-Layer Column Chromatography

Experiments involving Thin-layer chromatography (TLC) were performed using silica gel F254 coated on aluminium (Kieselgel 60 F_{254}, Merck) while column chromatography separations were performed with Kieselgel 60 (230-400 mesh, Merck). TLC was used for preliminary profiling of plant extracts and for immediate partial identification of compounds. Different solvent systems were prepared in TLC separations with the aim of determining purity of isolated or synthesised compounds and the R_f values. Samples (10 µg) were loaded on TLC plates and developed using mobile phase solutions in TLC chamber.

Visualization of compounds on TLC plates was done under UV light after staining with vanillin: sulphuric acid mixture or with methanol: sulphuric acid solution (95:5 % v/v). TLC analysis was done using silica gel G254 coated on aluminium plates.

3.4 Melting point

The melting points of samples were determined on a Veego (VMP-DS) Mel-Temp apparatus and data were recorded uncorrected.

3.5 Fourier transformed infrared (FTIR) spectroscopy

FTIR spectra of all samples were recorded on a Perkin Elmer UATR Spectrum Two spectrophotometer. Samples were scanned over a wavelength range of 4000 – 400 cm^{-1}.

3.6 NMR Analysis

^{1}H NMR experiments were performed on Agilent 600 MHz NMR spectrometer with spectra obtained in the range 0.5 ppm – 15 ppm. ^{13}C NMR spectra were recorded in the range 5 ppm – 250 ppm on Agilent 400 MHz NMR spectrometer using trimethylsilane (TMS) as internal standard. Samples (10 – 30 mg) were prepared in deuterated dimethyl sulfoxide (DMSO-d_6), or deuterated chloroform ($CDCl_3$).

3.7 Mass Spectroscopic Analysis

Mass spectroscopic analysis was done on a Bruker AmaZon Ion Trap instrument. The ESI-LC/MS analysis of samples (1 mg each) was carried out under the following conditions:

Table 3.1: HPLC Conditions for MS analysis

Conditions	Values
Polarity	Negative
Scan mode	MS/MS
Electrospray voltage	+ 4500 V
Dry gas flow	9.0 mL/min
Nebulizer gas pressure	50.0 psi
Dry temperature	350 ^{o}C

The HPLC instrument was equipped with Dionex ® 3000 RS pump, Dionex ® WPS-3000RS autosampler and Dionex ® DAD-3000RS Diode Array Detector. Separation was effected on Waters ® Sunfire C-18 reversed phase column (4.6x150 mm) at a column temperature of 30 ^{o}C. Samples were injected (injection volume of 10 µL) using the autosampler at a mobile phase multi gradient ratio (A-water, B-Acetonitrile, C-0.1% formic acid) from 2% B to 98% B within 80 minutes at a flow rate of 0.5 mL/min.

3.8 Collection of plant materials

The plant samples were collected for the extraction of target PTs and flavonoid. The PTs of interest were isolated from Mimusops *caffra, Tectona grandis, Syzygium aromaticum, Melaleuca salicina and Lavandula angustifolia* while the flavonoid was extracted from *Leptospermum petersonii.*

Fresh leaves of *Mimusops caffra* were obtained from Durban, South Africa in May 2015. The stem bark of *Tectona grandis* were collected from Ilorin, Nigeria in February 2016. Dried *Leptospermum petersonii* leaves were requested from an essential oil extraction factory in Australia in February 2016. *Syzygium aromaticum* was obtained from a spice shop in Cape Town in May 2016. The leaves of *Melaleuca salicina* and *Lavandula angustifolia* were collected from CPUT, Bellville campus, South Africa in August 2015. The plant samples were identified accordingly at Department of Horticulture, CPUT. All plant samples were air dried within the laboratory and pulverized using a mechanical grinder.

3.9 Extraction procedures

The extraction of starting materials, the pentacyclic triterpenes of interest (BA (**4**), OA (**5**) and UA (**6**)) and a target flavonoid compound from plant samples are highlighted in the following sub-sections.

3.9.1 Extraction of betulinic acid from *Tectona grandis*

The Teak tree (*Tectona grandis*, family *Lamiaceae*) is a deciduous hardwood mainly used for timber, especially furniture and boat building. The sawdust obtainable from teak wood had been used in several adsorption studies involving metal ions (Kumar et al., 2006). The different parts of teak tree have been utilized in traditional medicines due to the anti-inflammatory and anthelmintic activity (Nidavani & Mahalakshmi, 2014).

Figure 3.1: Teak tree

The dried stem bark of *T. grandis* was milled into powdery form. A weighed mass of 250 g of the plant sample was extracted twice with ethyl acetate under reflux conditions for 3 hours. The extracts were combined, filtered through Whatman No.1 filter paper and concentrated *in vacuo* in a rotary evaporator at 45 °C*.* Purification was carried out by subjecting crude extracts to column chromatography (silica gel), using a mixture of hexane: ethyl acetate as eluent, starting with 9:1 v/v followed by gradient increment. Fractions were collected and monitored by TLC. Similar fractions were combined and subsequently recrystallized from methanol to obtain purer product. All reactions were monitored by TLC.

TLC visualization was done under UV (254 nm) before and after spraying spotted TLC plates with 15% H_2SO_4 acid in methanol. The sprayed plates were heated gently for clear identification of spots.

3.9.2 Extraction of oleanolic acid from *Syzygium aromaticum* (Clove buds)

Cloves (*Syzygium aromaticum,* family *Myrtaceae)* is an aromatic flowering plant mainly cultivated for clove oil and used as spice. It is used in Ayurvedic as well as Chinese medicine for painkiller and anthelmintic properties. Essential oils from cloves have good antifungal activity (Pinto et al., 2009).

Figure 3.2: Clove buds

Cloves were obtained from Indian spice shops in Cape Town. The buds, weighing 980 g, were macerated in dichloromethane at room temperature for 72 hrs. Extraction was done twice. Afterwards, the mixture was filtered to remove the marc, and the filtrates were combined. The filtrate was concentrated under reduced pressure with a rotatory evaporator resulting in an oily product (extract) after removal of the solvent. This was followed by successive partitioning into organic solvent with low polarity. Specifically, the product was washed with hexane and subsequently, the filtration of the resulting mixture gave a solid (powdery) white material. Further purification was done using column chromatography. Column chromatography was carried out with silica gel and hexane: ethyl acetate in a gradient elution starting with (9:1 v/v). Isolates were monitored using TLC and similar fractions were combined.

3.9.3 Extraction of ursolic acid from *Mimusops caffra*

Mimusops caffra (family *Sapotaceae*) is an abundant tree found in Eastern Cape and KwaZulu-Natal areas of South Africa. Mimusops species have demonstrated chemopreventive potential (Saha et al., 2008) as well as potent antibacterial activity (Hazra et al., 2007).

Figure 3.3: *Mimusops caffra* (leaves and fruits)

The leaves of *Mimusops caffra* (500 g) that have been air-dried and pulverized was extracted with a freshly prepared solution of 4 L methanol containing 1 M NaOH (40 g dissolved in 1 L

of water). The mixture was filtered after 3 days. The filtrate was then concentrated under reduced pressure in a rotary evaporator at 42 ± 2 ^{0}C to one-tenth of the initial volume. To the concentrate was added about 10 mL of conc. sulphuric acid to initiate precipitation of the compounds of interest. The resultant precipitate was filtered and allowed to dry. The dried extract was subjected to column chromatography using silica gel 60 and mobile phase of hexane-ethyl acetate at a gradient elution of 5% successive increment. Similar fractions were combined based on their TLC profiles. The product was recrystallized in methanol to obtain UA (**6**).

3.9.4 Extraction of flavonoid from *Leptospermum petersonii*

Lemon-scented tea tree (*Leptospermum petersonii*, family Myrtaceae) is an ornamental plant that is mainly cultivated for essential oils. The essential oils from *L. petersonii* have been found to exhibit potent antifungal properties (Hood et al., 2010). An important characteristic of this study is the attempt to beneficiate spent (used) leaves of *L. petersonii* after the essential oils have been extracted from the leaves commercially, thus adding potential value to the plant product. The extraction of essential oils from *L. petersonii* has been widely studied; however, there is limited knowledge on the composition or extraction of secondary metabolites from the plant.

Figure 3.4: *L. petersonii* (Lemon-scented Tea Tree)

Dried leaves of *L. petersonii* (160g) was refluxed in methanol for 30 minutes. The methanolic extract was filtered, and the marc (insoluble residue) was extracted again under similar previous conditions. The combined extracts were concentrated under reduced pressure to one-tenth of the starting volume.

The (yellowish) concentrated extract was washed with hexane (200 mL) and then filtered to afford hexane soluble fraction (filtrate) and a residual material (12.432 g, 7.8%). After removal of solvents from the hexane filtrates, an oily gelatinous material (18.2 g) was obtained. Boiling the yellowish residual material in methanol and subsequent filtration afforded a yellowish solid residue material weighing 0.64 g. The methanol filtrate was kept overnight to precipitate a greenish product weighing 2.49 g.

TLC analysis of the yellowish solid material showed the plant contained flavonoid (suspected) and pentacyclic triterpene while the greenish product contained a mixture of triterpenes, when compared with standard samples. The solid material obtained was washed boiled in methanol and then filtered immediately while hot. The residue was purified using column chromatography (Silica gel 60) with a mobile phase of hexane-ethyl acetate (9:1 v/v). Similar fractions were combined based on their TLC profiles.

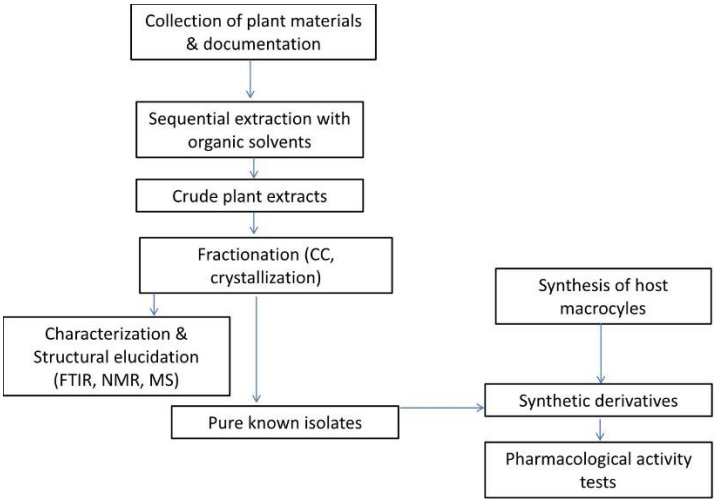

Figure 3.5: Project design overview

3.9.5 Extractives of *Melaleuca salicina*

M. salicina (family *Myrtaceae*), has been used widely by Aborigines in Australia traditional medicine for several years, especially for the active antimicrobial properties, and other medicinal activities (Sharifi-Rad et al., 2017). In this study, a rapid exploration of this plant was performed to assess the presence of target pentacyclic triterpene compounds in the plant.

Figure 3.6: *Melaleuca salicina* (Leaves and flower)

Fresh leaves from *M. salicina* plant were collected on CPUT Bellville campus and air-dried within the laboratory. A weighed amount (500 g) of the dried leaves was macerated in a solution containing methanol (3 L) and NaOH (50g in 1 L of water) for 3days at room temperature. After extraction, the mixture was filtered. The filtrate was concentrated to one-tenth of the original volume under reduced pressure. Subsequently, the concentrated extract was acidified with dil. H_2SO_4 to precipitate out UA from the extract. The precipitated material was filtered and allowed to dry. The product was then subjected to recrystallization.

The fruits (700 g, fresh) of *Melaleuca salicina* were extracted with methanol over a period of 3 days. The final extract was filtered. The filtrate obtained was concentrated under reduced pressure resulting in an orange coloured solid material. The product was analysed by TLC and checked for the presence of pentacyclic triterpenes.

3.9.6 Extractives of Lavandula angustifolia

The Lavender plant (*Lavandula angustifolia,* family *Lamiaceae)* is an aromatic flowering plant widely used in culinary as well as in herbal medicines.

Figure 3.7: Lavender plant

Lavender leaves were collected from CPUT, Bellville campus. A weighed mass (50 g) of the fresh leaves was subjected to hydro-distillation for 3 hours to extract the essential oil constituents. The marc obtained was air-dried within the laboratory. The dried leaves were then extracted exhaustively using methanol under reflux conditions at 45 °C (±3 °C) for 2 hours. Extraction was carried out twice. The mixture was filtered, and the combined filtrate was evaporated to dryness to yield a powdery product. The greenish material was washed twice with hexane, filtered and dried.

3.10 Synthesis of Derivatives

Semi-synthetic derivatives were prepared from the isolated PTs (BA (**4**), OA (**5**), UA (**6**)) and a flavonoid (**19**), by activating and/or protecting the C3 hydroxyl and C28 carbonyl functionalities of the PTs.

3.10.1 Acetylation and methylation of starting materials

Several reports abound on the synthesis and activities of acetylated, as well as methyl esters of pentacyclic triterpenes. In this work, these compounds served as starting materials for the conjugate hybrids, and provided a basis for comparison to justify whether the synthesis is necessary or not, based on the bioassay results.

3.10.1.1 3-*O*-Acetylbetulinic acid

The plant derived betulinic acid (**4**) (1 g, 2.2 mmol) was treated with pyridine (5 mL) and acetic anhydride (5 mL). The mixture was stirred for 24 hours at room temperature and monitored with TLC analysis to confirm reaction completion. Upon completion, water (50 mL) was added to the mixture, and stirred at room temperature for 20 min. The resultant solid was filtered under vacuum, and thoroughly washed with a solution of dilute HCl and distilled water. The dried crude product (white powdery solid material, 1.02 g) was recrystallized in *n*-hexane.

3.10.1.2 3-*O*-Acetyloleanolic acid

Oleanolic acid (OA) (**5**) was isolated from cloves. The plant-sourced OA (2.0019 g, 4.4 mmol) was acetylated as above and purified by silica gel column chromatography using gradient elution (90% hexane/ 10% ethyl acetate, to 85% hexane/15% ethyl acetate). Similar fractions were combined and evaporated to dryness using a rotatory evaporator.

3.10.1.3 3-*O*-Acetylursolic acid

UA (**6**) (2.20 g, 4.4 mmol) was acetylated as described in section 3.10.1.1. The product obtained was then chromatographed by silica gel chromatography (gradient elution: hexane/ethyl acetate) to afford a white powdery material.

3.10.1.4 Methyl betulinate

BA (**4**) (0.4025 g, 0.876 mmol) was added to K_2CO_3 (0.2622 g, 1.9 mmol), dimethyl formamide, DMF (20 mL), and methyl iodide, CH_3I (0.1099 mL, 1.752 mmol) in a 50 mL round bottom flask. The mixture was stirred at room temperature for 6 h, while monitoring progress of reaction with TLC to ascertain disappearance of starting material. Ethyl acetate (150 mL) was added, and stirred at room temperature for 5 min. The reacted mixture was transferred into a separating funnel and washed thrice with H_2O (50 mL). The separated organic layer was washed with saturated NaCl (50 mL) and dried over anhydrous $MgSO_4$. Removal of the solvent was done under reduced pressure. The solid residual material was recrystallized using methanol to afford white crystalline material.

3.10.1.5 Methyl oleanolate

The reaction of OA (**5**) (0.4019 g, 0.876 mmol) with CH_3I in presence of K_2CO_3 and DMF afforded the methylation of the carboxylic (COOH) group of OA (**5**) at C17 to yield methyl oleanolate (**24**) using the procedure described in section 3.10.1.4.

3.10.1.6 Methyl ursolate

UA (**6**) (0.4017 g, 0.876 mmol) was methylated as described in section 3.10.1.4. Dichloromethane was used in final extraction instead of ethyl acetate. The product obtained was purified by silica gel column chromatography (n-hexane / ethyl acetate 7: 3).

3.10.2 Synthesis of polyhydroxyl triterpene compounds

The synthesis of polyhydroxyl bearing PTs followed the methods reported by (Huang et al. 2015). Starting material PTs was oxidised using Jones reagent. The oxidised (3-ketone PTs) products (7.6 mmol) was dissolved in acetic acid (100 mL), and selenium oxide (920 mg) was added, and reaction mixture was refluxed to yield α,β-unsaturated ketones. The epoxy ketones were prepared by reacting α,β-unsaturated ketones (3.1 mmol) in methanol with NaOH (5 mL) in ice bath for 30 min, followed by addition of H_2O_2 (140 mL), after which solution was stirred at rt to obtain epoxidized products. The epoxy-3-hydroxyl compounds were synthesized by dissolving the epoxy ketones (2.4 mmol) in methanol, then slowly adding sodium borohydride

(456 mg) and stirred at rt. The product obtained (1 mol equivalent) was then dissolved in acetone, followed by dropwise addition of perchloric acid (2 equivalent) while stirring at rt. Final product was extracted with ethyl acetate, washed with $NaHCO_3$ and brine, and dried over $MgSO_4$, followed by purification using silica gel chromatography.

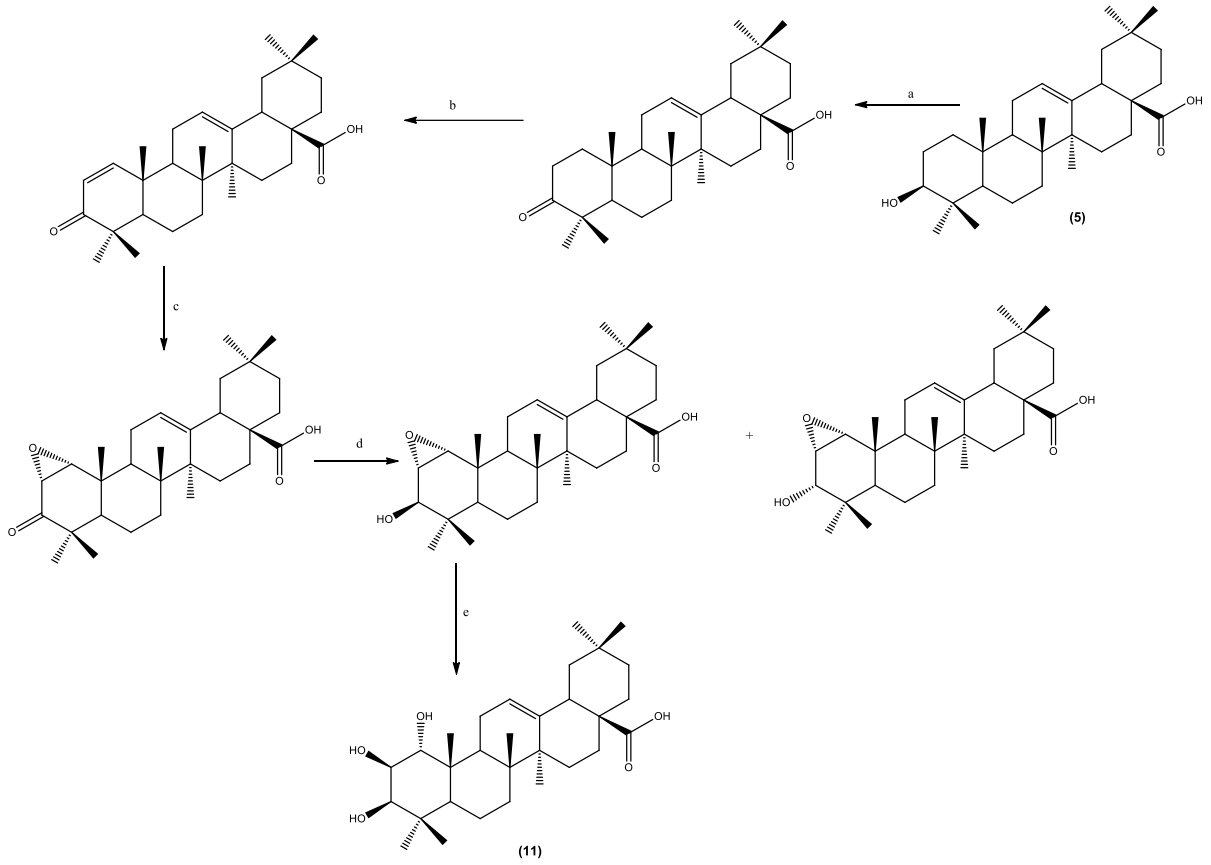

Scheme 3.1: Synthesis of polyhydroxyl derivatives of pentacyclic triterpenes. (a) Jones reagent, acetone, 0 ^oC; (b) selenium oxide, Ac_2O, reflux; (c) 30% H_2O_2, NaOH, MeOH, rt; (d) $NaBH_4$, MeOH, rt; (e) perchloric acid, acetone, rt

According to Scheme 3.1, the epoxidation of α,β-unsaturated ketones intermediates formed in the course of synthesizing the target polyhydroxyl compounds is often achieved with H_2O_2 in presence of NaOH in methanol. The choice of selective reagent is critical, taking note that there are double bonds in ring A and ring C of the triterpenes. Hence, hydrogen peroxide is a preferred choice, as this reagent is too weak to epoxidize the olefinic double bond in ring C by electrophilic addition. With the right experimental conditions, hydrogen peroxide can only attack the olefinic Ring C bond in presence of polyoxometalates or transition metal compounds. This characteristic selectivity enable the formation of an epoxide analogue on ring A. Hence, the selective epoxidation of the α,β-unsaturated double bond of ring A over the double bond in ring C is because H_2O_2/NaOH is a nucleophilic epoxidizing agent whereas the double bond in ring C will require an electrophilic epoxidizing agent.

3.10.3 Synthesis of pentacyclic triterpene conjugates

Conjugated triterpene anhydrides

The derivatives classified in this group followed a structural C28 – C28 anhydride-type linkage of two PT compounds. The conjugated hybrid compounds A13 – A18 were prepared by dissolving 0.1 g (0.22 mmol) of acetylated pentacyclic triterpenes (BAA (**20**), OAA (**21**), or UAA (**22**)) in dichloromethane, and then adding DCM (30 mL) and thionyl chloride (3 mL) to the solution, followed by stirring for 12 h at room temperature. Triethylamine (0.5 mL) was added. 0.1 g (0.22 mmol) of corresponding acetylated pentacyclic triterpene (BAA (**20**), OAA (**21**), or UAA (**22**)) was added to the reaction flask, depending on the target combination, and stirred at room temperature for 24 h. Upon completion, distilled H_2O (100 mL) was added to the mixtures. The organic layer was extracted thrice with DCM (30 mL) in a separating funnel and washed with saturated NaCl, and dried over anhydrous sodium sulfate (Na_2SO_4). The solvent was removed *in vacuo.* The residual products were recrystallized using suitable solvents. The method by (Sell and Kremers, 1938-a) was adapted. An illustration of the reaction scheme was given in scheme 3.3. The combinations are listed as follows:

Compound A13 (UAA – UAA conjugate)

Compound A14 (UAA – OAA conjugate)

Compound A14 A15 (OAA – OAA conjugate)

Compound A14 A16 (BAA – BAA conjugate)

Compound A14 A17 (UAA – BAA conjugate)

Compound A18 (OAA – BAA conjugate)

Conjugated triterpene esters

Other PT-PT conjugate hybrids were linked by ester-type bridge based on the C28-C3 coupling of two PTs. Compounds A22 – A30 were prepared as follows: 0.1 g (0.22 mmol) of acetylated pentacyclic triterpenes (BAA (**20**), OAA (**21**), UAA (**22**)) was dissolved in dichloromethane, DCM (30 mL), and then added thionyl chloride (3 mL) to the solution. The solution was stirred for 12 h at room temperature. Triethylamine (0.5 mL) was added, and then 0.1 g (0.22 mmol) of methyl esters of pentacyclic triterpenes (methyl betulinate (**23**), methyl oleanolate (**24**), or methyl ursolate (**25**)) was added, depending on the target combination. This was followed by stirring at room temperature for 24 h. The product work up followed the steps given earlier in section 3.10.3. The residual products were recrystallized using suitable solvents or subjected to column chromatography. The C28 position of (BAA (**20**), OAA (**21**), and UAA (**22**)) were coupled to the open C3 positions of other PTs using similar routine experiment reported by

(Sell & Kremers, 1938-a; Gnoatto et al. 2008). An illustration of the reaction scheme was given in scheme 3.2. The derivatives in this group are listed as follows:

A22 (BAA – methyl BA)

A23 (BAA – methyl OA)

A24 (BAA – methyl UA)

A25 (OAA – methyl BA)

A26 (OAA – methyl OA)

A27 (OAA – methyl UA)

A28 (UAA – methyl BA)

A29 (UAA – methyl OA)

A30 (UAA – methyl UA)

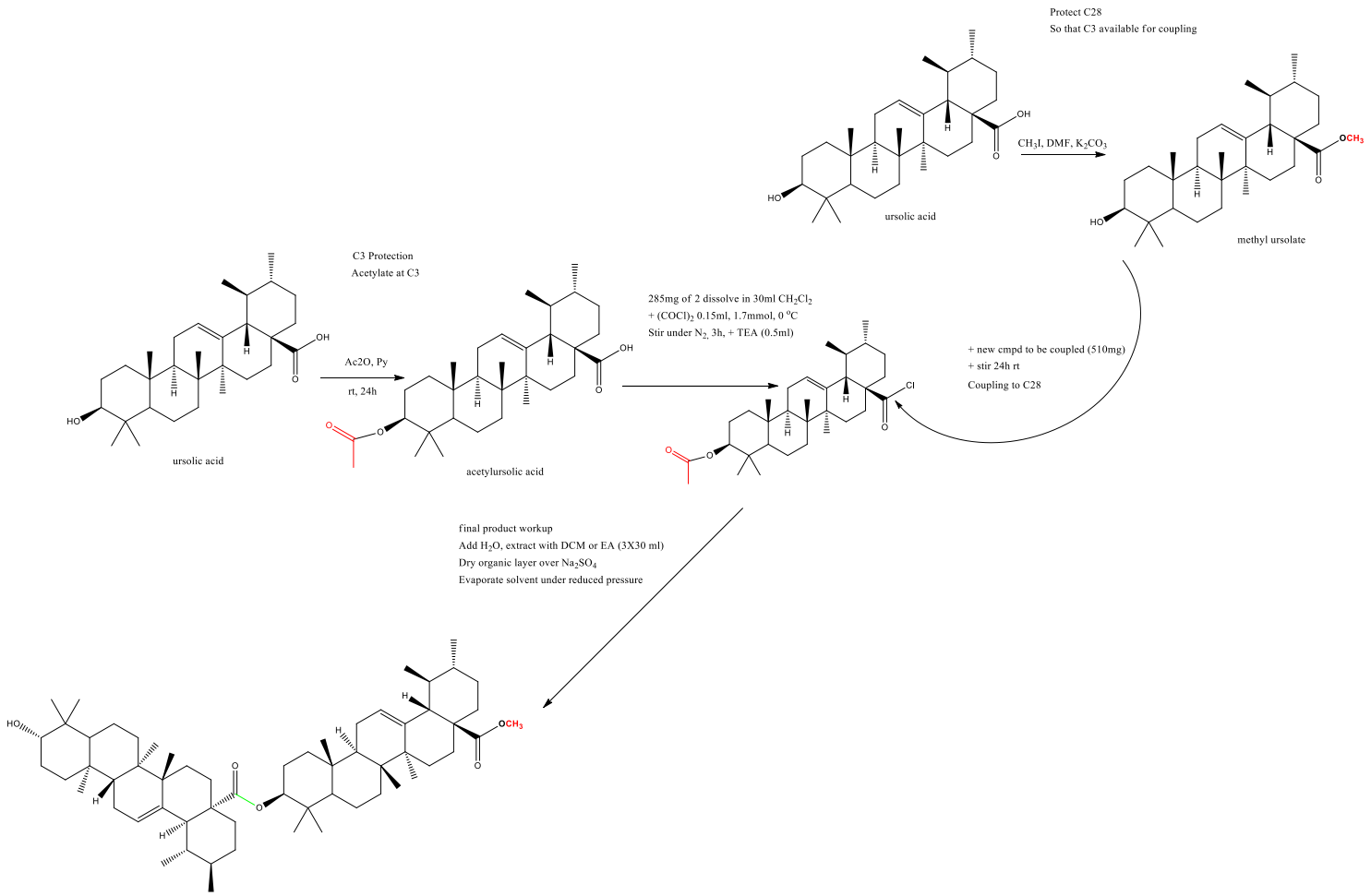

Scheme 3.2: Synthesis of conjugate esters of pentacyclic triterpenes (C28 - C3 coupling)

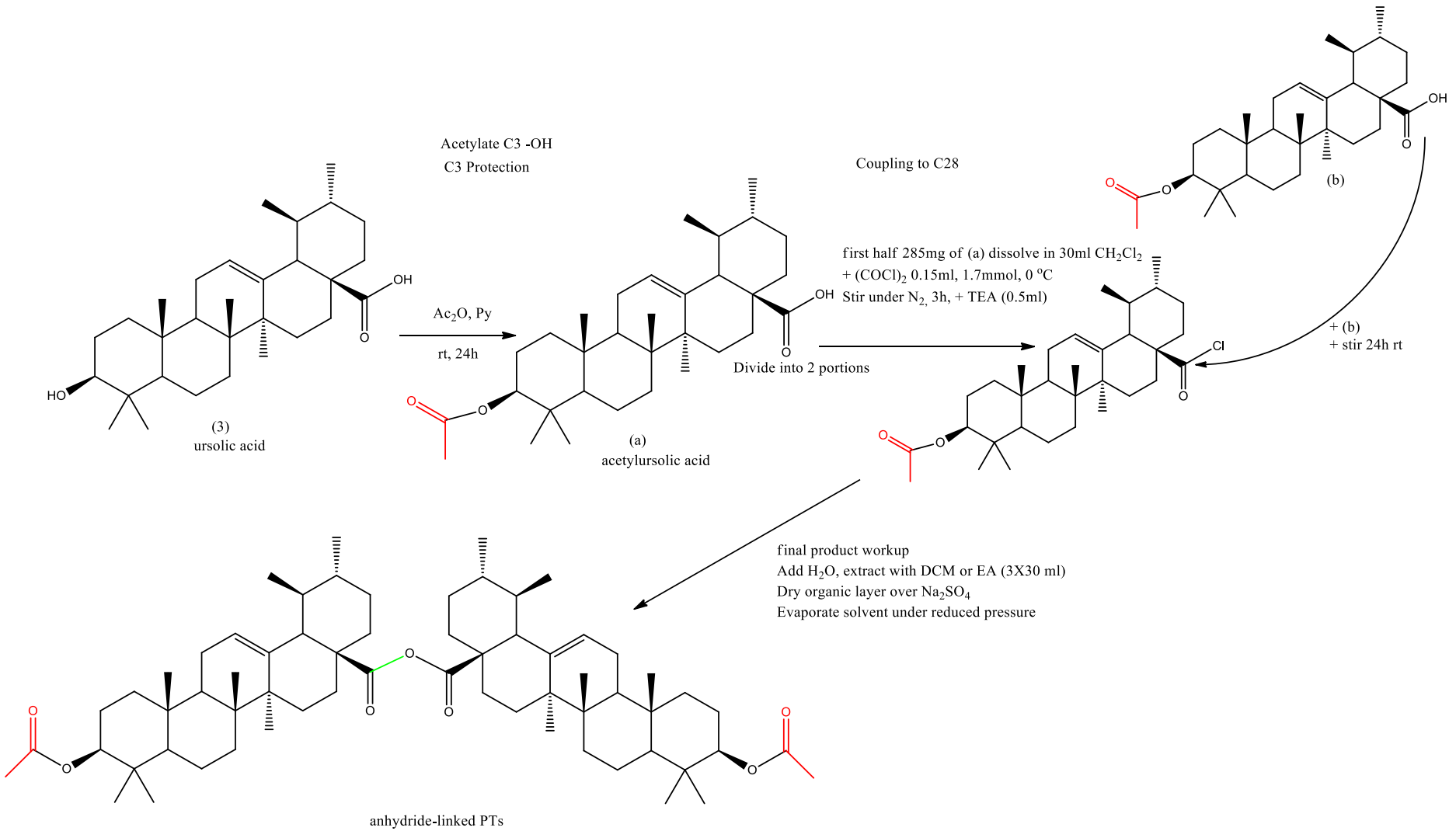

Scheme 3.3: Synthesis of conjugate anhydrides of pentacyclic triterpenes (C28 – C28 coupling)

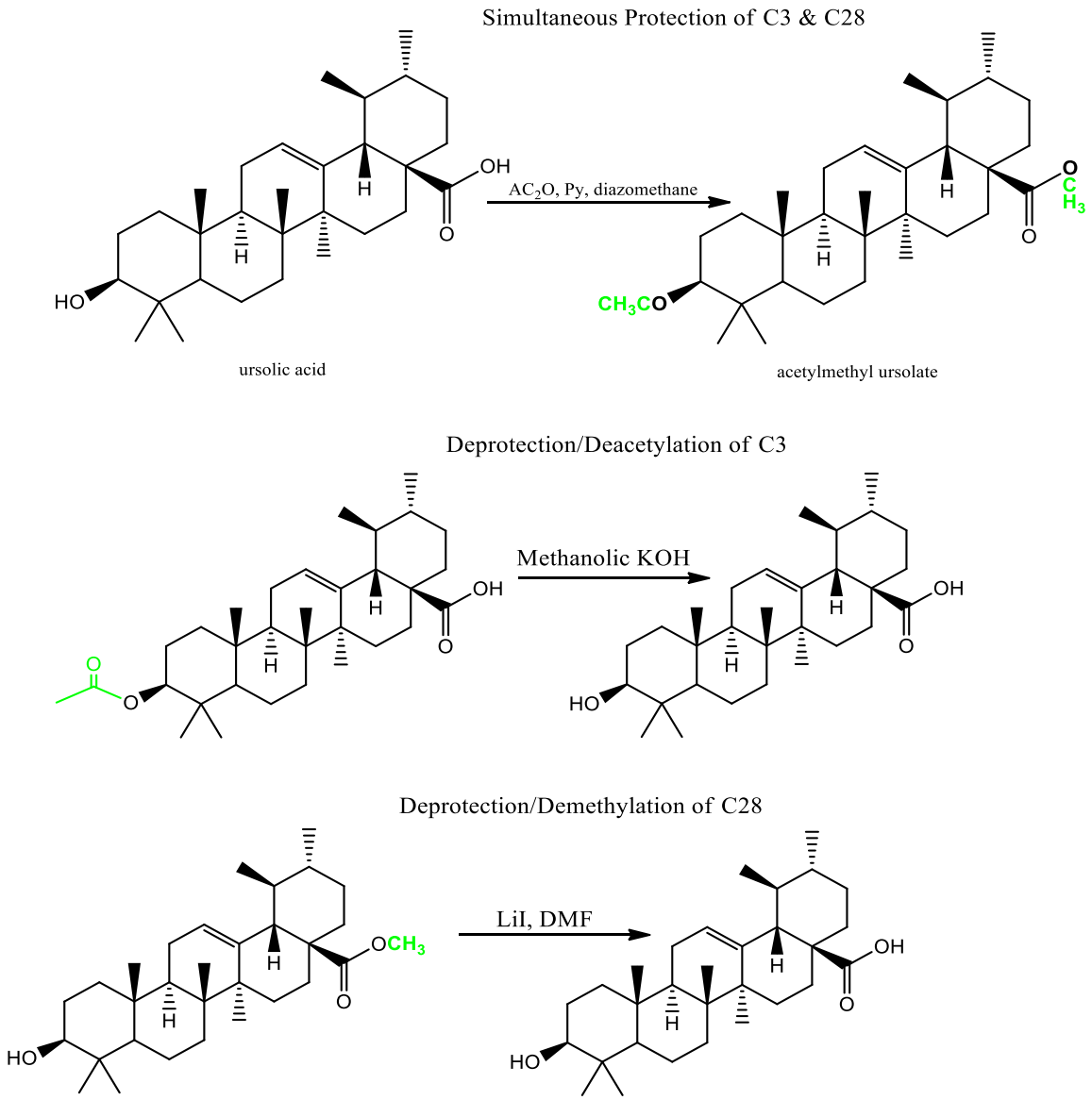

Scheme 3.4: Reaction schemes for protection and de-protection of triterpene

3.10.4 6-Methyltectochrysin based derivatives

This section discusses the preparation of derivatives of 6-methyltectochrysin (**19**). The sulfonation of (**19**) to form (compound A37), and methylated form of (**19**) (compound A38), and flavonoid-triterpene derivatives (compounds A31, A32, A33) were prepared via semi synthesis. The semi-synthetic modification of 5-hydroxy-7-methoxy-6-methylflavone (**19**) resulting in compounds A37 and A38 involve substitution of the hydroxyl functional group on the flavonoid. The triterpene – flavonoid conjugates were synthesized by exploiting the hydroxyl C5 position of the flavonoid, which was linked to the C28 position of acetylated pentacyclic triterpenes (BAA (**20**), OAA (**21**), and UAA (**22**)).

The preparation of intermediate triterpenoyl acid chlorides followed the same procedures discussed in section 3.10.3 for the conjugated esters. Acetylated pentacyclic triterpenes 0.1008 g (0.221 mmol) were reacted with thionyl chloride and TEA followed by addition of the flavonoid compound (0.0590 g, 0.223 mmol).

3.10.4.1 Synthesis of compound A31 (BAA – 6-Methyltectochrysin conjugate)

BAA (**20**) was reacted with thionyl chloride and TEA, and then added to 5-hydroxy-7-methoxy-6-methylflavone (**19**). The resulting product (light yellowish powdery material) was purified using silica gel column chromatography. The chromatographed product was labelled compound A31.

3.10.4.2 Synthesis of compound A32 (OAA – 6-Methyltectochrysin conjugate)

OAA (**21**) was reacted with 5-hydroxy-7-methoxy-6-methylflavone (**19**) as done above. The resulting product (light yellowish powdery material) was purified using silica gel column chromatography. The chromatographed product was labelled compound A32.

3.10.4.3 Synthesis of compound A33 (UAA – 6-Methyltectochrysin conjugate)

UAA (**22**) was reacted with thionyl chloride and TEA as above followed by addition of 5-hydroxy-7-methoxy-6-methylflavone (**19**). The resulting product (light yellowish powdery material) was purified using silica gel column chromatography. The chromatographed product was labelled compound A33

3.10.4.4 Synthesis of compound A37 (Na – sulfonic 6-Methyltectochrysin)

The sulfonation of target flavonoid compound was done by adapting the method of Woznicka et al. (2015). The isolated flavonoid (5-hydroxy-7-methoxy-6-methylflavone (19)) 0.071 g (0.27 mmol) was added to 5 mL of conc. H_2SO_4 in a 50 mL round bottom flask. The mixture was stirred at room temperature for 2 h. Then, ice-cold water (75 mL) was added, and the mixture was filtered using vacuum suction. The solid product was recrystallized from hot saturated water solution, filtered, and air dried at room temperature. The sulfonated solid material was neutralized with a solution of 20% NaOH to pH 4. The solution was filtered, and the residue was dried to afford the sodium salt of the derivative.

3.10.4.5 Synthesis of compound A38 (methylated flavonoid)

The methylation procedure reported by De Carvalho et al. (1996) was employed, with slight modification. A mixture of 5-hydroxy-7-methoxy-6-methylflavone (**19**) (0.1230 g, 0.46 mmol), dimethyl sulfate, Me_2SO_4 (1 mL), dry K_2CO_3 (0.0633 g, 0.46 mmol) and acetone (50 mL) was heated under reflux for 12 h. The mixture was cooled to room temperature, and distilled water (50 mL) was added to remove inorganic salts. The organic layer was dried over Na_2SO_4 and the solvent was removed *in vacuo*. The product was chromatographed on silica gel using hexane/ethyl acetate (5: 1) for elution.

3.10.5 Synthesis of calixarene-based derivatives

The synthesis of calix[4]arene (**18**) from 4- tert- butylphenol (**17**) is shown in scheme 3.5. The combination of (**18**) with PTs to assess influence of such combinations of calixarene -PT derivatives (of the forms of (**14**), (**15**) and (**16**)) on the level of bioactivities relative to the parent starting materials.

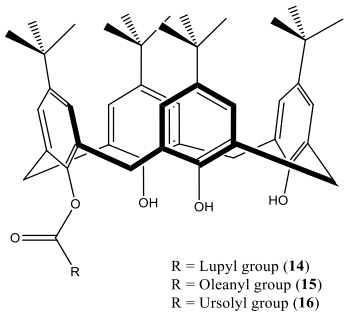

R = Lupyl group (**14**)
R = Oleanyl group (**15**)
R = Ursolyl group (**16**)

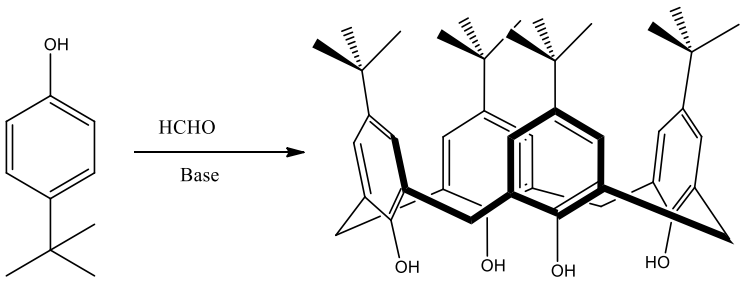

(**17**) (**18**)

Scheme 3.5: Synthesis of calix[4]arene (**18**)

3.10.5.1 Synthesis of p-*tert*-butylcalix[4]arene

In the preparation of calix[4]arene (**18**), the synthesis method by Gutsche et al. (1981) was adopted with little modifications. A mixture of of p-*tert*-butylphenol (**17**) (10 g, 66.7 mmol), NaOH (0.12 g, 0.045 equivalent of phenol), and formalin (6.1 ml, 66.7 mmol) in a round bottom flask was heated in an oil bath for 2 h at 120 °C. The experimental setup involved continuous stirring using an overhead stirrer. About 15 mins into the reaction, a color change was observed from clear to cloudy viscous material and upon reaction completion, a yellow gel-like solution was formed, which solidified after cooling to room temperature. The yellow precursor was broken into smaller pieces and suspended in 80 ml of diphenyl ether in a 2-neck round bottom flask (outlet for nitrogen and condenser). The contents were first heated gently on hot plate. Immediately after the yellow precursor dissolves, a gentle flow of nitrogen was blown into the flask to remove evolved water. The condenser was fixed just at the start of precipitate formation, and the mixture was refluxed for 2 h under nitrogen flow at 120 °C. Upon completion, the mixture was allowed to cool to room temperature, washed twice with ethyl acetate (10 ml x 2), and once with acetic acid (20 ml). The product was filtered and allowed to dry to afford a crude (mixture) of 5.9 g of white solid material. The crude was refluxed in 30 ml toluene for 30 min and filtered while hot. The residue was dried to yield 1.22 g of a creamy white powdery material (cyclic octamer suspected). The filtrate was cooled to afford crystal formation.

3.10.5.2 Synthesis of calixarene–triterpene conjugated derivatives

The triterpene–calixarene conjugates were synthesized by exploiting the C28 position of the acetylated pentacyclic triterpenes OAA (**21**), and UAA (**22**) to enable coupling with an available hydroxyl position of the calixarene. The coupling was done using the procedure discussed in section 3.10.3.

In separate experiments, OAA (**21**) (0.1004g, 0.22 mmol) or UAA (**22**) (0.1012 g, 0.22 mmol) was treated with thionyl chloride and TEA and allowed to react. Then calix[4]arene (**18**) (0.1438 g, 0.22 mmol) was added. The product work-up was done as with other hybrid derivatives above. The products (Compound A35 and Compound A36) were recrystallized from n-hexane.

3.11 Biological activity evaluation

This study assessed the biological activity of isolated compounds as well as all the synthesized derivatives. The biological assays involved the investigation of antipathogenic potential and level of activity of pure isolates of pentacyclic triterpenes, flavonoid, calixarene, and synthesized derivatives.

3.11.1 Antioxidant activity

The antioxidant capacity (ORAC, FRAP, and TEAC) of isolated pentacyclic triterpenes, flavonoid, calixarene, and synthesized derivatives were evaluated in this study.

3.11.1.1 Oxygen Radical Absorbance Capacity Assay (ORAC)

The ORAC method is a fluorescence-based simple and reliable technique for measuring peroxyl radical absorbing capacity of antioxidants using a fluorescence spectrophotometer. The assay protocols have been described in literature (Wu et al., 2004; Georgiev et al., 2010).

Preparation of solutions

The working solution for the ORAC assay was prepared by mixing 700 mL acetone, 295 mL distilled water and 5 mL glacial acetic acid, in a 1 L bottle.

The phosphate buffer (75 mM, pH 7.4) solution was prepared as follows: 1.035 g of sodium dihydrogen orthophosphate-1-hydrate ($NaH_2PO_4.H_2O$) was weighed in a 100 mL media bottle and 100 mL of double distilled water was added. The solution was mixed until all salts dissolved. Separately, 1.335 g of di-sodium hydrogen orthophosphate dehydrate ($Na_2HPO_4.2H_2O$) was weighed, transferred into a 100 mL media bottle and 100 mL double distilled water was added. The required buffer was prepared by mixing 18 mL of the first solution and 82 mL of the second solution. pH was adjusted as necessary with either of the phosphate solutions and the solution was stored at 4 °C

Preparation of fluorescein sodium salt stock solution was done by weighing 0.0225 g of sodium fluorescein ($C_{20}H_{10}Na_2O_5$) and dissolving in 50 mL phosphate buffer. The solution was mixed until dissolved and stored in a dark container at 4 °C.

Perchloric acid solution (0.5M) was prepared by mixing 195 mL distilled water and 15 mL 70% perchloric acid in a 250 mL Media bottle. The solution can be stored at room temperature and usable for up to 6 months.

A 500 µM Trolox standard stock solution was prepared as follows: 0.00625 g of 6-Hydroxy-2,5,7,8-tetra-methylchroman-2-carboxylic acid was weighed into a 50 mL screw cap tube, and 50 mL phosphate buffer was added, and mixed until dissolved.
To confirm quality of standard, dilute the stock twice (2x) and analyse the absorbance which should give an absorbance of 0.670 ±0.015 at 289nm.

A 250 µM Trolox Control solution was prepared as follows: 0.00312 g of 6-Hydroxy-2,5,7,8-tetra-methylchroman-2-carboxylic acid was weighed in 50 mL screw cap tube, and 50 mL phosphate buffer was added, and mixed until dissolved. For quality assurance, this solution should give an absorbance of 0.670±0.015 at 289 nm.

A measured amount of 150 mg of peroxyl radical, 2,2'-Azobis (2-methylpropionamidine) dihydrochloride (AAPH), was measured out of the 25 mg/mL stock into a 15 mL screw cap tube for sample assays. Preparation of AAPH solution for sample analysis must be done fresh for assays.

Sample analysis

Samples (isolated pentacyclic triterpenes, flavonoids and synthesized derivatives) were dissolved in acetone and mixed until dissolved, applying sonication where necessary. Any slightly turbid sample was centrifuged. To ensure quality control, reagents were prepared fresh on the day of analysis. The pH of phosphate buffer was rechecked prior to each assay.

The method by Wu et al. (2004) was used with slight modifications. Calibration standards in the range of 5 µM to 25 µM were prepared from a standard 500 µM stock solution of Trolox by dilution in phosphate buffer (75 mM, pH 7.4). Fluorescence filters (excitation wavelength of 485 nm and emission wavelength of 538 nm) were employed for the assay. The Fluoroskan ascent plate reader (Thermo Fisher Scientific, U.S.A.) equipped was equipped with an incubator (at a working temperature of 37 °C). Fluorescein stock solution was diluted with phosphate buffer to a final concentration of 14 µM per well in a black 96-microwell plate. AAPH (6 mL, 25 mg/mL in phosphate buffer) was then added to each well, resulting in a final AAPH concentration of 4.8 mM in each well. Sample wells contained 12 µL of each sample, in triplicates, while standard and control wells contained 12 µL of trolox standard and control solutions, respectively. The fluorescence from each well was recorded every 5 min for 2 h. Final ORAC values were calculated using the regression equation $y = ax^2 + bx + c$ between Trolox concentration (µM) and the area under the curve. Results were expressed as micromoles of Trolox equivalents per gram of sample weight.

3.11.1.2 Ferric Reducing Antioxidant Power Assay (FRAP)

The FRAP assay is based on application of oxidation/reduction reaction to assess the ability of a sample to reduce Fe (III) to Fe (II). Antioxidants are expected to donate electrons in a similar principle followed by a reductant in redox reactions. The FRAP assay is a fast and non-concentration dependent assay.

Preparation of solutions

An acetate Buffer (300 mM, pH 3.6) solution was prepared as follows: 1.627 g of Sodium acetate and 16 mL Glacial acetic acid was mixed and made up to 1 L with distilled water in a 1 L media bottle. The pH was checked, and the solution was stored at room temperature.

Dilute HCl (40 mM) solution was prepared by diluting 1.46 mL concentrated HCl (32% HCl) with distilled water and making up to I L in a 1 L media bottle. Solution was stored at room temperature.

A 10 mM solution of 2,4,6-tri[2-pyridyl]-s-triazine (TPTZ) was prepared as follows: 0.0093g of TPTZ and 3 mL of 40 mM HCl was mixed in a 15 mL conical tube. Solutions were freshly prepared for assay.

Iron (III) chloride hexahydrate (20 mM) was prepared by mixing 0.054 g $FeCl_3.6H_2O$ and 10 mL distilled water in a 15 mL conical tube. Solutions were prepared fresh for assay.

A 1.0 mM ascorbic acid standard stock solution was prepared as follows: 0.0088 g of ascorbic acid was weighed into a 50 mL centrifuge tube and 50 mL of distilled water was added. The solution was mixed until dissolved. Solutions were prepared fresh for assay. To ensure quality control, 125 µl of the stock solution was diluted with 1375 µl distilled water to obtain a concentration of 83 µM in an Eppendorf tube. This solution should give an absorbance of 0.830 $\pm$0.010 at 265 nm.

A 400 µM ascorbic acid control solution was prepared as follows: 0.00352 g of ascorbic acid was added to 50 mL distilled water in a 50 mL centrifuge tube. The solution was mixed until dissolved. To ensure quality control, 311 µl of the stock solution was diluted with 1189 µl distilled water to obtain a concentration of 83 µM in an Eppendorf tube. This solution should give an absorbance of 0.830 $\pm$0.010 at 265 nm.

The FRAP reagent was prepared by mixing 30 mL acetate buffer (300 mM, pH 3.6), 3 mL TPTZ (10 mM in 40 mM HCl), 3 mL $FeCl_3.6H_2O$ (20 mM) and 6.6 mL distilled water.

Sample analysis

Samples (isolated pentacyclic triterpenes, flavonoids and synthesized derivatives) were dissolved in ethanol and mixed until dissolved, applying sonication where necessary. Any

slightly turbid sample was centrifuged. To ensure quality control, reagents were prepared fresh on the day of analysis. The pH of phosphate buffer was rechecked prior to each assay.

The ferric reducing ability of the isolated pentacyclic triterpenes, flavonoid, and the synthesized derivatives was determined using the method described by Benzie and Strain (1996). Each sample (10 µL) was mixed with 300 µL FRAP reagent in a 96-well plate.

Samples were added in triplicates to different wells. Control wells contained 10 µl of control per well while ascorbic acid standard wells contained 10 µl of standard per well. The samples were incubated at 37 °C for 30 min, afterwards, the plates were read at a wavelength of 593 nm in a Multiskan Spektrum plate reader (Thermo Fisher Scientific). Ascorbic acid (AA) was used as standard. The results were expressed as µmol Ascorbic acid equivalents /100 g sample weights.

3.11.1.3 ABTS+ Radical Scavenging Activity Assay (TEAC)

The ABTS (2,2'-azino-di-3-ethylbenzthialozine sulphonate) radical cation scavenging assay can be used for total antioxidant status analysis. In this reaction, antioxidants scavenge ABTS radicals or interfere with the radical generation process.

Preparation of Solutions

In order to prepare 7mM solution of 2,2'-Azino-bis(3-ethylbenzothiazoline-6-sulfonic acid diammonium salt (ABTS), 0.0192 g of ABTS was weighed into a 15 mL screw cap tube and 5 mL of distilled water was added. The solution was mixed until dissolve. The ABTS solution was prepared fresh prior to assays.

Potassium-peroxodisulphate solution (140 mM) was prepared by weighing 0.1892 g of the salt ($K_2S_2O_8$) into a 15 mL screw cap tube and 5 mL of distilled water. The solution was mixed until dissolve. The solution was prepared fresh prior to assays.

Trolox (6-Hydrox-2,5,7,8-tetramethylchroman-2-carboxylic acid) standard stock solution (1.0 mM) was prepared as follows: 0.0125 g of Trolox was weighed into a 50 mL screw cap tube and 50 mL of ethanol was added. The solution was mixed until dissolved. The solution was prepared fresh prior to assays. To ensure quality control, the solution was diluted five times (5x) with ethanol. The diluted solution should give an absorbance of 0.650 ±0.015 at 289 nm.

A control solution (200µM) of Trolox (6-Hydroxy-2,5,7,8-tetramethylchroman-2-carboxylic acid) was prepared by weighing 0.0025 g of Trolox and mixing with 50 mL of ethanol in a 50 mL screw cap tube. The solution was prepared fresh prior to assays. To ensure quality control, the solution should give an absorbance of 0.650 ±0.015 at 289 nm.

The ABTS solution mix was prepared 24 hours prior to the assay. The solution was prepared by adding 88µl of the prepared potassium-peroxodisulphate solution and 5 mL of the ABTS solution in a 15 mL screw cap tube. The solution was mixed well and left in in the dark, at room temperature for 24 hours before use. The ABTS· solution was then diluted with ethanol (approximately 1 mL ABTS mix added to 20 mL ethanol) to give an absorbance of 1.50 at 734 nm.

Sample analysis

Samples (isolated pentacyclic triterpenes, flavonoids and synthesized derivatives) were dissolved in ethanol and mixed until dissolved, applying sonication where necessary. Any slightly turbid sample was centrifuged. To ensure quality control, reagents were prepared fresh on the day of analysis. The pH of phosphate buffer was rechecked prior to each assay.

The ABTS radical scavenging activity of the isolated pentacyclic triterpenes, flavonoids and synthesized derivatives was determined using the method described by Re et al. (1999). The dissolved samples were mixed with 300 µL ABTS· solution in a 96-well clear plate. The trolox standard wells contained 25 µL of standard solution per well while the control wells contained 25 µL of the control solutions. Sample wells contained 25 µL of samples in triplicates. The mixtures were incubated at room temperature for 30 mins. The recording of the plates was done in a Multiskan Spektrum plate reader (Thermo Fisher Scientific). Trolox was used as the standard. Results were expressed as µmol Trolox equivalents/ g sample weights.

3.11.2 Antimicrobial studies

The isolated and synthesized derivatives were screened to evaluate the in-vitro antimicrobial activity. All samples were tested against six pathogenic bacteria, comprising of three Gram-positive (*B. cereus, E. faecalis & S. aureus*) and three Gram-negative (*E. coli, K. pneumoniae & P. aeruginosa*) microbial strains.

The bacteria type, significance, drug resistance and optimal growth conditions for the strains that were used to determine the antimicrobial activity of the extracts are discussed as follows:

1. *Bacillus cereus,* Strain ATCC 10876 (genome sequenced)

B. cereus is a Gram-positive aerobic and facultative anaerobic bacterium found in multiple environments including soil, water, and food. *B. cereus* is a common cause of foodborne illness and have been implicated to cause food poisoning. The typical laboratory growth condition is in nutrient agar/broth incubated at 30°C.

2. *Enterococcus faecalis*, Strain ATCC 51299

E. faecalis is a Gram-positive bacterium responsible for several life-threatening nosocomial infections. It inhabits in the gastrointestinal tract of humans. *E. faecalis* is a low-level Vancomycin-resistant microbe, and resistant to Vancomycin (glycopeptide). It is sensitive to Teicoplanin (semisynthetic glycopeptide) and used in screening tests for high-level Aminoglycoside resistance. The typical laboratory growth condition is in brain heart infusion medium with 4 mcg/ml vancomycin and incubation at 37°C.

3. *Escherichia coli*, Strain ATCC 25922

E. coli (Gram-negative bacterium) is the major causative microorganism of food poisoning. E. coli is susceptible to Cephalexin (cephalosporin; class of β-lactam antibiotic), Cephaloglycin (1st generation cephalosporin; class of β-lactam antibiotic), Kanamycin (aminoglycoside), Cephaloridine (1st generation semisynthetic cephalosporin; class of β-lactam antibiotic), Cephalothin (1st generation cephalosporin; class of β-lactam antibiotic), Chloramphenicol, Colistin (polymyxin antibiotic – a polypeptide), Gentamicin (aminoglycoside), Nalidixic acid (quinolone antibiotic), Neomycin (aminoglycoside), and Tetracycline (polyketide antibiotic). The typical laboratory growth condition is in trypticase soy agar or broth with incubation done at 37°C.

***4. Klebsiella pneumoniae* subsp. *pneumoniae*, Strain ATCC 700603**

K. pneumoniae is a Gram-negative bacterium, and an important causative agent of nosocomial infections which produces beta-lactamase SHV-18. *K. pneumonia* is resistant to Ampicillin (β-lactam antibiotic), Aztreonam (synthetic monocyclic class of β-lactam antibiotic), Cefoxitin (2nd generation cephalosporin; class of β-lactam antibiotic), Cefpodoxime (3rd generation cephalosporin; class of β-lactam antibiotic), Ceftazidime (3rd generation cephalosporin; class of β-lactam antibiotic), Chloramphenicol, Piperacillin (class of β-lactam antibiotic), Tetracycline (polyketide antibiotic), and Ceftriaxone (3rd generation cephalosporin; class of β-lactam antibiotic).

K. pneumoniae has intermediate resistance for Cefotaxime (3rd generation cephalosporin; class of β-lactam antibiotic), Tobramycin (aminoglycoside), and Gentamicin (aminoglycoside). It is sensitive to Amoxicillin-clavulanate (class of β-lactam antibiotic and β-lactamase inhibitor combo), Cefepime (4th generation cephalosporin; β-lactam), Ciprofloxacin (2nd generation fluoroquinolone), Imipenem (carbapenem; β-lactam), Piperacillin-tazobactam (class of β-lactam antibiotic and β-lactamase inhibitor combo), and Trimethoprim-sulfamethoxazole (sulphonamide and additional synthetic antibiotic combo). The typical laboratory growth condition is in nutrient agar/broth, incubated at 37 °C.

***5. Pseudomonas aeruginosa*, Strain ATCC 27853**

P. aeruginosa (Gram-negative bacterium) is an opportunistic pathogen and causative agent of nosocomial infections. The optimum growth condition is in Trypticase soy agar or broth with incubation done at 37 °C.

***6. Staphylococcus aureus* subsp. *aureus*, Strain ATCC 33591**

S. aureus is a Gram-positive bacterium, and a common cause of nosocomial infections. It is also responsible for causing a range of illnesses. *S. aureus* is Methicillin resistant (narrow spectrum class of β-lactam antibiotic) and produces beta-lactamase. The typical laboratory growth condition is in nutrient agar/broth, incubated at 37 °C.

3.11.2.1 Preparation of the test strains

The microbial strains were inoculated into 5 mL of the appropriate growth media and incubated at the strains' optimum growth temperature for 24 hours. The optical density (OD) of the cultures was measured at 600nm and the culture OD adjusted to 0.5 prior to use in the assays.

3.11.2.2 Bioautography assay

This method afford rapid assessment of the antimicrobial activities of target compounds. The method reported by Rufaro Mabande (2018) was adapted with slight modifications. Briefly, 10 µg of sample (compound) was applied (in duplicate) onto silica thin layer chromatography plates. Sterile absorbent cotton wool was saturated with the test strains and applied to the surface of the TLC plate to allow for the transfer of the test strain. The TLC plates were placed in a plastic container containing moist paper towel and incubated at the test strains' optimal growth temperatures for 24 hours. The TLC plates were treated with the tetrazolium salt, MTT (0.25%, w/v in phosphate buffered saline), re-incubated for 3 - 6 h and evaluated for the appearance of purple spots (indicative of growth) or white bands (indicative of inhibition of microbial growth).

3.11.2.3 Broth dilution assays

The samples (1000 µg/ml stock solutions) were diluted in DMSO to give a final concentration of 500 µg/ml for each sample, which was used to prepare the following dilution set up:

Controls

Negative control: 160µl culture + 20µl DMSO

Positive control: 160µl culture + 20µl vancomycin (gram +ve) or ampicillin (for gram –ve)

Sterile control: 50µl broth + 80µl sterile distilled water + 50µl DMSO

Sample setup: 20µl sample + 160µl culture (giving a final concentration of 55.6 µg/ml)

The samples were setup in triplicates. The methods of European Committee for Antimicrobial Susceptibility Testing (EUCAST, 2003) was adapted. Microdilutions of each bacteria and samples were prepared in 96 well sterilized microtitre plates. The test strains were grown in optimal growth media as indicated previously. After 24 hours of growth, the OD600 of the culture was determined. The OD600 was adjusted to 0.8 for this experiment.

The samples and cultures were dispensed into microtiter plates as per setup (see figure below) and the plates were incubated for 24 hours at the optimal growth temperature of the test strains. 20 µl of 0.25% (w/v) MTT in PBS was added to each well and the plates were incubated at the optimal growth temperature of the test strains for 3 hours. Then, 100 µl DMSO was added to each well and incubated at room temperature for 4 hours. The OD of the samples were determined at 570 nm. The visual detection of turbidity in the wells as compared with the negative and positive controls indicated that there was no inhibition. Negative and positive controls were tested in parallel in all experiments. To rule out the effect of DMSO on the development of the studied microorganisms, all experiments were compared with control. The MIC is considered to be where all colour is lost as compared to the control containing the DMSO equivalent.

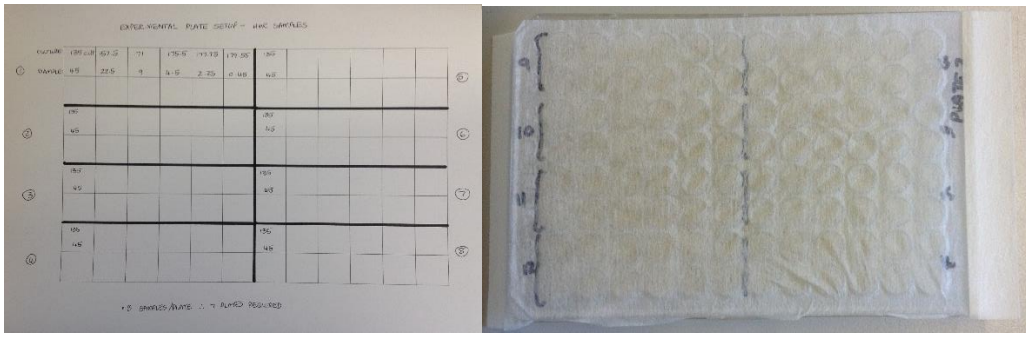

Figure 3.8: Layout of 96-well setup for antibacterial activity determination

Figure 3.9: Representative 96-well plate during broth dilution assays

3.12 Chapter Summary

The list of research materials including chemicals and plant materials have been provided. The different extraction procedures as well as information on synthesis of derivatives were given. The methodology for biological evaluations, which include antioxidant and antimicrobial assays have shown the steps required for the analysis of bioactivity of isolated compounds and synthesized derivatives. The results and detailed discussions on extraction of starting materials and their characterization follows in the next Chapter.

CHAPTER FOUR
RESULTS AND DISCUSSIONS

4.0 Chapter Introduction

The isolated compounds and synthesized derivatives derived from previous chapter are characterized in the following sections. This followed successful extraction of target compounds including triterpenes (BA (**4**), OA (**5**), UA (**6**)) and one flavonoid (6-methyltectochrysin), and the application of these starting materials to prepare semi-synthetic hybrid conjugate products.

4.1 Characterisation of natural product isolates

4.1.1 Characterisation of betulinic acid isolated from *Tectona grandis*

Betulinic acid, BA (**4**) was extracted from the stem bark (250 g) of Teak tree. The ethyl acetate extract (yellowish solution) was concentrated *in vacuo*, producing 4.8 g of a yellowish-white powdery material. Chromatographed product weighed 2.2 g, which was then recrystallized from methanol to afford a white amorphous powdery product (1.6 g, 0.64% yield). The TLC analysis of the product revealed one (light brown) visible spot (R_f = 0.56, hexane/ ethyl acetate 8:2). The product had a melting point of 315.6 °C, in agreement with literature values of 315 - 318 °C (Bhakuni et al., 1971).

Isolation of BA (**4**) from plants has been reported several times for decades with reports supporting economical scale production. Bhakuni et al. (1971) obtained pure BA (**4**) from the leaves and stem of *Diospyros buxifolia* (Blume) Hiern plant by subjecting an extracted crude material to recrystallization. According to the authors and other literature works, BA (**4**) often co-exist with its derivatives such as betulin, the acetate or the methyl ester acetate in same plant.

The FT-IR data was obtained by scanning the product over a frequency of 4000 – 400 cm^{-1}. The IR spectrum (see Appendix A - Figure 1.1) data depicting available functional moieties are as follows: IR (ν_{max} cm^{-1}): 3466, 2941, 2868, 1685, 1644, 1450, 1376, 1248, 1042.

FT-IR analysis revealed absorption bands at 3466 cm^{-1} and 1685 cm^{-1} representing hydroxyl (-OH) and carbonyl (C=O) functionalities respectively. The peaks at 2941 cm^{-1} and 2868 cm^{-1} are indicative of –C-H stretch. The C=C alkene functionality is assigned to the peak at 1644 cm^{-1} while presence of C-OH stretch is indicated by peak at 1042 cm^{-1}.

The mass spectral analysis (ESI-MS [M-H]-) for the compound gave an m/z 455.353 (calc. 456.7003); corresponding to the molecular formula $C_{30}H_{48}O_3$. The NMR data (see Appendix B – Figure 2.1) is presented as follows:

^{1}H NMR (600 MHz, DMSO-d_6) δ ppm: 0.64 (3H, *s*) 0.75 (3H, *s*) 0.85 (3H, *s*) 0.86 (3H, *s*) 0.92 (3H, *s*) 1.63 (3H, *s*) 4.55 (1H, *s*) 4.67 (1H, *s*).

The ^{1}H NMR spectrum revealed terminal methylene (olefinic) protons at δ 4.67 (Hb-29) and δ 4.55 (Ha-29). The allylic methyl group protons observed at δ 1.63 was in agreement with NMR data reported by Haque et al. (2013). Five tertiary methyl (-CH_3) peaks were found at δ 0.64, δ 0.75, δ 0.85, δ 0.86, and δ 0.92, conforming with Raza et al., 2015. The product was identified as 3-hydroxy-lup-20(29)-en-28-oic acid (betulinic acid, BA) (**4**).

^{13}C-NMR (400 MHz, DMSO-d_6) δ ppm: 14.81 (C27) 16.17 (C26) 16.22 (C25) 16.37 (C24) 18.39 (C6) 19.35 (C30) 20.89 (C11) 25.51 (C12) 27.54 (C2) 28.52 (C23) 29.63 (C21) 30.53 (C15) 32.15 (C16) 34.36 (C7) 36.78 (C10) 37.14 (C22) 38.03 (C18) 38.70 (C1) 38.91 (C4) 40.68 (C8) 42.42 (C14) 47.05 (C19) 48.97 (C13) 50.37 (C9) 55.33 (C5) 55.85 (C17) 77.26 (C3) 110.06 (C29) 150.73 (C20) 177.69 (C28)

The ^{13}C-NMR spectrum (Appendix B – Figure 2.2) showed 30 carbons. The data obtained is in agreement with literature values (Raza et al., 2015) as shown in Table 4.1.

Table 4.1: Comparison of ^{13}C-NMR data of isolated BA (**4**) with literature values.

	BA Product (**4**)	Literature
1	38.70	38.68
2	27.54	27.77
3	77.26	78.75
4	38.91	38.71
5	55.33	55.30
6	18.39	18.20
7	34.36	34.25
8	40.68	40.59
9	50.37	50.48
10	36.78	37.50
11	20.89	20.80
12	25.51	26.91
13	48.97	49.14
14	42.42	42.35
15	30.53	30.50
16	32.15	32.18
17	55.85	56.13
18	38.03	38.68
19	47.05	46.90
20	150.73	150.67
21	29.63	29.50
22	37.14	37.2
23	28.52	29.58
24	16.37	15.96
25	16.22	15.76
26	16.17	15.21
27	14.81	14.53
28	177.69	178.98
29	110.06	109.33
30	19.35	19.16

4.1.2 Characterisation of oleanolic acid and maslinic acid isolated from *Syzygium aromaticum*

OA (**5**) was isolated from dichloromethane extract of dried clove buds. The processed filtrate produced an oily crude extract weighing (73.03 g) which showed multiple spots on TLC plates. The product was washed with hexane, initiating the precipitation of a solid material that was filtered under suction and dried. The solid material (11.72 g, 1.2% yield) was suspected to contain a mixture of triterpenes after TLC analysis (2 spots) based on comparison with standards. The R_f values of the compounds in the mixture (0.67 and 0.16) was a match with standard samples of oleanolic acid (**5**) and maslinic acid (**11**), respectively.

Other methods were reported for the direct extraction of OA (**5**) from clove buds by removal of oil from the clove buds using steam distillation prior to soxhlet extraction procedure (Wicht, 2007). Different methods may lead to varying yield output or recovered OA (**5**).

A portion of the product (3.0 g) was purified using silica gel column chromatography. Similar fractions were combined to give 0.9 g of OA (**5**), 0.35 g of MA (**11**), and a mixture of OA & MA (1.37 g) that was difficult to separate. Alternative technique for achieving separation was by acetylating the mixture, and then using column chromatography for separation. The products were whitish powder in appearance.

The melting point for OA was 311 °C (literature: 310 °C), while the melting point of MA (**11**) was 272 °C (literature: 269 – 271 °C). These agreed with literature data (Ramirez-Espinosa et al., 2014; Xu et al., 2013).

The FT-IR (ν_{max} cm^{-1}) data: 3416, 2939, 2869, 1689, 1461, 1387, 1271, 1182, 1032, 997.

The FT-IR spectrum (Appendix A - Figure 1.2) of the product (suspected OA) consisted of hydroxyl (-OH) functionality at 3416 cm^{-1}, and a sharp prominent peak at 1689 cm^{-1} is assigned to carbonyl (C=O) groups. The absorption band at 2939 cm^{-1} and 2869 cm^{-1} are indicative of C-H stretch in CH_3 and CH_2 groups. The peak at 1461 cm^{-1} represents C-H of methyl (CH_3) groups while the peak at 1032 cm^{-1}, represents C-OH stretch of secondary alcohol groups.

The mass spectral analysis (ESI-MS [M-H]-) for the compound gave m/z 455.3252 (calc. 456.7003); corresponding to molecular formula $C_{30}H_{48}O_3$.

The NMR data generated (Appendix B – Figure 2.3) is presented as follows:

^{1}H NMR (600 MHz, $CDCl_3$) δ ppm: 0.77 (3H, *s*) 0.79 (3H, *s*) 0.80 (3H, *s*) 0.84 (3H, *s*) 0.90 (3H, *s*) 0.95 (3H, *s*) 1.03 (3H, *s*) 2.83 (1H, br *s*) 3.23 (1H, br *s*) 5.28 (1H, br *s*)

The methyl (21H, -CH_3 x 7) protons were represented at δ 0.77, 0.79, 0.80, 0.84, 0.90, 0.95 and 1.03. The olefinic H-12 was observed at δ 5.28 [lit. 5.26, (Ragasa et al., 2014)].

The ^{1}H-NMR data was compared with relevant literature (Table 4.2) and the structure of isolated product was established as 3- hydroxyolean-12-en-28-oic acid (oleanolic acid, OA) (**5**).

Table 4.2: Comparison of ^{1}H-NMR data of isolated OA (**5**) with published data.

OA Product **(5**)	Literature (Ragasa et al., 2014)
0.77 (3H, *s*)	0.73 (3H, s, CH_3-24)
0.79 (3H, *s*)	0.75 (3H, s, CH_3-26)
0.80 (3H, *s*)	0.88 (3H, s, CH_3-30)
0.84 (3H, *s*)	0.89 (3H, s, CH_3-25)
0.90 (3H, *s*)	0.91 (3H, s, CH_3-29)
0.95 (3H, *s*)	0.96 (3H, s, CH_3-23)
1.03 (3H, *s*)	1.11 (3H, s, CH_3-27)
2.83 (1H, br *s*)	2.81 (dd, J = 4.2, 13.8 Hz, H-18)
3.23 (1H, br *s*)	3.20 (dd, J = 4.2, 11.4 Hz, H-3)
5.28 (1H, br *s*)	5.26 (t, J = 3.6 Hz, H-12)

A second product was co-extracted with the OA (**5**) from the clove buds. The product (white powder) (MA (**11**)) has a melting point of 272 °C [lit. 269 – 271 °C (Xu et al., 2013)]. The FT-IR data was obtained by scanning the product over a frequency of 4000 – 400 cm^{-1}. The FTIR spectrum (Appendix A – Figure 1.3) data indicated the following peaks:

IR (ν_{max} cm^{-1}): 3376, 2931, 2864, 2665, 1689, 1612, 1519, 1457, 1366, 1269, 1195, 1051, 1032.

The FT-IR spectrum (Appendix A – Figure 1.3) of the product obtained (MA) (**11**) revealed a broad absorption band at 3376 cm^{-1}, indicating presence of hydroxyl (-OH) functionality.

The –OH absorption peak was observed to be broader than the –OH peak found in OA (**5**). The prominent peak at 1689 cm^{-1} is assigned to carbonyl (C=O) groups. The absorption band at 2931 cm^{-1} and 2864 cm^{-1} are indicative of C-H stretch in CH_3 and CH_2 groups. The peak at 1467 cm^{-1} represents C-H of methyl (CH_3) groups while the peak at 1032 and 1051 cm^{-1} represents C-OH stretch of secondary alcohol groups.

The mass spectral analysis (ESI-MS [M-H]-) for the compound gave an m/z 471.206 (calc. 472.36); corresponding to molecular formula $C_{30}H_{48}O_4$.

The ^{1}H NMR spectrum data (Appendix B – Figure 2.4) is summarised as follows:

^{1}H NMR (600 MHz, DMSO-d_6) δ ppm: 0.70 (6H, *d, J* = 2.34 Hz) 0.87 (6H, *s*) 0.89 (3H, *s*) 0.91 (3H, *s*) 1.08 (3H, *s*) 2.74 (1H, *d*, *J* = 9.37 Hz) 3.73 (1H, d, J = 10.54 Hz) 5.16 (1H, br *t*, *J* = 3.51 Hz)

The NMR data revealed olefinic (H-12) proton at δ 5.16 while the upfield region of the 1H NMR showed seven methyl signals at δ 0.70 (6H, CH_3 x 2), δ 0.87 (6H, CH_3 x 2), δ 0.89, δ 0.91 and δ 1.08. The H-2 and H-3 protons were signalled at δ 2.74 and δ 3.73, respectively [lit. 2.91 (1H, *d, J* = 10.0 Hz, H-3), 3.62 (1H, *m*, H-2), (Woo et al., 2014)]. These were further verified with the data by (Wang et al., 2015), and the product was identified as 2α,3β-dihydroxyolean-12-en-28-oic acid (maslinic acid, MA) (**11**).

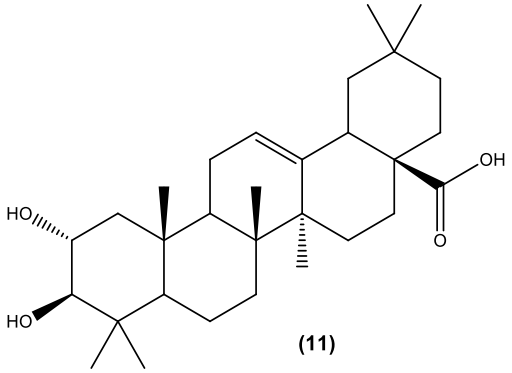

(11)

4.1.3 Characterisation of ursolic acid isolated from *Mimusops caffra*

UA (**6**) was extracted from dried leaves (500 g) of *Mimusops caffra* using alcoholic sodium hydroxide. The dried extract so obtained (greenish white powder, 24.20 g, 0.938%) was chromatographed using silica gel. Fractions that showed one similar spot after TLC analysis (pinkish spot) were combined and weighed after removal of solvent to give 4.69 g of whitish powdery material. The product was compared against known standards of UA using TLC analysis, revealing one (pinkish) spot upon visualization. (R_f = 0.61, hexane/ethyl acetate 8:2). The product has a melting point of 279 °C (literature: 279 - 283 °C, Simelane et al., 2013).

IR (ν_{max} cm^{-1}): 3416, 2926, 2871, 1688, 1456, 1388, 1377, 1032, 997.

The FT-IR spectrum (Appendix A – Figure 1.4) showed absorption bands at 3416 cm^{-1} and 1688 cm^{-1} indicating the presence of hydroxyl (-OH) and carbonyl (C=O) functional groups, respectively. The bands at 1388 cm^{-1} and 1377 cm^{-1} are due to a gem dimethyl group. The peaks at 2966 cm^{-1} and 2871 cm^{-1} represents –C-H stretch. The C=C alkene functionality is assigned to the peak at 1688 cm^{-1} while presence of C-OH stretch is indicated by peak at 1032 cm^{-1}. The mass spectral analysis (ESI-MS [M-H]-) for the compound was m/z 455.353 (calc. 456.7003); corresponding to the molecular formula $C_{30}H_{48}O_3$.

^{1}H NMR (600 MHz, DMSO-d_6) δ ppm: 0.67 (3H, *s*) 0.74 (3H, *s*) 0.81 (3H, *d, J*=12 Hz) 0.86 (3H, *s*) 0.88 (3H, *s*) 0.90 (3H, *s*) 1.03 (3H, *s*) 2.09 (1H, *d*, *J* = 11.72 Hz) 3.00 (1H, br *d*, J = 5.86 Hz) 5.12 (1H, *br s*)

The ^{1}H NMR spectrum (Appendix B – Figure 2.5) revealed one olefinic proton at δ 5.12, and seven methyl (-CH_3) at δ 0.67, δ 0.74, δ 0.81, δ 0.86, δ 0.88, δ 0.90 and δ 1.03, respectively.

The spectra data obtained agreed with literature report (Zacchigna et al., 2014; Labib et al., 2016), and shown in Table 4.3. The isolated product was identified as 3β- hydroxy-urs-12-en-28-oic acid (ursolic acid, UA) (**6**).

Table 4.3: Comparison of ^{1}H-NMR of isolated UA (**6**) with published data

#	UA (**6**)	Labib et al. (2016)
H-3	3.00 (1H, br *d*, J = 5.86 Hz)	3.17 (1H, *br s*)
H-12	5.12 (1H, *br s*)	5.12 (1H, *br s*)
H-18	2.09 (1H, br d, J = 11.72 Hz)	2.10 (1H, *d, J*=11.0 Hz)
H-23	0.67 (3H, *s*)	0.67 (3H, *s*, CH_3)
H-24	0.88 (3H, *s*)	0.89 (3H, *s*, CH_3)
H-25	0.86 (3H, *s*)	0.86 (3H, *s*, CH_3)
H-26	0.74 (3H, *s*)	0.74 (3H, *s*, CH_3)
H-27	1.03 (3H, *s*)	1.03 (3H, *s*, CH_3)
H-29	0.81 (3H, *d, J*=12 Hz)	0.81 (3H, *d, J*=6.4 Hz)
H-30	0.90 (3H, *s*)	0.90 (3H, *d, J*=6.4 Hz)

4.1.4 Characterisation of flavonoid isolated from *Leptospermum petersonii*

TLC revealed material contain two products with R_f values of 0.72 and 0.44 (hexane: ethyl acetate 8:2) respectively, and the suspected flavonoid component having a higher R_f.

A portion of the yellowish powdery material obtained (0.6 g) was subjected to silica gel column chromatography using a gradient elution (hexane: ethyl acetate) starting with 9:1 v/v and subsequent 5% ethyl acetate increment. Similar fractions obtained from the column were combined, and the removal of solvent gave a yellowish product (235 mg, one spot on TLC) corresponding to a known flavonoid compound while other fractions obtained were (suspected to be) mixtures of flavonoid and triterpenes. Haberlein and Tschiersch (1994) had reported on the phytochemistry of another Leptospermum specie, (*L. scoparium*). It was made known that the dichloromethane extracts contained triterpenoids and flavonoids. Leptospermum species have been utilised in traditional medicines as sedatives, treatment of respiratory infections and diarrhoea (Brooker et al., 1989).

The (flavonoid) product had a melting point of 214 °C (literature: 212 - 214 °C, Mayer, 1990). The FT-IR data of samples of the product was obtained by scanning the product over a frequency of 4000 – 400 cm^{-1}. The corresponding IR absorption results are shown as follows:

IR (ν_{max} cm^{-1}): 3065, 3004, 2922, 2852, 1660, 1611, 1590, 1493, 1450, 1381, 1333, 1133.

The IR data obtained from the FTIR spectrum (Appendix A – Figure 1.5) showed strong prominent carbonyl C=O absorption at 1660 cm^{-1}. The absorption bands at 1590 depicts aromatic rings, while 3004 cm^{-1} represents allylic C=CH stretch. The absorption peaks at 2922 cm^{-1} and 2852 cm^{-1} indicated CH groups. The mass spectral analysis (ESI-MS [M-H]-) for the compound was m/z 281.098 (calc. 282.29); corresponding to the molecular formula $C_{17}H_{14}O_4$.

^{1}H NMR (600 MHz, $CDCl_3$) δ ppm: 1.23 (1H, *s*) 2.27 (3H, *s*) 3.88 (3H, *s*) 6.38 (1H, *s*) 6.64 (1H, *s*) 7.51 (3H, *m*) 7.88 (2H, *m*)

The ^{1}H NMR spectrum (Appendix B – Figure 2.6) revealed aromatic protons at 7.90 (2H) and 7.54 (3H). The olefinic protons were shown at 6.64 (H-3) and at 6.36 (H-8). The 7-OMe and 6- Me protons were assigned at δ 3.88 and δ 2.27, respectively [lit. 3.96 (7-OMe), 2.13 (6-Me) (Mayer, 1990)]. The ^{13}C data is as follows:

^{13}C NMR (101 MHz, $CDCl_3$) δ ppm 7.74 56.03 95.00 104.00 105.09 105.21 126.26 129.13 131.72 131.78 154.53 160.26 163.27 163.78 183.03

The ^{13}C NMR NMR (Appendix B - Figure 2.7) was assigned, and compared with previous work reported in literature for the same compound, as shown in Table 4.4. The positions of the hydroxyl, methyl and methoxy is expected to have shielding effects and affects the frequencies observed in the NMR spectrum. These data were used, in part, to identify the isolated product as 5-hydroxy-7-methoxy-6-methylflavone (**19**) (6- methyltectochrysin).

Table 4.4: ^{1}H-NMR of 5-hydroxy-7-methoxy-6-methylflavone (**19**)

# position	5-hydroxy-7-methoxy-6-methylflavone (**19**)	Mayer, (1990)	De Carvalho et al. (1996)
2	163.27	163.4	162.0
3	105.09	106.0	108.3
4	183.03	182.2	176.6
5	160.26	158.3	158.3
6	105.21	109.1	105.9
7	163.78	163.4	158.3
8	95.00	89.4	108.3
9	154.53	155.9	150.4
10	104.00	105.4	105.9
1’	131.72	131.4	131.4
2’ , 6’	126.26	126.2	126.1
3’ , 5’	129.13	128.9	128.9
4’	131.78	131.6	131.3
7-OCH_3	56.03	55.9	55.9
6- Me	7.74	7.4	7.5

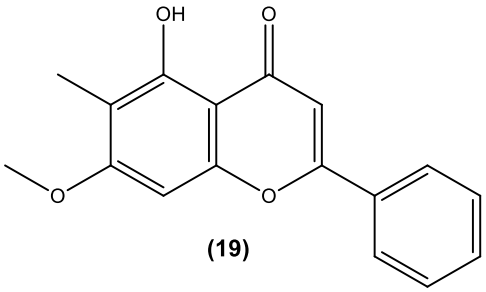

(19)

4.1.5 Extraction of triterpenes from *Melaleuca salicina*

The basified alcoholic extract of *M. salicina* leaves was acidified, and the resulting precipitated product was filtered, and dried. The crude extract yield obtained from the leaves weighed 26 g (5.2% yield). The methanolic extract obtained from the fruits yielded an orange-yellow powdery material (41 g, 5.9% yield). Part of the samples were dissolved in methanol for TLC analysis. TLC development showed two spots. Co-spotting with known standard samples of pentacyclic triterpenes (UA (**6**), BA (**4**), 3-*O*-acetyl UA (**22**) and 3-*O*-acetyl BA (**20**)) was done for the extracts from the leaves and the fruits of *Melaleuca salicina*. A variation in composition was observed. The leaves showed pinkish and brownish spots, suspected to contain UA (**6**) and BA (**4**) while the fruits contained a mixture of triterpenes (UA (**6**), BA (**4**), 3-*O*-acetyl UA (**22**) and 3-*O*-acetyl BA (**20**)). This showed the formation of naturally occurring esterified forms of the triterpenes in nature. This further iterate the complexity of natural products and the level of complex chemistry occurring in natural environment. Recrystallization of the products did not separate (resolve) the mixtures. Further separation and purification of the products, and confirmation using spectroscopic analysis was not included in this work. The desired quantities of triterpenes required for semi-synthesis work was extracted in other plants as discussed in previous sections. The extraction of triterpenes from *M. salicina* was carried out for exploratory purposes to test for the presence of target triterpene compounds.

4.1.6 Extraction of triterpenes from *Lavandula angustifolia*

The dried methanolic extract of *L. angustifolia* was washed with hexane to afford a greenish-white product (0.88 g, 1.76%). TLC analysis of the filtrate revealed 2 pinkish spots. Immediate co-spotting with available standard samples of pentacyclic triterpenes showed one of the spots as UA (**6**) while the other correlated with 3-*O*-acetyl UA (**22**). The filtrate was concentrated *in-vacuo* and a greenish powdery material was obtained. The product was boiled in methanol. After cooling, crystals of products were filtered and analysed by TLC (hexane: ethyl acetate, 8:2). Two spots were observed, showing R_f values of 0.54 and 0.86, respectively. The filtered product was brownish white (0.74 g) containing a mixture of triterpenes. The disappearance of greenish colour suggests removal of chlorophyll content after attempted recrystallization. Further separation and purification of the products, and confirmation using spectroscopic analysis was not included in this work. The extraction of triterpenes from Lavender was carried out for exploratory purposes to confirm presence of target triterpene compounds.

4.2 Characterization of semi-synthetic derivatives

Grouping of derivatives

The derivatives were grouped and coded for easy reference. These include Group I: substituted compounds (acetylated, methylated), Group II: pentacyclic triterpenenoyl anhydride -linked conjugated derivatives, Group III: pentacyclic triterpenoyl ester -linked derivatives, Group IV: calixarene - anchored triterpene derivatives, and Group V: flavonoid - triterpene conjugates.

4.2.1 Group I (Substituted derivatives)

This group of pentacyclic triterpene derivatives were synthesized by substituting the hydroxyl group at C3 position (acetylation), or by transforming the carboxylic acid functionality at the C28 position into a methyl ester group (esterification). Apart from being used in comparative studies to assess level of alterations in biological activities relative to the activities exhibited by the hybrid-conjugated derivatives, the acetylated and methylated compounds were used as starting materials to make the latter derivatives related to this work.

4.2.1.1 3-*O*-Acetylbetulinic acid

White crystalline compound, 0.61 g, (61%) was obtained. TLC analysis of the product showed one pinkish spot (R_f = 0.80, hexane/ ethyl acetate 8:2). The compound had a melting point of 293 °C (literature: 289 °C, Raza et al., 2015); (ESI-MS [M-H]-) m/z 497.3710 (calc. 498.74) corresponding to molecular formula $C_{32}H_{50}O_4$. It was further identified as 3-*O*-acetylbetulinic acid (**20**).

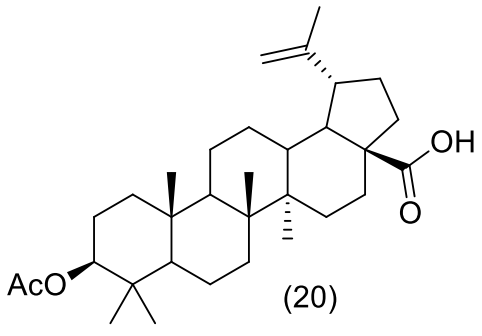

(20)

FT-IR (ν_{max} cm^{-1}): 3073, 2942, 2870, 1734, 1693, 1450, 1367, 1245, 1195, 1031, 980, 883.

The FT-IR data (Appendix A – Figure 1.6) of the product was compared with FT-IR data obtained for the starting material (BA, (**4**)) for any structural changes.

The major differences include absence of C3 hydroxyl band (found in BA (**4**) at 3466 cm^{-1}); substituted with the – OAc group. The peak at 1734 cm^{-1} (C=O of ester) was more prominent in the acetylated product, and peak at 1245 cm^{-1} attributed to (C - O) functionality is more prominent. The lup-20(29)-ene vinylidene group (=CH_2) absorption peaks were attributed to signals at 2942, 1693 and 883 cm^{-1} (Mbaze et al., 2007).

The ^{1}H NMR data (Appendix B – Figure 2.10) is as follows:

^{1}H NMR (600 MHz, $CDCl_3$) δ ppm: 0.80 (3H, *s*) 0.82 (6H, *d, J* = 4.69 Hz) 0.90 (3H, *s*) 0.94 (3H, *s*) 1.66 (3H, *s*) 2.01 (3H, *s*) 2.15 (1H, *td*, *J*=12.30, 3.51 Hz) 2.24 (1H, *dt*, *J*=12.89, 2.93 Hz) 4.44 (1H, *dd*, *J* = 10.84, 5.57 Hz) 4.58 (1H, *s*) 4.71 (1H, *s*)

The acetylated protons were due at δ 2.01. Other methyl protons (18H) are shown at 0.80, 0.82 (6H, CH_3 x 2), 0.90, 0.94, and 1.66. Other assignments are for H-18 olefinic proton at 2.15, and 4.71 (H_a-29), 4.58 (H_b-29), respectively [lit. 4.48 (1H, *dd*, *J* = 5.5, 10.5 Hz, H-3), 4.62 (1H, *br s,* H_b-29) 4.75 (1H, *br s,* H_a-29) (Ahmad et al., 2010)].

^{13}C NMR (151 MHz, $CDCl_3$) δ ppm: 14.62 (C27) 16.00 (C24) 16.13 (C25) 16.42 (C26) 18.12 (C2) 19.31 (C30) 20.81 (C6) 21.27 (C20) 23.65 (C11) 25.40 (C12) 27.91 (C23) 29.66 (C21) 30.53 (C15) 32.12 (C16) 34.19 (C7) 37.01 (C22) 37.09 (C10) 37.76 (C4) 38.34 (C13) 38.39 (C1) 40.65 (C8) 42.38 (C14) 46.90 (C19) 49.23 (C18) 50.35 (C9) 55.38 (C5) 56.36 (C17) 80.91 (C3) 109.70 (C29) 150.31 (C20) 171.02 (C=O ester) 182.11 (C28 COOH)

The ^{13}C NMR spectrum is shown in (Appendix B – Figure 2.11). The data for the acetylated product were compared with those from literature, and found to be in agreement [lit. 81.20 (C3), 171.31 (C1', C=O ester), 182.56 (C28, COOH), respectively (Ahmad et al., 2010)].

4.2.1.2 3-*O*-Acetyloleanolic acid

Final product weighed 1.61 g (81% yield). TLC analysis of the product showed one deep purple spot (R_f = 0.77, hexane/ ethyl acetate 8:2). The white compound obtained had a melting point of 265 °C (literature: 265 - 266 °C, Rali et al., 2016); (ESI-MS [M-H]-) m/z 497.364 (calc. 498.371) corresponding to molecular formula $C_{32}H_{50}O_4$, and further identified by the spectral properties as 3-*O*-acetyloleanolic acid (**21**).

FT-IR (ν_{max} cm^{-1}): 3197, 2942, 2877, 1722, 1700, 1448, 1369, 1249, 1180, 1027, 985

The FT-IR spectrum (Appendix A – Figure 1.7) of the product revealed absorption at 3197 (-OH, COOH), and prominent peaks at 1722 (-CO of carboxylic acid) and 1700 (-C=O of acetyl). These C=O functional group bands are more prominent in (**21**) relative to the starting material (oleanolic acid (**5**)), suggestive of successful acetylation reaction. The –C = C stretch was linked to absorption at 1448. A strong sharp peak at 1249 was attributed to carbonyl (C-O) group. The NMR data (Appendix B – Figure 2.12) is presented as follows:

^{1}H NMR (600 MHz, $CDCl_3$) δ ppm: 0.71 (3H, *s*) 0.81 (3H, *s*) 0.83 (3H, *s*) 0.87 (3H, *s*) 0.90 (6H, *d*, *J* = 5.86 Hz) 1.09 (3H, *s*) 2.04 (3H, *s*) 2.79 (1H,*br dd*, *J* = 13.47, 4.10 Hz) 4.46 (1H, *dd*, *J* = 9.37, 6.44 Hz) 5.24 (1H, *t*, *J* = 3.51 Hz) 8.78 (1H, *br s*)

Methyl groups were identified (3H) each at δ 0.71, δ 0.81, δ 0.83, δ 0.87, δ 0.90 (6H, CH_3 x 2) δ 1.09 and δ 2.04 (OAc). A deshielding effect (resulting from anisotropic field of acetate group) was observed for the H-3 with a shift at 4.46. The H-12 and H-18 protons were assigned at δ 5.24 and δ 2.79, respectively. NMR data was confirmed with literature [data: methine protons at 4.45 (C3) 5.25 (C12) and 2.34 (C18), respectively, (Rali, et al., 2016)].

^{13}C NMR (101 MHz, CHLOROFORM-*d*) δ ppm: 15.36 16.64 17.14 18.15 21.29 22.85 23.56 25.87 27.64 28.01 30.64 32.41 33.03 33.76 36.96 37.66 38.03 39.25 40.91 41.53 45.81 46.51 47.52 55.26 80.89 122.50 127.07 141.36 143.59 145.50 171.01 183.71

From the ^{13}C analysis (Appendix B – Figure 2.13), was revealed 32 carbon signals identified for the 3-acetyl-OA product including the reference peaks for C3 (80.89), C=O (171.01) and CH_3 of acetoxy –$OCOCH_3$ (21.29), and were in agreement with literature data [lit. C3 (80.93), C=O (171.05), OAc (21.31) (Rali, et al., 2016)].

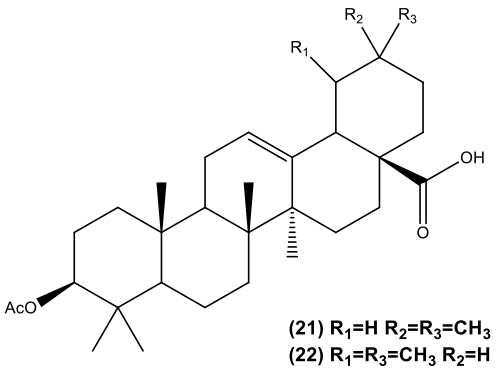

(21) R_1=H R_2=R_3=CH_3
(22) R_1=R_3=CH_3 R_2=H

4.2.1.3 3-*O*-Acetylursolic acid

The resulting white powdery product (1.9 g, 86%), had an R_f 0.76 (hexane/ ethyl acetate 8:2), melting point 198 °C (lit. 193 °C, Basir et al. 2014); (ESI-MS [M-H]-) m/z 497.293 (calc. 498.4) corresponding to molecular formula $C_{32}H_{50}O_4$, and further identified by spectral analysis as 3β- acetylursolic acid (**22**).

FT-IR (ν_{max} cm^{-1}): 2926, 2873, 1735, 1692, 1457, 1369, 1244, 1031, 1006, 985, 770, 662, 560. The FT-IR spectrum (Appendix A – Figure 1.8) revealed absorption at 1735 (-CO of carboxylic acid) and 1692 (-C=O of acetyl). The –C = C stretch was linked to absorption at 1457, and aliphatic C – H at 2926. A strong sharp peak at 1244 was attributed to carbonyl (C-O) group.

The parent pentacyclic triterpene, UA (**6**), has a broad –OH (C-3) absorption band at 3416, however, the absorption band was absent in the acetylated product due to conversion of –OH to –OAc.

^{1}H NMR (600 MHz, $CDCl_3$) δ ppm 0.74 (3H, *s*) 0.82 (3H, *s*) 0.83 (3H, *br s*) 0.84 (3H, *s*) 0.91 (3H, *s*) 0.93 (3H, *d*, *J* = 2.93 Hz) 1.04 (3H, *s*) 2.01 (3H, *s*) 2.15 (1H, *d*, *J* = 11.13 Hz) 4.47 (1H, *dd*, *J* = 10.54, 5.86 Hz) 5.20 (1H, *t*, *J* = 3.51 Hz) (Appendix B – Figure 2.14).

From ^{1}H NMR spectrum was identified eight methyl groups (24H) and olefinic H-12 proton at δ 5.20. The spectrum differs from the starting material with the prominent singlet for CH_3COO protons at δ 2.01. The H-3 proton also differs, as the effect of acetylation caused the de-shielded protons to be observed at δ 4.47. The splitting as doublet of doublet may also resulted from coupling to other two non-chemically equivalent protons due to acetylation. The data generated agreed with literature (Basir et al., 2014), and the product was identified as 3-acetylursolic acid (**22**).

4.2.1.4 Methyl betulinate

The white crystalline product (0.1456 g, 36%), had a melting point 264 °C (lit. 262 – 264 °C, Anjaneyulu & Prasad, 1983), (ESI-MS [M-H]-) m/z 469.74 (calc. 470.38) corresponding to molecular formula $C_{31}H_{50}O_3$, which might be a betulinic acid methyl ester (**23**).

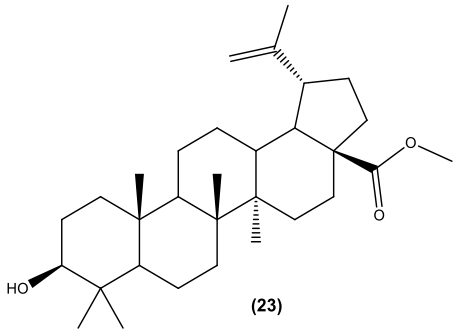

(23)

FT-IR information (Appendix A – Figure 1.9): IR (ν_{max} cm^{-1}): 3334, 2940, 2873, 1748, 1641, 1452, 1377, 1152, 1072, 1044, 993, 880, 786. The spectrum showed hydroxyl (-OH) absorption at 3334, and the band at 1748 due to carbonyl group. The absorption at 2940 was linked to C – H group. The NMR data (Appendix B – Figure 2.15) is presented as follows:

^{1}H NMR (600 MHz, $CDCl_3$) δ ppm: 0.73 (3H, *s*) 0.80 (3H, *s*) 0.90 (3H, *s*) 0.93 (6H, *s*) 1.85 (3H, *s*) 2.94 (1H, *d, J* = 3.51 Hz) 3.15 (1H, *dd*, *J* = 11.72, 4.69 Hz) 4.57 (1H, *s*) 4.70 (1H, *s*)

The ^{1}H NMR data showed the BA terminal protons at δ 4.57 (H-29a) and δ 4.70 (H-29b), and allylic position C30 methyl protons at δ 1.85. The H-3 and H-19 protons were assigned to δ 3.15 and δ 2.94, respectively [lit. (1.66, *s,* H-30), (3.15, H-3), (2.88, H-19) (Kojima, et al. 1987)].

Other data agreed with the proposed structure however a methoxy signal was not observed in the spectrum. The methyl ester derivative might not have been formed, although the product obtained differs from the starting material BA, but might not be the methylated derivative. Besides spectral difference, the crystalline product obtained had a melting point of 264 °C, TLC R_f 0.40, (hexane/ ethyl acetate 7:3), in contrast to the starting material BA (amorphous powdery, 315 °C, R_f 0.56).

4.2.1.5 Methyl oleanolate

The methylated OA (**24**) product obtained was colorless crystalline needles (0.1540 g, 38%), and had a melting point 201 °C (lit. 204 °C, Umehara et al., 1992), R_f 0.70 (hexane/ ethyl acetate 7:3), (ESI-MS [M-H]-) m/z 469.369 (calc. 470.376) corresponding to molecular formula $C_{31}H_{50}O_3$, and characterized for oleanolic acid methyl ester (**24**).

The FT-IR analysis of (**24**) revealed the following absorption bands: IR (ν_{max} cm^{-1}): 3365, 2942, 2862, 1726, 1712, 1462, 1433, 1386, 1381, 1254, 1190, 1163, 1032, 998, 825, 753, 668.

The FT- IR spectrum (Appendix A – Figure 1.10) showed absorption bands at 3365 cm^{-1}, 1728 cm^{-1}, and 1254 cm^{-1}, corresponding to presence of hydroxyl (-OH) and carbonyl (–C – O and -C=O) functionalities respectively.

^{1}H NMR (600 MHz, $CDCl_3$) δ ppm: 0.69 (3H, *s*) 0.75 (3H, *s*) 0.87 (6H, *d, J* = 5.27 Hz) 0.89 (3H, *s*) 0.96 (3H, *s*) 1.10 (3H, *s*) 2.83 (1H, *dd*, *J* = 14.06, 4.69 Hz) 3.18 (1H, *dd*, *J* = 11.42, 4.39 Hz) 3.59 (3H, *s*) 5.25 (1H, *t*, *J* = 3.81 Hz)

The ^{1}H NMR of (**24**) (Appendix A – Figure 2.16) consisted 24 methyl protons. The methyl ester proton was observed at δ 3.59, and methane protons at δ 2.83 (H-18), δ 3.18 (H-3) and δ 5.25 (H- 12). The results agreed with those reported in previous work by (Umehara et al., 1992).

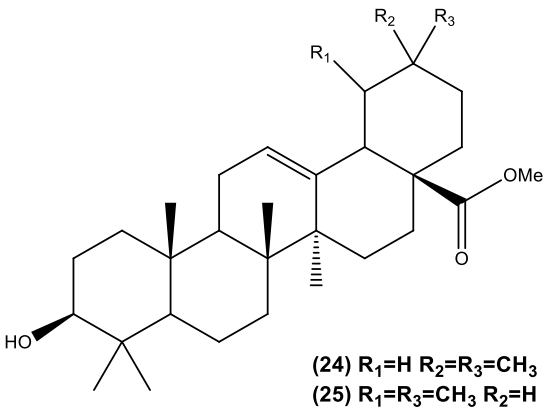

(24) R_1=H R_2=R_3=CH_3
(25) R_1=R_3=CH_3 R_2=H

4.2.1.6 Methyl ursolate

A white powdery product (0.1093 g, 27%), R_f 0.43 (hexane/ ethyl acetate 7:3), melting point 170 °C (lit. 170 - 171 °C, Sell & Kremers, 1938b), (ESI-MS [M-H]-) m/z 469.369 (calc. 470.376) corresponding to molecular formula $C_{31}H_{50}O_3$, and further identified as methyl ursolate (**25**).

The FT-IR analysis of (**25**) revealed the following absorption bands: IR (ν_{max} cm^{-1}): 3417, 2940, 2871, 1751, 1735, 1628, 1456, 1388, 1159, 1091, 994, 860, 828, 754, 662. The FT-IR spectrum (Appendix A – Figure 1.11) showed absorption bands at 3417 and 1735 corresponding to presence of hydroxyl (-OH) and carbonyl (–C – O) functionalities respectively. The –OH of carboxylic absorption band usually found at 3196 in parent pentacyclic triterpenes was absent in the methylated product due to esterification at C-28.

^{1}H NMR (600 MHz, $CDCl_3$) δ ppm: 0.75 (6H, *d*, *J* = 7.03 Hz) 0.83 (3H, *d*, *J* = 6.44 Hz) 0.89 (3H, *s*) 0.91 (3H, *d*, *J* = 6 Hz) 0.96 (3H, *s*) 1.05 (3H, *s*) 1.98 (1H, *td*, *J* = 13.47, 4.69 Hz) 2.19 (1H, *d*, *J* = 11.13 Hz) 3.19 (1H, *dd*, *J* = 11.13, 4.69 Hz) 5.22 (1H, *t*, *J* = 3.51 Hz).

The ^{1}H NMR (Appendix B – Figure 2.17) revealed 21H (CH_3 x 7), at δ 0.75, 0.83, 0.89, 0.91 and 1.05, and olefinic H-12 protons at δ 5.22. The H-18 proton was found at δ 2.19 and the proton H-3 at δ 3.19. The TLC and m.p. tests showed another product was formed, however, the expected methoxy signal was absent at δ 3.64 in the NMR spectrum. The expected methyl ester might not have been formed.

4.2.2 Group II (Conjugated triterpene anhydrides)

The derivatives classified in this group followed a structural C28 – C28 anhydride-type linkage of two PT compounds. The C3 positions of respective PTs were protected by acetylation, thus, leaving their C28 positions available for the target conjugate formation. Gnoatto et al. (2008) explained the activation of the carboxylic acid functionality, which is bonded to the C17 position using oxalyl chloride.

PTs were transformed to respective acetyl esters and then converted to corresponding acid chlorides by treating with thionyl chloride. An attempt was made to use oxalyl chloride, but the reagent was found to be very reactive and reactions were not successful. Derivatives were synthesized following preparation of chlorides of PTs using ($SOCl_2$) and treatment with triethylamine (TEA), and condensation with carbonyl group of alternating PTs, following the method of Sell and Kremers (1938a). Factors due to steric hindrance and lower nucleophilicity of C28 carboxylic functionality, and also the high reactivity of acid anhydride. These challenges pose difficulties to the synthesis and may affect integrity of final products. The effect of such modifications are, however assessed in the characterization data obtained to determine any structural changes as it may relate to observed level of biological activities.

4.2.2.1 Compound A13 (UAA – UAA conjugate)

Compound A13 (R_f = 0.84, hexane/ethyl acetate 7:3).

Yield: (0.1603 g, 80%); white powdery solid; m.p 235 °C; FT-IR (ν_{max} cm^{-1}): 2924, 2869, 1794, 1733, 1691, 1455, 1367, 1243, 1032, 1004, 967 (Appendix A – Figure 1.12).

The FTIR absorption bands at 1794 and 1733 may give a partial indication of the presence of anhydride group in the conjugated pair. The anhydride functionality Ar-CO-O-CO-Ar include the presence of carbonyl C=O and C-O functionalities. These were assigned according to literature (Pretsch et al. 2000). The C=O carbonyl signals of esters are assigned to absorption bands at 1690 and 1243, while C-O stretch expected of anhydrides is expected in the range 1300 – 900.

^{1}H NMR (600 MHz, $CDCl_3$) δ ppm: 0.74 (3H, *s*) 0.79 (3H, *s*) 0.83 (15H, *m*) 0.92 (9H, *d*, *J* = 7.62 Hz) 1.04 (6H, *d*, *J* = 5.86 Hz) 1.22 (6H, *s*) 2.01 (6H, *s*) 4.46 2H, *dd*, *J* = 9.96, 5.86 Hz) 5.21 (1H, *t*, *J* = 3.51 Hz) 5.28 (1H, *t*, *J* = 3.22 Hz) (Appendix B – Figure 2.18)

The spectrum of compound A13 differs from that that of UAA with the presence of sixteen methyl group protons at 0.74, 0.79, 0.83 (CH_3 x 5), 0.92 (CH_3 x 3), 1.04 (CH_3 x 2), and 1.22 (CH_3 x 2). The prominent singlet six methyl protons of ($COOCH_3$ x 2) attached to the C3 positions of the pair were found at δ 2.01. The H-12 proton from the two units exhibited different chemical shifts revealed as part A at δ 5.1 and part B at δ 5.28. The H-3 protons overlapped in the conjugate (2H) at δ 4.46. The chemical observed proton assignments alone cannot directly justify the anhydride bridge in the hybrid, but provided an indication of the composition of the product.

^{13}C NMR (75 MHz, $CDCl_3$) δ ppm: 15.54, 16.72, 17.02, 17.10, 18.17, 21.17, 21.18, 21.32, 23.28, 23.57, 24.09, 28.08, 29.71, 30.60, 32.85, 36.72, 36.90, 37.70, 38.27, 38.82, 39.03, 39.49, 41.93, 45.81, 47.45, 47.93, 52.58, 55.29, 80.93, 125.73, 137.96, 171.04

From the ^{13}C NMR spectrum (Appendix A – Figure 2.19), the chemical shifts for carbon in the C(O)O- (δ 171.04) and the methyl of CH_3C(O)O- (δ 21.18), and C3 (δ 80.93) of parent lupane agreed with literature reported by Raza et al 2015 [lit. C=O of acetyl (δ 171.08), OCOCH_3 (21.33), and C3 (δ 80.89), respectively)], however the usual C28 reference carboxyl (δ 182) was absent, or may have overlapped with the less deshielded C=O of acetoxy peak. The C28 carboxyl signal of the starting product UAA (**22**) was not found in the spectrum of Compound A13.

4.2.2.2 Compound A14 (UAA – OAA conjugate)

Compound A14: (R_f = 0.85, hexane/ethyl acetate 7:3). Yield: (0.1328 g, 80%); brownish white powder; m.p 277 °C.

FT-IR (ν_{max} cm^{-1}): 3396, 2946, 2697, 2510, 1802, 1732, 1694, 1655, 1457, 1366, 1243, 1091, 1026, 971 (Appendix A – Figure 1.13). The absorption peak at 1802, 1026 and 971 may be linked to the carbonyl of anhydride type conjugation. The carbonyl absorption were assigned to 1733 and 1243.

^{1}H NMR (600 MHz, $CDCl_3$) δ ppm: 0.72 (3H, *s*) 0.83 (15H, *m*) 0.87 (3H, *s*), 0.90 (9H, *d, J* = 7.62 Hz) 0.91 (3H, *s*) 1.04 (3H, *s*) 1.09 (3H, *s*) 1.22 (3H, *s*) 2.01 (6H, *s*) 2.78 (1H, *br dd*, *J* = 13.77, 4.39 Hz) 4.45 (2H, *dd*, *J* = 9.37, 6.44 Hz) 5.20 (1H, *t*, *J* = 3.51 Hz) 5.24 (1H, *t*, *J* = 3.51 Hz) (Appendix B – Figure 2.20).

The proton assignment for compound A14 indicated the olefinic proton (1H each) for UAA (**22**) and OAA (**21**) part of the conjugate at δ 5.20 and δ 5.24. The acetoxy protons (CH_3COO x 2) were referenced at δ 2.01 while a total of 48 methyl protons (CH_3 x 16) were identified. In the hybrid conjugate of (**22**) and (**21**), the H-3 protons (2H) overlapped at δ 4.45.

4.2.2.3 Compound A15 (OAA – OAA conjugate)

Compound A15 (R_f = 0.84, hexane/ethyl acetate 7:3). Yield: (0.1763 g, 88%); white crystals; m.p 245 °C; FT-IR (ν_{max} cm^{-1}): 2926, 2876, 1801, 1726, 1455, 1372, 1251, 1203, 1088, 1043, 999, 881, 803, 739, 668 (Appendix A – Figure 1.14). Comparison with OAA (**21**) showed appearance of absorption at 1801 and attenuation of the band at 1700 which may suggest structural changes around the C28 carboxyl functionality. Carbonyl absorption are assigned to the bands at 1726 and 1251.

^{1}H NMR (600 MHz, $CDCl_3$) δ ppm: 0.76 (6H, *s*) 0.82 (12H, *d*, *J* = 6 Hz) 0.88 (3H, *s*) 0.89 (12H, *d*, *J* = 4.1 Hz) 1.10 (6H, *s*) 1.22 (3H, *s*) 2.01 (6H, *s*) 2.79 (2H, *dd*, *J* = 13.18, 4.39 Hz) 4.45 (2H, *t, J* = 9 Hz) 5.27 (2H, *t*, *J* = 3.51 Hz) (Appendix B – Figure 2.21).

The assigned H-12 for the parent OAA (**21**) starting material were observed as overlapped protons at δ 5.27. The H-3 proton assignment for the two units overlapped at δ 4.45. Six methyl protons of ($-OC(O)CH_3$) were observed in the conjugate hybrid material at δ 2.01. Sixteen methyl groups ($8CH_3$ x 2) (48H) were found for the conjugate compound A15.

4.2.2.4 Compound A16 (BAA – BAA conjugate)

Compound A16 (R_f = 0.87, hexane/ethyl acetate 7:3). Yield: (0.1600 g, 80%); brownish white powder; m.p 273 °C; FT-IR (ν_{max} cm^{-1}): 3386, 2940, 2498, 2868, 1801, 1759, 1734, 1694, 1642, 1465, 13723, 1246, 1025, 967, 979, 883 (Appendix A – Figure 1.15). The IR spectrum showed extra C=O bands at 1759 and 1801 for the product. The spectrum differs relative to BAA (**20**). Carbonyl of anhydrides are linked to bands including 1025 and 967.

^{1}H NMR (600 MHz, $CDCl_3$) δ ppm: 0.79 (9H, *d*, *J*=8.49, 3.81 Hz) 0.81 (12H, *d*, *J* = 3.51 Hz) 0.89 (3H, *s*) 0.93 (6H, *s*) 1.65 (6H, *s*) 2.01 (6H, *s*) 2.15 (2H, *td*, *J* = 12.30, 3.51 Hz) 2.24 (2H, *m*) 2.97 (2H, *td*, *J* = 10.98, 4.98 Hz) 4.43 (2H, *dd*, *J* = 10.84, 5.57 Hz) 4.57 (2H, *s*) 4.69 (2H, *s*) (Appendix B – Figure 2.22).

Compound A16 has allylic methyl H-30 protons found as 6H (CH_3 x 2) at δ 1.65. The H-29a and H-29b protons of lupane-type conjugated triterpenoid were assigned at 4.57 (2H) and 4.69 (2H), suggestive of overlap of identical parts of the conjugate hybrid derivative. The deductions are suggestive preliminary elucidation and apparent distinctions observed for the synthesized product relative to the starting material.

^{13}C NMR (151 MHz, CHLOROFORM-*d*) δ ppm: 14.60, 16.00, 16.13, 16.42, 18.11, 19.29, 20.82, 21.27, 23.65, 25.40, 27.90, 29.64, 30.53, 32.12, 34.19, 37.00, 37.08, 37.75, 38.34, 38.39, 40.66, 42.38, 45.83, 46.89, 49.22, 50.35, 55.37, 56.29, 80.91, 109.65, 150.36, 170.99

The ^{13}C data for compound A16 (Appendix B – Figure 2.23) revealed chemical shifts 21.27 and 171.02 for the methyl and carbonyl of $–OCOCH_3$, respectively. The olefinic CH_2 of lupane at 109.65. The starting material BAA (**20**) was expected to exhibit C28 signal at 180.59 (Raza et al. 2015), however, the conjugate BAA – BAA hybrid has no such carboxyl peak. This may only be suggestive of activation and linkage via the C28 position.

4.2.2.5 Compound A17 (UAA – BAA conjugate)

Compound A17 (R_f = 0.85, hexane/ethyl acetate 7:3).Yield: (0.1395 g, 69%); white powder; m.p 248 °C; FT-IR (ν_{max} cm^{-1}): 3386, 2941, 2868, 1801, 1759, 1734, 1694, 1642, 1454, 1365, 1246, 1026, 979, 883 (Appendix A – Figure 1.16). Dual C=O asymmetric bands and C=O absorption were linked to 1734, 1694 and 1246, respectively. The carbonyl region is further characterized difference to starting materials by peaks found at 1801 and 1759.

^{1}H NMR (600 MHz, $CDCl_3$) δ ppm: 0.75 (3H, *s*) 0.79 (3H, *s*) 0.81 (9H, *m*) 0.83 (6H, *t*, *J* = 2.93 Hz) 0.89 (3H, *s*) 0.91 (3H, *d, J* = 2.93 Hz) 0.92 (3H, *s*) 1.04 (3H, *s*) 1.21 (3H, *s*) 1.65 (3H, *s*) 2.01 (6H, *d*, *J* = 4.2 Hz) 2.16 (2H, *br d, J* = 3.51 Hz) 2.21 (1H, *m*) 4.43 (2H, *dd*, *J* = 10.84, 5.56 Hz) 4.56 (1H, *d*, *J* = 2.34 Hz) 4.69 (1H, *d, J* = 2.34 Hz) 5.21 (1H, *t, J* = 3.51 Hz)

From the NMR data (Appendix B – Figure 2.24), a total of 45H protons (CH_3 x 15) were found. The acetylation of position C3 of the starting materials on (**20**) and (**22**) were observed in the conjugated product at 2.01 (6H, CH_3 x 2). The BAA (**20**) unit revealed H-29a and H-29b terminal CH_2 protons at 4.56 and 4.69, while the olefinic H-12 of UAA (22) is at 5.21. The H-3 and H-18 protons for both (**20**) and (**22**) overlapped in the conjugated product, emerging as two protons each at 4.43 and 2.16, respectively.

4.2.2.6 Compound A18 (OAA – BAA conjugate)

Compound A18 (R_f = 0.86, hexane/ethyl acetate 7:3). Yield: (0.1503 g, 75%); white powder; m.p 256 °C; FT-IR (ν_{max} cm^{-1}): 3042, 2946, 2873, 1803, 1733, 1644, 1454, 1391, 1366, 1243, 1090, 1032, 980 (Appendix A – Figure 1.17). Carbonyl C=O absorption assigned to 1733, 1454 and 1243, and anhydride region peak was identified at 1803.

^{1}H NMR (600 MHz, $CDCl_3$) δ ppm: 0.79 (12H, *m*) 0.83 (6H, *m*) 0.87 (3H, *d, J* = 6.44 Hz) 0.90 (6H, *s*) 0.93 (3H, *d*, *J* = 2.93 Hz) 1.10 (3H, *m*) 1.22 (3H, *s*) 1.65 (3H, *d, J* = 3.51 Hz) 2.01 (6H, *s*) 2.78 (1H, *br d*, *J* = 13.47 Hz) 2.97 (2H, *dd*, *J* = 10.69, 4.69 Hz) 4.45 (2H, *dd*, *J* = 9.37, 6.44 Hz) 4.58 (1H, *s*) 4.70 (1H, *s*) 5.27 (1H, *t, J* = 3.51 Hz) (Appendix B – Figure 2.25).

From the NMR spectrum, H-3 protons of both OAA (**21**) and BAA (**20**) was referenced as overlapped (2H) at δ 4.45, and the two acetoxy methyl units at δ 2.01 (6H). The H-18 of OAA is assigned at δ 2.78. A singlet for olefinic H-12 proton at 5.27 further may suggest presence of (**21**), while one proton each at δ 4.58 and δ 4.70 are assigned to (**20**).

^{13}C NMR (75 MHz, $CDCl_3$) δ ppm 14.65 15.34 16.18 (2C) 16.47 16.65 17.01 18.17 (3C) 19.35 20.87 21.33 (2C) 23.52 23.71 25.44 25.92 27.47 27.96 (2C) 29.71 (2C) 30.55 30.67 32.14 32.53 33.07 33.79 34.25 37.12 (3C) 37.69 37.81 38.08 38.38 (2C) 39.29 40.69 41.01 41.59 42.43 45.87 (4C) 46.51 46.92 47.54 49.26 50.40 50.50 55.32 55.42 56.33 80.93 (2C) 109.71 122.55 143.60 150.42 171.05 (2C)

In the ^{13}C spectrum (Appendix B – Figure 2.26), the signal δ 21.33 (CH_3 of –OAc), δ 171.05 (C=O of –OAc) are characteristic of the acetoxy groups attached to C3 of both (**21**) and (**20**). The absence of the characteristic carboxyl C28 around δ 182 differed from the chemical shift of the starting materials. 64 carbons were however counted in the spectrum of compound A18.

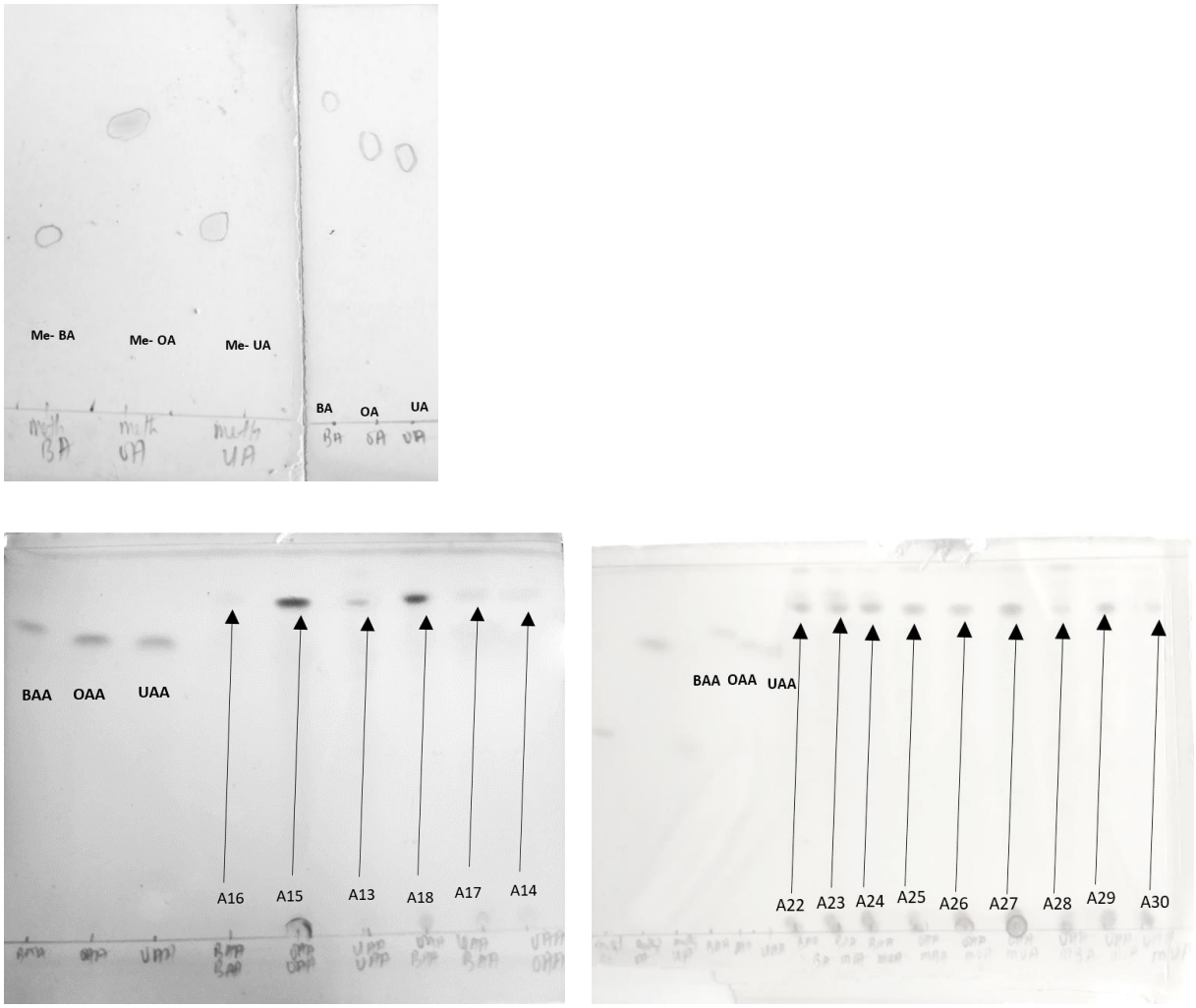

Figure 4.1: Sample TLC Illustration of Derivatives

4.2.3 Group III: Conjugated triterpene esters

4.2.3.1 Compound A22 (BAA – BA)

Compound A22 (R_f = 0.86, hexane/ethyl acetate 7:3). Yield: (0.1381 g, 69%); brownish crystals; m.p 329 °C; FT-IR (ν_{max} cm^{-1}): 3415, 2941, 2870, 1735, 1634, 1456, 1369, 1159, 1091, 1026, 991, 803, 665 (Appendix A – Figure 1.18). Carbonyl C=O stretch referenced at 1735, and C-O stretch due at 1026. The C-H alkyl stretch was attributed to peak at 2941.

^{1}H NMR (600 MHz, $CDCl_3$) δ ppm: 0.72 (3H, *s*) 0.79 (12H, *m*) 0.90 (6H, *s*) 0.93 (9H, *s*) 1.65 (6H, *d*, *J* = 6.44 Hz) 2.01 (3H, *s*) 2.21 (2H, *dd, J* = 7.62, 4.1 Hz) 2.95 (2H, *m*) 3.15 (1H, *dd*, *J*=11.13, 4.69 Hz) 4.43 (1H, *dd*, *J* = 10.54, 5.86 Hz) 4.57 (2H, *s*) 4.70 (2H, *s*) 11.35 (1H, *br s*) (Appendix B – Figure 2.27).

The H-3 proton (δ 3.15) is due to (**23**) while the H-3 for the acetylated component (**20**) was assigned to shift at 4.43. The lupane H-29a and H-29b protons overlapped at δ 4.57 and δ 4.70 revealing two protons each in the conjugated product. A total of thirteen CH_3 (39H) signals was found in the conjugate hybrid. No methoxy proton assignment was found, hence the

combination might have been BAA – BA. The BAA ($7CH_3$) and BA ($6CH_3$) might account for the total of 13 methyl groups (39H) in A22. This is a possibility. The spectrum of the product differs from those of the starting materials. It is not possible to confirm whether the desired coupling was formed or not. However, the activities of such combinations remained of interest.

4.2.3.2 Compound A23 (BAA – OA)

Compound A23 (R_f = 0.86, hexane/ethyl acetate 7:3). Yield: (0.1403 g, 70%); brown crystals; m.p 355 °C; FT-IR (ν_{max} cm^{-1}): 3414, 2945, 2870, 1733, 1642, 1456, 1366, 1244, 1159, 1095, 1027, 980, 881, 739, 665 (Appendix A – Figure 1.19). Carbonyl C=O was referenced at 1733, and additional C-O stretch at 1027.

^{1}H NMR (600 MHz, $CDCl_3$) δ ppm: 0.71 (3H, *s*) 0.75 (3H, *s*) 0.81 (9H, *m*) 0.87 (9H, *m*) 0.90 (3H, *s*) 0.93 (3H, *s*) 0.96 (3H, *s*) 1.10 (3H, *s*) 1.66 (3H, *s*) 2.00 (3H, *s*) 2.79 (1H, *br dd*, *J* = 13.77, 3.81 Hz) 3.18 (1H, *br dd*, *J* = 11.42, 3.81 Hz) 4.43 (1H, *dd*, *J* = 10.84, 5.56 Hz) 4.57 (1H, *s*) 4.70 (1H, *s*) 5.26 (1H, *t, J* = 3.22 Hz) 11.74 (1H, *br s*) (Appendix B – Figure 2.28).

The spectrum revealed characteristic 42H identified for $14CH_3$ groups, and the protons for terminal CH_2 of lupane was observed at δ 4.70 and δ 4.57. The H-3 chemical shift due to acetylation in BAA (20) was linked to δ 4.43 (1H). The oleanane component in the conjugate showed a reference H-12 at δ 5.26 H-18 proton at δ 2.79.

4.2.3.3 Compound A24 (BAA – UA)

Compound A24 (R_f = 0.86, hexane/ethyl acetate 7:3). Yield: (0.0989 g, 49%); brown crystals; m.p 325 °C.

FT-IR (ν_{max} cm^{-1}): 3406, 2944, 2871, 1735, 1694, 1642, 1463, 1367, 1245, 1186, 1029, 980, 883 (Appendix A – Figure 1.20). The carbonyl C=O stretch was identified at 1735. The absorption at 2644 is due to C-H stretch while band at 1029 is assigned to C-O functionality.

^{1}H NMR (600 MHz, $CDCl_3$) δ ppm: 0.75 (6H, *br d*, *J* = 7.62 Hz) 0.79 (3H, *s*) 0.81 (6H, *d*, *J* = 6.44 Hz) 0.88 (3H, *s*) 0.90 (3H, *s*) 0.91 (3H, *s*) 0.93 (3H, *s*) 0.95 (3H, *s*) 1.04 (3H, *s*) 1.22 (3H, *s*) 1.65 (3H, *s*) 2.00 (3H, *s*) 2.18 (2H, *br d*, *J* = 11.72 Hz) 2.24 (1H, *br d*, *J* = 12.89 Hz) 2.97 (1H, *td, J* = 10.54, 5.27 Hz) 3.18 (1H, *dd, J* = 11.13, 4.69 Hz) 4.43 (1H, *dd*, *J* = 10.84, 5.57 Hz) 4.57 (1H, *s*) 4.70 (1H, *s*) 5.21 (1H, *t*, *J* = 3.51 Hz) 11.41 (1H, *br s*) (Appendix B – Figure 2.29).

The 42 methyl proton signals (CH_3 x 14) were accounted in the spectrum of A24. The chemical shifts at δ 4.57 and δ 4.70 were assigned to the terminal CH_2 of BAA (**20**). The H-12 of (**25**) found at δ 5.21. The H-18 of the two units overlapped in the conjugated hybrid at δ 2.18.

4.2.3.4 Compound A25 (OAA – BA)

Compound A25 (R_f = 0.86, hexane/ethyl acetate 7:3). Yield: (0.1485 g, 49%); brownish white crystals; m.p 272 °C.

FT-IR (v_{max} cm^{-1}): 3405, 2944, 2870, 1732, 1643, 1456, 1375, 1247, 1034, 983 (Appendix A – Figure 1.21). The IR absorption was characterized to include C=O (1732), C-O stretch (1034) suggestive of carbonyl bearing compounds.

^{1}H NMR (600 MHz, $CDCl_3$) δ ppm: 0.72 (3H, *s*) 0.79 (3H, *s*) 0.82 (6H, *m*) 0.87 (3H, *s*) 0.90 (9H, *br d,* J = 4.1 Hz) 0.93 (6H, *s*) 1.10 (3H, *s*) 1.22 (3H, *s*) 1.65 (3H, *s*) 2.01 (3H, *s*) 2.78 (1H, *dd, J* = 13.47, 4.1 Hz) 2.94 (1H, *td, J* = 10.98, 4.39 Hz) 3.15 (1H, *dd, J* = 11.13, 4.69 Hz) 4.46 (1H, *t,* J = 8.1 Hz) 4.57 (1H, *s*) 4.70 (1H, *s*) 5.25 (1H, *t*, *J* = 3.51 Hz) 11.31 (1H, *br s*) (Appendix B – Figure 2.30).

The first part OAA (21) has identifiable H-3 (δ 4.46), methyl of –$OCOCH_3$ and olefinic H-12 (δ 5.25), while the methyl ester of BA (δ 23) was linked to δ 4.57 and δ 4.70 (olefinic terminal protons). It was further observed that the H-19 protons overlapped (2H) at δ 2.94. The spectrum showed 42 methyl proton signals (CH_3 x 14).

4.2.3.5 Compound A26 (OAA – OA)

Compound A26 (R_f = 0.86, hexane/ethyl acetate 7:3). Yield: (0.1294 g, 64%); white crystals; m.p 281 °C.

FT-IR (v_{max} cm^{-1}): 3406, 2946, 2877, 1801, 1733, 1462, 1365, 1244, 1032, 982, 826, 803 (Appendix A – Figure 1.22). The spectrum revealed carbonyl C=O stretch at 1733, and C-O stretch at 1032 and 1244 characteristic of an ester-containing compound.

^{1}H NMR (600 MHz, $CDCl_3$) δ ppm: 0.72 (6H, *d,* J = 5.27 Hz) 0.74 (3H, *s*) 0.82 (6H, *m*) 0.87 (12H, *d,* J = 3.51 Hz) 0.90 (6H, *d,* J = 5.86 Hz) 0.95 (3H, *s*) 1.09 (6H, *s*) 2.01 (3H, *s*) 2.77 (2H, *br d,* J = 14.06 Hz) 3.17 (1H, *dd,* J = 11.13, 4.1 Hz) 4.45 (1H, *dd*, *J* = 9.37, 6.44 Hz) 5.25 (2H, *t*, *J* = 3.51 Hz) 11.07 (1H, *br s*) (Appendix B – Figure 2.31).

It was observed that the H-12 protons for the conjugate hybrid overlapped as triplet at δ 5.25 and the H-18 protons from the pair overlapped as doublet at δ 2.77, respectively. The CH3COO methyl was found as singlet at δ 2.01. The OAA (8CH_3) and OA (7CH_3) might be linked to the total of 15 methyl groups (45H) observed in A26.

4.2.3.6 Compound A27 (OAA – UA)

Compound A27 (R_f = 0.86, hexane/ethyl acetate 7:3). Yield: (0.1068 g, 53%); white crystals; m.p 273 °C.

FT-IR (ν_{max} cm^{-1}): 3437, 2927, 2873, 1802, 1733, 1456, 1367, 1245, 1090, 1026, 988, 825, 803, 663 (Appendix A – Figure 1.23). Carbonyl absorption bands for C=O was assigned to 1801, and C-O to 1026.

^{1}H NMR (600 MHz, $CDCl_3$) δ ppm: 0.75 (9H, *m*) 0.82 (3H, *s*) 0.83 (3H, *s*) 0.89 (6H, *d,* J = 3.51 Hz) 0.90 (6H, *m*) 0.95 (3H, *s*) 1.04 (6H, *s*) 1.10 (3H, *d,* = 5.27 Hz) 1.22 (3H, *s*) 2.01 (3H, *s*) 2.19 (1H, *d*, *J* = 11.13 Hz) 2.78 (1H, *dd*, *J* = 13.47, 3.51 Hz) 3.18 (1H, *dd*, *J* = 11.72, 4.69 Hz) 4.46 (1H, *t,* J = 8.1 Hz) 5.22 (1H, *t,* J = 3.51 Hz) 5.27 (1H, *t,* J = 3.51 Hz) 11.33 (1H, *br s*) (Appendix B – Figure 2.32).

The assigned signals for H-3 for both units forming the conjugate are due to chemical shifts at δ 4.46 (1H) and δ 3.18 (1H). The H-12 (one proton each) were observed at δ 5.22 and δ 5.27 based on difference in methyl positioning in ring E of both starting materials. The OA component is reflected with H-18 proton at δ 2.78, while the H-18 proton of UA is found at δ 2.19. Fifteen methyl group protons (45H) were observed in A27.

4.2.3.7 Compound A28 (UAA – BA)

Compound A28 (R_f = 0.86, hexane/ethyl acetate 7:3). Yield: (0.1160 g, 58%); brownish crystals; m.p 276 °C.

FT-IR (ν_{max} cm^{-1}): 3439, 2943, 2870, 1734, 1643, 1455, 1376, 1244, 1033, 974, 880 (Appendix A – Figure 1.24). The C=O of carbonyl and associated C-O linked with ester group are referenced at 1734 and 1033, respectively. The C-H stretch was assigned with 2943.

^{1}H NMR (600 MHz, $CDCl_3$) δ ppm: 0.72 (3H, *s*) 0.75 (3H, *d, J* = 11.4 Hz) 0.79 (3H, *s*) 0.83 (9H, *m*) 0.90 (3H, *s*) 0.93 (9H, *d, J* = 6 Hz) 1.04 (3H, *s*) 1.22 (3H, *br s*) 1.64 (3H, *s*) 2.01 (3H, *s*) 2.94 (1H, *td*, *J* = 10.84, 4.69 Hz) 3.15 (1H, *dd*, *J* = 11.42, 4.39 Hz) 4.46 (1H, *dd*, *J* = 9.37, 6.44 Hz) 4.57 (1H, *s*) 4.69 (1H, *s*) 5.21 (1H, *t*, *J* = 3.22 Hz) 11.24 (1H, *s*) (Appendix B – Figure 2.33).

The H-12 olefinic proton of UAA was found at δ 5.21 while the terminal CH_2 of the lupane triterpenoid pair was observed as singlet at δ 4.57 and δ 4.69, (H-29_a, H-29_b), respectively. The H-3 of UAA was linked to δ 4.46 and the methyl protons of $COOCH_3$ was observed at δ 2.01. Fourteen methyl groups (42H) were found in A28.

4.2.3.8 Compound A29 (UAA – OA)

Compound A29 (R_f = 0.86, hexane/ethyl acetate 7:3). Yield: (0.1790 g, 90%); brownish crystals; m.p 283 °C.

FT-IR (ν_{max} cm^{-1}): 3387, 2935, 2873, 1734, 1652, 1459, 1366, 1244, 1162, 1103, 1013, 989 (Appendix A – Figure 1.25). The C=O of carbonyl and associated C-O linked with ester group are referenced at 1734 and 1013, respectively. The C-H stretch was assigned with 2935.

^{1}H NMR (600 MHz, $CDCl_3$) δ ppm: 0.71 (3H, *s*) 0.75 (6H, *s*) 0.83 (9H, *d, J* = 9.6 Hz) 0.87 (12H, *d, J* = 4.8 Hz) 0.92 (3H, *s*) 0.95 (3H, *s*) 1.04 (3H, *s*) 1.10 (3H, *s*) 2.01 (3H, *s*) 2.78 (1H, *dd*, *J* = 14.06, 4.69 Hz) 3.18 (1H, *dd*, *J* = 11.13, 4.10 Hz) 4.46 (1H, *dd*, *J* = 9.37, 6.44 Hz) 5.21 (1H, *t*, *J* = 3.51 Hz) 5.25 (1H, *t*, *J* = 3.81 Hz) 11.35 (1H, *s*) (Appendix B – Figure 2.34).

The H-12 olefinic protons for the triterpenoid pair were found at δ 5.21 and δ 5.25. The H-3 (δ 3.18) proton of the OA part in compound A29 differed from those of OA (δ 3.23). The H-3 of UAA was linked to δ 4.46 and the methyl protons of $COOCH_3$ was observed at δ 2.01. Fifteen methyl groups (45H) were found in compound A29.

4.2.3.9 Compound A30 (UAA – UA)

Compound A30 (R_f = 0.86, hexane/ethyl acetate 7:3). Yield: (0.1790 g, 90%); brownish crystals; m.p 233 °C.

FT-IR (ν_{max} cm^{-1}): 3397, 2926, 2872, 1734, 1631, 1456, 1370, 1244, 1151, 1091, 1032, 990 (Appendix A – Figure 1.26). The C=O of carbonyl and associated C-O linked with ester group are referenced at 1734 and 1091, respectively. The C-H stretch was assigned with 2926.

^{1}H NMR (600 MHz, $CDCl_3$) δ ppm: 0.73 (9H, *d, J* = 6 Hz) 0.81 (3H, *s*) 0.83 (6H, *d, J* = 2.34 Hz) 0.88 (3H, *s*) 0.91 (6H, *d, J* = 3.51 Hz) 0.95 (6H, *s*) 1.04 (9H, *s*) 2.01 (3H, *s*) 2.18 (2H, *d, J* = 11.9 Hz) 3.18 (1H, *dd, J* = 11.72, 4.69 Hz) 4.46 (1H, *dd*, *J* = 9.37, 6.44 Hz) 5.21 (2H, *br d*, *J* = 4.10 Hz) 11.34 (1H, *s*) (Appendix B – Figure 2.35).

Fifteen methyl groups (45H) were observed in the spectrum of compound A30. The H-3 of the UAA part was linked to δ 4.46, and the methyl protons of $COOCH_3$ was observed at δ 2.01. The H-3 (δ 3.18) proton of the UA part in compound A30 differed from those of UA (δ 3.00). The H-12 olefinic protons overlapped at δ 5.21.

4.3 Flavonoid – based derivatives

4.3.1 Compound A31 (BAA – flavonoid conjugate)

Compound A31 (R_f = 0.56, hexane/ethyl acetate 7:3). Yield: (0.1490 g, 93%); light yellowish crystals; m.p 219 °C.

FT-IR (ν_{max} cm^{-1}): 2946, 2871, 1081, 1735, 1662, 1611, 1591, 1450, 1379, 1333, 1273, 1242, 1216, 1136, 1033, 1013, 979, 888, 840, 803, 761, 681, 662 (Appendix A – Figure 1.27).

The IR spectrum showed combined peaks observed in the IR data for each of BAA (**20**) and 6-methyltectochrysin (**19**). C-H stretches are indicated with the absorption bands at 2871. Multiple carbonyl C=O absorption was referenced including 1735, 1662, and 1611, while C-O stretch was assigned to 1033.

^{1}H NMR (600 MHz, $CDCl_3$) δ ppm: 0.81 (6H, *s*) 0.91 (3H, *d*, *J* = 7.5 Hz) 0.94 (6H, *s*) 1.66 (3H, *s*), 2.01 (3H, *s*) 2.27 (3H, *s*) 3.88 (3H, *s*) 4.45 (1H, *dd*, *J* = 10.84, 5.57 Hz) 4.59 (1H, *d, J* = 10.5 Hz) 4.70 (1H, *d*, *J* = 5.86 Hz) 6.39 (1H, *s*) 6.64 (1H, *s*) 7.51 (3H, *m*) 7.89 (2H, *dd*, *J* = 7.91, 1.46 Hz) (Appendix B – Figure 2.36).

The flavone component showed aromatic ring B protons at δ 7.31 (3H) and δ 7.89 (2H). The H-30 methyl protons of the lupane component in compound A31 were reflected at 1.66, and a total of nine methyl group protons for BAA- were found. The methoxy component of the flavonoid has three protons signal at δ 3.88. For the lupine part, characteristic geminal CH_2 protons were assigned to chemical shift at δ 4.59 (1H) and δ 4.70 (1H), respectively, while the signal due to CH_3COO at position C3 were referenced as three protons methyl signal at δ 2.01.

4.3.2 Compound A32 (OAA – flavonoid conjugate)

Compound A32 (R_f = 0.58, hexane/ethyl acetate 7:3).

Yield: (0.1500 g, 94%); light yellowish crystals; m.p 214 °C.

FT-IR (ν_{max} cm^{-1}): 2945, 2869, 1730, 1661, 1611, 1592, 1450, 1381, 1333, 1246, 1216, 1136, 1033, 999, 983, 838, 803, 762, 682, 663 (Appendix A – Figure 1.28). The IR spectrum was observed to contain carbonyl C=O (1730, 1611) and C-O (1033, 1246) stretch.

^{1}H NMR (600 MHz, $CDCl_3$) δ ppm: 0.77 (3H, *s*) 0.84 (6H, *d, J* = 5.86 Hz) 0.88 (3H, *s*) 0.90 (6H, *d, J* = 4.1 Hz) 1.11 (3H, *s*) 1.22 (1H, *s*) 2.02 (3H, *s*) 2.27 (3H, *s*) 2.80 (1H,*br dd*, *J* = 13.47, 4.10 Hz) 3.88 (3H, *s*) 4.46 (1H, *t,* J = 8.1 Hz) 5.28 (1H, *t*, *J* = 3.51 Hz) 6.39 (1H, *s*) 6.64 (1H, *s*) 7.51 (3H, *m*) 7.89 (2H, *dd*, *J* = 7.91, 1.46 Hz) (Appendix B – Figure 2.37).

Eight methyl groups of the OAA component of the hybrid conjugate were identified at δ: 0.77 (3H), 0.84 (6H), 0.88 (3H), 0.90 (6H), 1.11 (3H) and 2.02 (3H). The protons correlating with the flavonoid unit include the olefinic type protons at δ 6.64 (1H) and δ 6.39 (1H), and aromatic ring B protons at δ 7.31 (3H) and δ 7.89 (2H) respectively. The presence of OAA (21) was confirmed with the oleanane H-3 proton at δ 4.46, H-12 proton at δ 5.28 and methyl of acetoxy group at δ 2.02.

4.3.3 Synthesis of compound A33 (UAA – flavonoid conjugate)

Compound A33 (R_f = 0.54, hexane/ethyl acetate 7:3). Yield: (0.1340 g, 84%); light yellowish crystals; mp 270 °C.

FT-IR (ν_{max} cm^{-1}): 2926, 2860, 1802, 1733, 1661, 1611, 1591, 1450, 1381, 1333, 1273, 1244, 1215, 1136, 1022, 836, 803, 761, 681, 662 (Appendix A – Figure 1.29). The presence of multiple carbonyl functionalities can be linked to absorption at 1733, 1661, 1611 due to C=O stretches and additional C-O type bands at 1022.

^{1}H NMR (600 MHz, $CDCl_3$) δ ppm: 0.84 (12H, *m*) 0.92 (6H, *m*) 1.05 (3H, *s*) 1.23 (1H, *s*) 2.02 (3H, *s*) 2.27 (3H, *s*) 3.89 (3H, *s*) 4.47 (1H, *dd*, *J* = 9.96, 5.86 Hz) 5.23 (1H, *t*, *J* = 3.51 Hz) 6.40 (1H, *s*) 6.64 (1H, *s*) 7.52 (3H, *d*, *J* = 7.62 Hz) 7.89 (2H, *m*) (Appendix B – Figure 2.38).

The ^{1}H assignment for UAA (**22**) was confirmed in compound A33 (**22**) with the protons of methyl of acetoxy group that were linked to chemical shift at δ 2.02, while the H-3 and olefinic H-12 were found at δ 4.47 and δ 5.23, respectively. The spectrum for the conjugate hybrid compound A33 (**22**) also showed signals for the flavonoid as referenced with the aromatic protons at δ 7.52 (3H) and δ 7.89 (2H), and protons of the methoxy substituent at δ 3.89.

4.3.4 Compound A37 (Sulfonic 6-methyltectochrysin)

Yield: (0.0589 g, 83%); whitish yellow powdery material; m.p 228 °C; FT-IR (ν_{max} cm^{-1}): 3062, 3003, 2922, 2853, 1662, 1649, 1591, 1544, 1449, 1424, 1382, 1333, 1273, 1215, 1164, 1135, 1033, 1014, 917, 834, 761, 681, 662, 568 (Appendix A – Figure 1.30). C-H stretches are indicated with the absorption bands at 2853. Multiple carbonyl C=O absorption was referenced including 1662, and 1649. The C-O stretch was assigned to 1033. The characteristic S=O absorption bands are expected as stretching vibrations at 1350-1300 and 1160-1120. The absorption bands at 1333 and 1135 may be due to S=O. The antisymmetric SOH bending can be linked to absorption at 1164, which is consistent with Jaganathan, et al. 2016

^{1}H NMR (600 MHz, DMSO-d_6) δ ppm: 1.22 (1H, *s*) 2.23 (3H, *s*) 3.44 (3H, *s*) 6.54 (1H, *s*) 6.98 (1H, *s)* 7.59 (3H, *br d*, *J* = 7.03 Hz) 8.07 (2H, *s*) (Appendix B – Figure 2.39).

The proton NMR data revealed aromatic protons of ring B at δ 7.59 (3H) and δ 8.07 (2H), and the protons assignments for the methoxy is seen at δ 3.44, while the 6-Me is shown at δ 2.23. The product might still contain traces of the starting materials as it was found that the proton for H-8 is still present in the final product. The NMR proton assignment was similar to the data by flavonoidsulfonate synthesized by Li and Zhang (2018) other than the presence of extra 6-Me in compound A37.

4.3.5 Compound A38 (methyl-flavonoid)

Yield: (0.1190 g, 96%); yellowish powder; m.p 276 °C.

FT-IR (ν_{max} cm^{-1}): 3062, 3003, 2923, 2854, 1661, 1610, 1591, 1496, 1450, 1424, 1382, 1333, 1273, 1215, 1160, 1135, 1033, 1013, 917, 833, 802, 761, 681, 662, 569 (Appendix A – Figure 1.31). The presence of carbonyl functionalities can be linked to absorption at 1661 and 1610 due to C=O stretches and additional C-O type bands at 1033.

^{1}H NMR (600 MHz, $CDCl_3$) δ ppm: 1.22 (1H, *s*) 2.25 (3H, *s*) 3.87 (3H, *s*) 6.36 (1H, *s*) 6.62 (1H, *s*) 7.50 (3H, *m*) 7.86 (2H, *dd*, *J* = 7.91, 1.46 Hz)

The signals observed in the spectral data (Appendix B – Figure 2.40) failed to account for additional methyl protons expected from the methylation of (**19**). The data obtained was similar to the starting material (**19**) suggesting the methylation was not successful. This may be due to the OH being at C5 position attached through strong hydrogen bonding with the C4 carbonyl group, hence making it difficult to be methylated.

4.4 Calix[4]arene derivatives

The recrystallized product afforded 2.46 g of colourless crystal cyclic tetramer (p-*tert*-butylcalix[4]arene (**18**)).

The crystals of the compound (**18**) melted at 342 °C (literature 344 – 346 °C, Gutshce et al., 1981).

FT-IR (ν_{max} cm^{-1}): 3187, 3052, 2954, 2869, 1603, 1485, 1452, 1393, 1362, 1292, 1202, 1118, 1032, 981, 913, 873, 816, 783, 729, 668, 625 (Appendix A – Figure 1.32). The hydroxyl group was due to the absorption band at 3187, and the C-H stretch at 2954, while C-O may be due to absorption at 1032. C-H bend vibrations of aromatics were observed at 729 and 668. Aromatic C-H out of plane vibrations is due to absorption at 873.

^{1}H NMR (400 MHz, $CDCl_3$) δ ppm: 1.28 (36H, *s*) 4.23 (8H, *s*) 6.99 (4H, *s*) 7.38 (8H, *s*).

The NMR data (Appendix B – Figure 2.41) of the synthesized calix[4]arene (**18**) showed thirty-six methyl protons at δ 1.28 (CH_3 x 12), eight CH_2 protons at δ 4.28 (CH_2 x 4), four hydroxyl protons at δ 6.99 (OH x 4), and eight aromatic protons at δ 7.38 (Ar-H x 8).

^{13}C NMR (151 MHz, pyridine- d_5) δ ppm: 31.43 (12 CH3) 32.31 (4 C(CH3)) 33.92 (4 CH2) 125.61 (8 Ar CH) 128.42 (8 Ar C(CH2)) 143.29 (4 Ar C-C(CH3)) 149.94 (4 Ar C-OH) (Appendix B – Figure 2.42)

4.4.1 Compound A35 (OAA – Calixarene conjugate)

Recrystallized Compound A35 (R_f = 0.91, hexane/ethyl acetate 9:1).

Yield: (0.2306 g, 95%); white crystals; mp 339 °C; FT-IR (ν_{max} cm^{-1}): 3381, 2954, 2873, 2699, 2511, 1731, 1647, 1479, 1393, 1363, 1245, 1201, 1043, 872, 839, 817, 782, 740 (Appendix A – Figure 1.33). The absorption at 3381 may be attributed to hydroxyl groups, while the C-H stretch is linked to 2954. The C-O functionality may cause the absorption at 1245 and 1043. Aromatic C-H vibrations may be due to the band at 839 and 872.

^{1}H NMR (600 MHz, pyridine-d_5) δ ppm 0.81 (6H, *s*) 0.86 (3H, *s*) 0.88 (3H, *s*) 0.94 (3H, *s*) 0.97 (3H, *s*) 0.99 (3H, *s*) 1.16 (36H, *s*) 1.26 (8H, *s*) 2.04 (3H, *s*) 4.67 (1H, *dd, J* = 11.82, 4.73 Hz) 5.45 (1H, *m*) 5.67 (4H, *m*) 7.23 (8H, *s*) (Appendix B – Figure 2.43).

The acetoxy proton of OAA was found at δ 2.04 while the associated H-3 proton and olefinic H-12 proton were assigned to the chemical shifts at δ 4.67 and δ 5.45. The methyl protons of the calixarene unit were assigned at δ 1.16. The presence of starting materials in the final product was established.

4.4.2 Compound A36 (UAA – Calixarene conjugate)

Recrystallized Compound A36 (R_f = 0.90, hexane/ethyl acetate 9:1).

Yield: (0.2157 g, 88%); white crystals; m.p 307 °C; FT-IR (ν_{max} cm^{-1}): 3154, 2956, 2869, 1734, 1604, 1481, 1394, 1363, 1286, 1242, 1201, 1160, 1124, 1103, 1028, 946, 872, 818, 782, 741, 699, 677 (Appendix A – Figure 1.34).

The FTIR results of the conjugated hybrid consisting calix[4]arene and PTs showed presence of hydroxyl in the region 3150-3600, and C-O due aromatic alcohols around 1242. Aromatic C-H out of plane vibrations expected in the range 840-970 were observed. The acetate region of the PT may be assigned as C=O at 1731 and *O*-methine C-H at 2867. The C-C-O aromatic alcohol ester of the form –COOAryl which may be expected at the ester bridge to form

compound A35 might be linked to the double absorption peaks at 1200 and 1245 which falls within expected range 1185-1290 otherwise not prominent in starting materials.

^{1}H NMR (600 MHz, $CDCl_3$) δ ppm: 0.76 (3H, *s*) 0.80 (3H, *s*) 0.82 (6H, *d, J* = 4.69 Hz) 0.92 (3H, *s*) 0.93 (3H, *s*) 1.05 (3H, *s*) 1.18 (36H, *s*) 2.02 (3H, *s*) 3.48 (4H, *d, J* = 12.89 Hz) 4.22 (4H, *d, J* = 13.47 Hz) 4.47 (1H, *dd, J* = 10.25, 5.57 Hz) 5.22 (1H, *t, J* = 3.81 Hz) 7.02 (8H, *s*) 10.31 (3H, *s*) (Appendix B – Figure 2.44).

From the UAA-calixarene conjugate hybrid product (compound A36), thirty-six methyl protons of calixarene were observed as singlet at δ 1.18 and eight aromatic protons (CH x 8) at δ 7.02, and the aromatic –OH at δ 10.31. The UAA (**22**) component was referenced at δ 5.22 (olefinic H-12), δ 4.47 (H-3), and eight methyl group protons at δ 0.76, 0.80, 0.82 (CH_3 x 2), 0.92, 0.93, 1.05 and 2.02 (methyl of acetoxy).

Calixarenes were first discovered in Adolph von Baeyer's laboratories in the nineteenth century. Since then, there has been modifications to their route of synthesis, including the common one-pot synthesis from para-substituted phenols and formaldehyde.

Calixarenes are important complexing agents as well as good enzyme mimics. Their basket-shape form enables their applications in host-guest chemistry. Calixarenes have been explored as host molecules in host-guest chemistry for enhancement of pharmacological profile of potential drug agents, and although calixarenes serve useful host molecule in host-guest chemistry (Shinkai, 1986; Baudry et al., 2003), and sensor applications (Deska et al., 2015), few studies explored the therapeutic applications of calixarenes, including controlled drug releases and cancer chemotherapy (Yousaf et al., 2015). Some derivatives of calixarenes, especially the water-soluble ones have been reported to exhibit significant bioactivities (Da Silva, 2004). Calixarenes were included for exploration in this study based on some findings stating that these compounds are able interact with organic and inorganic molecules and biomolecules, and can be designed to form water soluble derivatives as well as amphiphilic derivatives with bioactive compounds for pharmaceutical applications (Da Silva, 2004).

The activities of conjugate hybrid calixarene – triterpene formulations, phenolic – triterpene hybrids, and flavonoid – triterpene hybrids constitute preliminary compounds for our ongoing fundamental research and library of information on hybrid combination products.

4.5 Chapter Summary

Pentacyclic triterpenes - BA (**4**), OA (**5**), and UA (**6**) were extracted from *T. grandis*, *S. aromaticum*, and *M. caffra,* respectively, while 6-methyltectochrysin (**19**) was extracted from *L. petersonii*. An attempt was made to synthesize conjugate hybrid derivatives by the activation and/or protection of the C28 or C3 of these PTs. Preliminary assessment of the biological activities of these compounds are discussed in the next chapter.

CHAPTER FIVE
BIOLOGICAL STUDIES

5.1 Chapter Introduction

Preliminary biological *in-vitro* assays were carried out to assess the antioxidant and antimicrobial activities of the compounds prepared in this study. The total antioxidant capacities assays followed ORAC, FRAC and TEAC (ABTS+ free radical) tests. The antimicrobial study involved bioautography and broth dilution assays against six multi-drug resistant pathogenic bacteria strains.

5.1.1 Antioxidant Studies

Antioxidants have the potential to reduce or neutralize the bio-destructive effects of free radicals. Radical scavenging compounds react by donating electrons to free radicals, causing stability and eventually eliminating any further radical damages in the body. The compounds proposed in this work are non-enzymatic in nature, and have been obtained exogenously from plant sources, and used to prepare other derivatives. The total antioxidant capacity of the samples are presented in Table 5.1.

Table 5.1: Total antioxidant capacities

Compound / Code number*	ORAC assay (µmol TE /g DW)	FRAP assay (µmol/g DW)	TEAC (ABTS+) assay (µmol TE /g DW)
Ascorbic acid	2567.72	-	-
Group A - Plant sourced pentacyclic triterpenes			
Betulinic acid (A1)	14.34	-0.81	-23.1
Oleanolic acid (A2)	93.17	39.60	39.9
Ursolic acid (A3)	18.13	-8.94	8.1
Maslinic acid (A7)	3109.89	1783.81	654.1
Group B - Substituted derivatives			
3-*O*-Acetylbetulinic acid (A4)	37.59	17.18	-10.4
3-O-Acetyloleanolic acid (A5)	43.28	6.59	9.0
3-O-Acetylursolic acid (A6)	16.18	-0.07	-21.8
Methyl-betulinate (A19)	22.82	9.79	-25.8
Methyl-oleanolate (A20)	42.21	19.89	6.9
Methyl-ursolate (A21)	24.42	4.12	28.7
Group C - Conjugated anhydride-linked pentacyclic triterpene derivatives			
Compound A13	35.37	49.70	55.2
Compound A14	31.66	-2.28	-16.4
Compound A15	38.60	28.64	-23.1
Compound A16	41.39	-0.07	12.8
Compound A17	6.75	-0.07	-31.0
Compound A18	-1.50	-2.04	-29.0
Group D - Conjugated ester-type pentacyclic triterpene derivatives			
Compound A22	32.98	18.66	21.3
Compound A23	12.06	2.40	-2.1
Compound A24	12.40	7.32	-8.3
Compound A25	6.73	-6.72	-34.6
Compound A26	20.66	-2.04	-17.5
Compound A27	9.58	4.32	8.7
Compound A28	7.10	-3.54	27.6
Compound A29	48.01	12.94	-1.4
Compound A30	-2.26	-4.80	6.9
Group E - Flavonoid and derivatives			
5-hydroxy-7-methoxy-6-methylflavone (A10)	48.93	22.35	62.1
Compound A31	22.05	17.76	39.0
Compound A32	3.89	22.83	69.1
Compound A33	25.05	26.89	34.5
Compound A37	37.44	43.62	130.4
Compound A38	30.28	32.97	123.1

Group F - Calixarene and derivatives			
Calix[4]arene (A11)	42.63	259.14	333.0
Compound A35	37.92	19.53	216.0
Compound A36	30.28	33.86	184.4
Group G - Crude extracts (mixtures)			
A8 (OA – MA mixture)	311.47	382.58	354.7
A9 (OA – BA mixture)	46.79	41.82	58.0
A12 (*L. petersonii* crude)	101.76	165.51	191.5
* All values were means of three measurements. Some compounds have been given code numbers for easy reference. Other compounds maintained their compound codes from Chapter 4 & 5.			

The ORAC assay examines the peroxyl radical absorbing capacity of antioxidants while the ABTS (2,2'-azino-di-3-ethylbenzthialozine sulfonate) assay informs on the potential of antioxidants to scavenge ABTS radical cation or interfere with the radical generation process. The FRAP assay assesses the ability of antioxidant compounds to reduce Fe (III) to Fe (II) by donating electrons. These assays have been used to determine the antioxidant capacity of the compounds of interest.

PTs have shown antioxidant activities in several other studies. (Liu, 1995; Montilla, et al. 2003). From the results obtained in this study, Table 5.1 showed that MA (**11**) has the highest activity across the tested compounds. It was observed that (**11**) contains vicinal C2 and C3 hydroxyls, and C28 carboxyl functionality that may jointly contribute to the high antioxidant property of the compound (Allouche et al. 2010). The same observation on the influence of dihydroxy group was reported by (Fan, et al. 2010). The activity of the ascorbic acid control, a known antioxidant was compared with the derivatives. Other than MA, none of the derivatives were as potent as ascorbic acid.

Combination of PTs with flavonoid decreased the activity of 6-methyltectochrysin (A10). The crude extract of the *L. petersonii* was however found to exhibit better activity than the isolated flavonoid. Crude extracts have been reported to often possess good antioxidant activity (AsokKumar, 2009).

The antioxidant activity of the synthesized calix[4]arene (**18**) was higher than those of the parent PTs. This activity was depressed when combined in hybrids with PTs. The 5-hydroxy-7-methoxy-6-methylflavone (**19**) compound also showed interesting FRAP and TEAC results, and has a better antioxidant activity than the parent PTs. It was observed that BA (**4**) exhibited lesser activities relative to OA (5) and UA (5). The differences may be linked to the skeletal structure differences. BA (**4**) has terminal methylene and no olefinic groups in ring C. The aromatic ring of pentacyclic triterpenes and the hydroxyl group attached has been reported to influence antioxidant activity (David et al. 2004). This phenomenon may account for the better

activities observed for calixarenes, and may suggest the importance of aromaticity and hydroxyl functionality for antioxidant activities.

In group B, replacement of hydroxyl functionality with an acetoxy reduced antioxidative property. The oxygen reducing capacities decreased from 93.17 in OA (**5**) to 43.28 for OAA (**24**), and from 18.13 in UA (**6**) to 16.18 for UAA (**25**). This theory failed to hold for lupane type triterpenoid as it was found that the oxygen reducing antioxidant capacities of BAA (**20**) and methyl-BA (**23**) were higher than the level observed for the parent pentacyclic triterpene, BA (**4**). Previous study by Osusanmi et al. (2019) reported a similar activity, stating that BAA (**20**) showed higher antioxidant activity than BA (**4**).

In group C (A13 – A18), an increase in both the ferric reducing power and ABTS radical scavenging was observed when two UAA (**22**) molecules are conjugated via their C28 carbonyl functionalities to form compound A13. In Compound A13 (UAA – UAA conjugate), the ORAC, FRAP and TEAC results showed an increased activity (35.37, 49.70 and 55.20 respectively), relative to the non-conjugated single pentacyclic triterpene starting material UA (**6**) at the same concentration (16.18, -0.07, -21.8 respectively).

Combination of OAA (**21**) and UAA (**22**) in compound A14 resulted in a decreased antioxidant activity. For the OAA – OAA derivative (compound A15), the ferric reducing power was improved, while the ORAC and TEAC values were reduced when compared to OAA (Compound A5). The compound A16 integrated two BAA compounds, resulting in increased oxygen radical and ABTS radical reducing capacity but a diminished ferric reducing power. In compound A17, it was observed that the conjugation of UAA – BAA (ORAC 6.75) lowered overall activity of UAA (ORAC 16.18) and BAA (ORAC 37.59). The compound A18 (OAA – BAA conjugate) exhibited no antioxidant activity.

A decreased antioxidant power was observed for Group D. Only compound A22 and compound A27 showed positive activity across ORAC, FRAP and TEAC assays. All derivatives with this form of conjugation exhibited positive peroxyl radical reducing acitivity except compound A30. The compounds A22, A23, A24, A27, A29 could reduce Fe (III) to Fe (II) in FRAP assays whereas compounds A25, A26, A28, and A30 showed no negative FRAP activities. All Group D compounds except compounds A22, A27, A28 and A30 showed no ABTS radical scavenging activity.

The flavonoid compound (5-hydroxy-7-methoxy-6-methylflavone, A10) isolated from *L. petersonii* showed positive antioxidant activity. The values were 48.93, 22.35 and 62.1 for ORAC, FRAP and TEAC (ABTS) assays as shown in Group E. In compound A37 (sulfonated derivative), the ferric reducing power and the ABTS radical scavenging power of the derivatized flavonoid was doubled compared to the non-derivatized flavonoid. The peroxyl radical (ORAC assay) was slightly reduced. A similar trend was observed for methylated derivative of the

flavonoid (A38), showing a higher FRAP values and TEAC values but a lower ORAC value. The flavonoid-PT compounds (A31), (A32) and (A33) showed decreased antioxidant activities than the flavonoid.

The synthesized calix[4]arene (compound A11) showed positive antioxidant activity (Group F) which may have resulted from the four hydroxyl group functionalities found in the structural composition. The antioxidant potentials of calixarenes have been previously reported (Li et al. 2017). Rosenau et al. (2002) synthesized calixarene-type macrocycles that exhibited high antioxidant activity, twice as vitamin E. in other hybrid products, the conjugation of calix[4]arene with the pentacyclic triterpenes decreased the antioxidant power of the calixarene.

A mixture of OA – MA (A8) exhibited higher antioxidant than OA alone. The mixture of OA – BA have been obtained from *L. petersonii*, and it was observed that the mixture has a lower antioxidant value relative to the ethyl acetate crude extract (A12). The antioxidant capacity was higher in the case of the extracts, thus confirming synergistic action of natural compounds present in the crude extracts towards radical scavenging potential. The synergistic effect of compounds in crude extracts has been linked to improved antioxidant activity (Adebayo et al. 2015).

Antioxidants have been identified to possess inhibitory activity that reduces progression of heart-related and general ageing degenerative diseases. Antioxidants, including flavonoids, triterpenoids and polyphenolic compounds exhibit several health improving beneficial properties since they have been correlated with radical scavenging activities (Kaur & Kapoor, 2001). The observed levels of antioxidant activity between the samples showed that hybrid formulations did not create super antioxidant agents *per se* across the different groups.

Table 5.2: Comparison of antioxidant power in order of descending activity

Compound / Code number*	ORAC assay (µmol TE /g DW)**
Maslinic acid (A7)	3109.89
Ascorbic acid control	2567.2
A8 (OA – MA mixture)	311.47
A12 (*L. petersonii* crude)	101.76
Oleanolic acid (A2)	93.17
5-hydroxy-7-methoxy-6-methylflavone (A10)	48.93
Compound A29	48.01
A9 (OA – BA mixture)	46.79
3-O-Acetyloleanolic acid (A5)	43.28
Calix[4]arene (A11)	42.63
Methyl-oleanolate (A20)	42.21
Compound A16	41.39
Compound A15	38.6
Compound A35	37.92
3-O-Acetylbetulinic acid (A4)	37.59
Compound A37	37.44
Compound A13	35.37
Compound A22	32.98
Compound A14	31.66
Compound A38	30.28
Compound A36	30.28
Compound A33	25.05
Methyl-ursolate (A21)	24.42
Methyl-betulinate (A19)	22.82
Compound A31	22.05
Compound A26	20.66
Ursolic acid (A3)	18.13
3-*O*-Acetylursolic acid (A6)	16.18
Betulinic acid (A1)	14.34
Compound A24	12.4
Compound A23	12.06
Compound A27	9.58
Compound A28	7.1
Compound A17	6.75
Compound A25	6.73
Compound A32	3.89
Compound A18	-1.5
Compound A30	-2.26

Compound / Code number*	FRAP assay (µmol/g DW)***
Maslinic acid (A7)	1783.81
A8 (OA – MA mixture)	382.58
Calix[4]arene (A11)	259.14
A12 (*L. petersonii* crude)	165.51
Compound A13	49.7
Compound A37	43.62
A9 (OA – BA mixture)	41.82
Oleanolic acid (A2)	39.6
Compound A36	33.86
Compound A38	32.97
Compound A15	28.64
Compound A33	26.89
Compound A32	22.83
5-hydroxy-7-methoxy-6-methylflavone (A10)	22.35
Methyl-oleanolate (A20)	19.89
Compound A35	19.53
Compound A22	18.66
Compound A31	17.76
3-O-Acetylbetulinic acid (A4)	17.18
Compound A29	12.94
Methyl-betulinate (A19)	9.79
Compound A24	7.32
3-O-Acetyloleanolic acid (A5)	6.59
Compound A27	4.32
Methyl-ursolate (A21)	4.12
Compound A23	2.4
3-*O*-Acetylursolic acid (A6)	-0.07
Compound A16	-0.07
Compound A17	-0.07
Betulinic acid (A1)	-0.81
Compound A18	-2.04
Compound A26	-2.04
Compound A14	-2.28
Compound A28	-3.54
Compound A30	-4.8
Compound A25	-6.72
Ursolic acid (A3)	-8.94

Compound / Code number*	TEAC ABTS+) assay (µmol TE /g DW) ****
Maslinic acid (A7)	654.1
A8 (OA – MA mixture)	354.7
Calix[4]arene (A11)	333
Compound A35	216
A12 (*L. petersonii* crude)	191.5
Compound A36	184.4
Compound A37	130.4
Compound A38	123.1
Compound A32	69.1
5-hydroxy-7-methoxy-6-methylflavone (A10)	62.1
A9 (OA – BA mixture)	58
Compound A13	55.2
Oleanolic acid (A2)	39.9
Compound A31	39
Compound A33	34.5
Methyl-ursolate (A21)	28.7
Compound A28	27.6
Compound A22	21.3
Compound A16	12.8
3-*O*-Acetyloleanolic acid (A5)	9
Compound A27	8.7
Ursolic acid (A3)	8.1
Methyl-oleanolate (A20)	6.9
Compound A30	6.9
Compound A29	-1.4
Compound A23	-2.1
Compound A24	-8.3
3-O-Acetylbetulinic acid (A4)	-10.4
Compound A14	-16.4
Compound A26	-17.5
3-O-Acetylursolic acid (A6)	-21.8
Betulinic acid (A1)	-23.1
Compound A15	-23.1
Methyl-betulinate (A19)	-25.8
Compound A18	-29
Compound A17	-31
Compound A25	-34.6

5.2 Antimicrobial studies

Bioautography assays and *in vitro* broth dilution assays was carried out against six species of multi-drug resistant pathogenic bacteria strains including three gram-negative (*Escherichia coli, Klebsiella pneumoniae*, & *Pseudomonas aeruginosa*) and three gram positive (*Bacillus cereus, Staphylococcus aureus*, & *Enterococcus faecalis*) bacteria.

5.2.1 Bioautography assay results

The bioautography assay can provide information on basic antimicrobial potential of samples. The tested materials can either enhance or inhibit the growth of the microorganisms. The activity of the natural product compounds and synthesized derivatives were assessed visually, whereby visible purple spots indicated no inhibition or continual growth of the tested microbial strains, while white spots indicated inhibition and killing of the microbial strains. The assay involved microbial activity testing against a wide range of bacteria. These include multidrug resistant *Acinetobacter baumannii* ATCC 19606; multidrug (Ciproflaxin, Ceftazidime; Cefepime) resistant *Acinetobacter baumannii* ATCC BAA-16505; *Enterobacter cloacae* subsp. *cloacae* ATCC BAA-1143; *Listeria monocytogenes* ATCC 19111; vancomycin resistant *Enterococcus faecalis* ATCC 29212; multidrug (Ampicillin, Aztreonam, Cefoxitin, Cefpodoxime, Ceftazidimi, Chloramphenicol) resistant *Klebsiella pneumoniae* subsp. *pneumoniae* ATCC 700603; vancomycin-resitant / Teicoplanin sensitive *Enterococcus faecalis* ATCC 51299; oxacillin sensitive *Staphylococcus aureus* subsp. *aureus* ATCC 29213; *Pseudomonas aeruginosa* ATCC 27853; *Escherichia coli* ATCC 25922; *Bacillus cereus* ATCC 10876 (genome sequenced) and *Candida albicans* ATCC 24433.

Figure 5.1 showed the different (visual) observations illustrating activity of the samples. The positive results are those with visible zones of inhibition.

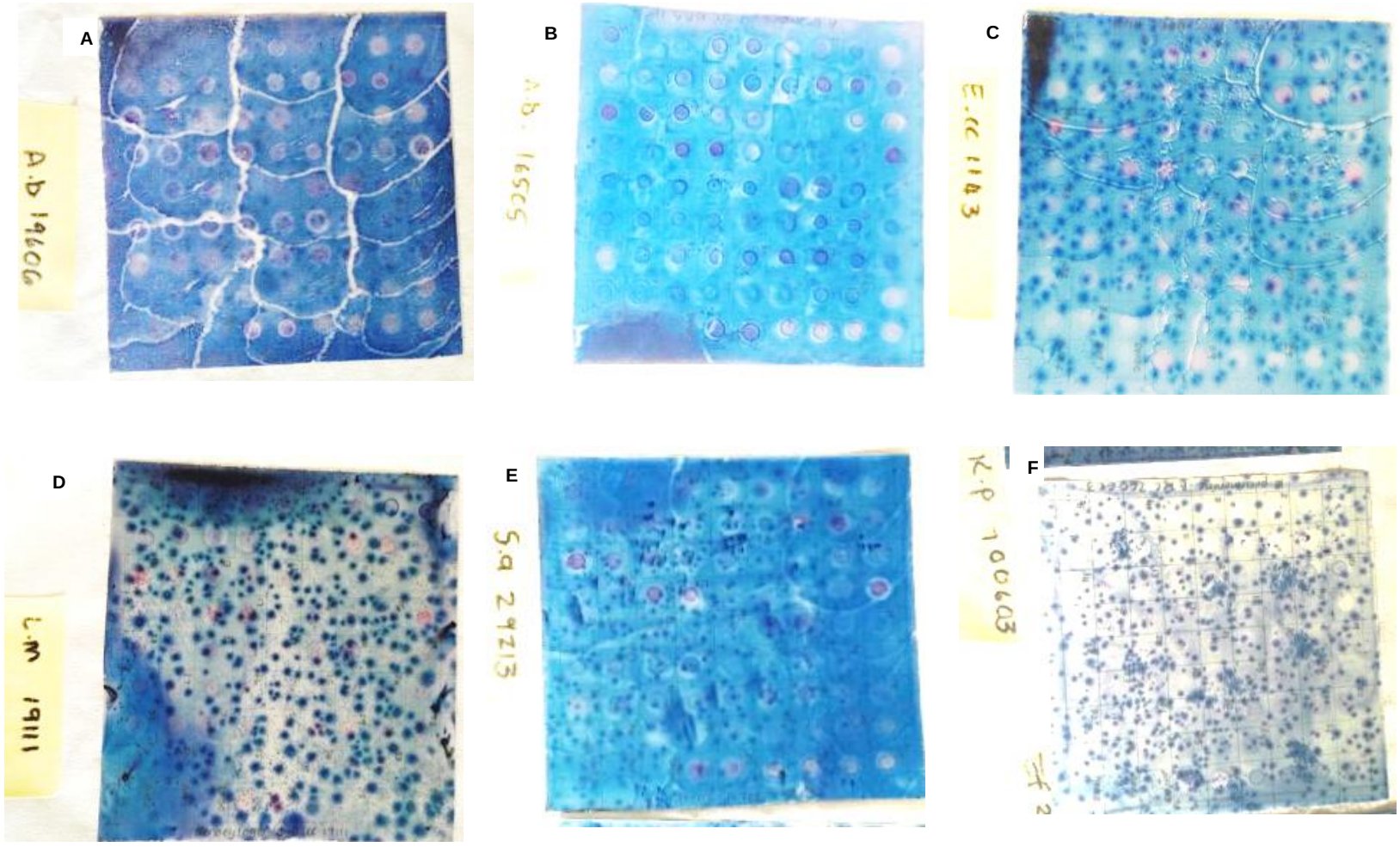
A
B
C
D
E
F

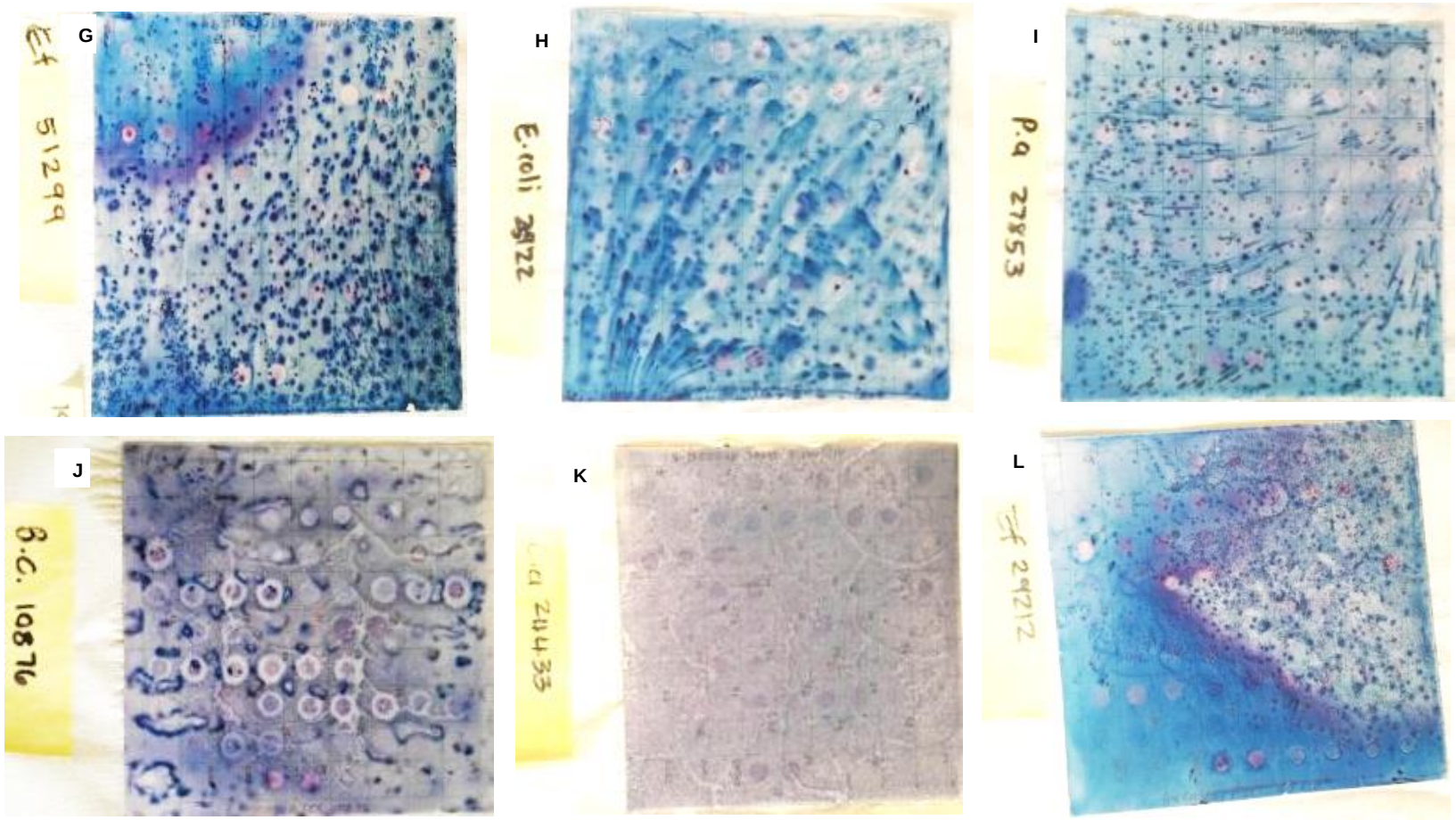

A = *Acinetobacter baumannii* ATCC 19606; B = *Acinetobacter baumannii* ATCC 16505; C = *Enterobacter cloacae* ATCC 1143; D = *Listeria monocytogenes* ATCC 19111;
E = *Staphylococcus aureus* ATCC 29213; F = *Klebsiella pneumoniae* ATCC 700603; G = *Enterococcus faecalis* ATCC 51299; H = *Escherichia coli* ATCC 25922;
I = *Pseudomonas aeruginosa* ATCC 27853; J = *Bacillus cereus* ATCC 10876; K = *Candida albicans* ATCC 24433; L = *Enterococcus faecalis* ATCC 29212

Figure 5.1: Images of TLC plates for bioautographic assays

Some of the plates were difficult to read or examined for a conclusive reference. The test against *A. baumannii*, *B. cereus, E. cloacae*, E. coli, and P. *aeruginosa,* a clear zone of inhibition might be indicative of the presence of inhibitory activities. This suggests that there was certain level of antimicrobial interactions, and that some of the samples inhibited the growth of the tested bacteria. The zone of inhibition cannot be confirmed for all samples. Hence, broth dilution assays were carried out on selected strains in order to gain measurable and conclusive insight on the potential antibacterial activities of the samples.

5.2.2 Broth Dilution Assays

The pentacyclic triterpenes, BA (**4**), OA (**5**), UA (**6**); and the isolated flavonoid (5-hydroxy-7-methoxy-6-methylflavone (**19**)), calix[4]arene (**18**) and their derivatives were tested for antibacterial activity against six bacterial strains by using the micro-dilution method. The determination of MIC require for the testing of antibacterial activity up to concentrations at which no visible bacterial growth is observed. However, in this study, growth of the microorganisms was still observed within the range of tested concentrations, thus implying that MIC has not been reached, and a higher sample concentration (up to 500 µg/mL) is required. The synthesis work is limited by low yields; hence, small amount of samples was available for all assays. This background work focused on establishing the activity of various pentacyclic triterpenes and relative bioactivities resulting from chemical modifications into derivatives. The level of antibacterial inhibition (against six different microbial strains) observed at tested concentration is shown in Table 5.3 and 5.4.

Table 5.3: Antimicrobial activity of samples

Samples	B. cereus	E. faecalis	S. aureus	E. coli	K. pneumoniae	P. aeruginosa
Positive control	Vancomycin			Ampicillin		
	71%	14%	27%	6%	n/a	11%
A1	13%	21%	-36%	0%	-10%	-18%
A2	48%	-13%	-88%	-6%	-8%	-23%
A3	54%	35%	-94%	10%	10%	8%
A4	71%	13%	-77%	8%	13%	-9%
A5	7%	16%	-22%	5%	-11%	-15%
A6	53%	-5%	-120%	-31%	-2%	-48%
A7	69%	19%	-89%	28%	20%	23%
A8	50%	-13%	-126%	-24%	3%	-17%
A9	58%	15%	-21%	-6%	5%	-12%
A10	-91%	2%	-97%	-16%	4%	-30%
A11	-18%	35%	-32%	5%	-7%	-6%
A12	61%	17%	-40%	5%	23%	-28%
A13	67%	-32%	-102%	-28%	-16%	-35%
A14	69%	19%	-84%	-47%	-40%	-44%
A15	71%	8%	2%	7%	-22%	10%
A16	70%	20%	-96%	3%	9%	3%
A17	71%	-39%	-115%	-41%	-13%	-44%
A18	71%	12%	-69%	8%	-8%	20%
A19	10%	-17%	-46%	-7%	3%	-7%
A20	68%	-7%	-26%	-23%	4%	-22%
A21	59%	-28%	-60%	-6%	5%	13%
A22	61%	-31%	-31%	10%	10%	11%
A23	65%	-2%	-39%	10%	21%	12%
A24	69%	-21%	-58%	10%	8%	-10%
A25	42%	11%	-88%	17%	5%	27%
A26	17%	-28%	-23%	2%	6%	18%
A27	32%	-27%	-93%	10%	8%	6%
A28	36%	-14%	-99%	-3%	7%	8%
A29	59%	-56%	-62%	-18%	4%	-21%
A30	60%	-63%	-49%	-5%	-4%	-7%
A31	-44%	-21%	-50%	-16%	4%	-49%
A32	-25%	-19%	-24%	-23%	-6%	-49%
A33	11%	-39%	-56%	-7%	18%	-51%
A34	-5%	-115%	-66%	10%	2%	-25%
A35	20%	19%	-31%	3%	14%	-19%
A36	2%	-11%	-4%	9%	-4%	-6%
A37	-87%	-13%	-76%	-21%	-5%	-80%
A38	-118%	-33%	-80%	-18%	3%	-94%

[antibiotic] = 111 µg/mL [samples] = 55.6 µg/mL

A1 (BA); A2 (OA); A3 (UA); A4 (BAA); A5 (OAA); A6 (UAA); A7 (MA); A8 (OA+MA); A9 (OA+BA); A10 (Flavonoid); A11 (Calix[4]arene); A12 (*L. petersonii* crude); A13 (Compound A13); A14 (Compound A14); A15 (Compound A15); A16 (Compound A16); A17 (Compound A17); A18 (Compound A18); A19 (BA-Me); A20 (OA-Me); A21 (UA-Me); A22 (Compound A22); A23 (Compound A23); A24 (Compound A24); A25 (Compound A25); A26 (Compound A26); A27 (Compound A27); A28 (Compound A28); A29 (Compound A29); A30 (Compound A30); A31 (Compound A31); A32 (Compound A32); A33 (Compound A33); A34 (Compound A34); A35 (Compound A35); A36 (Compound A36); A37 (Compound A37); A38 (Compound A38)

Table 5.4: Antimicrobial activity of samples in order of decreasing power

B. cereus		E. coli		E. faecalis		K. pneumoniae		P. aeruginosa		S. aureus	
vancomycin	71%	ampicillin	6%	vancomycin	14%	ampicillin	n/a	ampicillin	11%	vancomycin	27%
A4	71%	**A7**	28%	**A3**	35%	**A12**	23%	**A25**	27%	**A15**	2%
A15	71%	**A25**	17%	**A11**	35%	**A23**	21%	**A7**	23%	**A36**	-4%
A17	71%	**A3**	10%	**A1**	21%	**A7**	20%	**A18**	20%	**A9**	-21%
A18	71%	**A22**	10%	**A16**	20%	**A33**	18%	**A26**	18%	**A5**	-22%
A16	70%	**A23**	10%	**A7**	19%	**A35**	14%	**A21**	13%	**A26**	-23%
A7	69%	**A24**	10%	**A14**	19%	**A4**	13%	**A23**	12%	**A32**	-24%
A14	69%	**A27**	10%	**A35**	19%	**A3**	10%	**A22**	11%	**A20**	-26%
A24	69%	**A34**	10%	**A12**	17%	**A22**	10%	**A15**	10%	**A22**	-31%
A20	68%	**A36**	9%	**A5**	16%	**A16**	9%	**A3**	8%	**A35**	-31%
A13	67%	**A4**	8%	**A9**	15%	**A24**	8%	**A28**	8%	**A11**	-32%
A23	65%	**A18**	8%	**A4**	13%	**A27**	8%	**A27**	6%	**A1**	-36%
A12	61%	**A15**	7%	**A18**	12%	**A28**	7%	**A16**	3%	**A23**	-39%
A22	61%	**A5**	5%	**A25**	11%	**A26**	6%	**A11**	-6%	**A12**	-40%
A30	60%	**A11**	5%	**A15**	8%	**A9**	5%	**A36**	-6%	**A19**	-46%
A21	59%	**A12**	5%	**A10**	2%	**A21**	5%	**A19**	-7%	**A30**	-49%
A29	59%	**A16**	3%	**A23**	-2%	**A25**	5%	**A30**	-7%	**A31**	-50%
A9	58%	**A35**	3%	**A6**	-5%	**A10**	4%	**A4**	-9%	**A33**	-56%
A3	54%	**A26**	2%	**A20**	-7%	**A20**	4%	**A24**	-10%	**A24**	-58%
A6	53%	**A1**	0%	**A36**	-11%	**A29**	4%	**A9**	-12%	**A21**	-60%
A8	50%	**A28**	-3%	**A2**	-13%	**A31**	4%	**A5**	-15%	**A29**	-62%
A2	48%	**A30**	-5%	**A8**	-13%	**A8**	3%	**A8**	-17%	**A34**	-66%
A25	42%	**A2**	-6%	**A37**	-13%	**A19**	3%	**A1**	-18%	**A18**	-69%
A28	36%	**A9**	-6%	**A28**	-14%	**A38**	3%	**A35**	-19%	**A37**	-76%
A27	32%	**A21**	-6%	**A19**	-17%	**A34**	2%	**A29**	-21%	**A4**	-77%
A35	20%	**A19**	-7%	**A32**	-19%	**A6**	-2%	**A20**	-22%	**A38**	-80%
A26	17%	**A33**	-7%	**A24**	-21%	**A30**	-4%	**A2**	-23%	**A14**	-84%
A1	13%	**A10**	-16%	**A31**	-21%	**A36**	-4%	**A34**	-25%	**A2**	-88%
A33	11%	**A31**	-16%	**A27**	-27%	**A37**	-5%	**A12**	-28%	**A25**	-88%
A19	10%	**A29**	-18%	**A21**	-28%	**A32**	-6%	**A10**	-30%	**A7**	-89%
A5	7%	**A38**	-18%	**A26**	-28%	**A11**	-7%	**A13**	-35%	**A27**	-93%
A36	2%	**A37**	-21%	**A22**	-31%	**A2**	-8%	**A14**	-44%	**A3**	-94%
A34	-5%	**A20**	-23%	**A13**	-32%	**A18**	-8%	**A17**	-44%	**A16**	-96%
A11	-18%	**A32**	-23%	**A38**	-33%	**A1**	-10%	**A6**	-48%	**A10**	-97%
A32	-25%	**A8**	-24%	**A17**	-39%	**A5**	-11%	**A31**	-49%	**A28**	-99%
A31	-44%	**A13**	-28%	**A33**	-39%	**A17**	-13%	**A32**	-49%	**A13**	-102%
A37	-87%	**A6**	-31%	**A29**	-56%	**A13**	-16%	**A33**	-51%	**A17**	-115%
A10	-91%	**A17**	-41%	**A30**	-63%	**A15**	-22%	**A37**	-80%	**A6**	-120%
A38	-118%	**A14**	-47%	**A34**	-115%	**A14**	-40%	**A38**	-94%	**A8**	-126%
[antibiotic] = 111 µg/mL [samples] = 55.6 µg/mL											

PTs are known to be active antibacterial agents that can target the cell envelope of bacteria. The antibacterial properties of PTs isolated from other plant sources have been reported in literature (Siddique & Saleem, 2011; Kuete et al., 2011; Kamaraj et al., 2012; do Nascimento et al., 2014). In this exploratory study, the isolated compounds and synthesized derivatives were tested against standard bacteria strains. The results on the activities of the compounds against each microbial strain are discussed in detail as follows.

***Bacillus cereus* ATCC 10876**

The samples were tested against gram-positive *B. cereus*. It was observed that the conjugated including UAA – UAA (A13), UAA – OAA (A14), OAA – OAA (A15), BAA – BAA (A16), UAA – BAA (A17), and OAA – BAA (A18) showed inhibitory activities in the range 67% – 71%. Same level of activity was observed for BAA (compound A4) which inhibited microbial growth by 71%. These activities were obtained at a sample concentration of 55 µg/mL, which reflected a higher efficacy than the reference standard antibiotic, vancomycin (71% inhibition at a concentration of 111 µg/mL). This may indicate some improvements relative to the activity recorded for parent PTs BA (A1, 13%), OA (A2, 48%) and UA (A3, 54%). The antimicrobial activities of PTs and the acetylated derivatives are available in literature (Rivero-Cruz, et al. 2008; Sultana & Ata, 2008), however, the combination of these compounds in the hybrid derivatives disclosed in this work is yet to be reported in prior art. The approach to antimicrobial activities of PTs is often similar, but differs due to the nature of strains employed and the kind of derivatives used.

The activities of the samples against *B. cereus* (ATCC 10876 - genome sequenced) was assessed. In a previous study (do Nascimento et al. 2014), UA was isolated from *Sambucus australis*, and the antimicrobial activity of the compound, including the activities of derivatives of UA prepared by chemical modifications at C3 position were investigated. Weaker activities were reported for the parent UA (MIC > 1024 µg/mL). It is worth noting that the researchers attempted to assess the synergistic effect of mixing (physically) UA with different antibiotics, and found that the resulting formulations exhibited improved activities than antibiotics or the PT alone.

Compounds A20 and A21 that were the derivatives of UA and OA, were found to exhibit 68% and 59% inhibitory activities respectively, better than the parent UA and OA. On the contrary, the derivative of BA (compound A19) showed less activities (10%) relative to parent BA compound. The conjugated anhydride type compounds showed positive antibacterial activity A22 – A24 (61% - 69%), compounds 25, 27, 28 (32% – 42%) and compound A26 at 17% activity.

The flavonoid compound (A10) and its derivatives (A31, A32, A37, and A38) were inactive active against *B. cereus*. Although the flavonoid compound isolated from *L. petersonii* was

inactive against *B. cereus*, the crude extract (A12) of the plant showed significant activity (61% inhibition) at the tested concentration. This may suggest a synergistic action of the components of the crude towards the observed antibacterial activity. This agrees with the work done by de Fatima et al. (2009). The flavonoid and the synthesized calix[4]arene (A11) showed no inhibitory activity.

Kamaraj et al. (2012) investigated the antibacterial activity of PTs isolated from some Indian medicinal plants. The authors reported that crude extracts exhibited wide antibacterial properties at tested concentrations ranged 22.6 µg/mL – 28.4 µg/mL against gram-positive and gram-negative bacteria, including *B. cereus*. The synergistic activity of compounds in the crude might be responsible for the observed level of activities, but since quantitation and determination of the active element in the crude is essential, determination of the separate activities of the main bioactive ingredients may give a better insight to understand the causes of observed activities.

Calixarenes are useful in water purification, fluorescent sensors and drug delivery systems (Boudebbouze et al., 2013; Uysal Akku, 2015; Makwana et al., 2015). There was no prior work combining calix[4]arenes with PTs with an aim to assess variation in level of bioactivity, nor the assessment of bioactive properties of such compounds on selected strains reported in this study. The relevance of calixarene-antibiotic mixture was explored by Casnati et al. (1996). The researchers synthesized new vancomycin mimics via D- or L- alanine linkage between aromatic nuclei of calix[4]arene, and found that the MIC of the synthesized derivatives were in the range 4 – 64 mg/mL against strains of *S. aureus* and 16 mg/mL against *B. cereus*. However, in this study calixarene-anchored derivative formed with OAA (A35 and A36) showed inhibition of 20% and 2% respectively against *B. cereus* at a tested concentration of 55 µg/mL.

Samples A10, A11, A31, A32, A34, A37, and A38 were observed to lack inhibition and contained more thriving microbial loads as compared to the control. Figure 5.2 illustrates the activities of tested samples against *B. cereus*, whereby a level below that of negative control indicated inhibition (killing) of the bacteria whereas there is no activity for samples showing higher microbial load relative to the control.

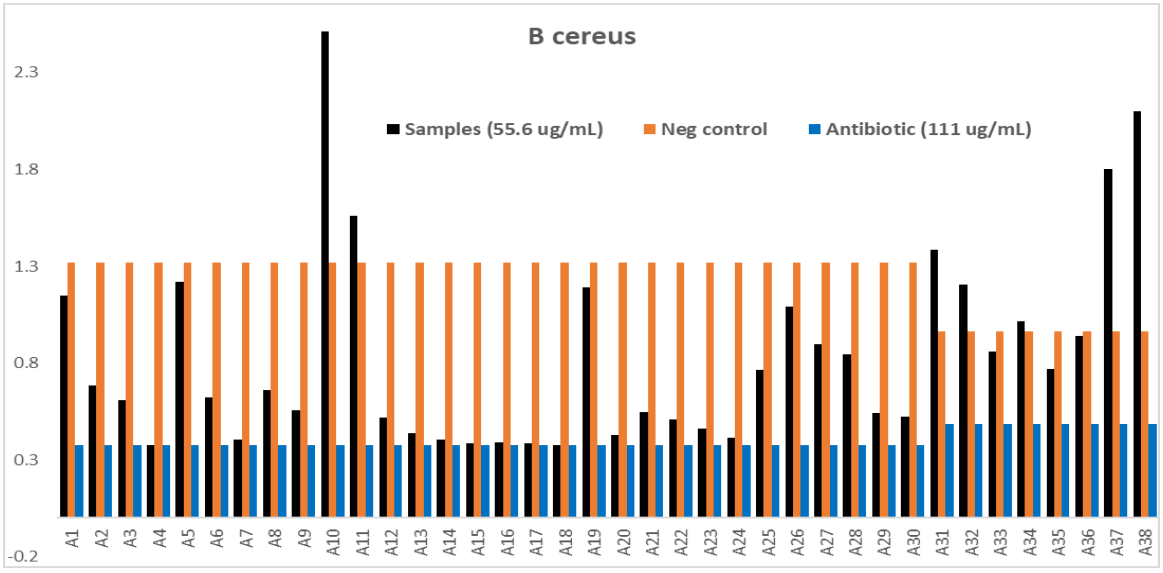

Figure 5.2: Antimicrobial activities against *B. cereus*

Escherichia coli ATCC 25922

E. coli are gram-negative bacteria widely contracted by humans from the environment via contaminated food and water, and some strains of these bacteria cause diarrhoea, respiratory diseases or urinary tract infections. In recent times, *E. coli* is becoming increasingly resistant to conventional antibiotics.

The strength of inhibition of a standard antibiotic (ampicillin, 111 µg/mL) against the *E. coli* (ATCC 25922) strain was found to be relatively low (6%), indicating the level of drug resistance exhibited by the bacteria strain. Sample A7 (MA), showed the best antibacterial activity against *E. coli* with a percentage bacteria reduction of 28% at 55.6 µg/mL. This showed about 5 times more potent activity than the ampicillin even when the amount of A7 used in the assay was half of the concentration of the antibiotic.

Pavel et al. (2016) investigated the antibacterial effect of MA and the synthetic acetylated derivative bearing benzylamide functionality and reportedly found no activity against bacteria including *E. coli, E. faecalis* and *P. aeruginosa*. Horiuchi et al. (2007) conducted studies on activities of pentacyclic triterpenes on Vancomycin-Resistant strains of Enterococci and reported significant activity against drug resistant strains. The data from this study are in line with the observation of the latter study.

The conjugation of OAA – methyl BA (A25, 17%) improved the antibacterial activity of parent pentacyclic triterpenes OA (A2, not active) and BA (A1, not active). The absence of significant activity of the PTs is consistent with a prior study (Chandramu et al. 2003) on antibacterial activity of BA and UA isolated from *Vitex negundo L.,* whereby these pentacyclic triterpenes showed insignificant antibacterial activity against *E. coli* even at a concentration of 1000 µg/disc.

Other ester-linked conjugated triterpenes including BAA – BA (A22, 10%), BAA – OA (A23, 10%), BAA – UA (A24, 10%) and OAA – UA (A27, 10%) exhibited positive antibacterial activity at the tested concentration. Although at a lower level of inhibition, (BAA, A4) and OA (OAA, A5) showed some antibacterial compounds relative to inactive parent pentacyclic triterpenes. Acetylated UA (UAA, A6) was inactive.

The synthesized calix[4]arene showed an inhibition activity of 5% at the tested concentration. The activity of this synthesized compound was doubled when combined with BA and UA respectively to make derivatives A34 (10%) and A36 (10%) respectively. The combination of calix[4]arene with OA (A35, 3%) lowered the antibacterial activity. Some of the anhydride-linked combined pentacyclic triterpenes (A18, A15, and A16) could also inhibit *E. coli* (8%, 7%, and 3% respectively).

The mixtures (natural crude) containing OA and MA (sample A8), OA and BA (sample A9) showed no activity. The flavonoid compound (A10) and its derivatives (A31, A32, A33, A37, and A38) were also inactive against *E. coli* whereas the crude extract of the same plant (A12) showed very little activity (inhibition activity of 5%). The non-activity of pentacyclic triterpenes against *E. coli* was reported by (Pavel et al. 2016).

Compounds A7, A18, A22, A23, A24, A25, A27, A34 and A36 has microbial load level lower than the amount in the negative control. Figure 5.3 illustrates the activities of samples against *E. coli*, whereby a level below that of negative control indicated inhibition (killing) of the bacteria, while in cases where the level of the sample is higher than that of the negative control, indicates no activity and the bacteria flourishes.

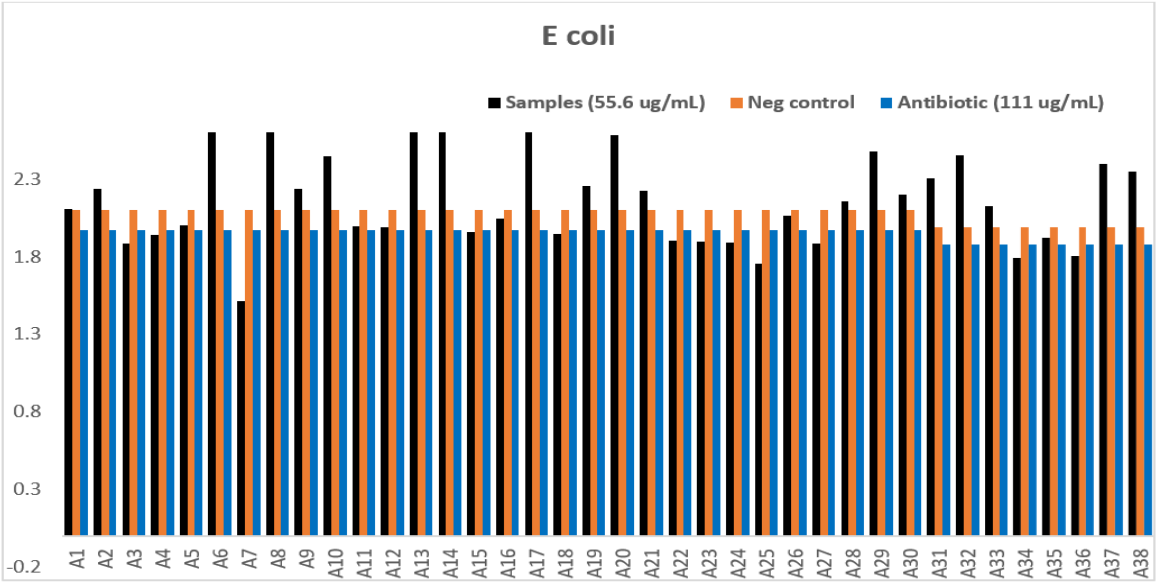

Figure 5.3: Antimicrobial activities against *E. coli*

Enterococcus faecalis ATCC 29212

E. faecalis (gram-positive bacteria), commonly found inhabiting in gastrointestinal tracts of mammals including humans has been implicated in severe life-threatening infections such as nosocomial infections. *E. coli* is often difficult to treat due to resistant to standard antibiotics including penicillin, oxacillin and vancomycin (Kau et al., 2005). In this study, the percentage inhibition by the antibiotic (vancomycin) was only 14% at 111 µg/mL.

Only 15 out of the 38 samples showed some level of antibacterial inhibition properties against *E. faecalis*. Ursolic acid, UA (A3) exhibited highest bioactivity against E. faecalis, by inhibiting the growth of the microorganism by 35%. BA (A1, 21%) showed good activity, however OA (A2) was inactive against *E. faecalis*. On the other hand, MA (A7), which is an isomer of OA was positively correlated for inhibition at 19%.

Acetylated BA (BAA, A4) and acetylated OA (OAA, A5) prevented microbial growth at 13% and 16% respectively. Thus, acetylation improved the antimicrobial properties of OA. Acetylated UA was inactive. This indicated that acetylation improved the activity of OA but resulted in a reverse action in UA.

The synthesized calix[4]arene (A11, 35%) showed positive inhibition activities. The combination of calixarene with OAA (A35, 19%) exhibited killing of the bacteria, but at a lower capacity relative to the synthesized calixarene. Other calixarene-anchored derivatives (A34, A36) were inactive. The flavonoid isolated from *L. petersonii* (A10) was nearly insignificant (2%) at 55 µg/mL, and its derivatives (A31, A32, A33, A37, and A38) were inactive against *E. faecalis*. In contrast, the crude extract of *L. petersonii* (A12) showed positive inhibitory properties.

Some of the conjugated triterpenes (A14, A15, A16, A18, and A25) showed interaction with the bacterial that resulted in inhibition. While a mixture of OA and BA (A9) was active, a mixture of OA and MA (A8) was found to be inactive.

With reference to the control, samples A1, A3, A7, A11, A12, A14, A15, A16, A25 and A35 contained lower microbial load, indicative of inhibition of growth. Figure 5.4 illustrates the activities against *E. faecalis*, whereby a level below that of negative control indicated inhibition (killing) of the bacteria, and in contrast, in cases where the level of the sample is higher than that of the negative control, indicates no activity and the bacteria flourishes.

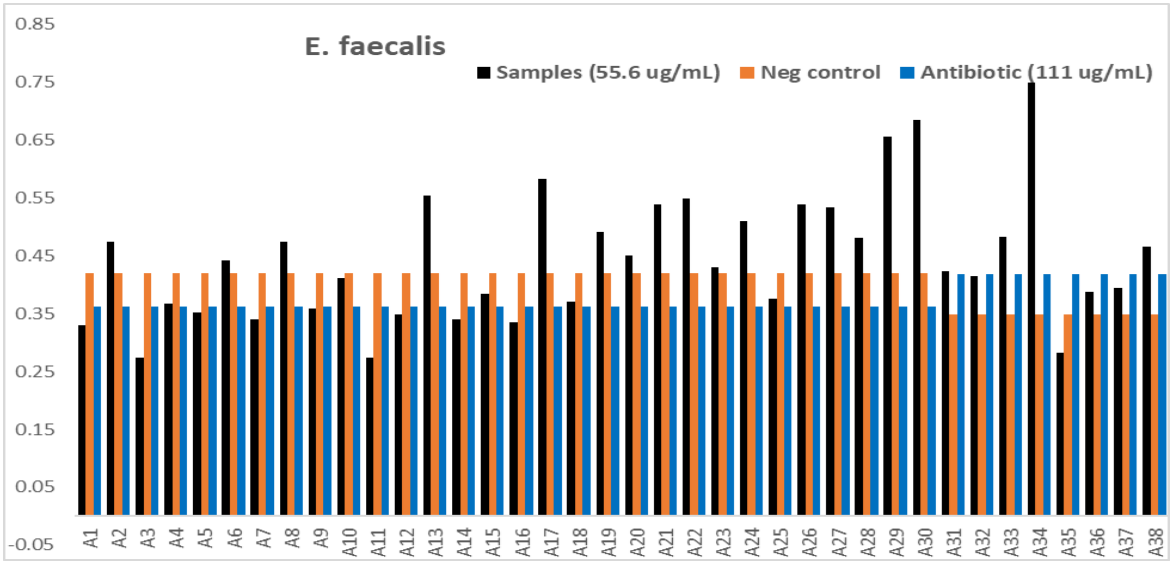

Figure 5.4: Antimicrobial activities against *E. faecalis*

***Klebsiella pneumoniae* ATCC 700603**

K. pneumonia is a gram-negative bacterium that have exhibited diversified epidemiology in different regions of the world, thereby leading to complications in finding precise treatment options. *K. pneumoniae* is often contracted from hospitals (nosocomial), and could lead to pneumonia, blood stream infections, wound infections, meningitis and urinary tract infections. The management of this bacteria is complex, and the mortality of K. pneumoniae infected patients is very high (Munoz-Price et al., 2013). Treatment options often involve combination of multiple antibiotics including colistin, imipenem and tigecycline (Munoz-Price et al., 2013). O, nly few antibiotic alternatives are remaining to combat this multi-drug resistant bacterium.,

From the results illustrated in Table 7.2, the activity of tested antibiotic was compared with those of isolated pentacyclic triterpenes, flavonoid, calixarene and their derivatives. The standard antibiotic (ampicillin) at a concentration of 111 µg/mL was inactive against the strain of *K. pneumonia* ATCC 700603.

Of the 38 samples that were tested, 24 of these showed certain level of antibacterial activities (2% - 23%) against K. pneumonia. The best activity was observed for crude extract of L. petersonii (A12, 23%) at 55 µg/mL, and this was significant considering the inactivity of ampicillin at 111 µg/mL. However, the flavonoid compound isolated from the crude extract had reduced activity (A10, 4%). Combination of the flavonoid with UAA (A33, 18%) improved the observed activity of the derivative-combined compound relative to the activities of parent flavonoid and UAA because the acetylated UA (A6) was inactive. The parent pentacyclic triterpenes BA (A1) and OA (A2) were inactive, but UA (A3) and MA (A7) were active.

The acetylated pentacyclic triterpenes, OAA (A5) and UAA (A6) were non-active whereas acetylation of BA (A4) produced a compound with 14% level of inhibition against *K. pneumoniae*. The ester-linked pentacyclic triterpene combinations A22, A23, A24, A25, A26, A27, A28 and A29 exhibited positive inhibitory properties against the bacteria. Methylation of pentacyclic triterpenes BA, and OA to produce compounds A19, and A20 respectively, showed that alkylation increased the antibacterial activities of the pentacyclic triterpenes, whereas the same chemical transformation halved the activity of UA (10%) to (A21, 5%).

Positive activity was also observed for conjugated ester-linked BAA – OA compound (A23). The calix[4]arene and its derivative when combined with UAA (A36) were non-active against the tested microbial strain. However, calixarene – BAA conjugate (A34, 2%) and calixarene – OAA conjugate (A35, 14%) showed some level of inhibition. Calixarene - UAA was inactive, and in contrast for Calixarene - OAA .

The activities of some samples including compounds A7, A12, A16, A23, A33 and A35 whereby inhibition of microorganism was observed is further shown by the microbial load relative to the negative control. Figure 5.5 illustrates the activities of the tested samples against *K. pneumonia*, whereby a level below that of negative control indicated inhibition (killing) of the bacteria, and in cases where the level of the tested sample is higher than that of the negative control, this indicates that the sample was inactive.

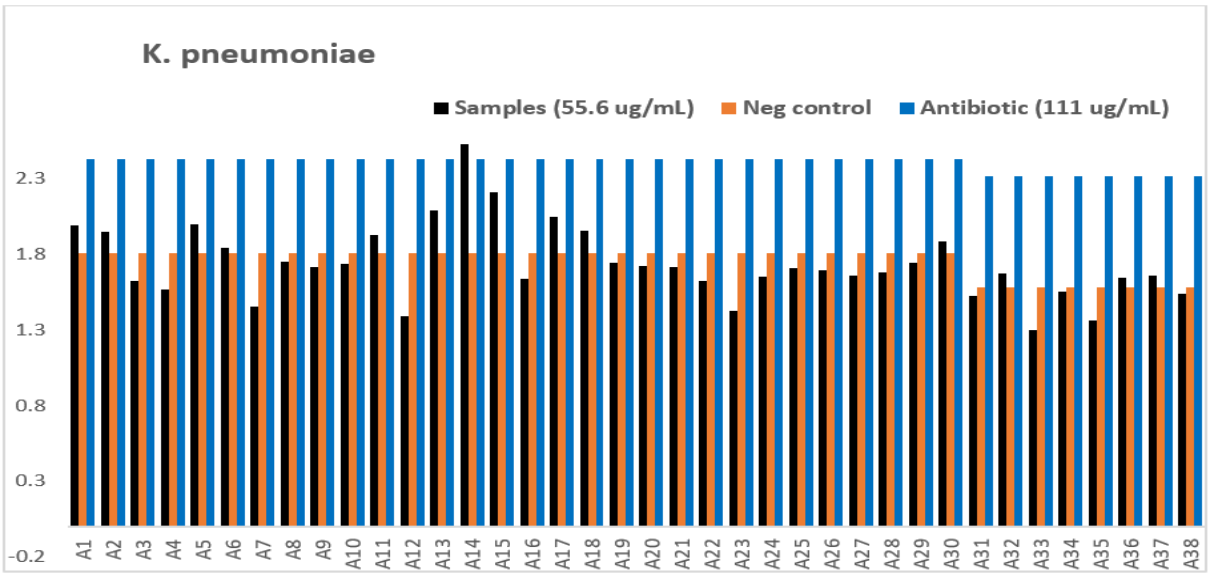

Figure 5.5: Antimicrobial activities against *K. pneumonia*

Pseudomonas aeruginosa ATCC 27853

P. aeruginosa, a gram-negative pathogenic bacterium possess well-developed membrane barriers and has shown the highest multi-drug resistance among non-spore-forming bacteria (Cloete, 2003).

Only twelve samples out of 38 tested samples were active (3% - 27% inhibition) at a concentration of 55 µg/mL. The standard antibiotic (vancomycin) destroyed and prevented the growth of the bacterial strain (*P. aeruginosa* ATCC 27853) by 11% at a concentration of 111 µg/mL, indicating that some of the tested samples possess better antibacterial activities relative to vancomycin. The parent pentacyclic triterpenes, BA (A1) and OA (A2) were inactive at tested concentration, while UA (A3) showed 8% activity. MA showed good antibacterial activities. The combination of OAA and methylated BA to form ester-linked derivative (A25) resulted in formation of the best antimicrobial compound against *P. aeruginosa* ATCC 27853. Similarly, samples A22, A23, A26, A27 and A28 that contained the same ester-linkage in their pentacyclic triterpene conjugations showed positive antibacterial activities against the tested bacterium.

The illustration made with reference to the control showed the samples containing lower microbial load relative to the negative control. Particularly, it was observed that there might have been inhibition by samples A3, A7, A15, A16, A18, A21, A22, A23, A25, A26, A 27, and A28, Figure 5.6 illustrates the activities of the tested samples against *P. aeruginosa*, whereby a level below that of negative control indicated inhibition (killing) of the bacteria, and in cases where the level of the tested sample is higher than that of the negative control, this indicates that the sample was inactive.

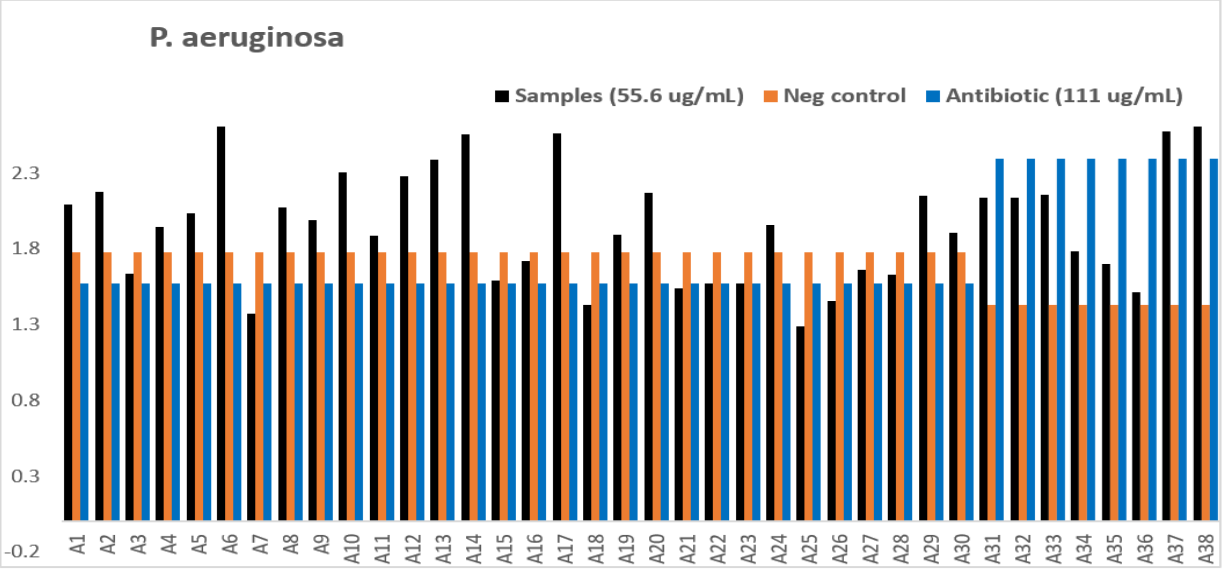

Figure 5.6: Antimicrobial activities against *P. aeruginosa*

***Staphylococcus aureus* ATCC 29213**

There has been numerous efforts to discover novel antibacterial agents (obtainable from plants) with remarkable potency against drug resistance microorganisms including methicillin-resistant strains of *Staphylococcus aureus* (MRSA). In this study, the reference control antibiotic (vancomycin, 111 µg/mL) showed 27% inhibition rate. Only compound A15 (OAA – OAA conjugate) showed positive 2% inhibition activity against *S. aureus* at the tested concentration (55 µg/mL).

It was observed that vancomycin and the PT samples exhibited poor activities in the pure form, however, previous work by by Chung and coworkers (Chung et al., 2011) showed an improved activity was increased for antibiotic (vancomycin) against methicillin-resistant and methicillin-sensitive strains of *S. aureus* by 50% by combining (mixing) pentacyclic triterpenes with the antibiotic, leading to an observed synergistic antimicrobial activity that was higher than when the antibiotic was applied alone. This provides an area for future exploration, where the synthesized compounds could be combined with antibiotics to assess potential variations in overall activities resulting from such synergistic interactions.

Figure 5.7 illustrates the activities of the tested samples against *S. aureus*, whereby a level below that of negative control indicated inhibition (killing) of the bacteria, and in cases where the level of the tested sample is higher than that of the negative control, this indicates that the sample was inactive.

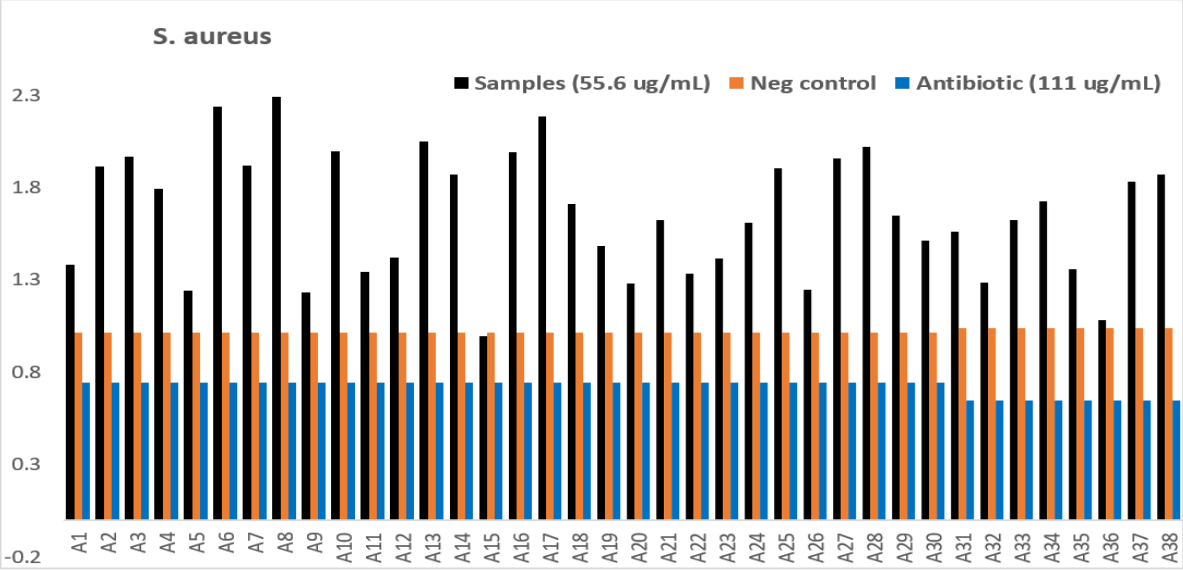

Figure 5.7: Antimicrobial activities against *S. aureus*

The derivatives of BA, OA and UA showed differed antimicrobial activities relative to the starting compounds. This observation is in line with the findings of Fontanay et al. (2008). The classification of potency of plant-derived bioactive agents depend on activities at various concentrations. It has been reported that plant extracts with MIC values < 8000 µg/mL exhibit anti-pathogenic properties, showing various antimicrobial and anti-infective activities. (Gibbons, 2004). Plant extracts with MIC values of <1000 µg/mL are often researched further for their activities (Rios & Recio, 2005). A lower concentration is considered for pure compounds. According to Gibbons (2004) and Fabry et al. (1998), pure isolates with MIC values < 64 µg/mL exhibits significant antimicrobial activities but a MIC of < 10 µg/mL must be exhibited by pure compounds before they can be considered as potential clinical trial candidates.

The persistence of drug resistant pathogenic microbes (such as drug-resistant strains of *M. tuberculosis*, methicillin resistant *Staphylococcus aureus* etc.) poses a major problem to public health globally. The prevalence of drug resistant pathogens has been attributed to overuse and misuse of antibiotics (Yong et al., 2009) and unfortunately, majority of conventional antibiotic drugs are now less efficient or showing no activity because they were originally designed for the treatment of pathogens with less complicated disruptive nature (Li & Ma, 2015). These warranted the continual development of new derivative drugs which are often embarked by Improving upon existing therapeutic compounds.

BAA showed similar level of antimicrobial activities with vancomycin against *Bacillus cereus* ATCC 10876 multi- drug resistant strain at a sample: antibiotic concentration of 1:2. The flavonoid and the derivatives showed poor activities against *B. cereus.*

Parent pentacyclic triterpenes (BA (**4**), and UA (**6**)) were inactive against *E. coli*. Acetylated products agreed with known knowledge in literature, and showed fairly improved activity in BAA (**20**) and OAA (**21**), but not UA (**22**). The introduction of additional hydroxyl and C-O made available when two different pentacyclic triterpenes were combined may be responsible for the increased activity.

Pentacyclic triterpenes UA (**6**) and BA (**4**) inhibited the growth of *E. faecalis*, however, OA (**5**) showed no activity. The difference in antibacterial property of UA (**6**) and OA (**5**) against *E. faecalis* was significant. Although UA and OA are isomers, the slight variation due to position of methyl functionality on Ring-E of both compounds might influence antibacterial activities of these compounds against *E. faecalis*. Similarly, MA (**11**), which is an isomer of OA (**5**), exhibited antibacterial activities against *E. faecalis*. The synthesized calix[4]arene was active against the bacteria but there was loss in potency after transformation into derivatives. While the crude of *L. petersonii* was active against E. faecalis, the isolated flavonoid and its

derivatives showed poor or no activity at the tested concentrations. Acetylation of OA (**5**) improved the antimicrobial activity against *E. faecalis* but caused a loss in activity for UA (**6**).

K. pneumonia is highly resistant to multiple drugs. This study found that the crude of *L. petersonii* was active against the tested strain, and performed better than any other synthesized derivative. The purification of pure flavonoid from the plant's crude extract resulted in decreased antimicrobial activity against *K. pneumoniae*. The parent pentacyclic triterpenes showed poor activities against the bacteria, however, the methylated pentacyclic triterpenes showed positive inhibitory properties, thus confirming that alkylation resulted in improved antibacterial actions against *k. pneumonia.*

In addition to UA (**6**) and MA (**11**), the ester-linked combinations of pentacyclic triterpenes constituted the active compounds found to exhibit good activities against *K. pneumonia*. The parent pentacyclic triterpenes generally showed poor antibacterial interactions against *K. pneumoniae*, and the formation of anhydride linkage between other derivatives of combined pentacyclic triterpenes showed poor activities. The different combinations of pentacyclic triterpenes further resulted in variation in level of activity of the synthesized compounds relative to the parent compounds. Overall, acetylation did not show much improvement in the antibacterial activities of the pentacyclic triterpenes and flavonoid.

Pentacyclic triterpenes were weak when tested individually against drug resistant strains of *S. aureus*. The beneficiation of pentacyclic triterpenes to make several derivatives does not improve potency against this microorganism. Earlier studies have established the existence of different mechanistic pathway for activity of pentacyclic triterpenes alone and when combined with other compounds (synergistic studies), hence, further studies can explore these derivatives in combination with standard antibiotics.

Unresolved chromatographed mixtures, such as OA–MA, and OA–BA showed better activity relative to parent OA and BA, but lower activity than MA. Hence, further work should consider mixtures of the triterpenes in varying proportions but at constant concentration to provide further understanding on the cooperative activity of these compounds when not linked chemically via new bond formation.

5.3 Chapter Summary

The antioxidant and antimicrobial activities of the various samples were assessed. The antimicrobial properties were tested against a wide range of gram-positive and gram-negative bacteria. There might have been solvent interference in the bioautography assays, hence the application of broth dilution assays afforded the assessment of antibacterial activity of the compounds. It was observed that MA (**11**) is a potent antioxidant. Other pentacyclic triterpenes

showed activity in the order OA (**5**) > UA (**5**) > BA (**4**), although the order was greatly changed after derivatives of the pentacyclic triterpenes were made. UA (**5**) showed very little peroxyl and ABTS radical reducing potential, with no ferric reducing activity, similarly, UAA (**22**) showed poor to no antioxidant activity, however, the radical scavenging potential was was improved in the case of UAA-UAA conjugate hybrids.

Some derivatives showed some positive antioxidative activities while hybrid combination resulted in loss of activity for others, for example, compound A18 (OAA – BAA) conjugate. Other OA derivatives may be exploited for the antioxidant properties. The parent flavonoid and calixarene compounds showed reduced bioactivities after derivatization.

CHAPTER SIX
CONCLUSIONS AND RECOMMENDATIONS

6.1 Chapter Introduction

This report accounts for efforts made to synthesise some derivatives of PTs, and some preliminary biological studies carried out to assess any potential bioactivity of the derivatives. This section provides concluding summary of the work carried out and highlights some proposed future work.

6.2 Conclusions

PTs were isolated from *Tectona grandis, Syzygium aromaticum, Mimussops caffra, Lavandula angustifolia*, and *Melaleuca salicina*, while a flavonoid compound was isolated from *Leptospermum petersonii*. There are previous studies on biological properties of PTs and 6-methyltectochrysin, but the PT-conjugate derivatives discussed in this work have not been earlier reported. Similar route of synthesis was used to prepare the PT derivatives. The parent PTs and their derivatives were checked for antioxidant properties, and tested *in-vitro* against multi-drug resistant microorganisms.

Proposed structures were given with some preliminary characterization to determine presence of triterpene skeleton in the synthesized derivatives. A major limitation to the synthesis work was low yield thus affecting available sample for multiple assays. The exact structures for the hybrid derivatives have not been claimed within the scope of this work. The formation of such large molecules could be further hindered by steric hindrance and stability issues.

Some PT hybrid combinations were prepared. Some analytical physico-chemical observations were reported. The bioactivities of the synthesized derivatives were compared with the activities of the parent PTs. The presence of hydroxyl at C3 and the carboxylic group at C17 were linked to decreased antimicrobial activities. The parent PTs exhibited lower level of inhibitions relative to derivative products. The standard antibiotics showed a lower inhibition (6%) against the resistant *E-coli* strain. The ester-linked PTs showed the best activity against *E. coli* (about 5 times better than the antibiotic). Some of the anhydride-linked PT-PT conjugates showed positive antibacterial activity compared to the parent PTs. The ester linked PT-PT conjugates were positive inhibitors against *K. pneumoniae* bacterium, whereas anhydride-linked conjugate hybrids showed poor activities.

The crude product of *L. petersonii* showed positive bioactivities, however the purification into pure compound resulted in loss of activity. The flavonoid and its derivatives were generally inactive antimicrobial as shown in this study. Future work might explore the toxicity of the crude

in comparison to the pure flavonoid compound extracted from the plants' leaves. The calixarene and its derivatives exhibited good biological activities, but calixarene and the synthesized compounds were limited due to low solubility in aqueous systems. Further beneficiation and refinement of calixarene to create more soluble and beneficial non-toxic bioactive agents should be reviewed in future studies.

It was found that the bioactivities of the parent pentacyclic triterpenes differ from those of the hybrid products. This may suggest the effects of the combinations on the observed biological activities. Although inventiveness of the derivatives is subjective in the intellectual property discourse, we understand that there have been no previous reports on the disclosed conjugated hybrid derivatives. To the best of our knowledge, no previous studies have considered combinations of such derivative products listed in this work, especially calix[4]arene - triterpenes, or flavonoid - pentacyclic triterpene formulations.

6.3 Recommendations and future work

The use of comprehensive analytical techniques and acquisition of robust data is required for detailed and accurate structural identification and elucidation of the prepared derivatives. Progress was hindered due to limited resources, and the lack of NMR instrument at the host research institution. An exact structural representation of the hybrid derivatives has not claimed within the scope of this work, however, proposed structures were shown, along with some preliminary characterization which determines presence of core reference units in the derivatives. The level of bioactivities obtained was not within the range that would encourage exhaustive structural elucidation at this stage, however, further work listed below could facilitate the drive to pursue such exercise in other studies. Future work might consider:

- Wider range of antimicrobial assays and antisickle-cell studies (on-going).
- Betulinic acid is known for its antitumor activity. The derivatives from this work could be further explored for their anticancer properties
- Exploring synergistic or antagonistic antimicrobial activities of the derivatives in presence of standard antibiotics, as well as toxicity studies.
- "Full-house" and exhaustive spectroscopic analysis of some of the derivative products.

REFERENCES

Abe, F., Yamauchi, T., Nagao, T., Kinjo, J., Okabe, H., Higo, H. & Akahane, H. 2002. Ursolic acid as a trypanocidal constituent in rosemary. *Biol. Pharm. Bull*., 25, p.1485-1487.

Ackermann, A., Karagöz, A.Ç., Ghoochani, A., Buchfelder, M., Eyüpoglu, I., Tsogoeva, S.B. and Savaskan, N. 2017. Cytotoxic profiling of artesunic and betulinic acids and their synthetic hybrid compound on neurons and gliomas. *Oncotarget*, *8*(37), p.61457.

Ahmad, F.B.H., Ghaffari Moghaddam, M., Basri, M. and Abdul Rahman, M.B., 2010. Anticancer activity of 3-O-acylated betulinic acid derivatives obtained by enzymatic synthesis. *Bioscience, biotechnology, and biochemistry*, *74*(5), pp.1025-1029.

Al Qaraghuli, M.M., Alzahrani, A.R., Niwasabutra, K., Obeid, M.A. & Ferro, V.A. 2017. Where traditional drug discovery meets modern technology in the quest for new drugs. Annals of Pharmacology and Pharmaceutics, 2(11), p.1-5.

Anjaneyulu, A.S.R. & Prasad, A.R. 1983. Structure of terminic acid, a dihydroxytriterpene carboxylic acid from Terminalia arjuna. *Phytochemistry*, *22*(4), p.993-998.

Appelbaum, P.C. 1992. Antimicrobial resistance in Streptococcus pneumoniae: an overview. *Clinical Infectious Diseases*, *15*(1), p.77-83.

Aruoma, O.I. 1994. Nutrition and health aspects of free radicals and antioxidants. *Food and Chemical Toxicology*, *32*(7), p.671-683.

Azwanida N.N. 2015. A Review on the Extraction Methods Use in Medicinal Plants, Principle, Strength and Limitation. *Med Aromat Plants*, 4 (3):196, p.1-6. doi:10.4172/2167-0412.1000196

Babalola, I.T. & Shode, F.O. 2013. Ubiquitous ursolic acid: A potential pentacyclic triterpene natural product. *Journal of pharmacognosy and phytochemistry*, 2(2), p.214 – 222.

Basir, D., Julinar, J., Agustriana, E. & Untari, B. 2014. Oxidation and Acetylation of Ursolic and Oleanolic Acids Isolated from Fragraea fragrans fruits; Antiproliferation of P388 Leukemia Cells. *Indonesian Journal of Chemistry*, 14(3), p.269-276.

Benzie, I.F.F. & Strain, J.J. 1996. The ferric reducing ability of plasma (FRAP) as a measure of antioxidant power': the FRAP assay. *Anal Biochem,* 239, p.70–76.

Bhakuni, D.S., Satish, S., Shukla, Y.N. & Tandon, J.S. 1971. Chemical constituents of Diospyros buxifolia, D. tomentosa, D. ferra, D. lotus, Rhus parviflora, Polygonum recumbens, Balanites aegyptiaca and Pyrus pashia. *Phytochemistry*, 10(11), p.2829-2831.

Bhatia, A., Kaur, G. & Sekhon, H. 2015. Anticancerous Efficacy of Betulinic acid: An Immunomodulatory Phytochemical. *Journal of PharmaScience and Technology*, 4(2), p.39-46.

Bignell, D. R., Huguet-Tapia, J. C., Joshi, M. V., Pettis, G. S. & Loria, R. 2010. What does it take to be a plant pathogen: genomic insights from Streptomyces species. *Antonie van Leeuwenhoek*, 98(2), p.179-194.

Bori, I.D., Hung, H.Y., Qian, K., Chen, C.H., Morris-Natschke, S.L. & Lee, K.H. 2012. Anti-AIDS agents 88. Anti-HIV conjugates of betulin and betulinic acid with AZT prepared via click chemistry. Tetrahedron letters, 53(15), pp.1987-1989.

Boudebbouze, S., Coleman, A.W., Tauran, Y., Mkaouar, H., Perret, F., Garnier, A., Brioude, A., Kim, B., Maguin, E. & Rhimi, M. 2013. Discriminatory antibacterial effects of calix [n] arene capped silver nanoparticles with regard to Gram positive and Gram negative bacteria. *Chemical Communications*, 49(64), p.7150-7152.

Braude, E.A. & Nachod, F.C. eds. 2013. Determination of organic structures by physical methods. Elsevier. Academic Press Inc., London. Vol. 1, p.118-124

Brooker, S.G., Cambie, R.C. & Cooper, R.C. 1989. Economic native plants of New Zealand. *Economic botany*, 43(1), p.79-106.

Butler, M.S. 2004. The role of natural product chemistry in drug discovery. *Journal of natural products*, *67*(12), p.2141-2153.

Caragay, A.B. 1992. Cancer preventive foods and ingredients. *Food Technol.*, *4*, p.65-68.

Casnati, A., Fabbi, M., Pelizzi, N., Pochini, A., Sansone, F., Unguro, R., Di Modugno, E. & Tarzia, G. 1996. Synthesis, antimicrobial activity and binding properties of calix [4] arene based vancomycin mimics. *Bioorganic & Medicinal Chemistry Letters*, 6(22), p.2699-2704.

Castro, M.J., Richmond, V., Romero, C., Maier, M.S., Estévez-Braun, A., Ravelo, Á.G., Faraoni, M.B. & Murray, A.P. 2014. Preparation, anticholinesterase activity and molecular docking of new lupane derivatives. *Bioorganic & medicinal chemistry*, 22(13), p.3341-3350.

Chakravarti, B., Maurya, R., Siddiqui, J. A., Bid, H. K., Rajendran, S. M., Yadav, P. P. & Konwar, R. 2012. In vitro anti-breast cancer activity of ethanolic extract of Wrightia tomentosa: role of pro-apoptotic effects of oleanolic acid and ursolic acid. *Journal of ethnopharmacology*, p.142 (1), 72-79.

Chandramu, C., Manohar, R.D., Krupadanam, D.G. & Dashavantha, R.V. 2003. Isolation, characterization and biological activity of betulinic acid and ursolic acid from Vitex negundo L. *Phytotherapy research*, 17(2), p.129-134.

Chen, Q. H., Liu, J., Zhang, H. F., He, G. Q. & Fu, M. L. (2009). The betulinic acid production from betulin through biotransformation by fungi. *Enzyme and Microbial Technology*, 45(3), p.175-180.

Chouna, J.R., Tamokou, J.D.D., Nkeng-Efouet-Alango, P., Lenta, B.N. & Sewald, N. 2015. Antimicrobial triterpenes from the stem bark of Crossopteryx febrifuga. *Zeitschrift für Naturforschung C*, *70*(7-8), p.169-173.

Chung, P.Y., Navaratnam, P. & Chung, L.Y. 2011. Synergistic antimicrobial activity between pentacyclic triterpenoids and antibiotics against Staphylococcus aureus strains. *Annals of Clinical Microbiology and Antimicrobials*, 10(1), p.25.

Cloete, T.E. 2003. Resistance mechanisms of bacteria to antimicrobial compounds. *International Biodeterioration & Biodegradation*, 51(4), p.277-282.

Cowan, M.M. 1999. Plant products as antimicrobial agents. *Clinical microbiology reviews*, *12*(4), p.564-582.

Daglia, M. 2012. Polyphenols as antimicrobial agents. *Current opinion in biotechnology*, *23*(2), p.174-181.

De Carvalho, M.G., Cranchi, D.C. & De Carvalho, A.G. 1996. Chemical constituents from Pinus strobus var. chiapensis. *J Braz Chem Soc*, 7(3), p.187-191.

De Carvalho, M.G., Cranchi, D.C. and De Carvalho, A.G., 1996. Chemical constituents from Pinus strobus var. chiapensis. *J Braz Chem Soc*, *7*(3), pp.187-191.

de Fatima, Â., Fernandes, S.A. & Sabino, A.A. 2009. Calixarenes as new platforms for drug design. *Current Drug Discovery Technologies*, *6*(2), p.151-170.

del Carmen Recio, M., Giner, R.M., Manez, S., Gueho, J., Julien, H.R., Hostettmann, K. & Rios, J.L. 1995. Investigations on the steroidal anti-inflammatory activity of triterpenoids from Diospyros leucomelas. Planta medica, 61(01), pp.9-12.

do Nascimento, P.G., Lemos, T.L., Bizerra, A., Arriaga, A., Ferreira, D.A., Santiago, G.M., Braz-Filho, R. & Costa, J.G.M. 2014. Antibacterial and antioxidant activities of ursolic acid and derivatives. *Molecules*, 19(1), p.1317-1327.

Ellis, W.Y., Lim, P. and Maniar, M. 2009. *Methods for the formulation and manufacture of artesunic acid for injection*. U.S. Patent Application 12/315,209.

European Committee for Antimicrobial Susceptibility Testing (EUCAST) of the European Society of Clinical Microbiology and Infectious Diseases (ESCMID). (2003). Determination of minimum inhibitory concentrations (MICs) of antibacterial agents by broth dilution. Clinical Microbiology and Infection, 9(8), pp.ix-xv.

Fabry, W., Okemo, P.O. & Ansorg, R. 1998. Antibacterial activity of East African medicinal plants. *Journal of Ethnopharmacology*, 60(1), p.79-84.

Fan, W. W., Yuan, G. Q., Li, Q. Q. & Lin, W. 2014. Antibacterial mechanisms of methyl gallate against Ralstonia solanacearum. *Australasian Plant Pathology*, 43(1), p.1-7.

Feng, H., Li, Y. & Liu, Q. 2013. Endophytic bacterial communities in tomato plants with differential resistance to Ralstonia solanacearum. *African Journal of Microbiology Research*, 7(15), p.1311-1318.

Ferrer-Gallego, R., Pérez-Gregorio, R., Hernández-Hierro, J.M., Quijada-Morín, N. & García-Estévez, I. 2017. Polyphenols and Food Quality. *Journal of Food Quality*, 2017, p.1-2.

Fontanay, S., Grare, M., Mayer, J., Finance, C. & Duval, R.E. 2008. Ursolic, oleanolic and betulinic acids: antibacterial spectra and selectivity indexes. *Journal of ethnopharmacology*, *120*(2), p.272-276.

Fukushima, E.O., Seki, H., Ohyama, K., Ono, E., Umemoto, N., Mizutani, M., Saito, K. & Muranaka, T. 2011. CYP716A subfamily members are multifunctional oxidases in triterpenoid biosynthesis. *Plant and Cell Physiology*, 52(12), p.2050-2061.
Gibbons, S. 2004. Anti-staphylococcal plant natural products. *Natural product reports*, 21(2), p.263-277.

Gnoatto, S.C., Susplugas, S., Dalla Vechia, L., Ferreira, T.B., Dassonville-Klimpt, A., Zimmer, K.R., Demailly, C., Da Nascimento, S., Guillon, J., Grellier, P. & Verli, H. 2008. Pharmacomodulation on the 3-acetylursolic acid skeleton: Design, synthesis, and biological evaluation of novel N-{3-[4-(3-aminopropyl) piperazinyl] propyl}-3-O-acetylursolamide derivatives as antimalarial agents. *Bioorganic & medicinal chemistry*, *16*(2), p.771-782.

Guo, Z. 2017. The modification of natural products for medical use. *Acta Pharmaceutica Sinica B*, 7(2), p.119-136.

Gutsche, C.D., Dhawan, B., No, K.H. & Muthukrishnan, R. 1981. Calixarenes. 4. The synthesis, characterization, and properties of the calixarenes from p-tert-butylphenol. *Journal of the American Chemical Society*, 103(13), p.3782-3792.

Guvench, O. 2016. Computational functional group mapping for drug discovery. *Drug discovery today*, *21*(12), p.1928-1931.

Haberlein, H. & Tschiersch, K.P. 1994. Triterpenoids and flavonoids from Leptospermum scoparium. *Phytochemistry*, 35(3), p.765-768.

Haddad, R., Milagre, H.M., Catharino, R.R. & Eberlin, M.N. 2008. Easy ambient sonic-spray ionization mass spectrometry combined with thin-layer chromatography. *Analytical Chemistry*, *80*(8), p.2744-2750.

Halabalaki, M., Vougogiannopoulou, K., Mikros, E. & Skaltsounis, A.L., 2014. Recent advances and new strategies in the NMR-based identification of natural products. Current opinion in biotechnology, 25, pp.1-7.

Halliwell, B. 2007. Biochemistry of oxidative stress. *Biochemical Society Transactions*, 35(5), p.1147-1150. DOI: 10.1042/BST0351147

Halliwell, B., Aeschbach, R., Löliger, J. & Aruoma, O.I. 1995. The characterization of antioxidants. *Food and Chemical Toxicology*, *33*(7), p.601-617.

Haque, A., Siddiqi, M.M.A., Rahman, A.M., Hasan, C.M. & Chowdhury, A.S., 2013. Isolation of Betulinic Acid and 2, 3-Dihydroxyolean-12-en-28-oic Acid from the Leaves of Callistemon linearis. *Dhaka University Journal of Science*, *61*(2), p.211-212.

Hashimoto, F., Kashiwada, Y., Cosentino, L. M., Chen, C. H., Garrett, P. E. & Lee, K. H. 1997. Anti-AIDS agents—XXVII. Synthesis and anti-HIV activity of betulinic acid and dihydrobetulinic acid derivatives. *Bioorganic & medicinal chemistry*, 5(12), p.2133-2143.

Hazra, K.M., Roy, R.N., Sen, S.K. & Laskar, S. 2007. Isolation of antibacterial pentahydroxy flavones from the seeds of Mimusops elengi Linn. *African journal of Biotechnology*, *6*(12), pp. 1446-1449.

Herrera, M.D., Rodríguez-Rodríguez, R. & Ruiz-Gutiérrez, V. 2006. Functional Properties of Pentacyclic Triterpenes Contained in “Orujo” Olive oil. Current Nutrition & Food Science, 2(1), p.45-49.

Hood, J.R., Burton, D.M., Wilkinson, J.M. & Cavanagh, H.M.A. 2010. The effect of Leptospermum petersonii essential oil on Candida albicans and Aspergillus fumigatus. *Medical mycology*, *48*(7), p.922-931.

Horiuchi, K., Shiota, S., Hatano, T., Yoshida, T., Kuroda, T. & Tsuchiya, T. 2007. Antimicrobial activity of oleanolic acid from Salvia officinalis and related compounds on vancomycin-resistant enterococci (VRE). *Biological and Pharmaceutical Bulletin*, *30*(6), p.1147-1149.

Hossain, M.A. & Ismail, Z. 2013. Isolation and characterization of triterpenes from the leaves of Orthosiphon stamineus. *Arabian Journal of Chemistry*, 6(3), p.295-298.

Huang, L., Luo, H., Li, Q., Wang, D., Zhang, J., Hao, X. & Yang, X. 2015. Pentacyclic triterpene derivatives possessing polyhydroxyl ring A inhibit Gram-positive bacteria growth by regulating metabolism and virulence genes expression. *European journal of medicinal chemistry*, 95, p.64-75.

Hughes, D. & Karlen, A. 2014. Discovery and preclinical development of new antibiotics. *Upsala journal of medical sciences*, 119(2), p.162-169.

Jachak, S. M. & Saklani, A. 2007. Challenges and opportunities in drug discovery from plants. *Current Science-Bangalore*, 92(9), p.1251-1257.

Jaganathan, J.R., Sivapragasam, M. and Wilfred, C.D., 2016. Thermal characteristics of 1-butyl-3-methylimimidazolium based oxidant ionic liquids. *Journal of Chemical Engineering & Process Technology*, *7*, p.32.

Jager, S., Trojan, H., Kopp, T., Laszczyk, M. N. & Scheffler, A. 2009. Pentacyclic triterpene distribution in various plants–rich sources for a new group of multi-potent plant extracts. *Molecules*, 14(6), p.2016-2031.

JC Furtado, N., Pirson, L., Edelberg, H., M Miranda, L., Loira-Pastoriza, C., Preat, V., Larondelle, Y. and André, C., 2017. Pentacyclic triterpene bioavailability: an overview of in vitro and in vivo studies. *Molecules*, *22*(3), p.400.

Joshi, H., Saxena, G. K., Singh, V., Arya, E. & Singh, R. P. 2013. Phytochemical investigation, isolation and characterization of betulin from bark of Betula utilis. *Journal of Pharmacognosy and Phytochemistry*, 2(1), p.145-151.

Juan, M.E., Planas, J.M., Ruiz-Gutierrez, V., Daniel, H. & Wenzel, U. 2008. Antiproliferative and apoptosis-inducing effects of maslinic and oleanolic acids, two pentacyclic triterpenes from olives, on HT-29 colon cancer cells. *British Journal of Nutrition*, 100(1), p.36-43.

Kamaraj, C., Rahuman, A.A., Siva, C., Iyappan, M. & Kirthi, A.V. 2012. Evaluation of antibacterial activity of selected medicinal plant extracts from south India against human pathogens. *Asian Pacific Journal of Tropical Disease*, 2, p.S296-S301.

Kanamoto, T., Kashiwada, Y., Kanbara, K., Gotoh, K., Yoshimori, M., Goto, T., Sano, K. & Nakashima, H. 2001. Anti-human immunodeficiency virus activity of YK-FH312 (a betulinic acid derivative), a novel compound blocking viral maturation. Antimicrobial agents and chemotherapy, 45(4), pp.1225-1230.

Kashiwada, Y., Hashimoto, F., Cosentino, L. M., Chen, C. H., Garrett, P. E. & Lee, K. H. 1996. Betulinic Acid and Dihydrobetulinic Acid Derivatives as Potent Anti-HIV Agents 1. *Journal of medicinal chemistry*, 39(5), p.1016-1017.

Kashiwada, Y., Chiyo, J., Ikeshiro, Y., Nagao, T., Okabe, H., Cosentino, L. M., Fowke, K., Natschke, S. L. M. & Lee, K. H. 2000. Synthesis and anti-HIV activity of 3-alkylamido-3-deoxy-betulinic acid derivatives. *Chemical and pharmaceutical bulletin*, 48(9), p.1387-1390.

Kau, A.L., Martin, S.M., Lyon, W., Hayes, E., Caparon, M.G. & Hultgren, S.J. 2005. Enterococcus faecalis tropism for the kidneys in the urinary tract of C57BL/6J mice. *Infection and immunity*, 73(4), p.2461-2468.

Kaur, C. & Kapoor, H.C. 2001. Antioxidants in fruits and vegetables–the millennium's health. *International journal of food science & technology*, 36(7), p.703-725.

Khwaza, V., Oyedeji, O. & Aderibigbe, B. 2018. Antiviral Activities of Oleanolic Acid and Its Analogues. *Molecules*, 23(9), p.2300.

Kojima, H., Tominaga, H., Sato, S. and Ogura, H., 1987. Pentacyclic triterpenoids from Prunella vulgaris. *Phytochemistry*, *26*(4), pp.1107-1111.

Koparde, A. A., Doijad, R. C., & Magdum, C. S. (2019). Natural Products in Drug Discovery. In *Pharmacognosy-Medicinal Plants*. IntechOpen. DOI: 10.5772/intechopen.82860

Kowalski, R. 2007. Studies of Selected Plant Raw Materials as Alternative Sources of Triterpenes of Oleanolic and Ursolic Acid Types. *Journal of Agricultural and Food Chemistry*, 55(3), p. 656-662.

Krasutsky, P. A. 2006. Birch bark research and development. *Natural product reports*, 23(6), p.919-942.

Kuete, V., Alibert-Franco, S., Eyong, K.O., Ngameni, B., Folefoc, G.N., Nguemeving, J.R., Tangmouo, J.G., Fotso, G.W., Komguem, J., Ouahouo, B.M.W. & Bolla, J.M. 2011. Antibacterial activity of some natural products against bacteria expressing a multidrug-resistant phenotype. *International journal of antimicrobial agents*, 37(2), p.156-161.

Kumar, Y.P., King, P. & Prasad, V.S.R.K. 2006. Zinc biosorption on Tectona grandis Lf leaves biomass: equilibrium and kinetic studies. *Chemical engineering journal*, *124*(1-3), p.63-70.

Kwan, E.E. & Huang, S.G. 2008. Structural elucidation with NMR spectroscopy: practical strategies for organic chemists. *European journal of organic chemistry*, *2008*(16), p.2671-2688.

Labib, R.M., Ebada, S.S., Youssef, F.S., Ashour, M.L. and Ross, S.A., 2016. Ursolic acid, a natural pentacylcic triterpene from Ochrosia elliptica and its role in the management of certain neglected tropical diseases. *Pharmacognosy magazine*, *12*(48), p.319.

Laszczyk, M.N. 2009. Pentacyclic triterpenes of the lupane, oleanane and ursane group as tools in cancer therapy. *Planta medica*, *75*(15), p.1549-1560.

Leonti, M., Stafford, G.I., Dal Cero, M., Cabras, S., Castellanos, M.E., Casu, L. & Weckerle, C.S. 2017. Reverse ethnopharmacology and drug discovery. *Journal of ethnopharmacology*, *198*, p.417-431.

Liu, J. 1995. Pharmacology of oleanolic acid and ursolic acid. *Journal of ethnopharmacology*, 49(2), p.57-68.

Lin, Y., Vermeer, M. A. & Trautwein, E. A. 2011. Triterpenic acids present in hawthorn lower plasma cholesterol by inhibiting intestinal ACAT activity in hamsters. *Evidence-Based Complementary and Alternative Medicine*, p.1-9.

Li, X. & Ma, S. 2015. Advances in the discovery of novel antimicrobials targeting the assembly of bacterial cell division protein FtsZ. *European journal of medicinal chemistry*, 95, p.1-15.

Li, H., Zhong, Y., Wu, W., Zhang, L., Lai, X. and Zeng, X., 2017. Phenolic antioxidants based on calixarene: Synthesis, structural characterization, and antioxidative properties in natural rubber. *Journal of Applied Polymer Science*, *134*(31), p.45144.

Li, W-W. and Zhang, Z-T. 2018. Synthesis, crystal structure and antitumor activity of tectochrysin-6-sulfonate. *Structural Chemistry*, 2018, pp.97-104.

Makwana, B.A., Vyas, D.J., Bhatt, K.D., Jain, V.K. & Agrawal, Y.K. 2015. Highly stable antibacterial silver nanoparticles as selective fluorescent sensor for Fe 3+ ions. Spectrochimica Acta Part A. *Molecular and Biomolecular Spectroscopy*, 134, p.73-80.

Mallavadhani, U. V., Panda, A. K. & Rao, Y. R. 2001. Diospyros melanoxylon Leaves: A Rich Source of Pentacyclic Triterpenes. *Pharmaceutical Biology*, 39(1), p.20–24.

Manayi, A., Nikan, M., Nobakht-Haghighi, N. and Abdollahi, M., 2018. Advances in the anticancer value of the ursolic acid through nanodelivery. *Current medicinal chemistry*, *25*(37), pp.4866-4875.

Mayer, R. 1990. Flavonoids from Leptospermum scoparium. *Phytochemistry*, 29(4), p.1340-1342.

Mbaze, L.M.A., Poumale, H.M.P., Wansi, J.D., Lado, J.A., Khan, S.N., Iqbal, M.C., Ngadjui, B.T. & Laatsch, H. 2007. α-Glucosidase inhibitory pentacyclic triterpenes from the stem bark of Fagara tessmannii (Rutaceae). *Phytochemistry*, 68(5), p.591-595.

Moellering, R.C. 2011. Discovering new antimicrobial agents. *International journal of antimicrobial agents*, *37*(1), p.2-9.

Montilla, M.P., Agil, A., Navarro, M.C., Jiménez, M.I., García-Granados, A., Parra, A. & Cabo, M.M. 2003. Antioxidant activity of maslinic acid, a triterpene derivative obtained from Olea europaea. *Planta medica*, *69*(05), p.472-474.

Moreira, V. M., Salvador, J. A., Simões, S., Destro, F. & Gavioli, R. 2013. Novel oleanolic vinyl boronates: synthesis and antitumor activity. *European journal of medicinal chemistry*, 63, p.46-56.

MR de Melo, M., MA Domingues, R., JD Silvestre, A. & M Silva, C. 2014. Extraction and purification of triterpenoids using supercritical fluids: from lab to exploitation. *Mini-Reviews in Organic Chemistry*, *11*(3), p.362-381.

Munoz-Price, L.S., Poirel, L., Bonomo, R.A., Schwaber, M.J., Daikos, G.L., Cormican, M., Cornaglia, G., Garau, J., Gniadkowski, M., Hayden, M.K. & Kumarasamy, K. 2013. Clinical epidemiology of the global expansion of Klebsiella pneumoniae carbapenemases. *The Lancet infectious diseases*, 13(9), p.785-796.

Nazaruk, J. & Borzym-Kluczyk, M. 2015. The role of triterpenes in the management of diabetes mellitus and its complications. *Phytochemistry Reviews*, *14*(4), p.675-690.

Nazzaro, F., Fratianni, F., Granese, T., Cozzolino, A., Maione, M., Ombra, M. N. & Coppola, R. 2013. Antimicrobial property of the hydro-alcoholic extract from purple basil (Ocimum basilicum var. purpurascens). *Worldwide Research Efforts in the Fighting Against Microbial Pathogens*, p.68-71.

Newman, D.J. & Cragg, G.M. 2016. Natural products as sources of new drugs from 1981 to 2014. *J. Nat. Prod*, *79*(3), p.629-661.

Nidavani, R.B. & Mahalakshmi, A.M. 2014. Teak (tectona grandis linn.): A renowned timber plant with potential medicinal values. *Inter J Pharm Pharm Sci*, *6*(1), p.48-54.

Pai, S. R. & Joshi, R. K. 2014. Distribution of betulinic acid in plant kingdom. *Plant Science Today*, 1(3), p.103-107.

Paterson, I. and Anderson, E.A., 2005. The renaissance of natural products as drug candidates. *Science*, *310*(5747), pp.451-453.

Patocka, J., 2003. Biologically active pentacyclic triterpenes and their current medicine signification. *J Appl Biomed*, *1*(1), pp.7-12.

Paul, S., Emmanuel, T., Matchawe, C., Alembert, T.T., Elisabeth, Z.O.M., Sophie, L., Luce, V.E., Maurice, T.F., Joel, Y.G.A., Atchade, D.T.A. & Joseph, M.T., 2014. Pentacyclic triterpenes and crude extracts with antimicrobial activity from Cameroonian brown propolis samples. *J App Pharm Sci*, 4(07), p.001-009.

Pavel, I.Z., Danciu, C., Oprean, C., Dehelean, C.A., Muntean, D., Csuk, R. & Muntean, D.M. 2016. In vitro evaluation of the antimicrobial ability and cytotoxicity on two melanoma cell lines of a benzylamide derivative of maslinic acid. *Analytical Cellular Pathology*, p.*2016*.

Pinto, E., Vale-Silva, L., Cavaleiro, C. & Salgueiro, L. 2009. Antifungal activity of the clove essential oil from Syzygium aromaticum on Candida, Aspergillus and dermatophyte species. *Journal of medical microbiology*, *58*(11), p.1454-1462.

Pisha, E., Chai, H., Lee, I. S., Chagwedera, T. E., Farnsworth, N. R., Cordell, G. A., Beecher, C. W., Fong, H. S., Kinghorn, A. D., Brown, D. M., Wani, M. C., Wall, M. E., Heiken, T. J., Gupta, T. K. &

Pezzuto, J. M. 1995. Discovery of betulinic acid as a selective inhibitor of human melanoma that functions by induction of apoptosis. *Nature medicine*, 1(10), p.1046-1051.

Pollier, J. & Goossens, A. 2012. Oleanolic acid. *Phytochemistry*, 77, p.10-15.

Pollier, J., Moses, T. & Goossens, A. 2011. Combinatorial biosynthesis in plants: a (p) review on its potential and future exploitation. *Natural product reports*, 28(12), p.1897-1916.

Pretsch, E., Buehlmann, P., Affolter, C., Pretsch, E., Bhuhlmann, P. & Affolter, C. 2000. *Structure determination of organic compounds*. 4th ed. Springer-Verlag Berlin Heidelberg, p.108

Qiu, W. W., Shen, Q., Yang, F., Wang, B., Zou, H., Li, J. Y., Li, J. & Tang, J. 2009. Synthesis and biological evaluation of heterocyclic ring-substituted maslinic acid derivatives as novel inhibitors of protein tyrosine phosphatase 1B. *Bioorganic & medicinal chemistry letters*, 19(23), p.6618-6622.

Ragasa, C.Y., Ng, V.A.S., Ebajo Jr, V.D., Fortin, D.R., De Los Reyes, M.M. & Shen, C.C. 2014. Triterpenes from *Shorea negrosensis*. *Der Pharmacia Lettre*, 6 (6), p.453-458.

Rainsford, K.D., Powanda, M.C. & Whitehouse, M.W. 2015. Novel Natural Products: Therapeutic Effects on Pain, Arthritic and Gastrointestinal Diseases. Springer Basel Heidelberg, New York Dordrecht, London, p.133-153.

Rali, S., Oyedeji, O.O., Aremu, O.O., Oyedeji, A.O. & Nkeh-Chungag, B.N. 2016. Semisynthesis of derivatives of oleanolic acid from Syzygium aromaticum and their antinociceptive and anti-inflammatory properties. *Mediators of inflammation,* (2016). Available at http://dx.doi.org/10.1155/2016/8401843.

Ramírez-Espinosa, J.J., Rios, M.Y., Paoli, P., Flores-Morales, V., Camici, G., de la Rosa-Lugo, V., Hidalgo-Figueroa, S., Navarrete-Vázquez, G. & Estrada-Soto, S. 2014. Synthesis of oleanolic acid derivatives: In vitro, in vivo and in silico studies for PTP-1B inhibition. *European journal of medicinal chemistry*, *87*, p.316-327.

Rao, L. R, Rao, C.S. & Ramaiah, T.S. 1966. The Chemical Examination of *Diospyros* Species. *Current Science*, 35, p.457-458.

Rather, I.A., Kim, B.C., Bajpai, V.K. & Park, Y.H. 2017. Self-medication and antibiotic resistance: Crisis, current challenges, and prevention. *Saudi journal of biological sciences*, *24*(4), p.808-812.

Raza, R, Ilyas, Z., Ali, S. & Nisar, M. 2015. Identification of Highly Potent and Selective α-Glycoside inhibitors with antiglycation potential, isolated from Rhododendron arboretum. *Rec. Nat. Prod*. 9:2, p.262-266.

Re, R., Pellegrini, N., Proteggente, A., Pannala, A., Yang, M. & Rice-Evans, C. 1999. Antioxidant activity applying an improved ABTS radical cation decolorization assay. *Free Radic Biol Med* 26, p.1231–7.

Reutrakul, V., Anantachoke, N., Pohmakotr, M., Jaipetch, T., Yoosook, C., Kasisit, J., Napaswa, C., Panthong, A., Santisuk, T., Prabpai, S. & Kongsaeree, P. 2010. Anti-HIV-1 and Anti-Inflammatory Lupanes from the Leaves, Twigs, and Resin of Garcinia hanburyi. Planta medica, 76(04), pp.368-371.

Rios, J. L. & Recio, M. C. 2005. Medicinal plants and antimicrobial activity. *Journal of ethnopharmacology*, 100(1), p.80-84.

Rivero-Cruz, J.F., Zhu, M., Kinghorn, A.D. and Wu, C.D., 2008. Antimicrobial constituents of Thompson seedless raisins (Vitis vinifera) against selected oral pathogens. *Phytochemistry Letters*, *1*(3), pp.151-154.

Robertson, A., Soliman, G. & Owen, E. C. 1939. Polyterpenoid compounds. Part I. Betulic acid from Cornus florida, L. *Journal of the Chemical Society*, p.1267-1273.

Rosenau, T., Potthast, A., Hofinger, A. and Kosma, P., 2002. Calixarene-type macrocycles by oxidation of phenols related to vitamin E. *Angewandte Chemie International Edition*, *41*(7), pp.1171-1173.

Rufaro Mabande, E. 2018. Antimicrobial discovery from South African marine algae. Masters theis, University of the Western Cape, p.49.

Rufino-Palomares, E.E., Pérez-Jiménez, A., J Reyes-Zurita, F., García-Salguero, L., Mokhtari, K., Herrera-Merchán, A., P Medina, P., Peragón, J. & A Lupianez, J., 2015. Anti-cancer and anti-angiogenic properties of various natural pentacyclic tri-terpenoids and some of their chemical derivatives. Current Organic Chemistry, 19(10), pp.919-947.

Saha, M.R., Hasan, S.M.R., Akter, R., Hossain, M.M., Alam, M.S., Alam, M.A. & Mazumder, M.E.H., 2008. In vitro free radical scavenging activity of methanol extract of the leaves of Mimusops elengi Linn. *Bangladesh Journal of Veterinary Medicine*, *6*(2), p.197-202.

Saratha, V., Iyyam Pillai, S. & Subramanian, S. 2011. Isolation and characterization of lupeol, a triterpenoid from Calotropis gigantea latex. *International Journal of Pharmaceutical Sciences Review and Research*, 10(2), p.54-57.

Segneanu, A.E. Gozescu, I. Dabici, A. Sfirloaga, P. & Szabadai, Z. 2012. Organic Compounds FT-IR Spectroscopy. *Macro To Nano Spectroscopy*, Dr. Jamal Uddin (Ed.), ISBN: 978-953-510664-7, InTech, Croatia, p.145-164. Available from: http://www.intechopen.com/books/macro-to-nano-spectroscopy/organiccompounds-ft-ir-spectroscopy

Sell, H.M. & Kremers, R.E. 1938a. The Synthesis of Esters of Ursolic ACID. *Journal of Biological Chemistry*, 125(2), p.451-453.

Sell, H.M. & Kremers, R.E. 1938b. The methylation of ursolic acid. *Journal of Biological Chemistry*, 126(2), p.501-503.

Shahidi, F. 1997. *Natural antioxidants: chemistry, health effects, and applications*. The American Oil Chemists Society, AOCS press, Champaign, Illinois, p.601-617.

Sharifi-Rad, J., Salehi, B., Varoni, E.M., Sharopov, F., Yousaf, Z., Ayatollahi, S.A., Kobarfard, F., Sharifi-Rad, M., Afdjei, M.H., Sharifi-Rad, M. & Iriti, M. 2017. Plants of the Melaleuca genus as antimicrobial agents: from farm to pharmacy. *Phytother. Res*., 31: 1475–1494. doi: 10.1002/ptr.5880.

Sharma, H., Kumar, P., Deshmukh, R.R., Bishayee, A. and Kumar, S., 2018. Pentacyclic triterpenes: New tools to fight metabolic syndrome. *Phytomedicine*.

Sheng, H. & Sun, H. 2011. Synthesis, biology and clinical significance of pentacyclic triterpenes: a multi-target approach to prevention and treatment of metabolic and vascular diseases. *Natural product reports*, *28*(3), p.543-593.

Siddique, H.R. & Saleem, M. 2011. Beneficial health effects of lupeol triterpene: a review of preclinical studies. *Life sciences*, 88(7-8), p.285-293.

Silva, M., David, J. P., Silva, L. C., Santos, R. A., David, J. M., Lima, L. S., Reis, P. S., & Fontana, R. 2012. Bioactive oleanane, lupane, and ursane triterpene acid derivatives. *Molecules*, 17(10), p.12197-12205.

Simelane, M.B., Shonhai, A., Shode, F.O., Smith, P., Singh, M. & Opoku, A.R. 2013. Anti-Plasmodial Activity of some Zulu medicinal plants and of some triterpenes isolated from them. *Molecules*, *18*(10), p.12313-12323.

Singh, S., Singh, S.K., Chowdhury, I. & Singh, R. 2017. Understanding the Mechanism of Bacterial Biofilms Resistance to Antimicrobial Agents. *The open microbiology journal*, *11*, p.53.

Smina, T.P., Mathew, J., Janardhanan, K.K. & Devasagayam, T.P.A. 2011. Antioxidant activity and toxicity profile of total triterpenes isolated from Ganoderma lucidum (Fr.) P. Karst occurring in South India. *Environmental toxicology and pharmacology*, *32*(3), p.438-446.

Şoica, C. M., Dehelean, C. A., Peev, C. I., Coneac, G., & Gruia, A. T. 2008. Complexation with hydroxypropyl-γ-cyclodextrin of some pentacyclic triterpenes. Characterisation of their binary products. *Farmacia*, LVI(2), p.182-190.

Sommerwerk, S. & Csuk, R. 2014. Convenient and chromatography-free partial syntheses of maslinic acid and augustic acid. *Tetrahedron Letters*, 55(37), p.5156-5158.

Spivak, A.Y., Nedopekina, D.A., Shakurova, E.R., Khalitova, R.R., Gubaidullin, R.R., Odinokov, V.N., Dzhemilev, U.M., Bel'skii, Y.P., Bel'skaya, N.V., Stankevich, S.A. & Korotkaya, E.V. 2013. Synthesis of lupane triterpenoids with triphenylphosphonium substituents and studies of their antitumor activity. *Russian Chemical Bulletin*, *62*(1), p.188-198.

Spivak, A.Y., Nedopekina, D.A., Khalitova, R.R., Gubaidullin, R.R., Odinokov, V.N., Bel'skii, Y.P., Bel'skaya, N.V. & Khazanov, V.A. 2017. Triphenylphosphonium cations of betulinic acid derivatives: synthesis and antitumor activity. *Medicinal Chemistry Research*, *26*(3), p.518-531.

Sporn, M. B., Liby, K. T., Yore, M. M., Fu, L., Lopchuk, J. M., & Gribble, G. W. 2011 New synthetic triterpenoids: potent agents for prevention and treatment of tissue injury caused by inflammatory and oxidative stress. *Journal of natural products*, 74(3), p.537-545.

Stohs, S. J., Miller, H. & Kaats, G. R. 2012. A review of the efficacy and safety of banaba (Lagerstroemia speciosa L.) and corosolic acid. *Phytotherapy Research*, 26(3), p.317-324.

Suleiman, M.M., McGaw, L.I., Naidoo, V. & Eloff, J., 2010. Detection of antimicrobial compounds by bioautography of different extracts of leaves of selected South African tree species. African Journal of Traditional, Complementary and Alternative Medicines, 7(1), p.64-78

Szakiel, A., Grzelak, A., Dudek,P. & Janiszowska, W. 2005. Biosynthesis of oleanolic acid and its glycosides in Calendula offıcinalis suspension culture. *Plant Physiology and Biochemistry*, 41, p.271–275.

Szakiel, A., Pączkowski, C., Pensec, F. & Bertsch, C. 2012. Fruit cuticular waxes as a source of biologically active triterpenoids. Phytochemistry Reviews, 11(2-3), p.263-284.

Sultana, N. and Ata, A., 2008. Oleanolic acid and related derivatives as medicinally important compounds. *Journal of enzyme inhibition and medicinal chemistry*, *23*(6), pp.739-756.

Szent-Gyorgyi, A. 1963. Lost in the twentieth century. *Annual review of biochemistry*, 32(1), p.1-15.

Tezuka, Y., Stampoulis, P., Banskota, A.H., Awale, S., Tran, K.Q., Saiki, I. & Kadota, S. 2000. Constituents of the Vietnamese medicinal plant Orthosiphon stamineus. *Chemical and Pharmaceutical Bulletin*, 48(11), p.1711-1719.

Thimmappa, R., Geisler, K., Louveau, T., O'Maille, P. & Osbourn, A. 2014. Triterpene biosynthesis in plants. *Annual review of plant biology*, 65, p.225-257.

Umehara, K., Takagi, R., Kuroyanagi, M., Ueno, A., Taki, T. & Chen, Y.J. 1992. Studies on differentiation-inducing activities of triterpenes. *Chemical and pharmaceutical bulletin*, 40(2), p.401-405.

University of Granada. 2007. Compound from Olive-pomace Oil Inhibits HIV Spread. ScienceDaily. Retrieved January 26, 2018 from www.sciencedaily.com/releases/2007/07/070709111536.htm

Uysal Akku¸, G., Al, E. & Korcan, S.E. 2015. Selective extraction of toxic heavy metals and biological activity studies using pyrimidylthioamide functionalised calix [4] arene. *Supramolecular Chemistry*, 27(7-8), p.522-526.

Vagi, E., Rapavi, E., Hadolin, M., Vasarhelyine Peredi, K., Balazs, A., Blazovics, A. & Simandi, B. 2005. Phenolic and triterpenoid antioxidants from Origanum majorana L. herb and extracts obtained with different solvents. *Journal of agricultural and food chemistry*, *53*(1), p.17-21.

Vázquez, L. H., Palazon, J. & Navarro-Ocaña, A. 2012. The pentacyclic triterpenes α-, β-amyrins: A review of sources and biological activities. *Phytochemicals-A Global Perspective of Their Role in Nutrition and Health*, 23, p.487-502.

Vicini, P., Fields, O., Lai, E., Litwack, E.D., Martin, A.M., Morgan, T.M., Pacanowski, M.A., Papaluca, M., Perez, O.D., Ringel, M.S. & Robson, M. 2016. Precision medicine in the age of big data: The present and future role of large-scale unbiased sequencing in drug discovery and development. *Clinical Pharmacology & Therapeutics*, *99*(2), p.198-207.

Wang, B. & Jiang, Z.H. 1992. Studies on oleanolic acid. *Chinese Pharmaceutical Journal*, 27, p.393-397.

Wang, X., Perumalsamy, H., Kwon, H.W., Na, Y.E. & Ahn, Y.J. 2015. Effects and possible mechanisms of action of acacetin on the behavior and eye morphology of Drosophila models of Alzheimer's disease. *Scientific reports*, 5, p.16127.

Wang, Z., Li, L., Jiang, Y., Liu, Y. and Liang, H., 2019. Oleanolic acid: Biological activities and therapeutic potential in chronic diseases. *system*, *11*, pp.49-52.

Wegner, S., Wambaugh, J., Ring, C. & Dix, D.J. 2016. High-Throughput Screening Provides an Opportunity to Predict the Potential for Additive Endocrine Bioactivity from Cumulative Chemical Exposures. *Endocrine Disrupting Chemicals*, p.04

WHO, (World Health Organization). 2014. *Antimicrobial resistance: global report on surveillance*. World Health Organization. Retrieved June 15, 2017 from http://apps.who.int/iris/bitstream/10665/112642/1/9789241564748_eng.pdf

Wicht, M. M. 2007. Oleanic acid: its isolation and derivatisation to potential antimicrobial compounds. *CPUT Theses & Dissertations*. Paper 347. http://dk.cput.ac.za/td_cput/347

Woo, K.W., Han, J.Y., Choi, S.U., Kim, K.H. & Lee, K.R. 2014. Triterpenes from Perilla frutescens var. acuta and their cytotoxic activity. *Natural Product Sciences*, 20(2), p.71-75.

Woznicka, E., Pieniążek, E., Zapała, L., Trojnar, I. & Kopacz, M. 2015. New sulfonic derivatives of quercetin as complexing reagents: synthesis, spectral, and thermal characterization. *Journal of Thermal Analysis and Calorimetry*, 120(1), p.351-361.

Wu, P.P., Zhang, B.J., Cui, X.P., Yang, Y., Jiang, Z.Y., Zhou, Z.H., Zhong, Y.Y., Mai, Y.Y., Ouyang, Z., Chen, H.S. & Zheng, J. 2017. Synthesis and biological evaluation of novel ursolic acid analogues as potential α-glucosidase inhibitors. *Scientific Reports*, *7*, p.45578.

Wu, X., Beecher, G.R., Holden, J.M., Haytowitz, D.B., Gebhardt, S.E. & Prior, R.L. 2004. Lipophilic and hydrophilic antioxidant capacities of common foods in the United States. *J Agric Food Chem* **52**:4026–37.

Xu, H.X., Zeng, F.Q., Wan, M. & Sim, K.Y. 1996. Anti-HIV triterpene acids from Geum japonicum. *Journal of natural products*, 59(7), p.643-645.

Xu, K., Wang, P., Yuan, B., Cheng, Y., Li, Q. & Lei, H. 2013. Structural and bioactive studies of terpenes and cyclopeptides from the Genus Rubia. *Chemistry Central Journal*, *7*(1), p.81.

Xu, S., Norton, R.A., Crumley, F.G. & Nes, W.D. 1988. Comparison of the chromatographic properties of sterols, select additional steroids and triterpenoids: gravity-flow column liquid chromatography, thin-layer chromatography, gas—liquid chromatography and high-performance liquid chromatography. *Journal of chromatography A*, *452*, p.377-398.

Yin, M.C. 2015. Inhibitory effects and actions of pentacyclic triterpenes upon glycation. *Biomedicine*, *5*(3), p.1-8.

Yong, D., Toleman, M. A., Giske, C. G., Cho, H. S., Sundman, K., Lee, K. & Walsh, T. R. 2009. Characterization of a new metallo-β-lactamase gene, blaNDM-1, and a novel erythromycin esterase gene carried on a unique genetic structure in Klebsiella pneumoniae sequence type 14 from India. *Antimicrobial agents and chemotherapy*, 53(12), p.5046-5054.

Yoshikawa, T., Toyokuni, S., Yamamoto, Y. & Naito, Y. 2000. Free radicals in Chemistry. *Biology and Medicine,* OICA International, London.

Yu, D., Sakurai, Y., Chen, C.H., Chang, F.R., Huang, L., Kashiwada, Y. & Lee, K.H. 2006. Anti-AIDS agents 69. Moronic acid and other triterpene derivatives as novel potent anti-HIV agents. Journal of medicinal chemistry, 49(18), p.5462-5469.

Zacchigna, M., Cateni, F., Drioli, S., Procida, G. & Altieri, T. 2014. PEG–Ursolic Acid Conjugate: Synthesis and In Vitro Release Studies. *Scientia pharmaceutica*, 82(2), p.411-422.

Zhang, H., Boghigian, B. A., Armando, J. & Pfeifer, B. A. 2011. Methods and options for the heterologous production of complex natural products. *Natural product reports*, 28(1), p.125-151.

Zhou, M., Zhang, R.H., Wang, M., Xu, G.B. & Liao, S.G. 2017. Prodrugs of triterpenoids and their derivatives. European journal of medicinal chemistry, 131, p.222-236.

Zhou, Y., Boudreau, D.M. & Freedman, A.N. 2014. Trends in the use of aspirin and nonsteroidal anti-inflammatory drugs in the general US population. *Pharmacoepidemiology and drug safety*, 23(1), p.43-50.

Ziegler, H.L., Franzyk, H., Sairafianpour, M., Tabatabai, M., Tehrani, M.D., Bagherzadeh, K., Hägerstrand, H., Stærk, D. & Jaroszewski, J.W. 2004. Erythrocyte membrane modifying agents and the inhibition of Plasmodium falciparum growth: structure–activity relationships for betulinic acid analogues. Bioorganic & medicinal chemistry, 12(1), pp.119-127.

Zupancic, A. 2001. Topical anti-inflammatory activity of Salvia officinalis L. leaves: the relevance of ursolic acid. *J. Ethnopharm*, 75, p.125-132.

APPENDICES

APPENDIX A: FT-IR spectra figures

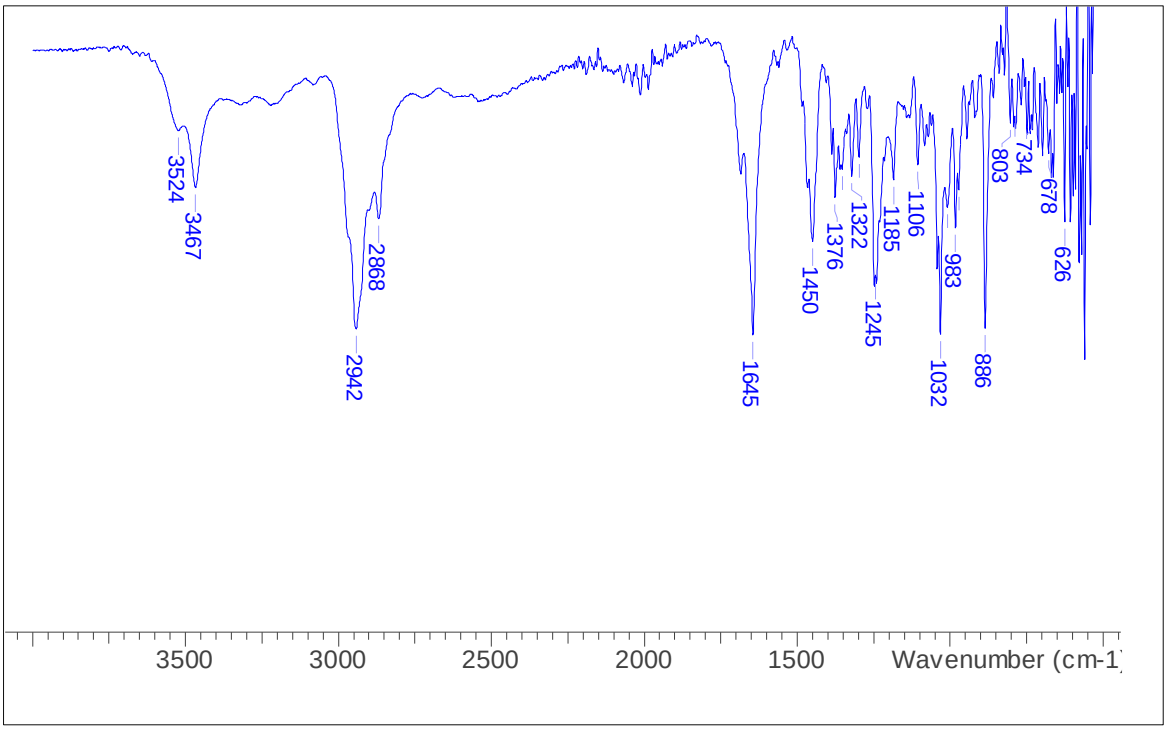

Figure 1.1: FT-IR spectrum of BA (**4**)

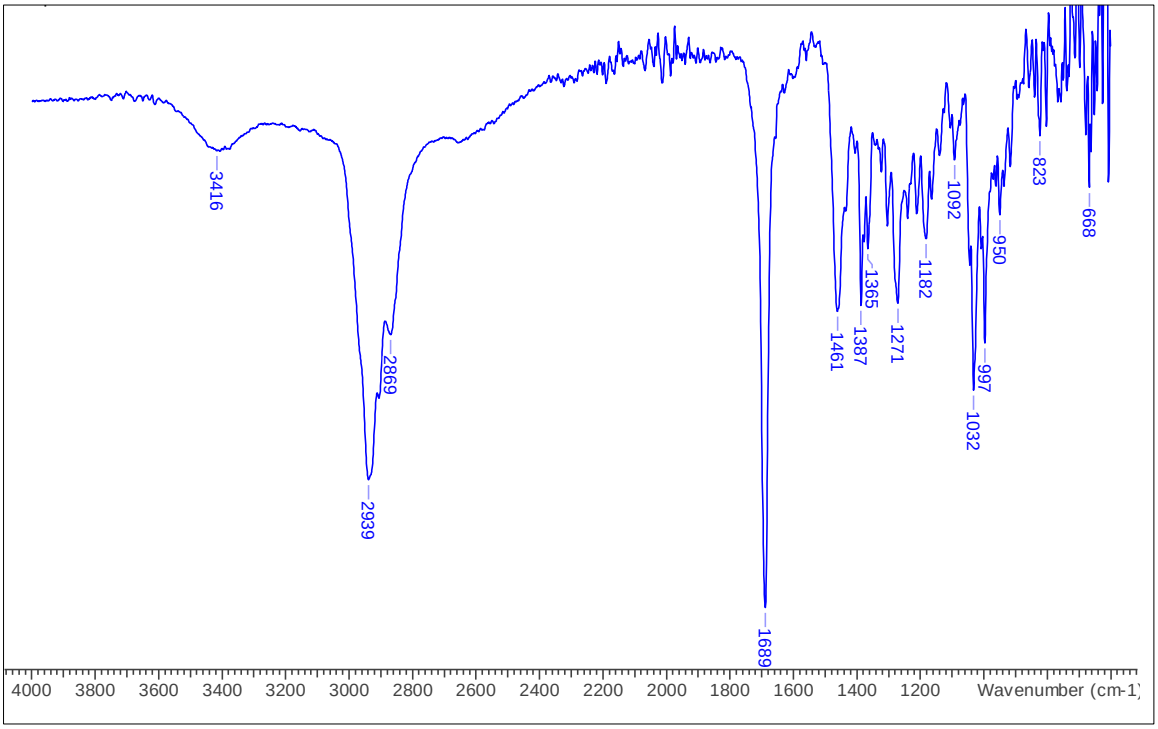

Figure 1.2: FT-IR spectrum of OA (**5**)

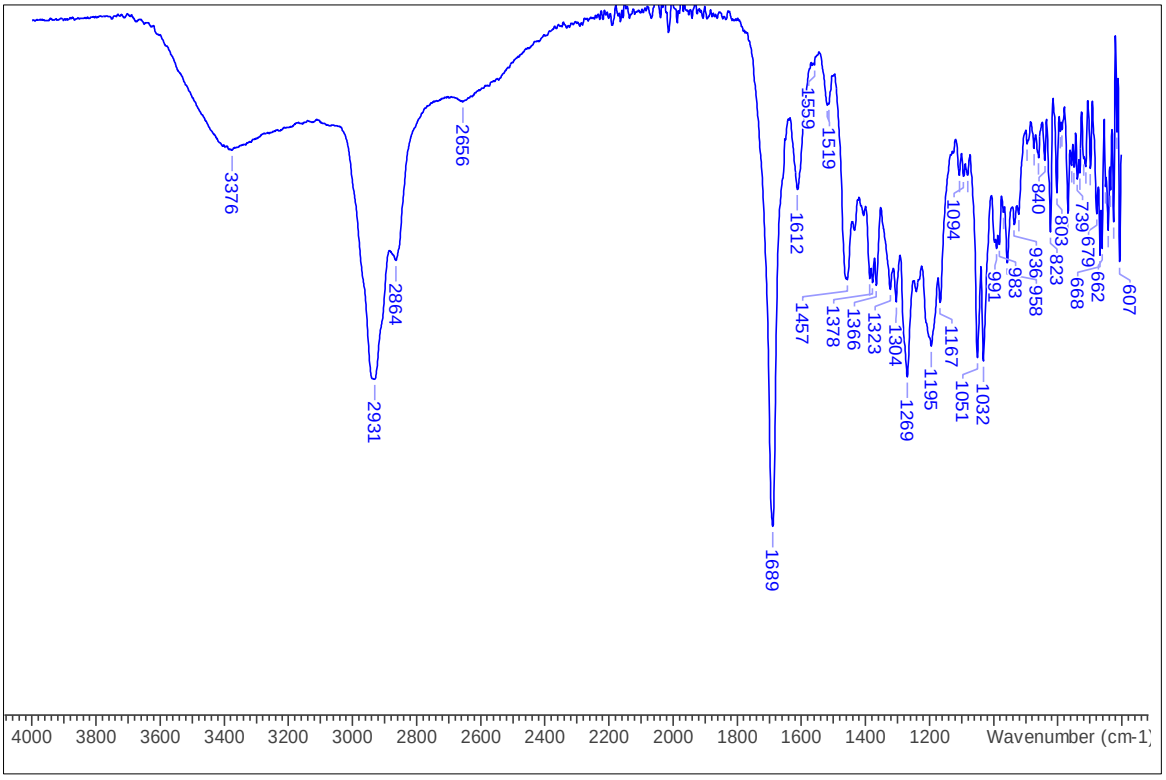

Figure 1.3: FT-IR spectrum of MA (**11**)

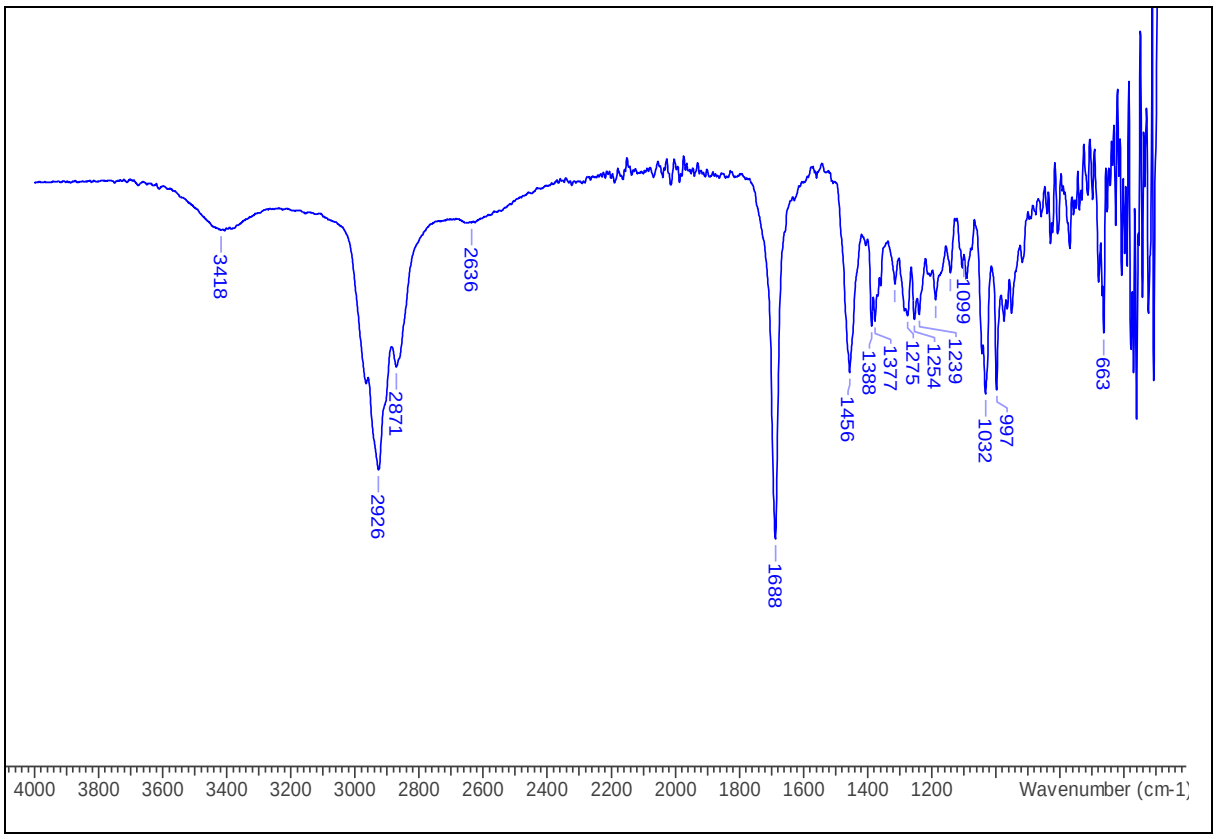

Figure 1.4: FT-IR spectrum of UA (**6**)

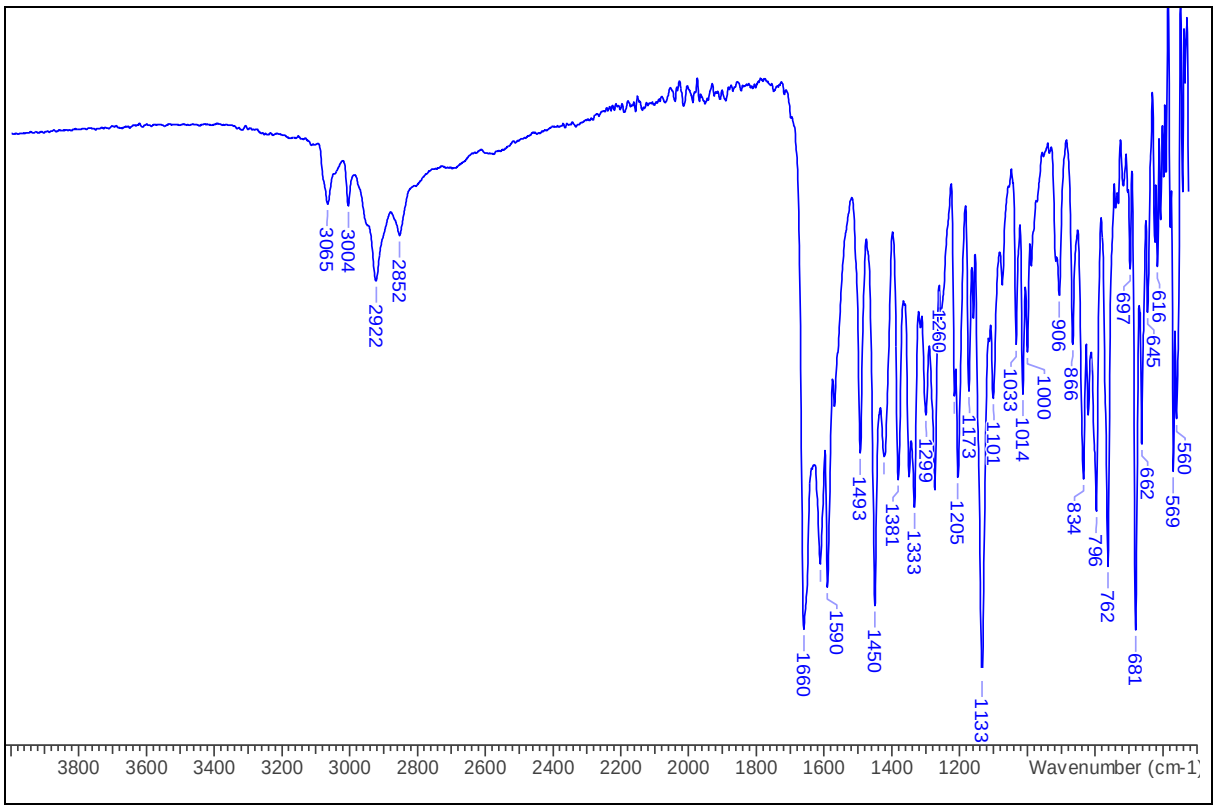

Figure 1.5: FT-IR spectrum of 5-hydroxy-7-methoxy-6-methylflavone (**19**)

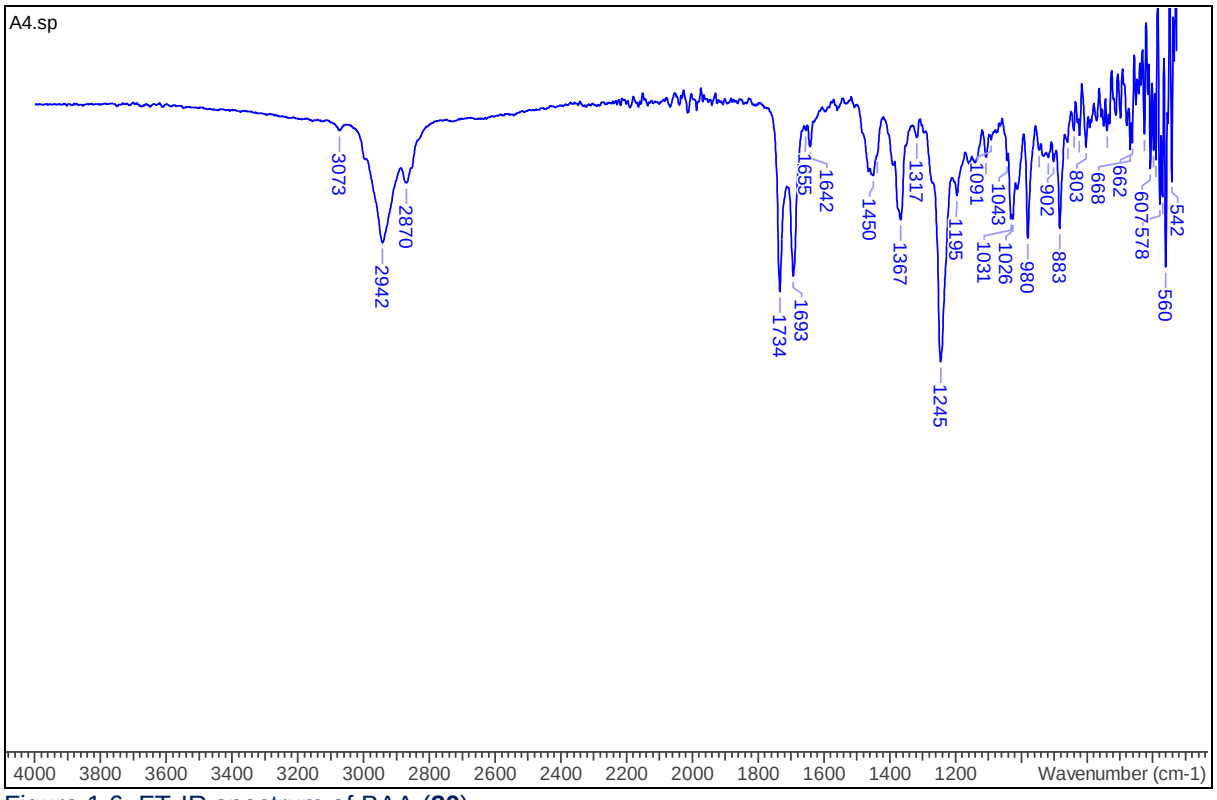

Figure 1.6: FT-IR spectrum of BAA (**20**)

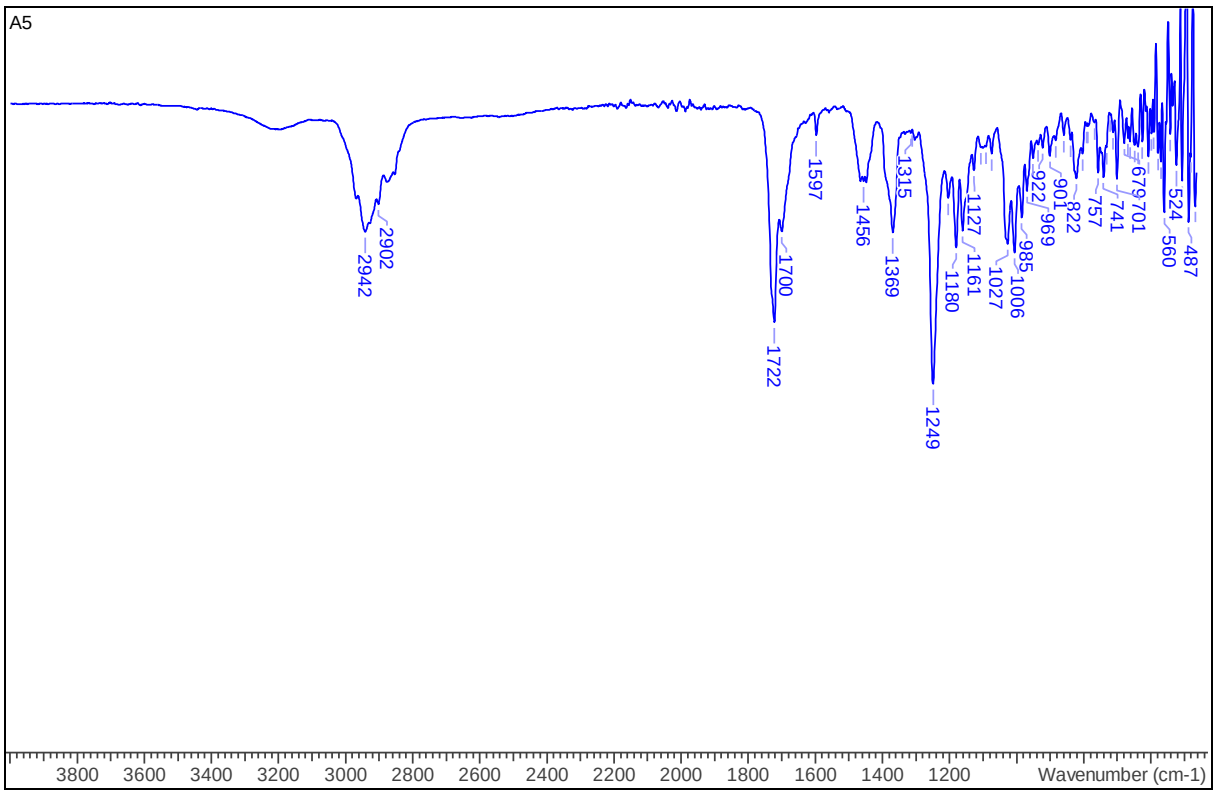

Figure 1.7: FT-IR spectrum of OAA (**21**)

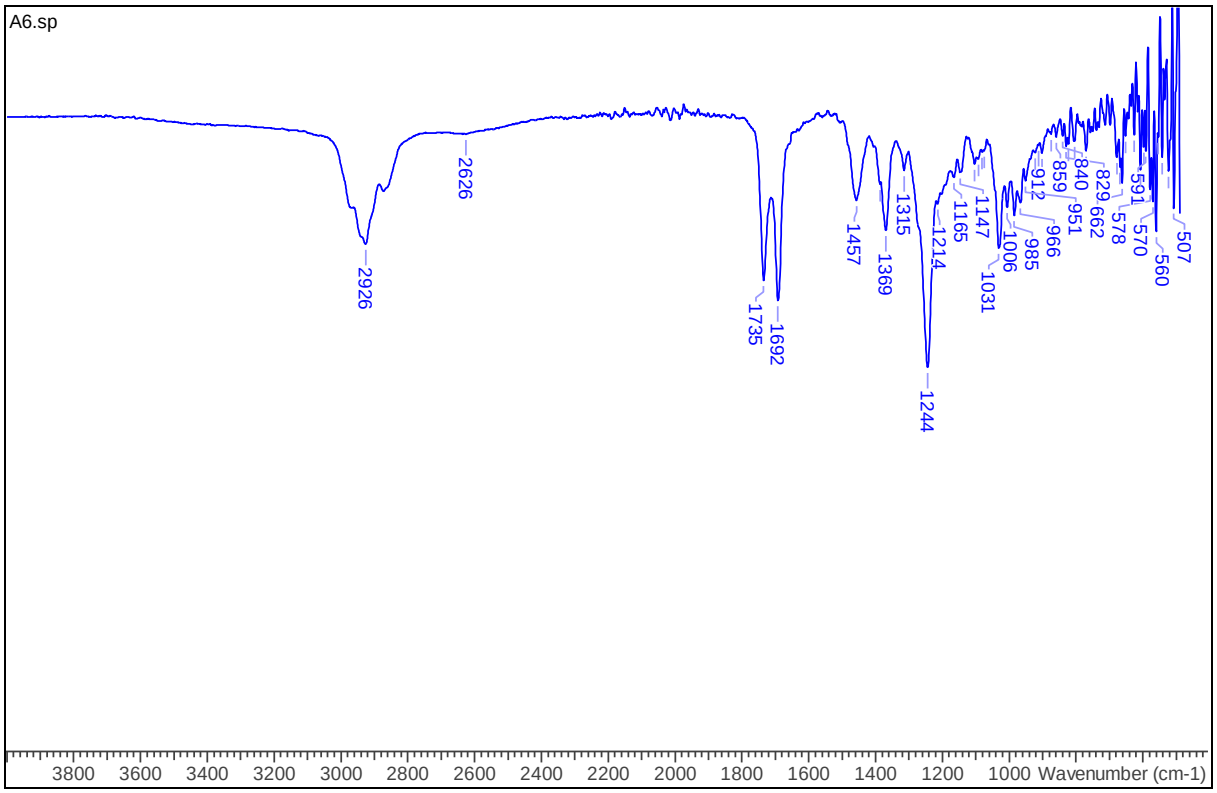

Figure 1.8: FT-IR spectrum of UAA (**22**)

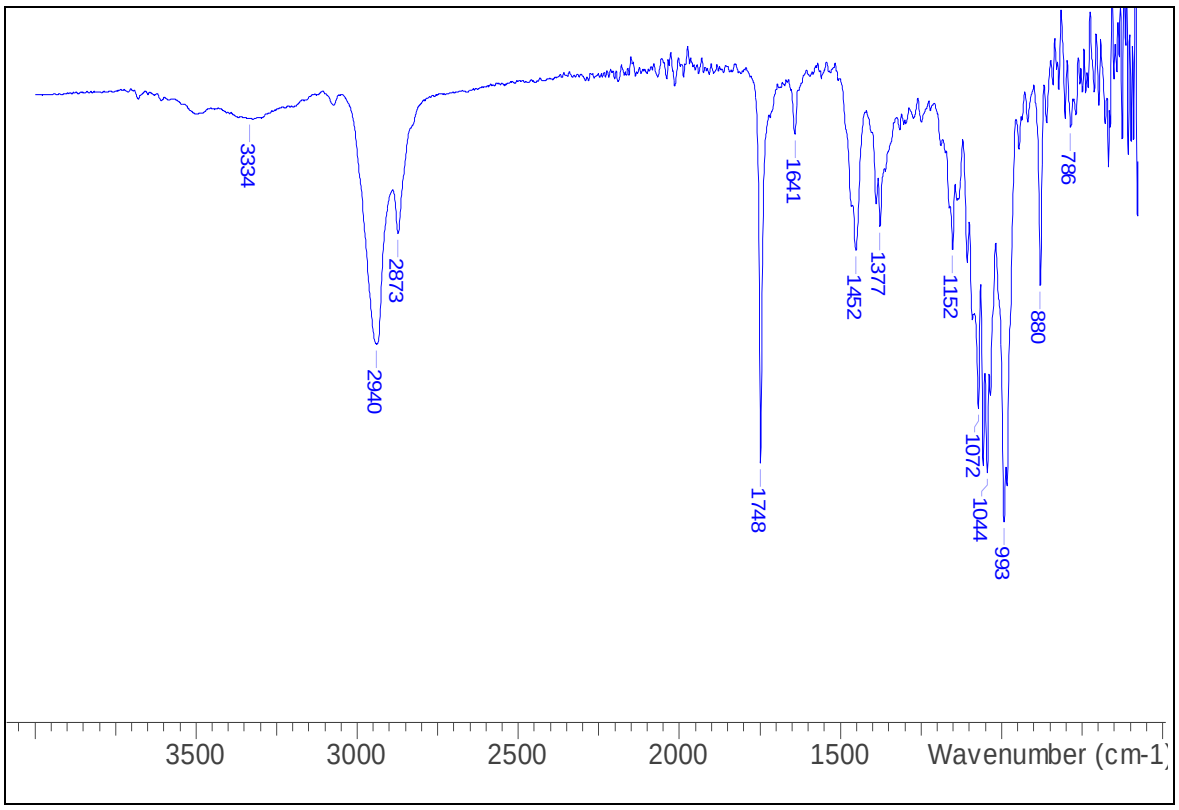

Figure 1.9: FT-IR spectrum of compound (**23**)

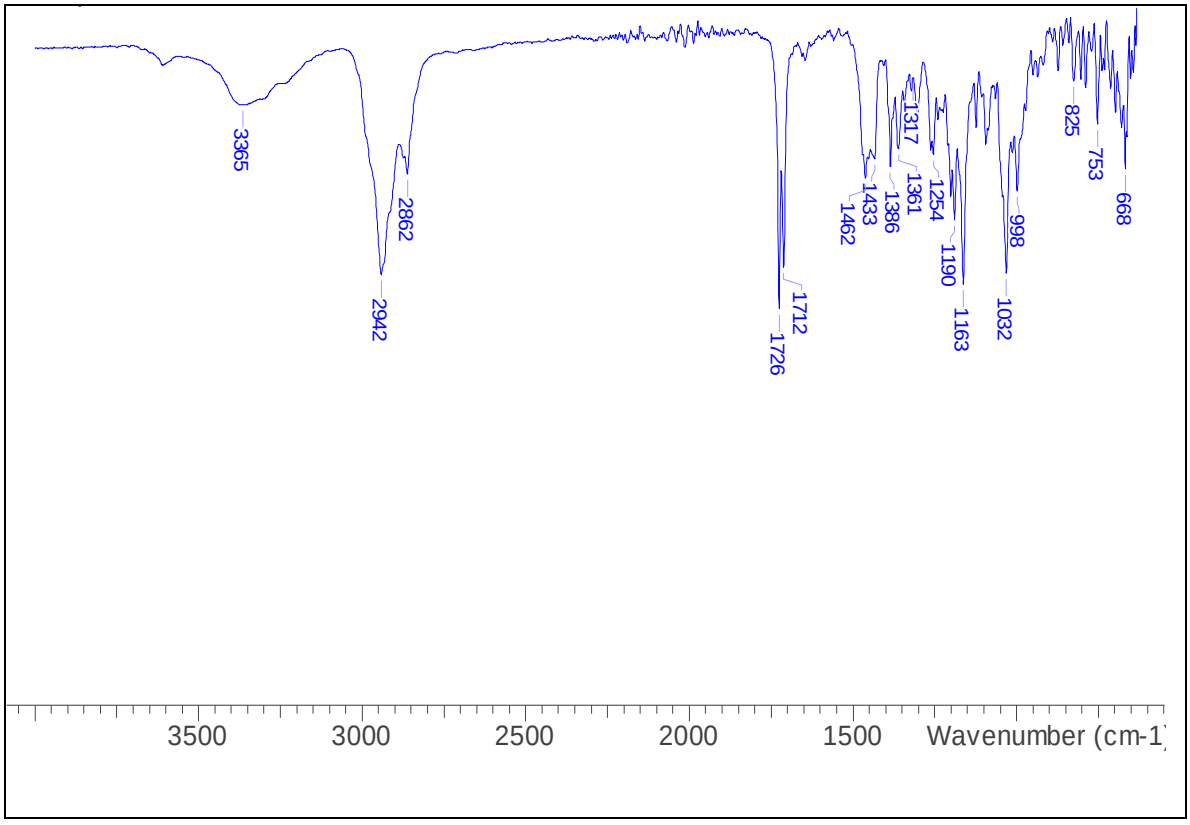

Figure 1.10: FT-IR spectrum of methyl oleanolate (**24**)

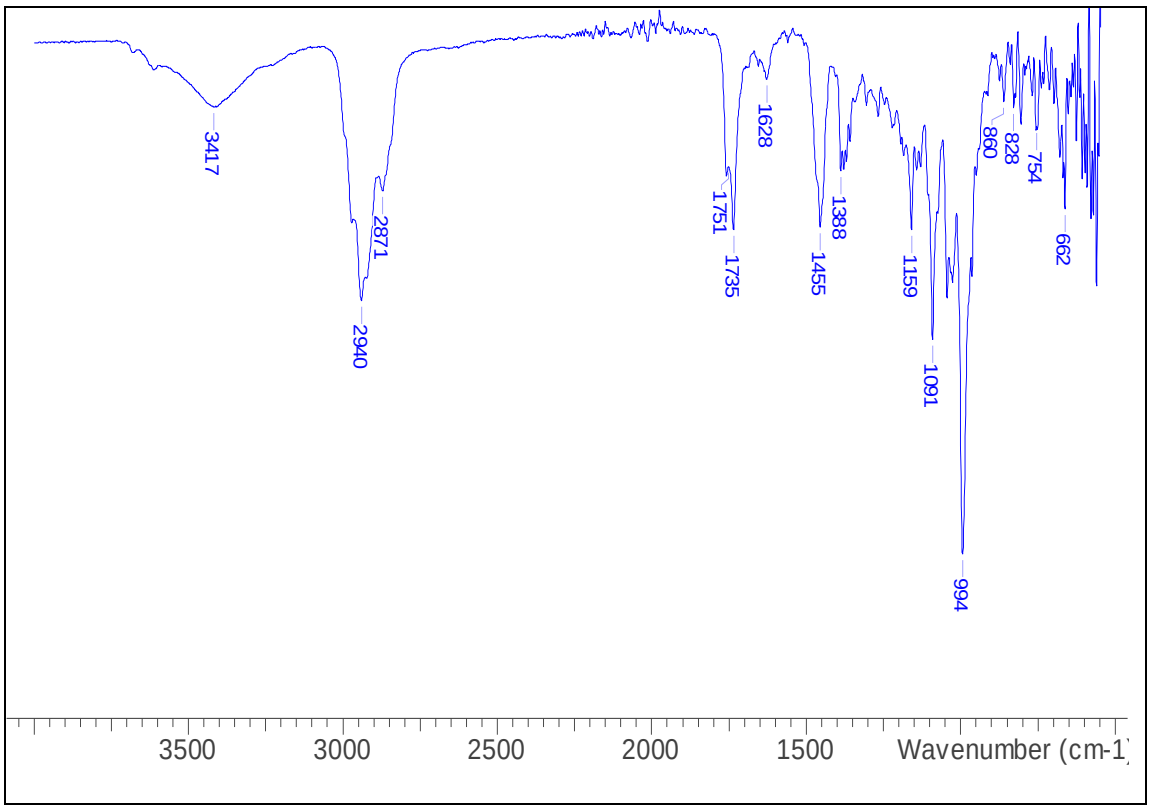

Figure 1.11: FT-IR spectrum of compound (**25**)

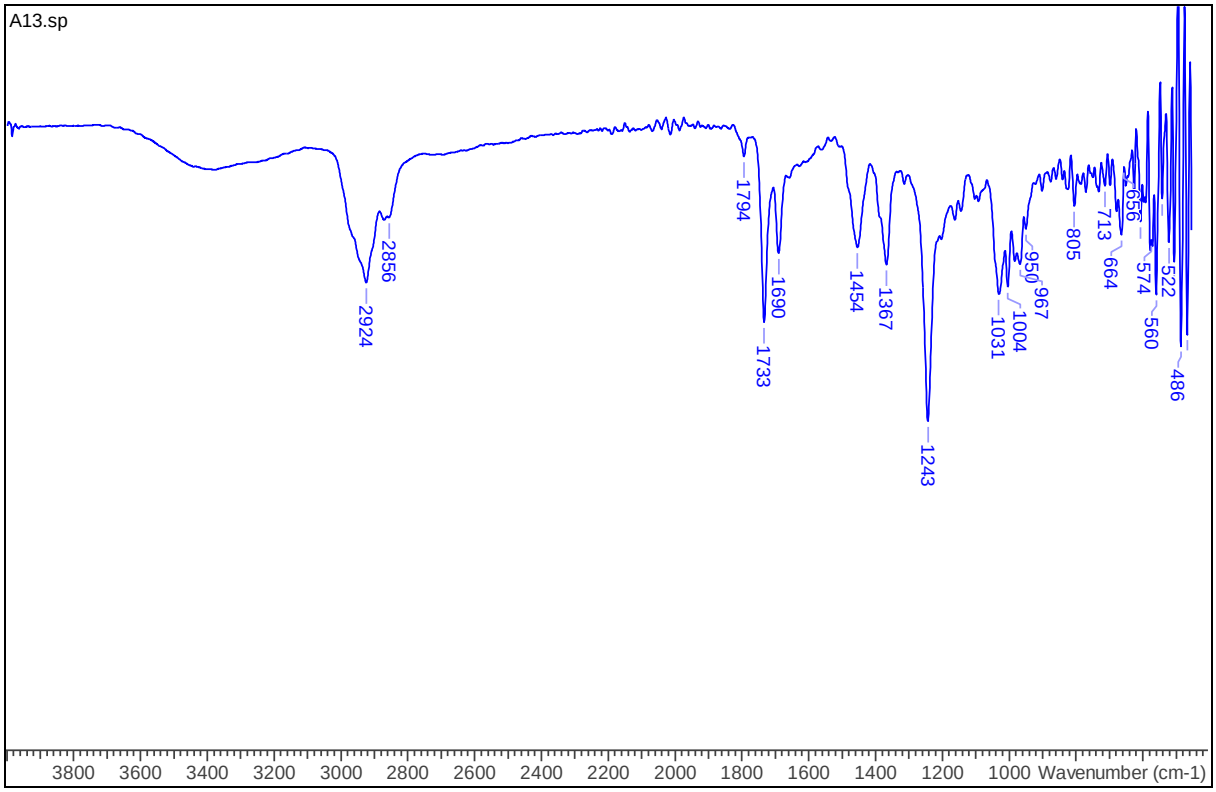

Figure 1.12: FT-IR spectrum of Compound A13

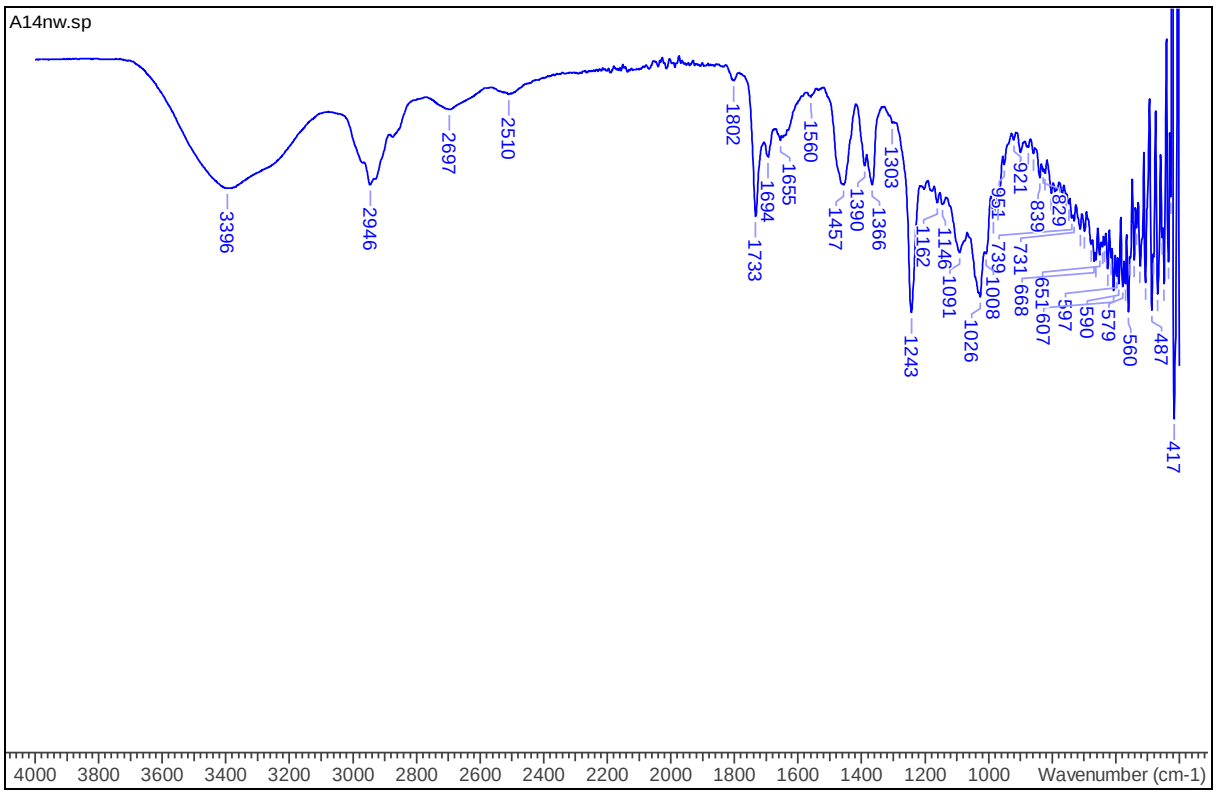

Figure 1.13: FT-IR spectrum of Compound A14

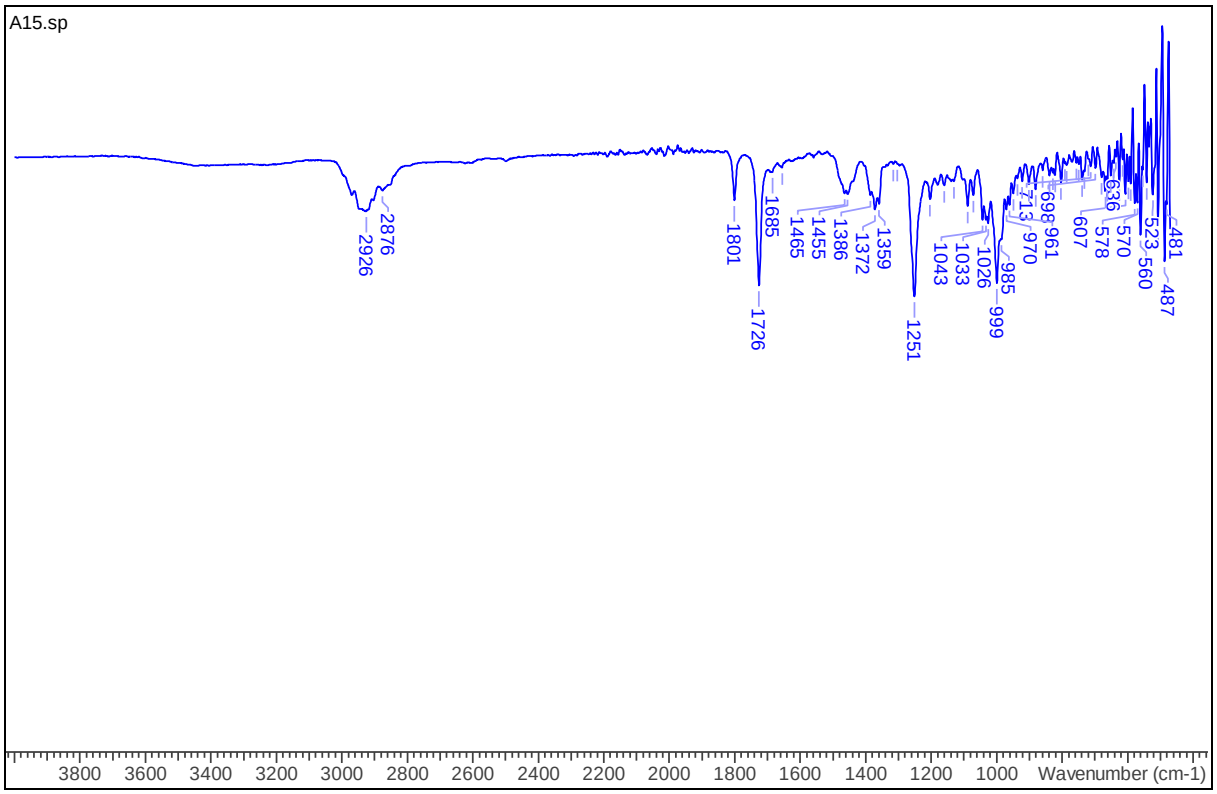

Figure 1.14: FT-IR spectrum of Compound A15

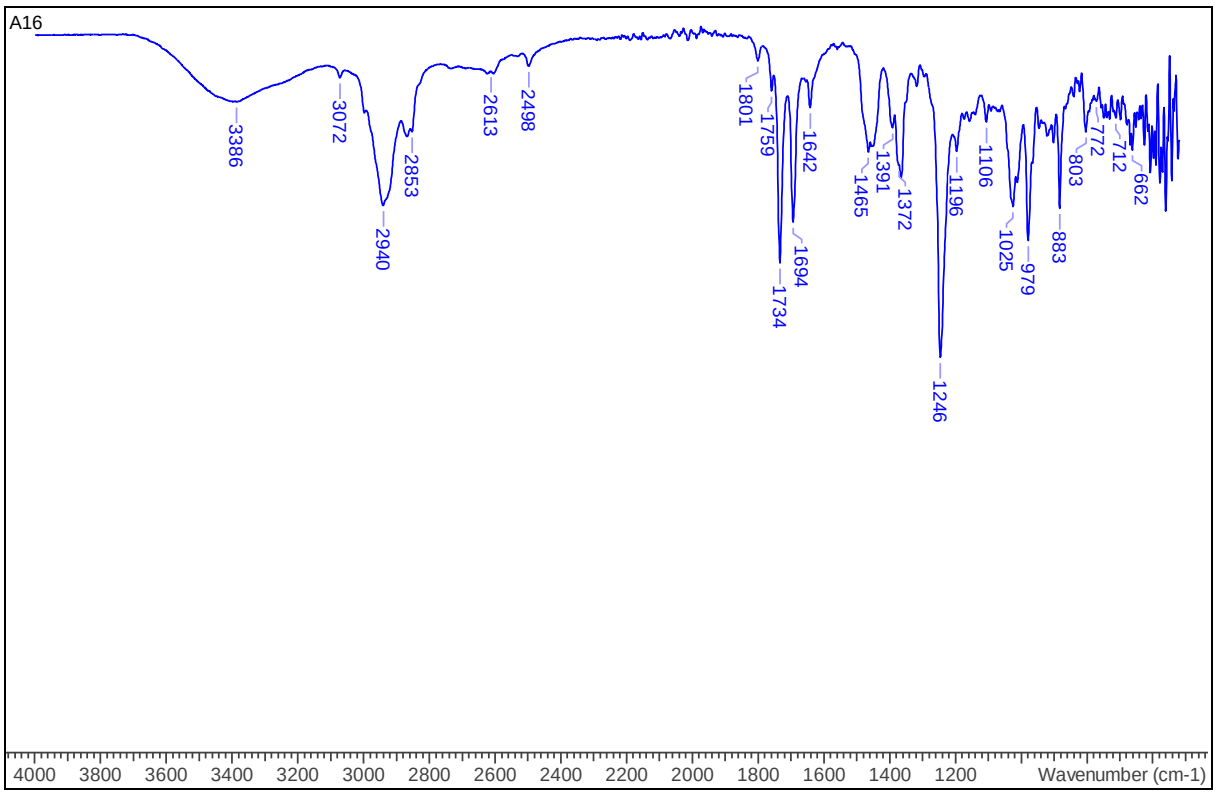

Figure 1.15: FT-IR spectrum of Compound A16

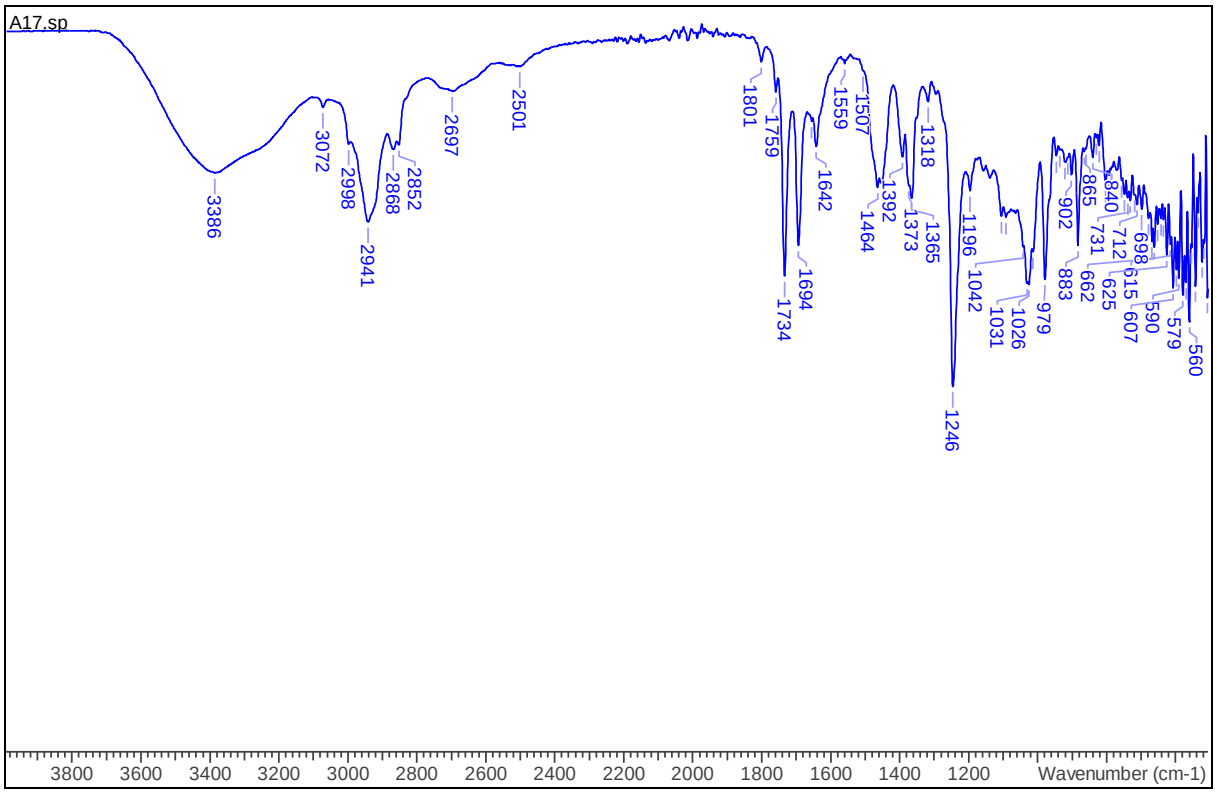

Figure 1.16: FT-IR spectrum of Compound A17

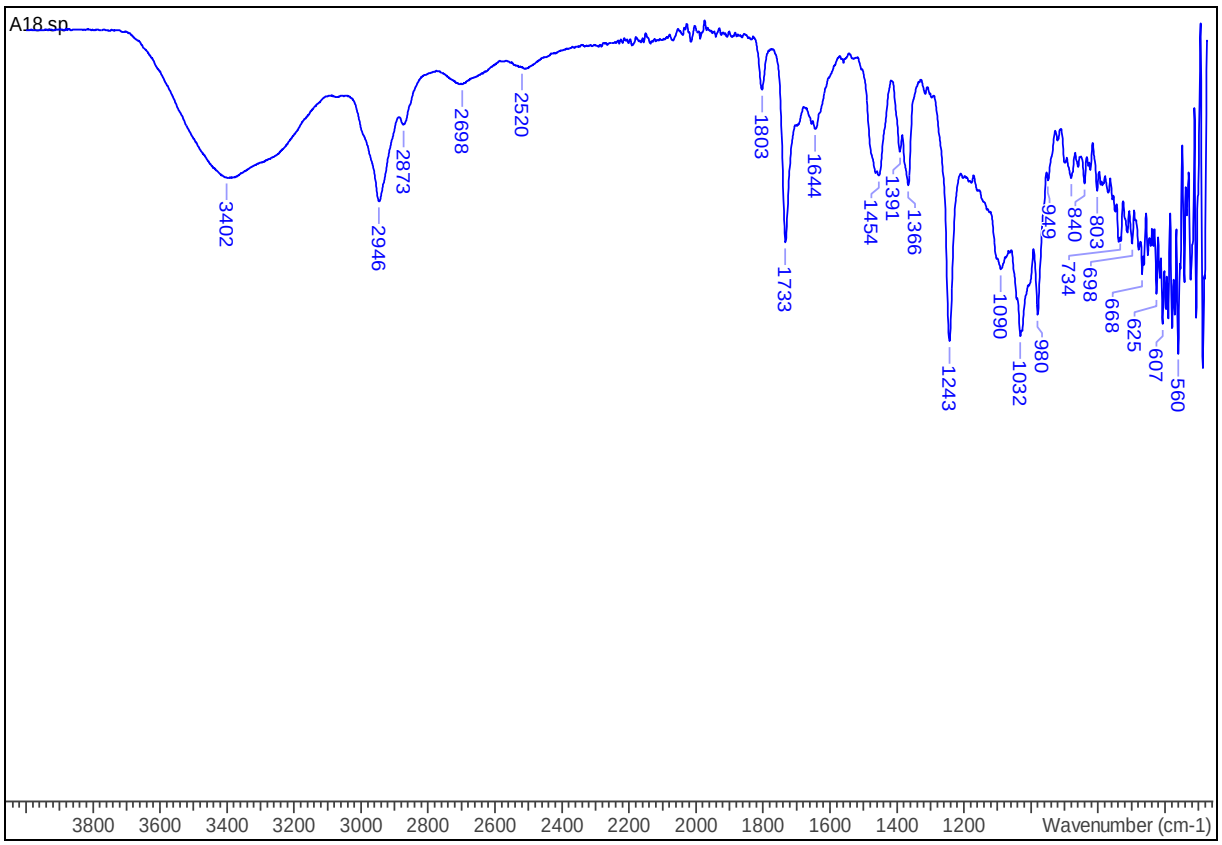

Figure 1.17: FT-IR spectrum of Compound A18

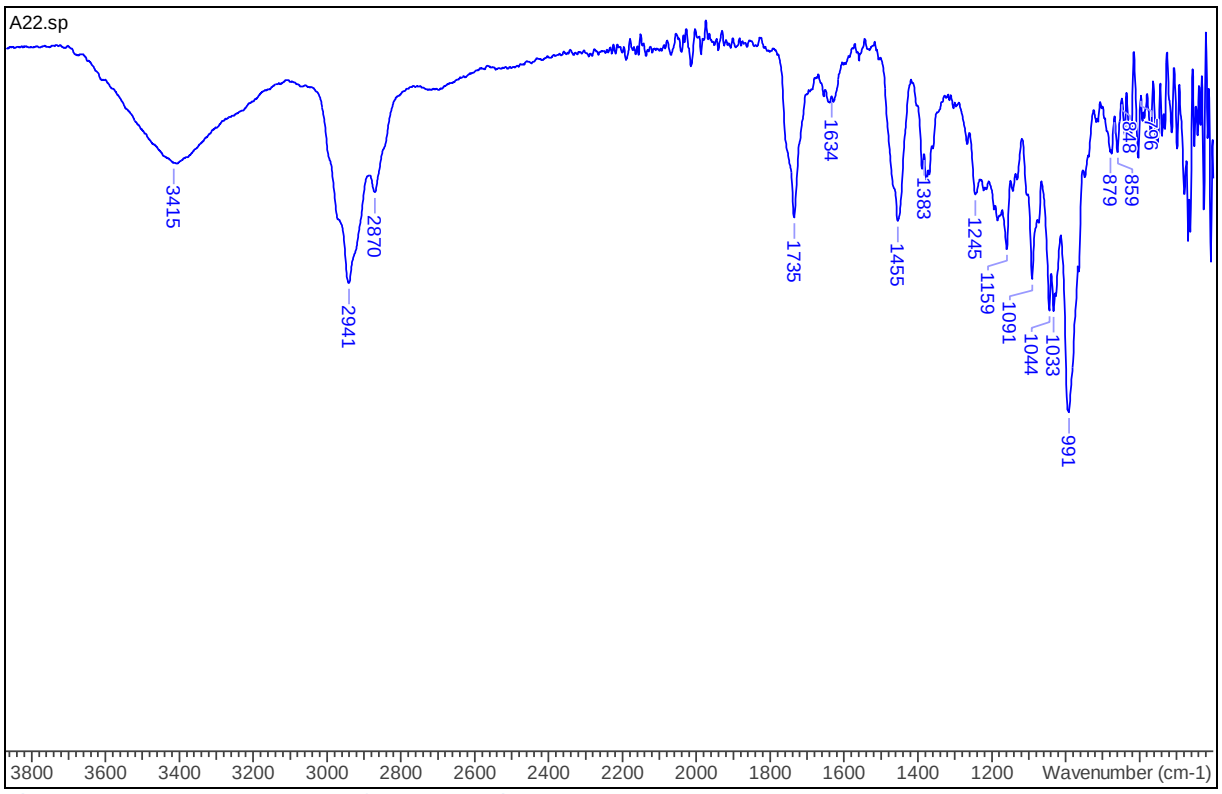

Figure 1.18: FT-IR spectrum of Compound A22

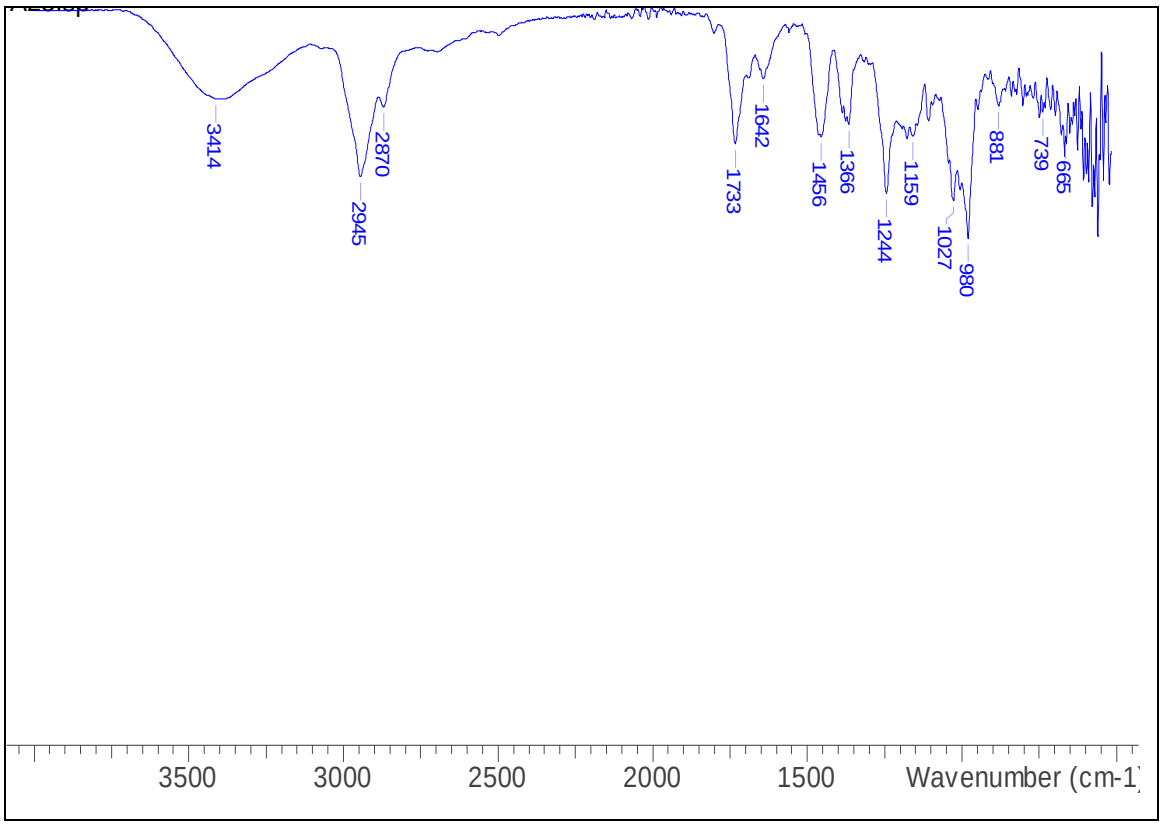

Figure 1.19: FT-IR spectrum of Compound A23

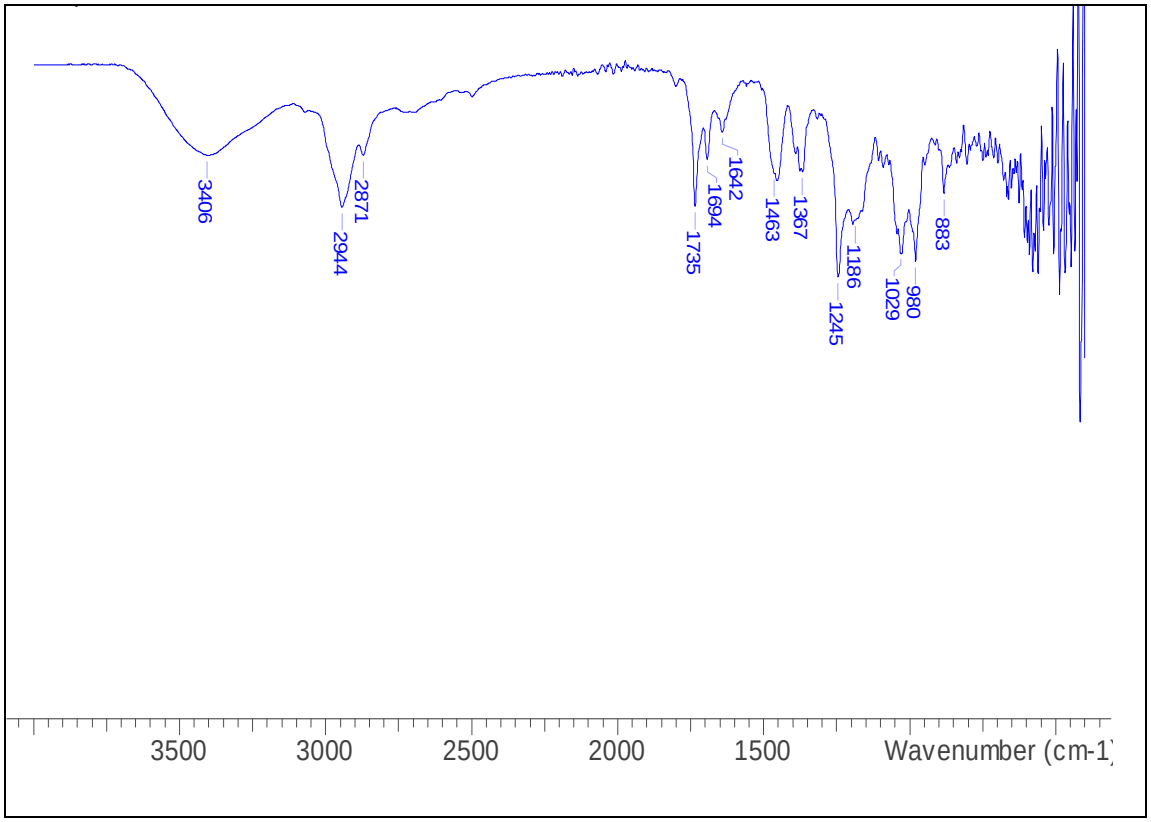

Figure 1.20: FT-IR spectrum of Compound A24

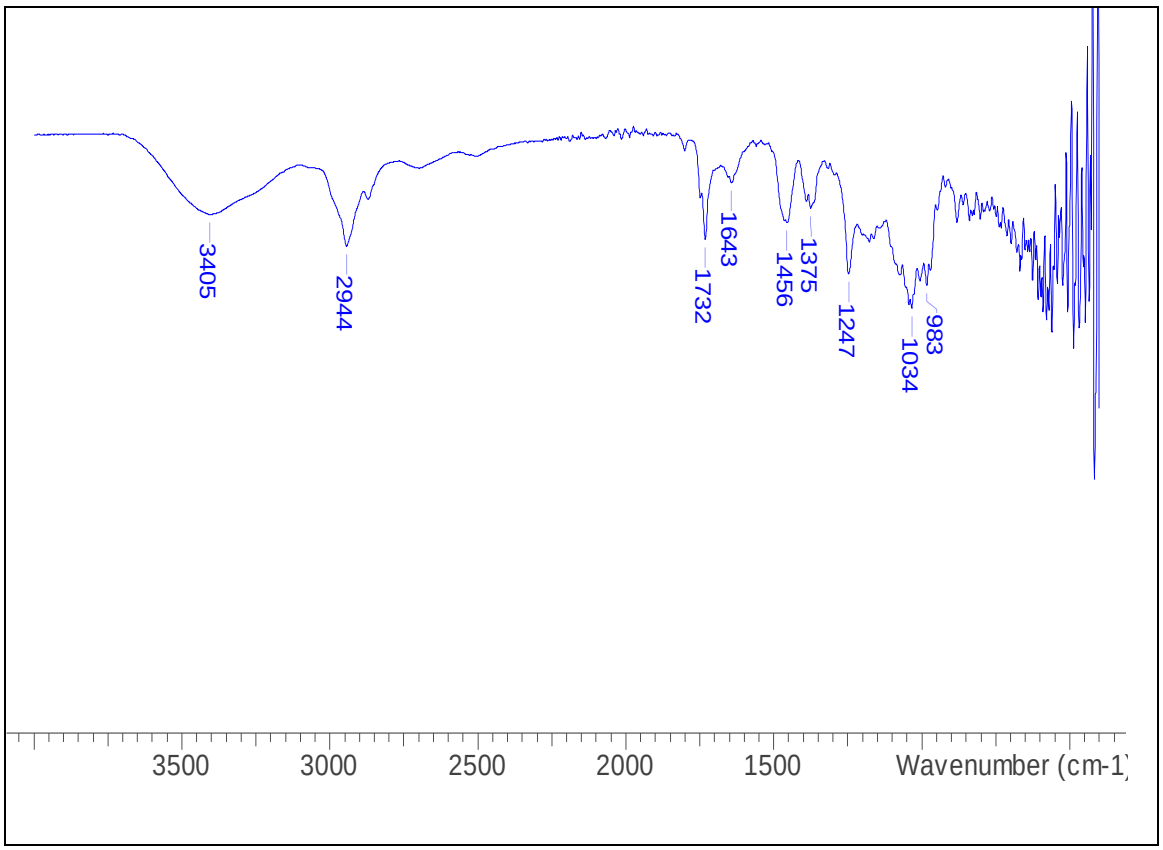

Figure 1.21: FT-IR spectrum of Compound A25

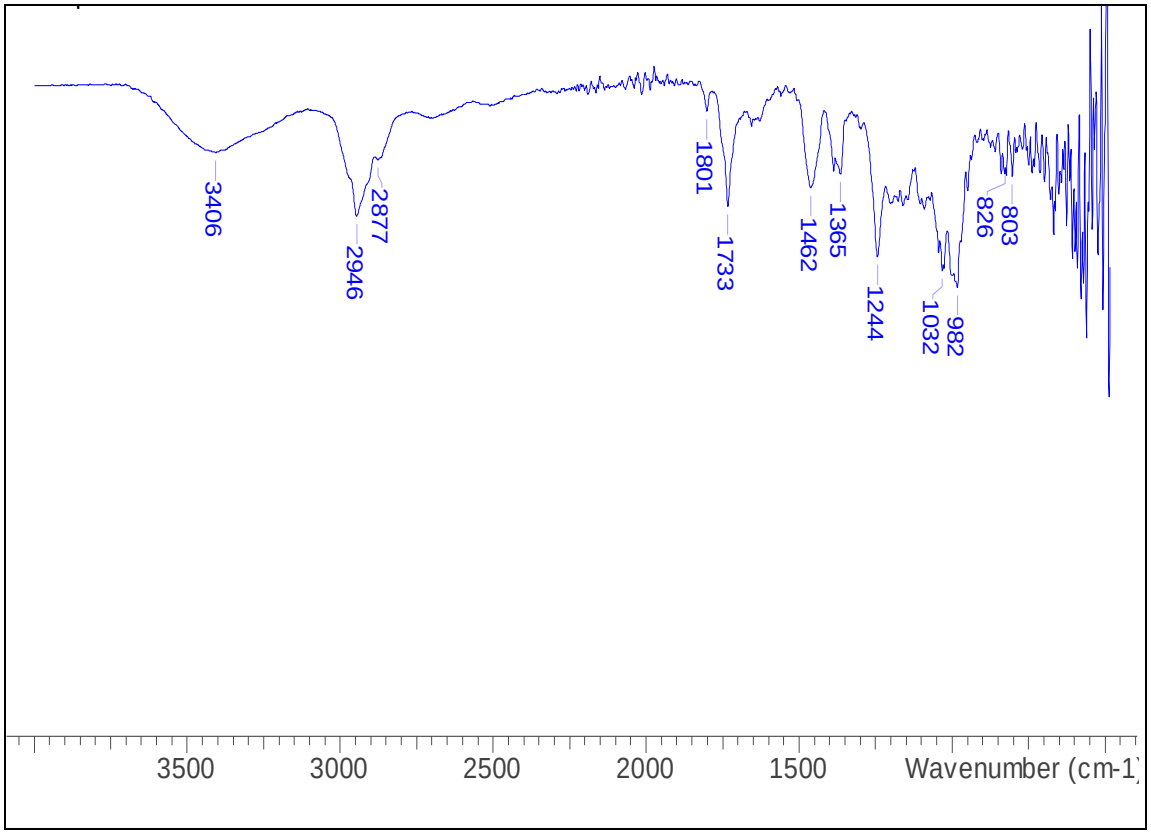

Figure 1.22: FT-IR spectrum of Compound A26

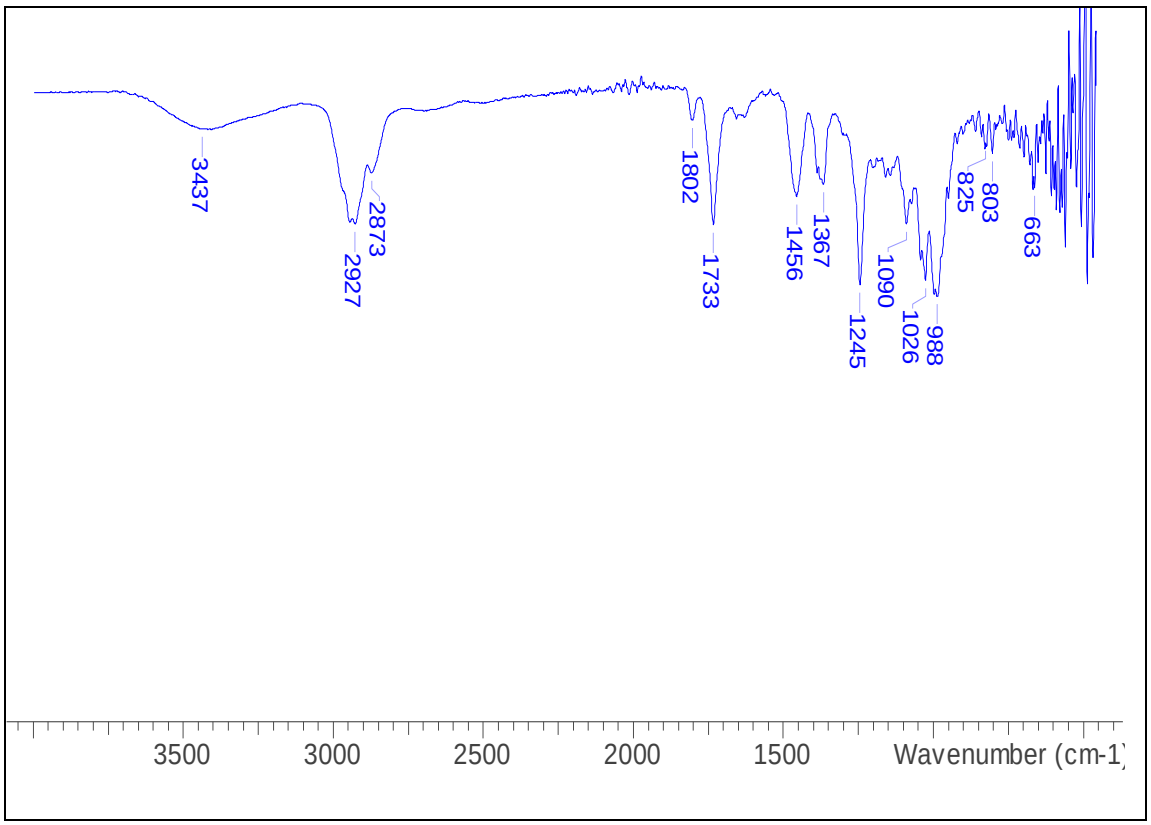

Figure 1.23: FT-IR spectrum of Compound A27

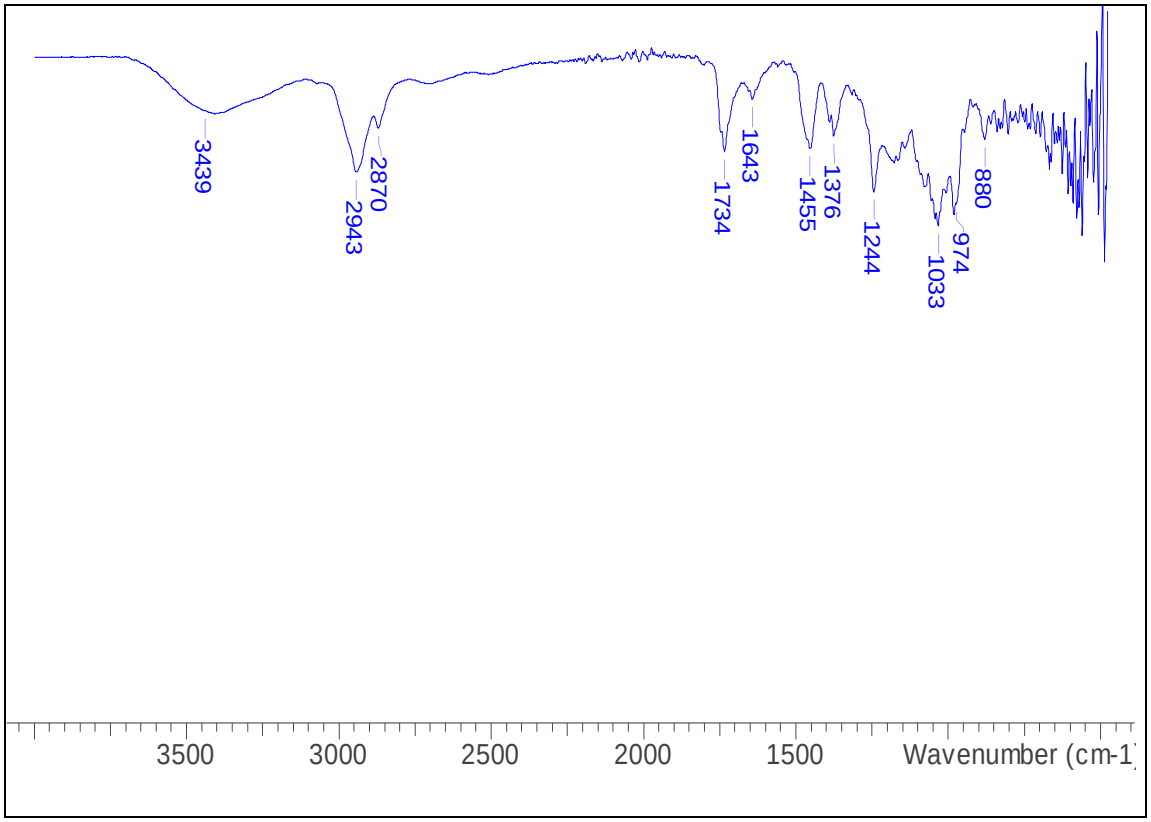

Figure 1.24: FT-IR spectrum of Compound A28

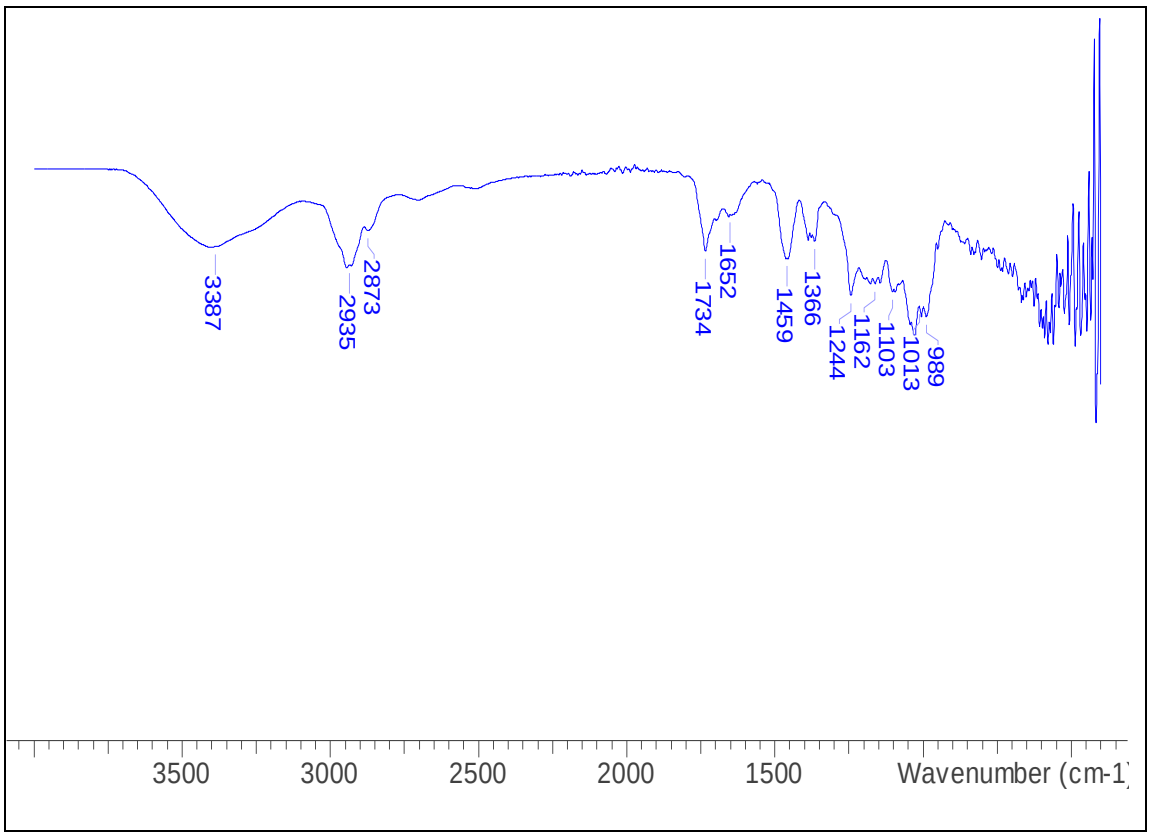

Figure 1.25: FT-IR spectrum of Compound A29

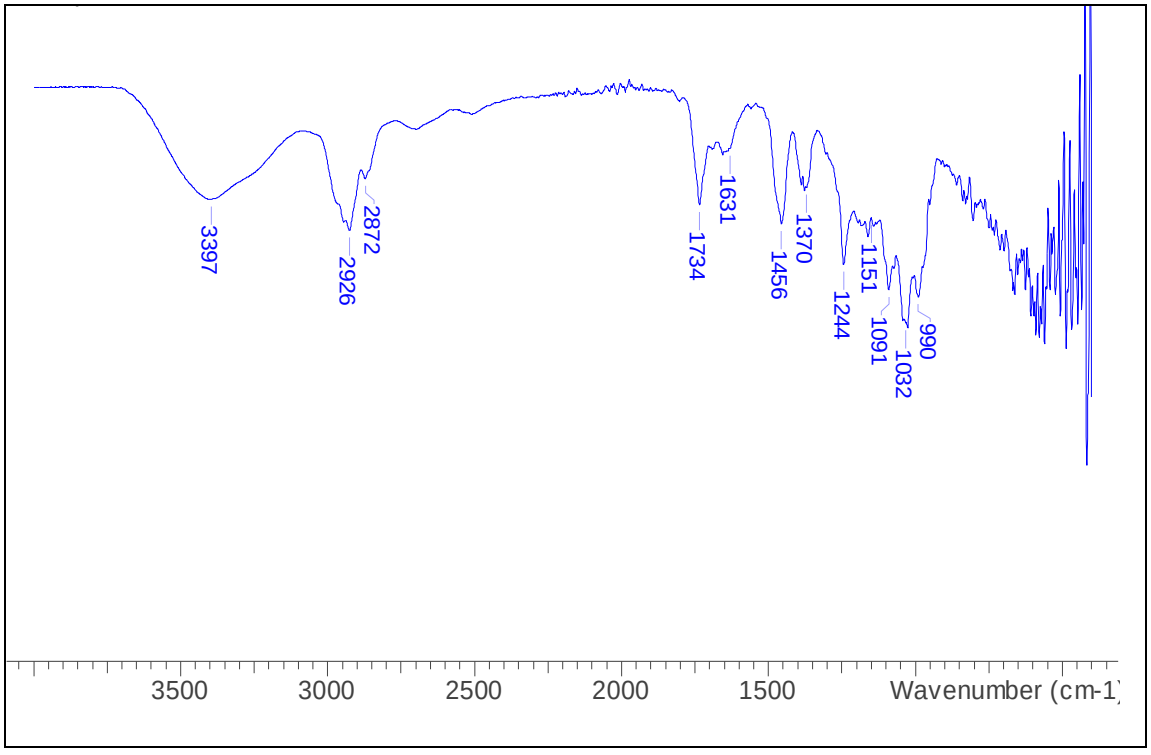

Figure 1.26: FT-IR spectrum of Compound A30

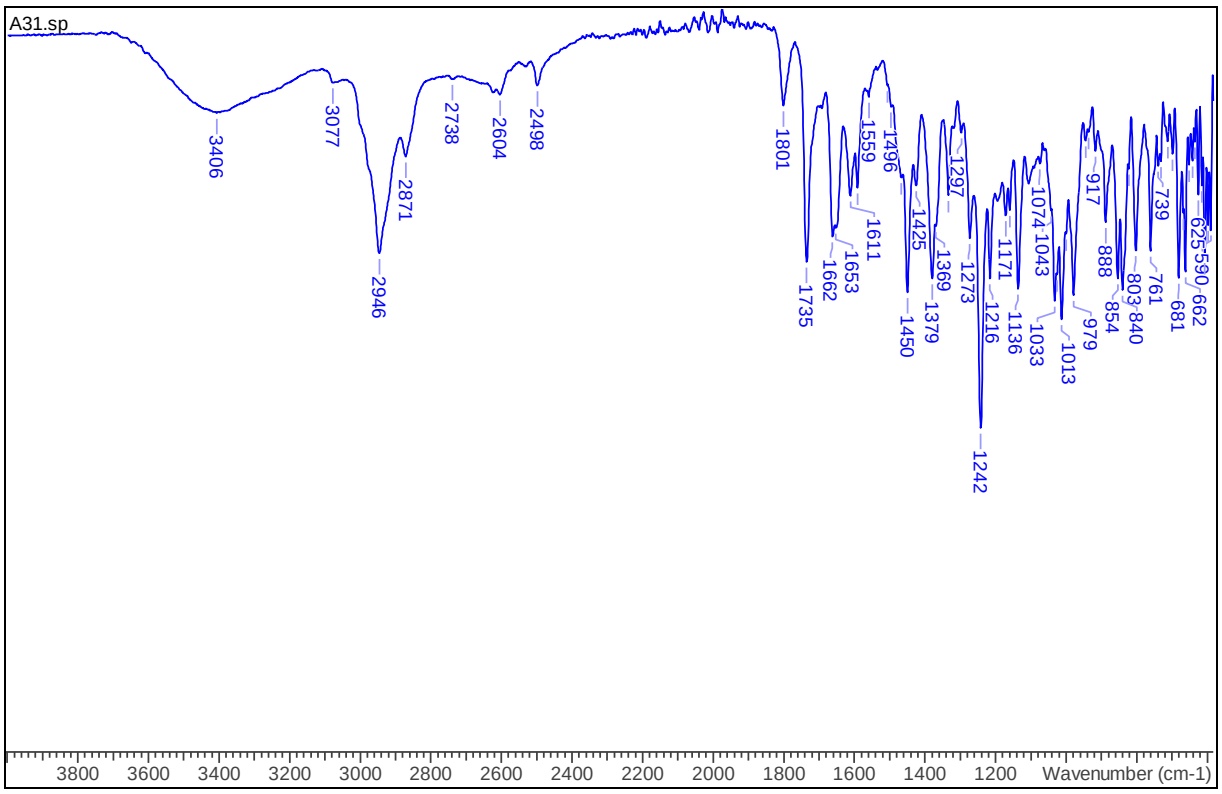

Figure 1.27: FT-IR spectrum of Compound A31

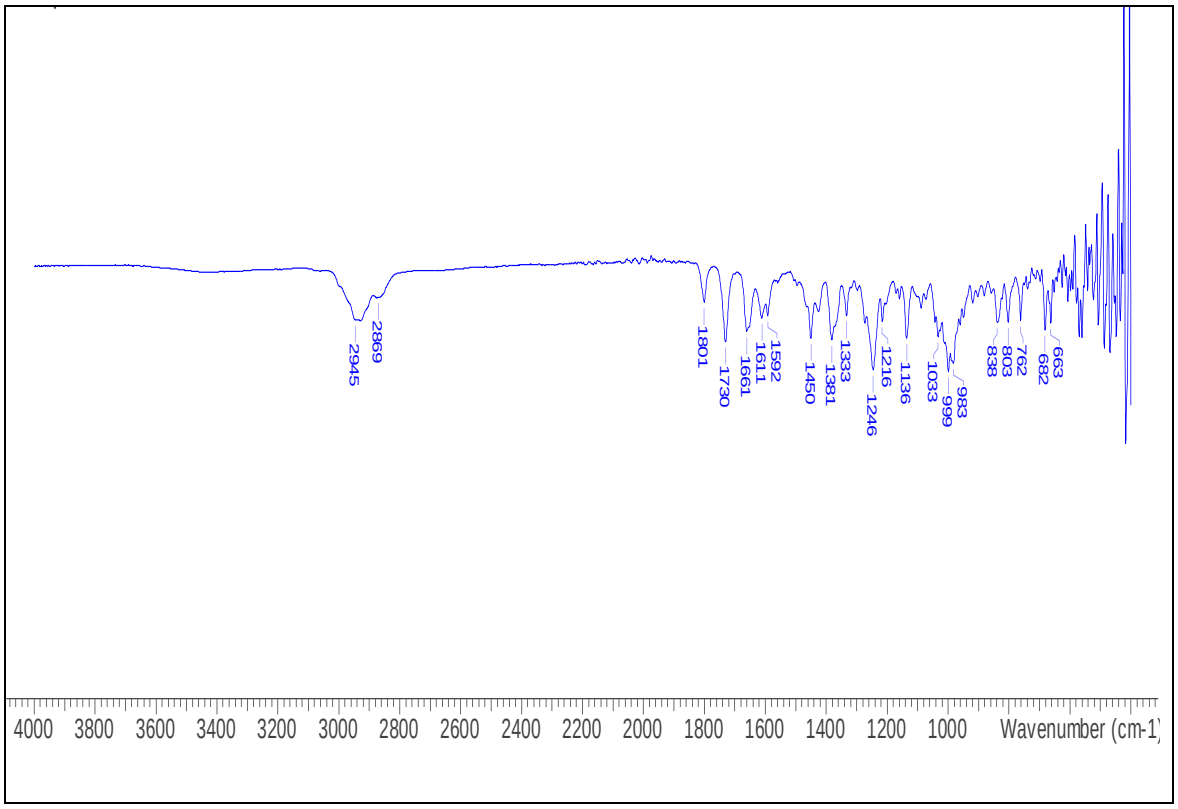

Figure 1.28: FT-IR spectrum of Compound A32

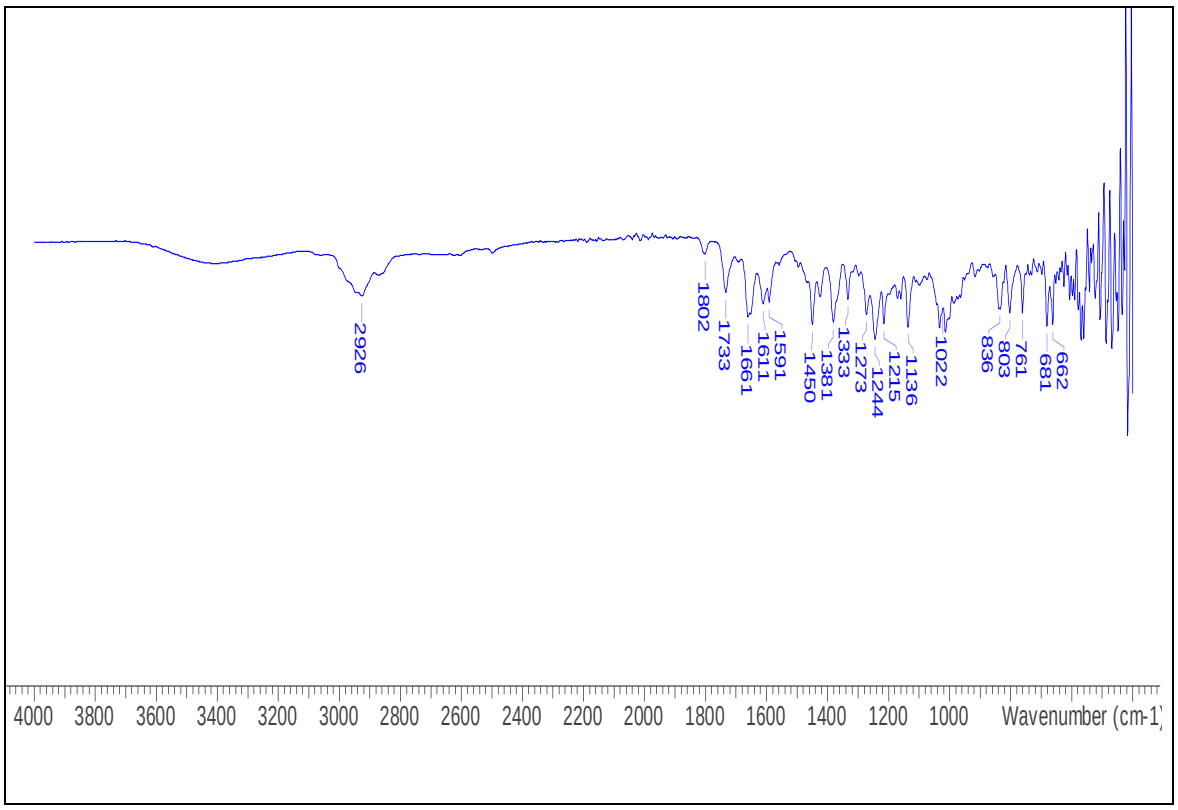

Figure 1.29: FT-IR spectrum of Compound A33

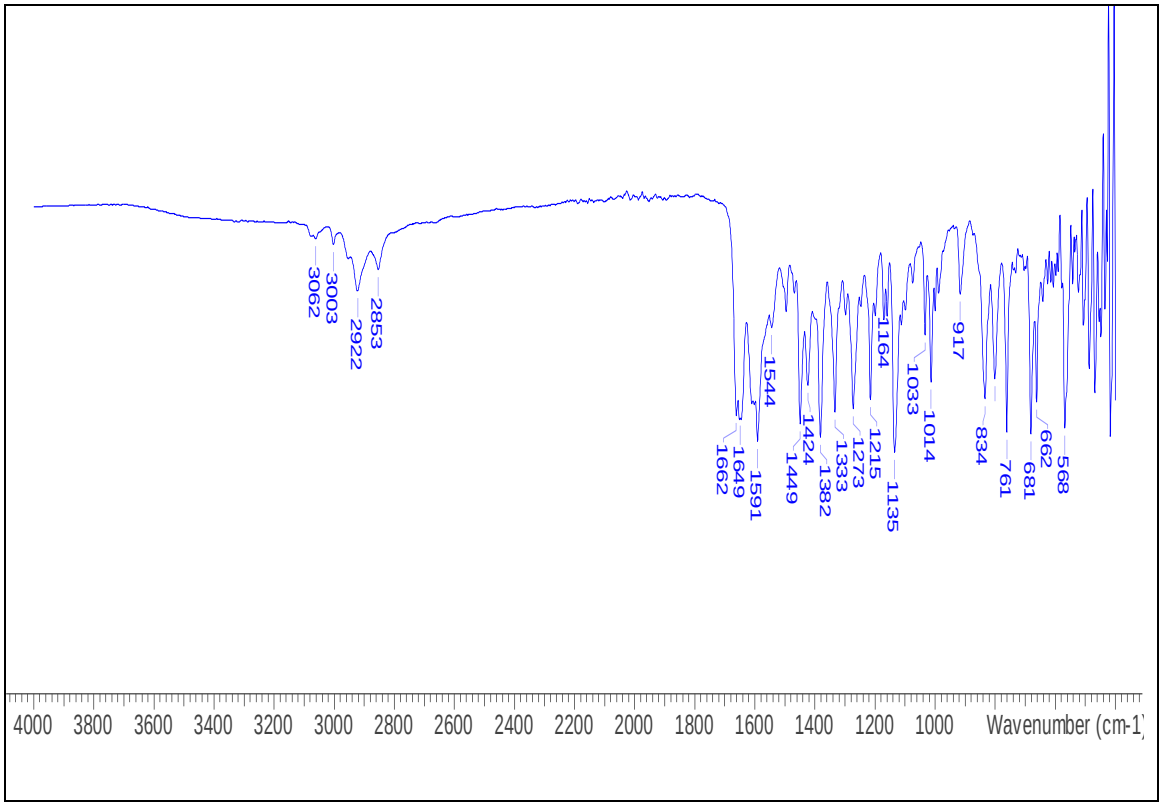

Figure 1.30: FT-IR spectrum of Compound A37

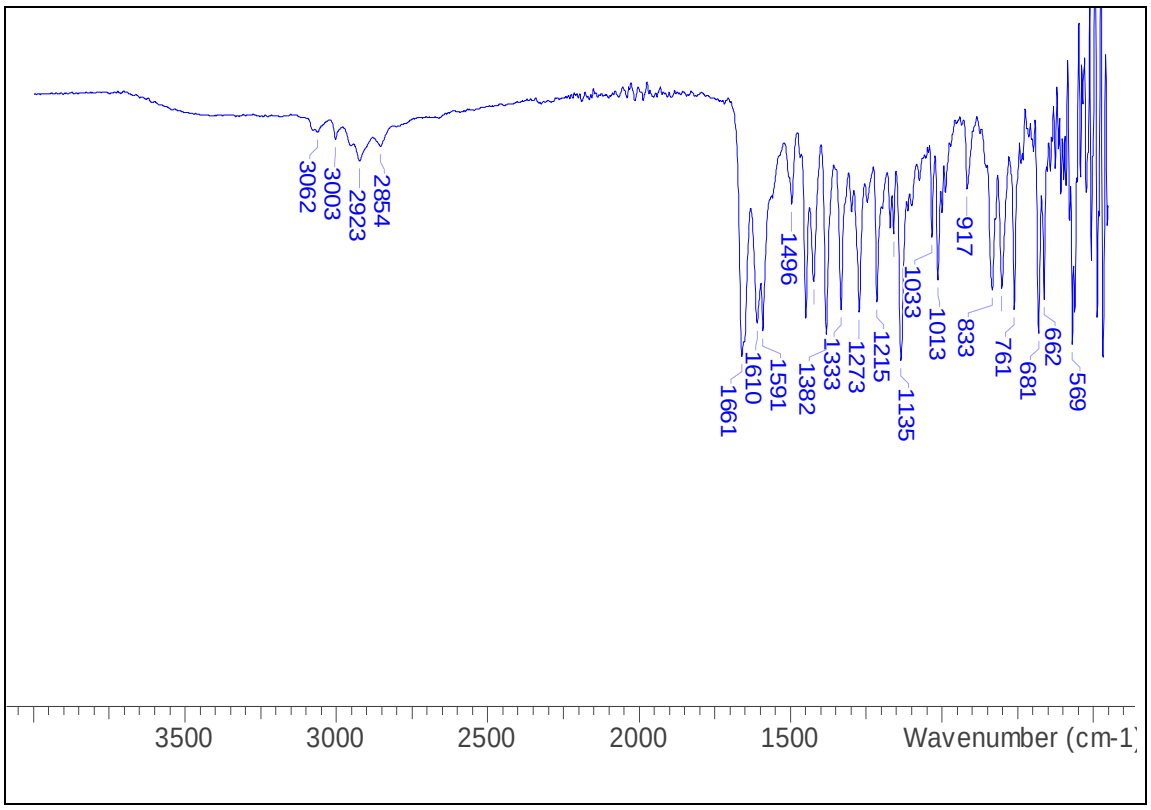

Figure 1.31: FT-IR spectrum of Compound A38

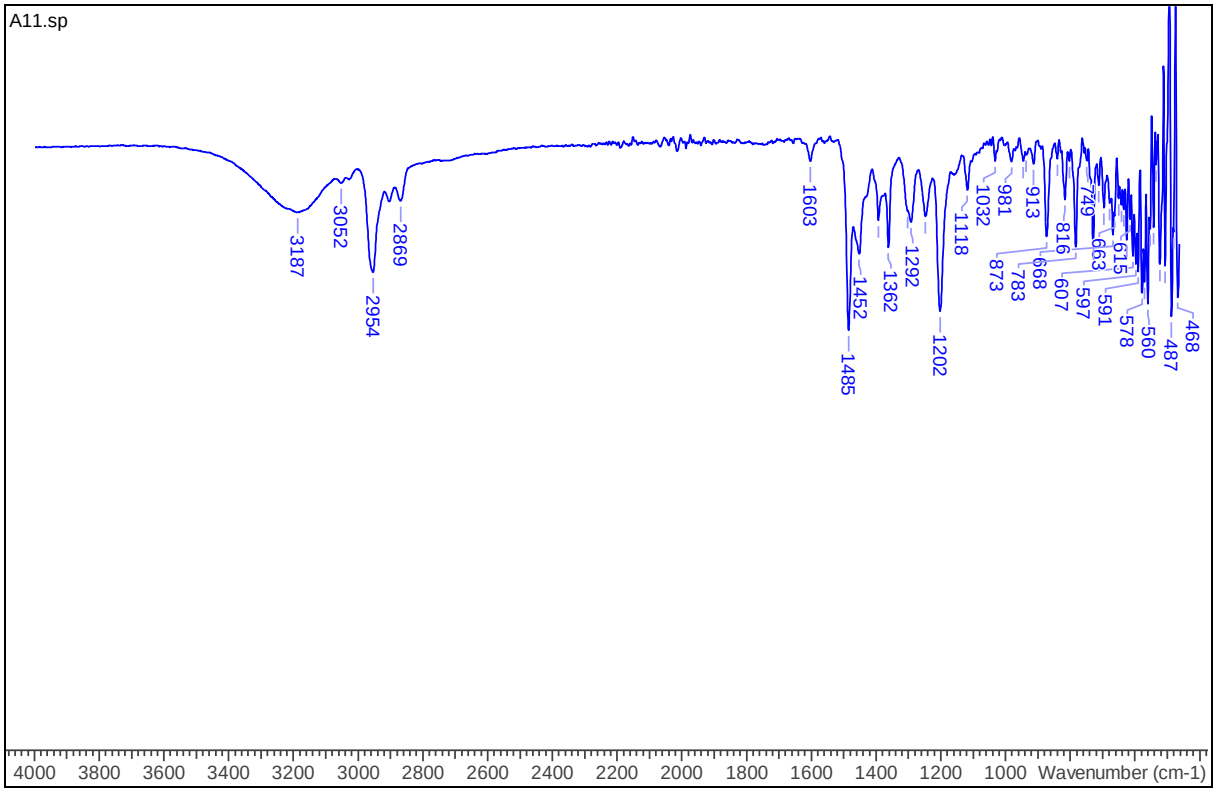

Figure 1.32: FT-IR spectrum of p-tertbutylcalix[4]arene (**18**)

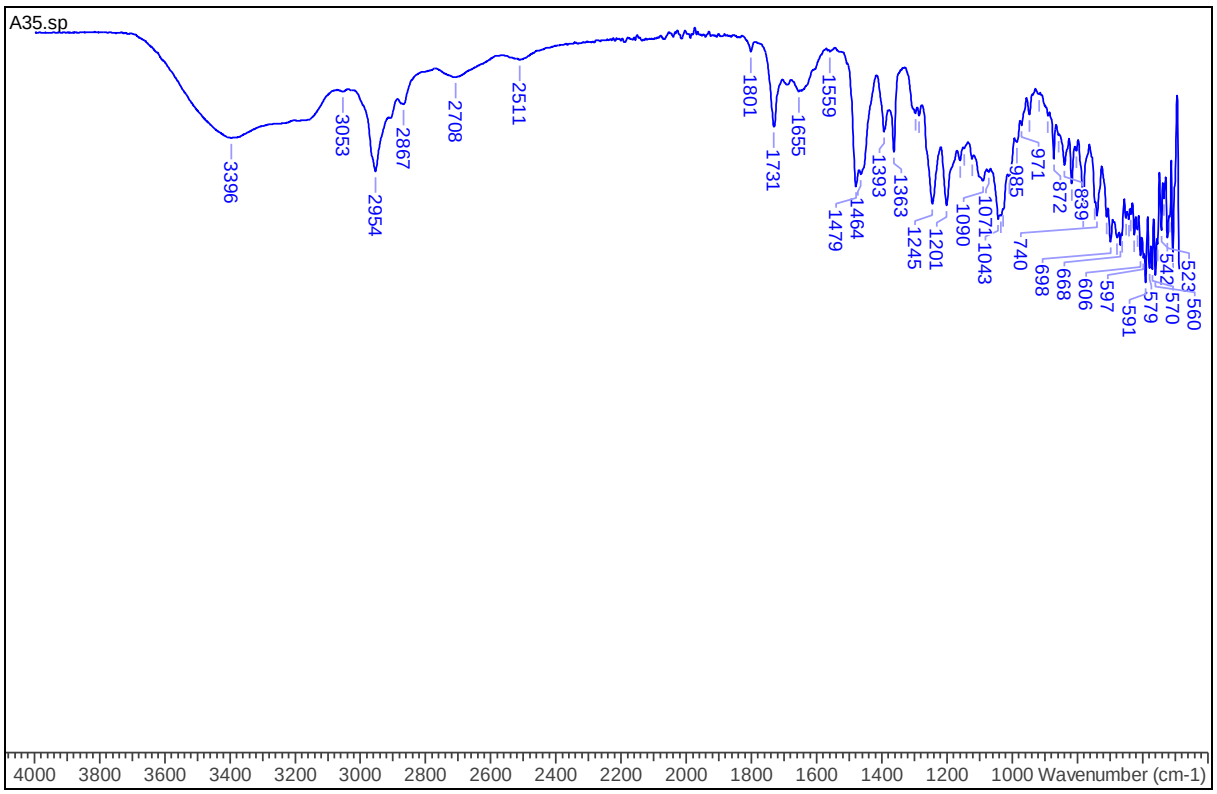

Figure 1.33: FT-IR spectrum of Compound A35

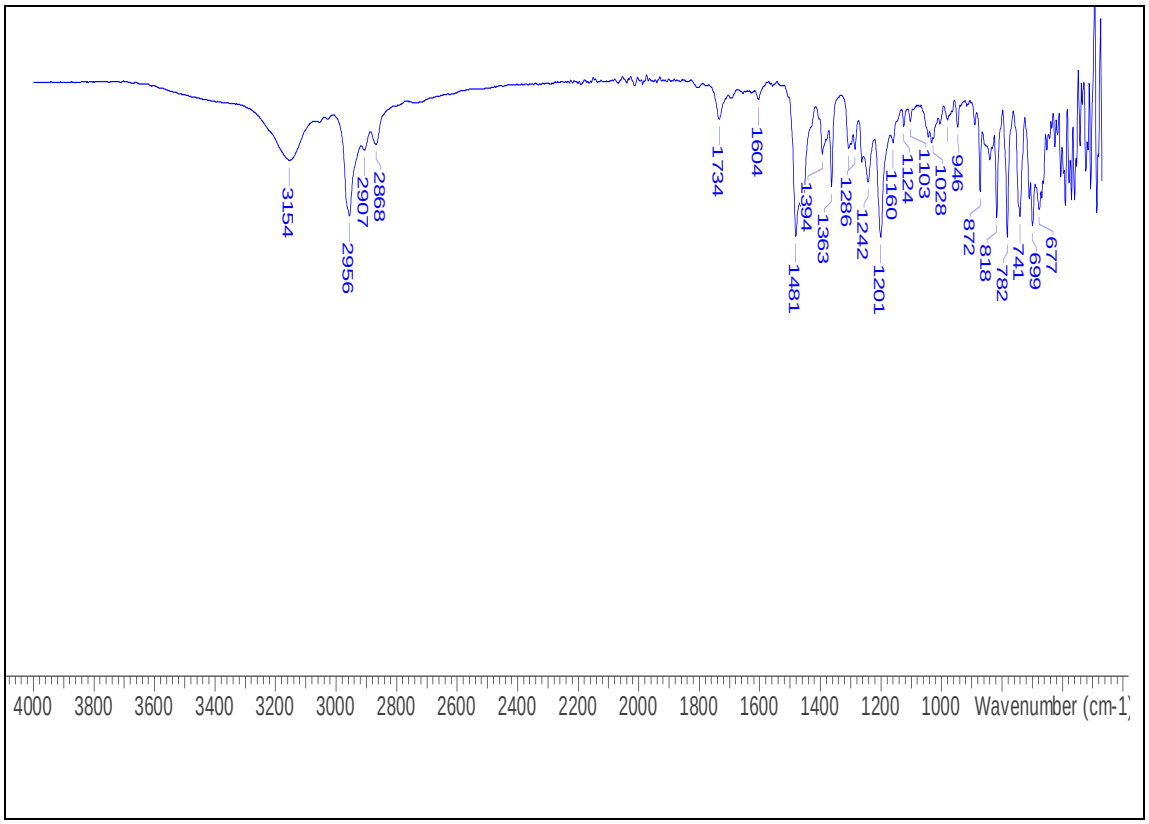

Figure 1.34: FT-IR spectrum of Compound A36

APPENDIX B: NMR spectra figures

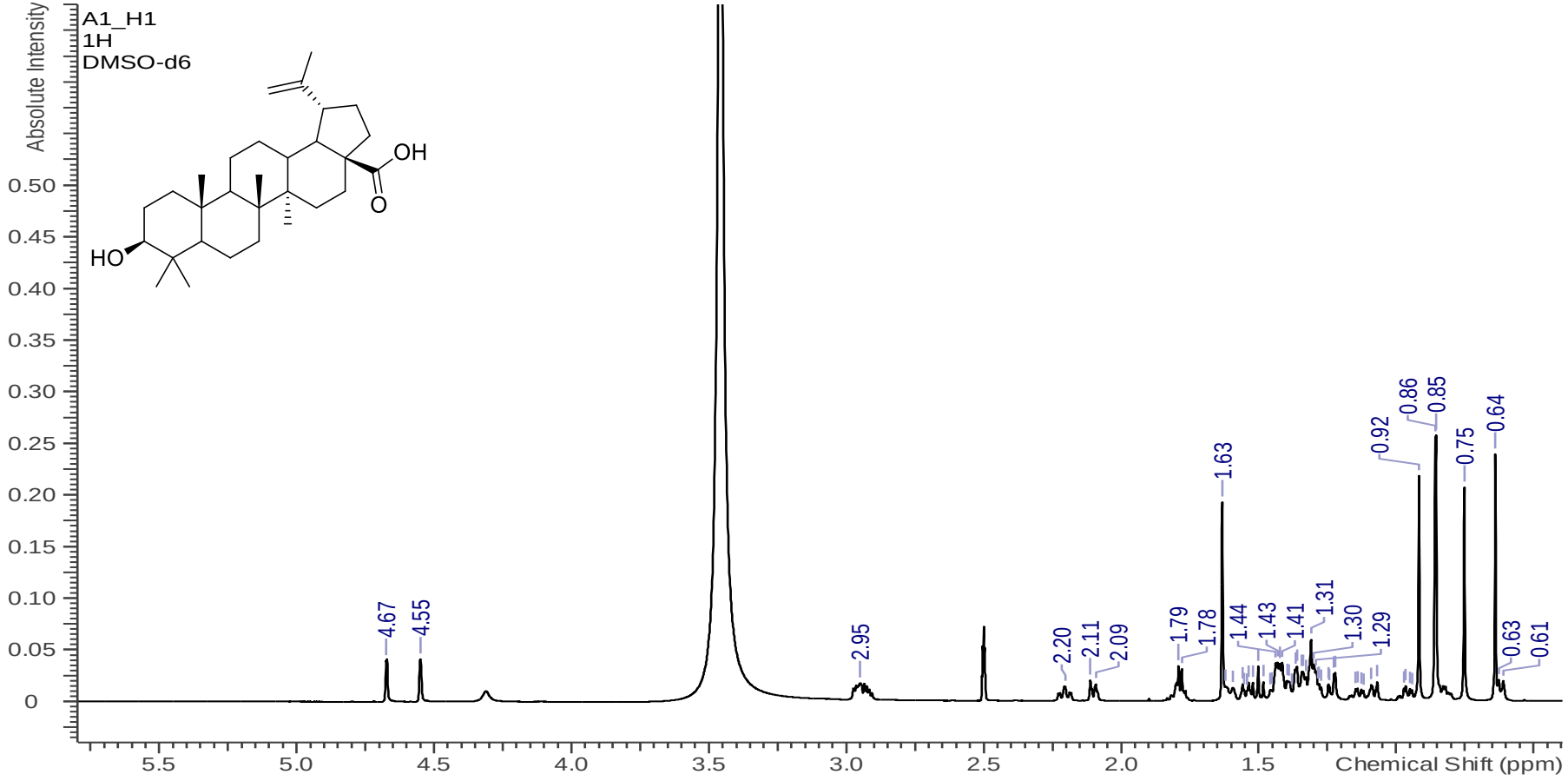

Figure 2.1: ^{1}H-NMR spectrum of BA (**4**)

*Note: The spectra provided in this section were the data obtained from NMR analysis of samples. Structures have been proposed for ease of reference, but not claimed 100% in some cases due to lack of other data.

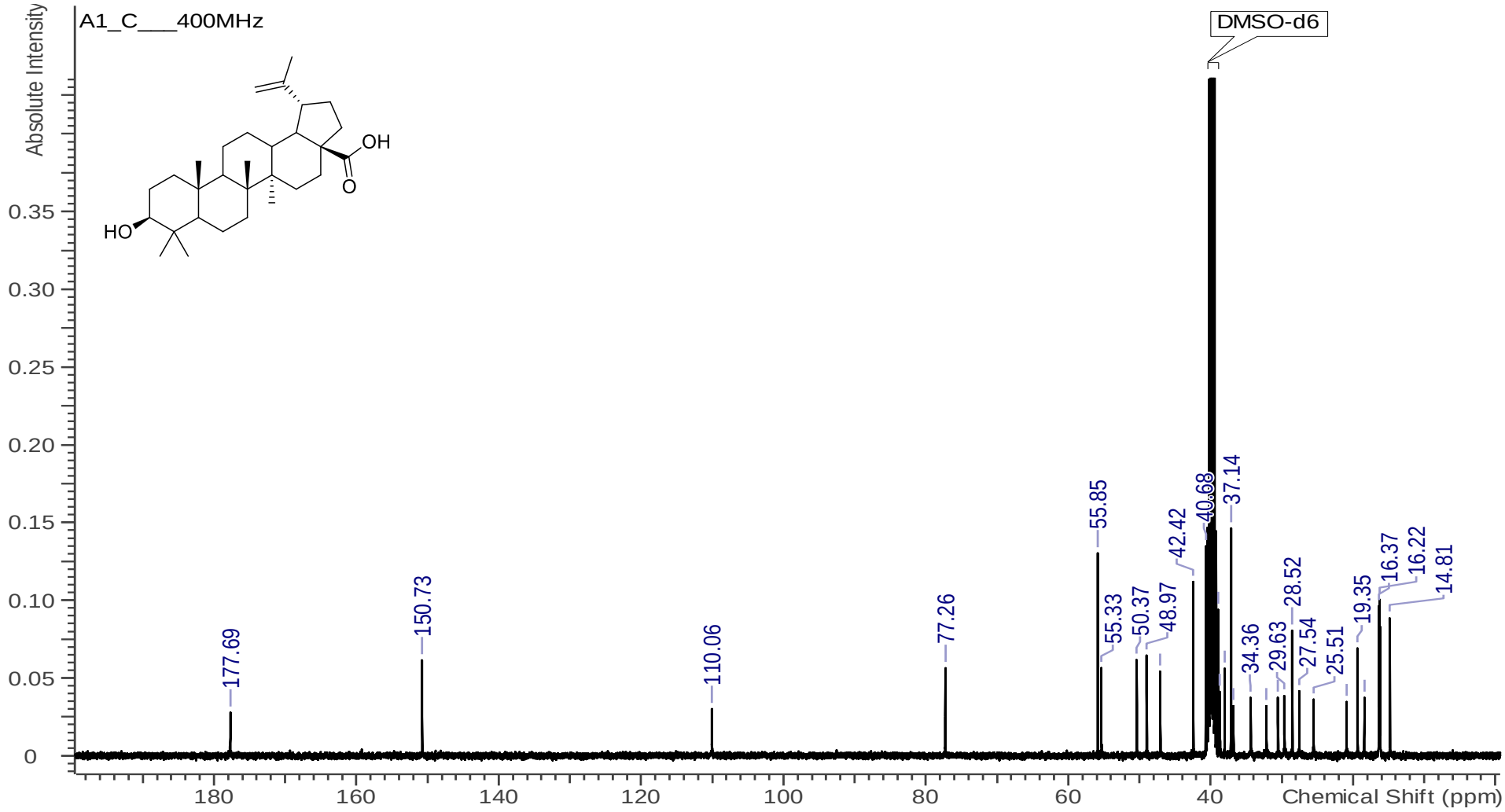

Figure 2.2: ^{13}C-NMR spectrum of BA (**4**)

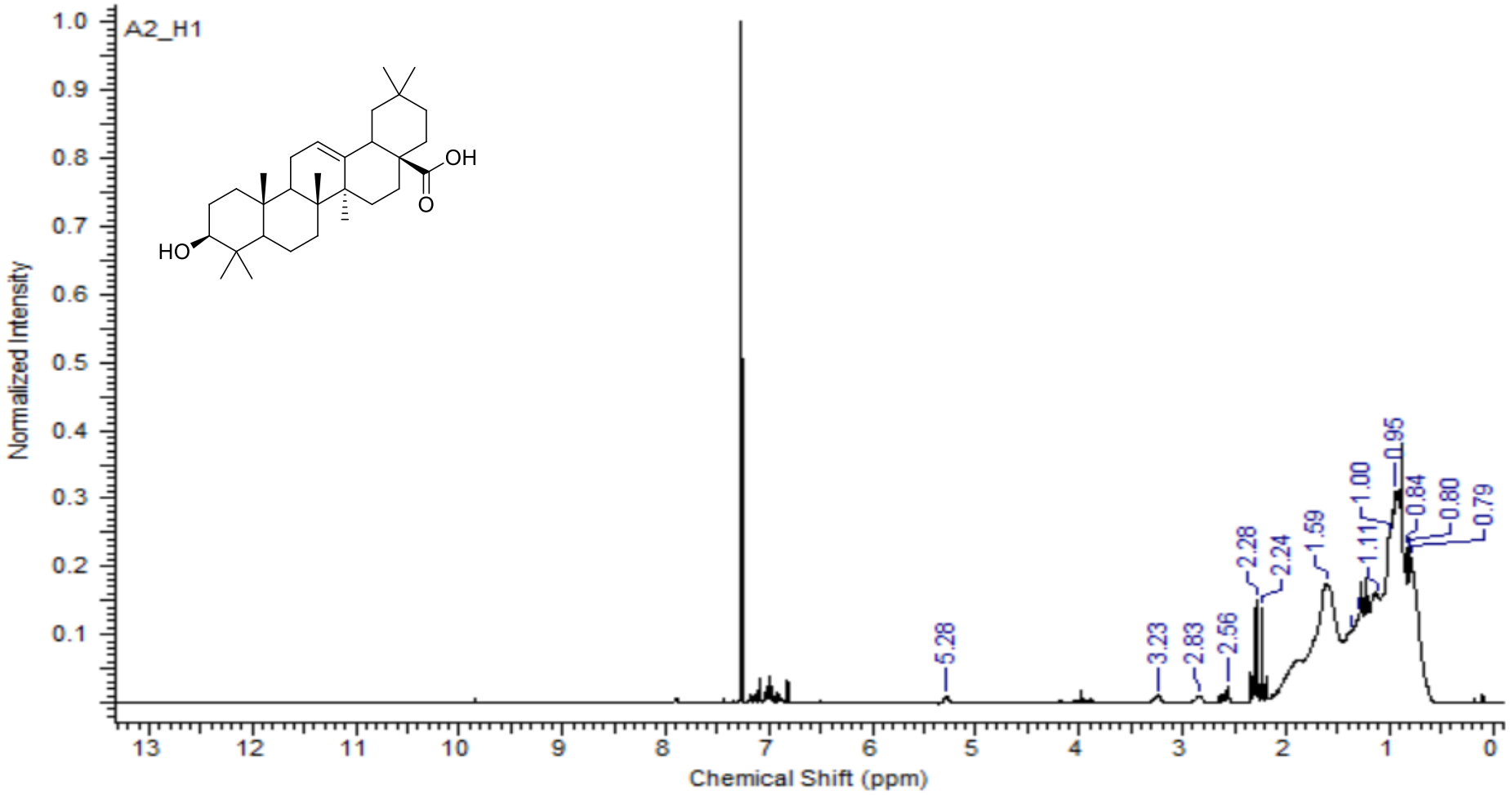

Figure 2.3: ^{1}H-NMR spectrum of OA (**5**)

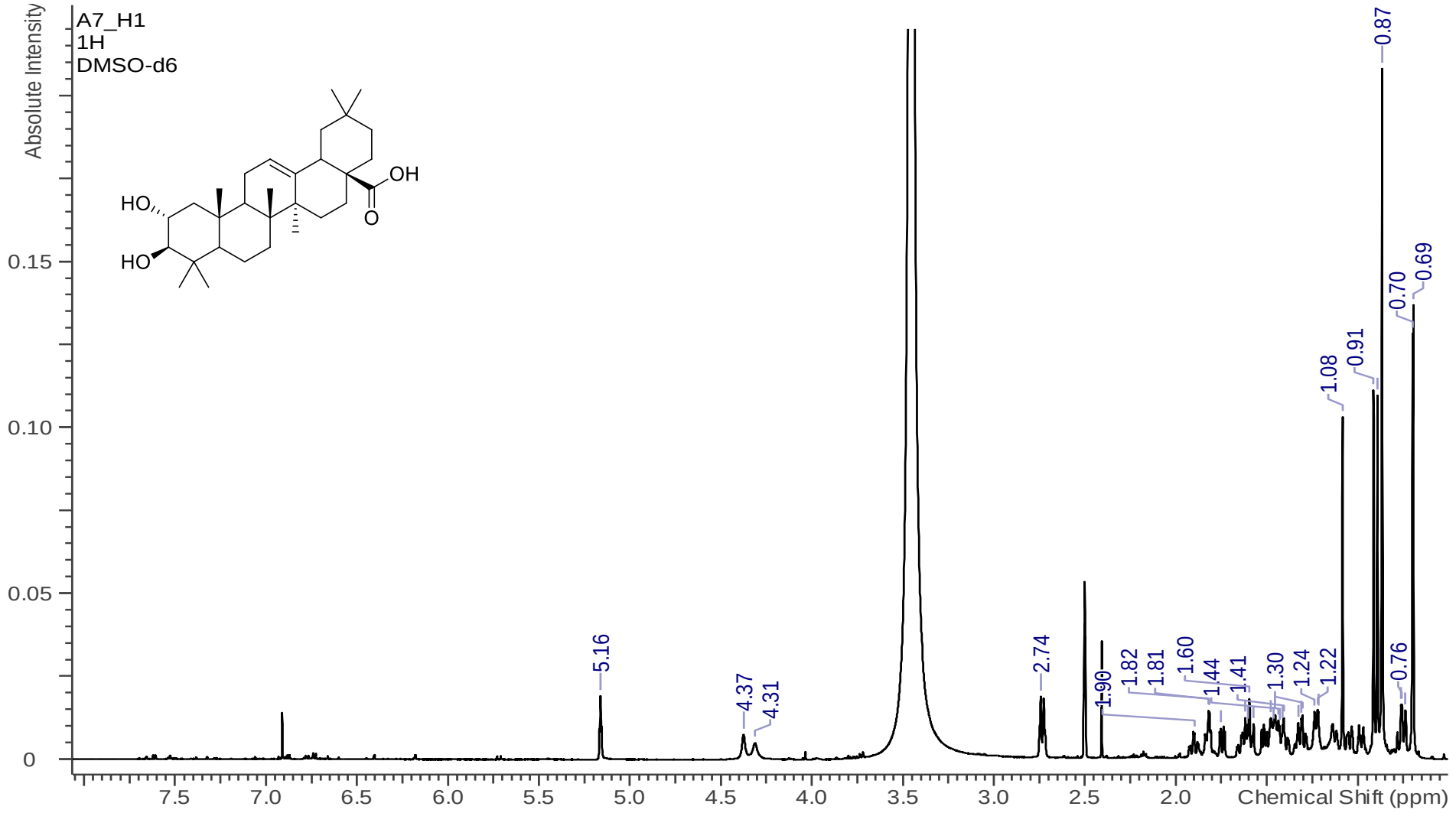

Figure 2.4: ^{1}H-NMR spectrum of MA (**11**)

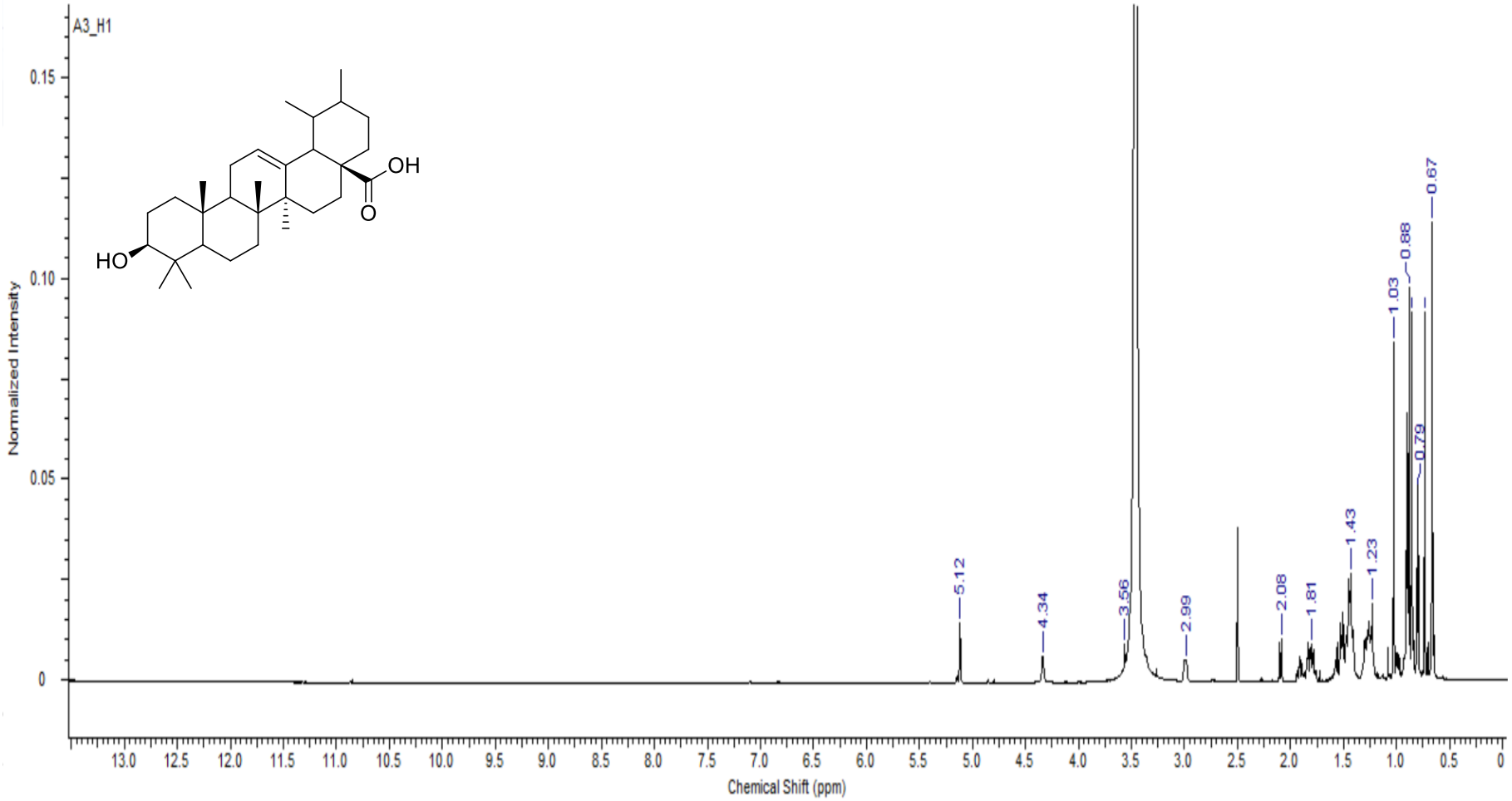

Figure 2.5: ^{1}H-NMR spectrum of UA (**6**)

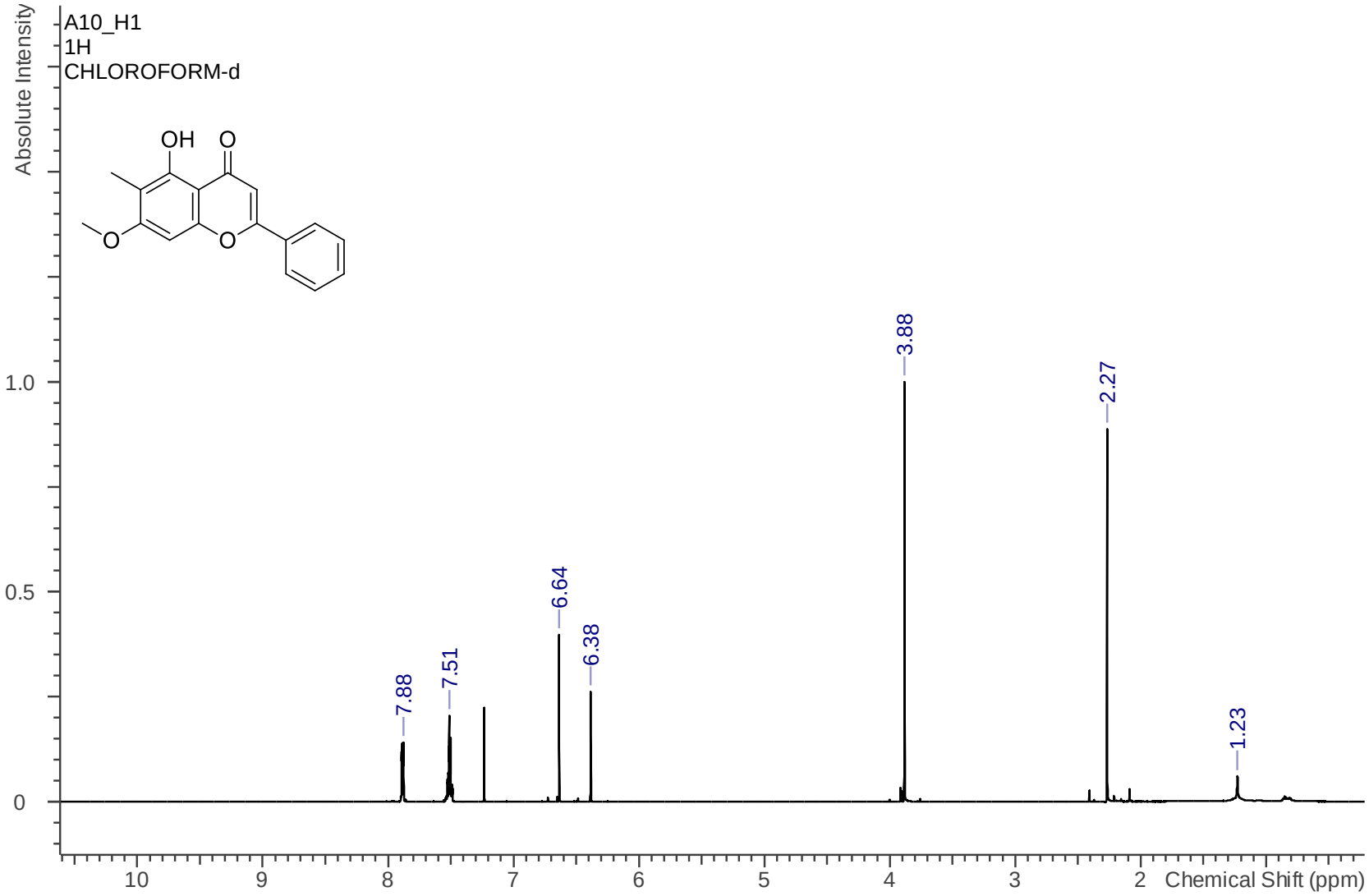

Figure 2.6: ^{1}H-NMR spectrum of 5-hydroxy-7-methoxy-6-methylflavone (**19**)

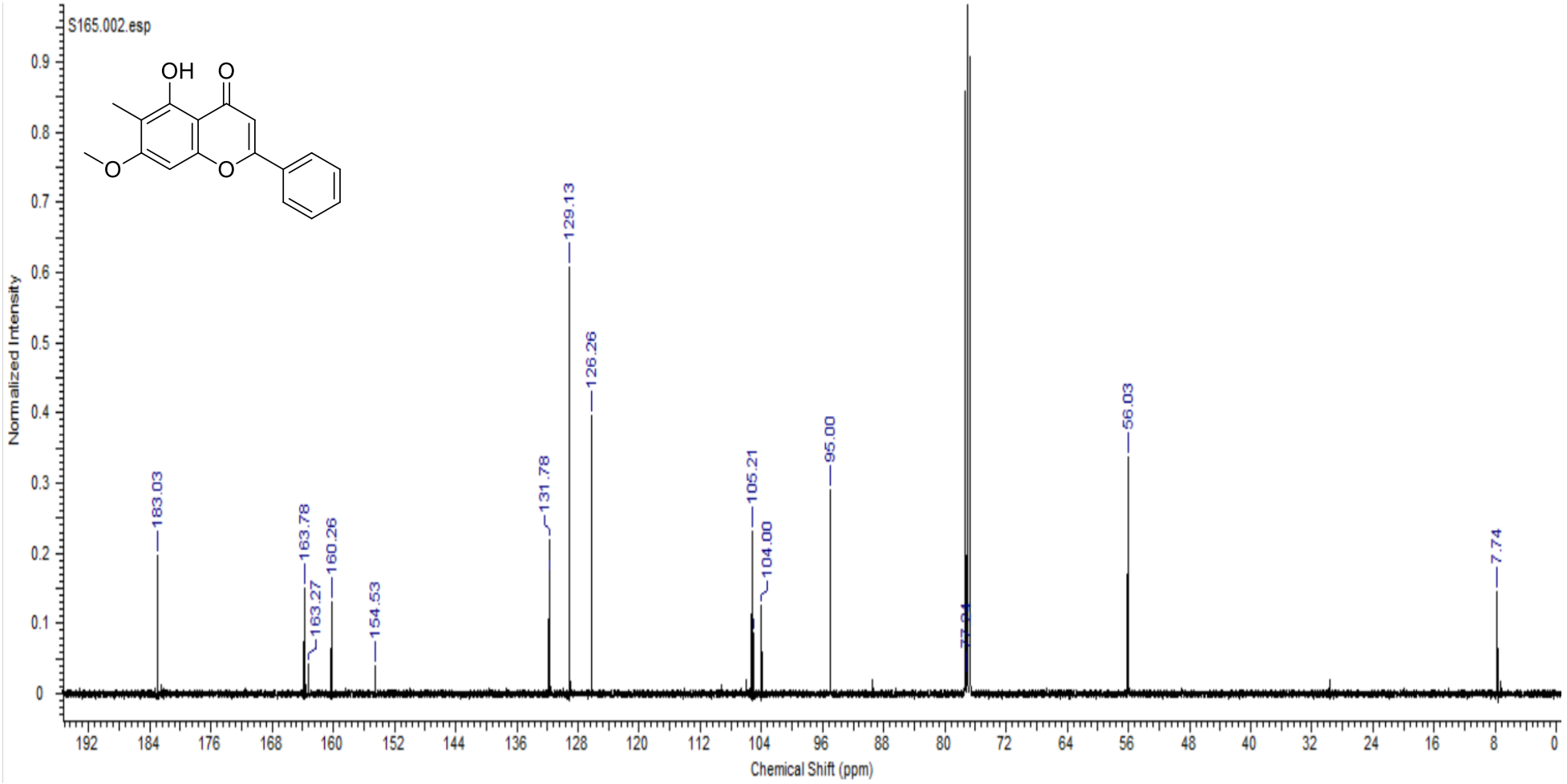

Figure 2.7: ^{13}C-NMR spectrum of 5-hydroxy-7-methoxy-6-methylflavone (**19**)

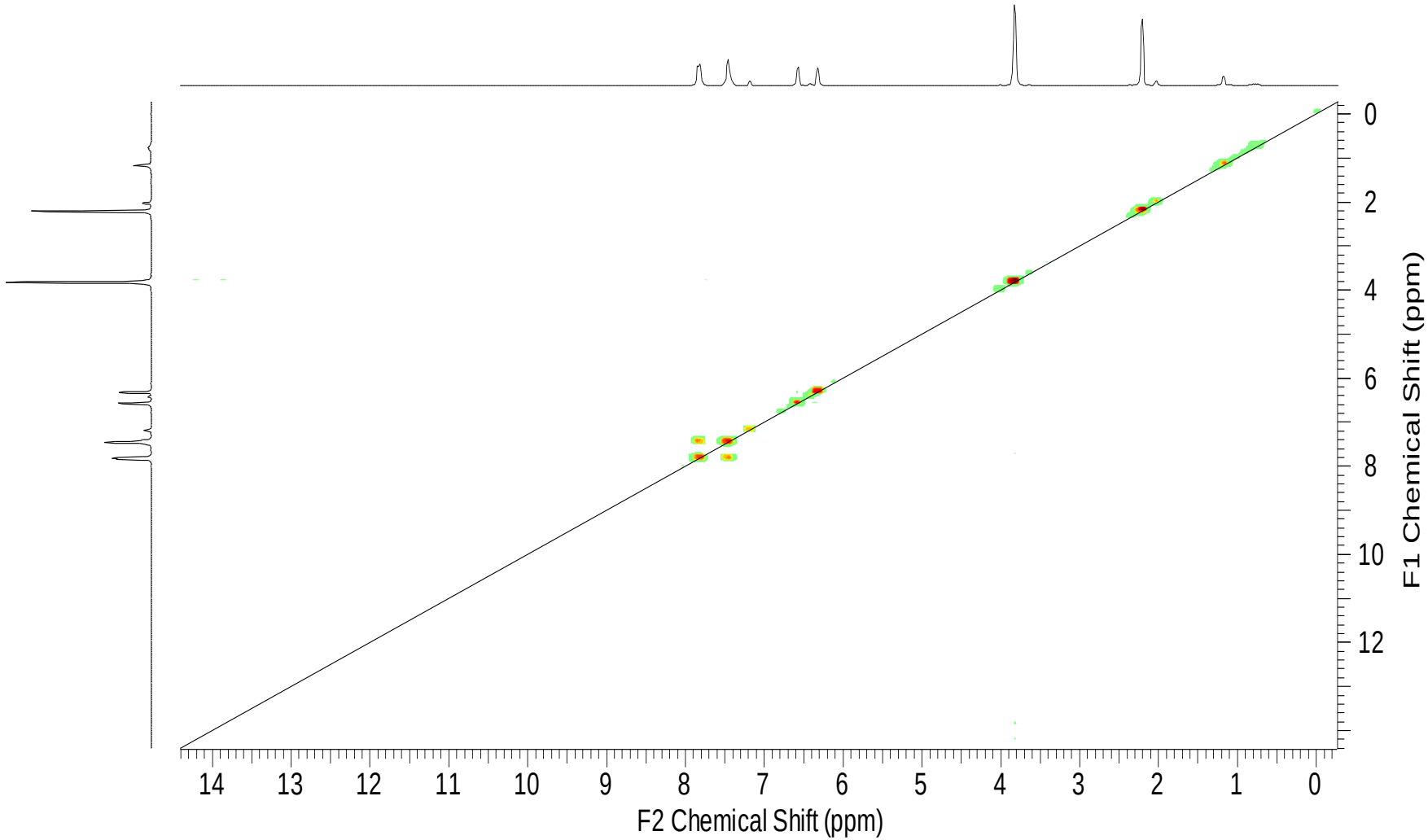

Figure 2.8: H-H COSY NMR spectrum of 5-hydroxy-7-methoxy-6-methylflavone (**19**)

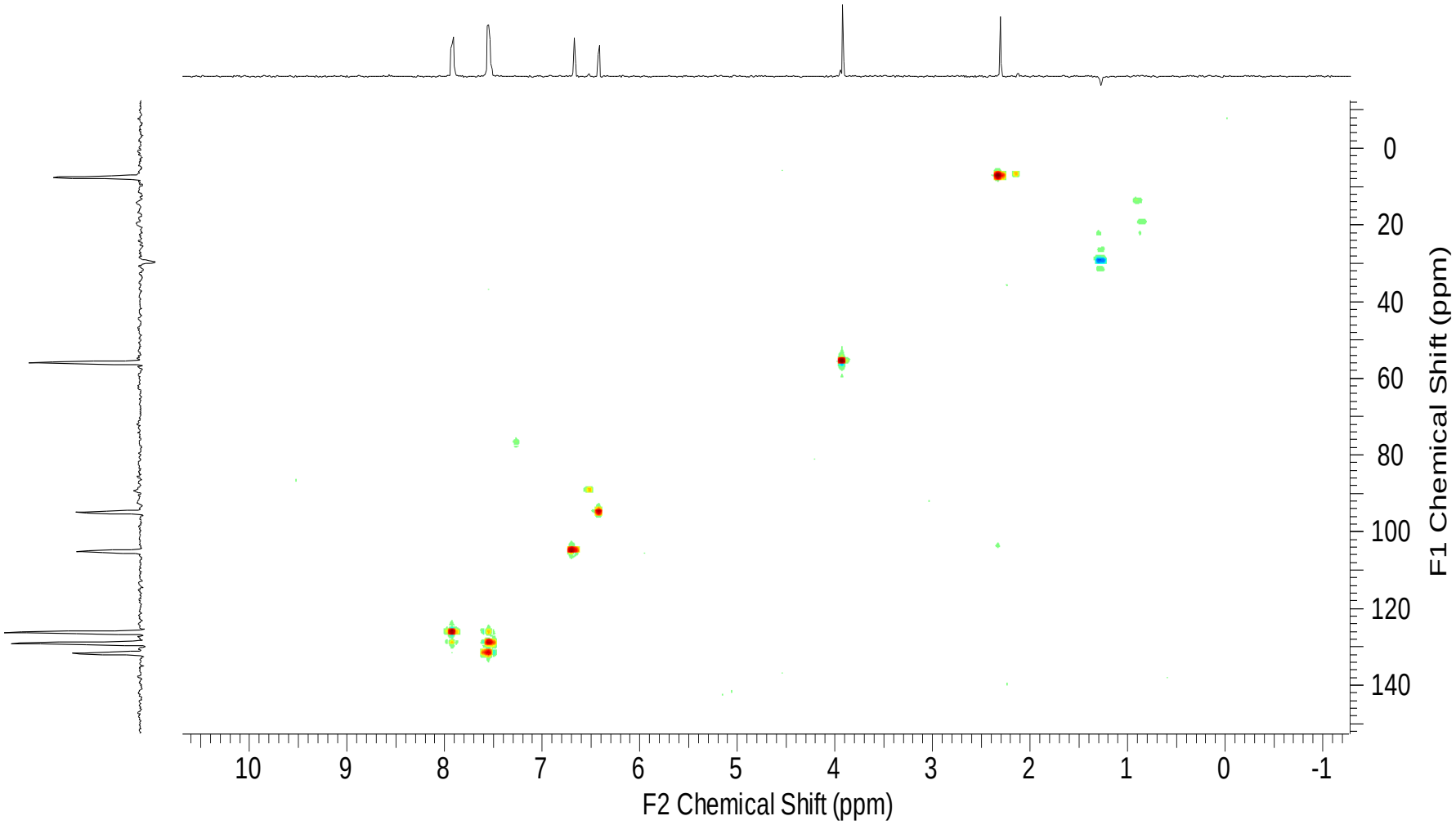

Figure 2.9: HSQC NMR spectrum of 5-hydroxy-7-methoxy-6-methylflavone (**19**)

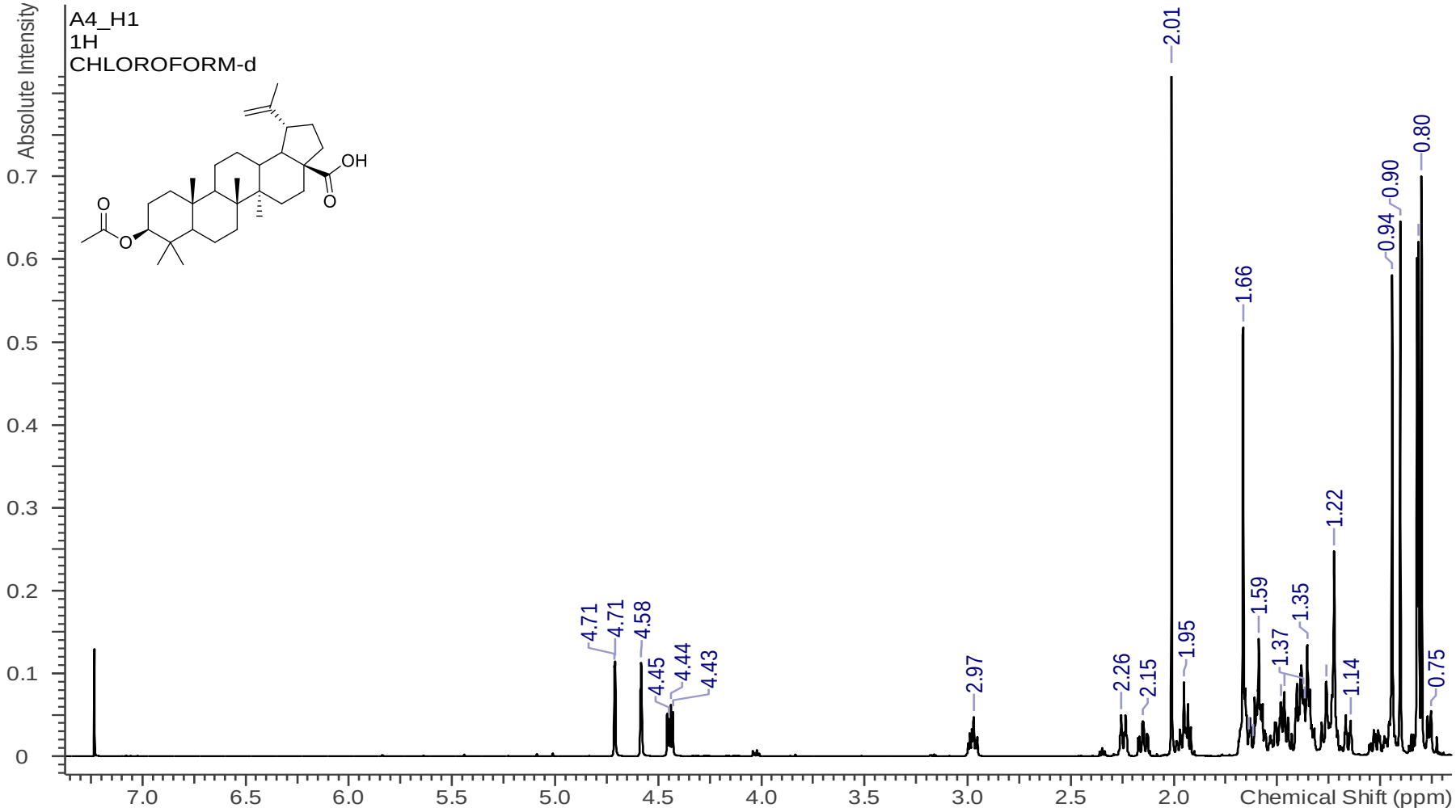

Figure 2.10: ^{1}H-NMR spectrum of BAA (**20**)

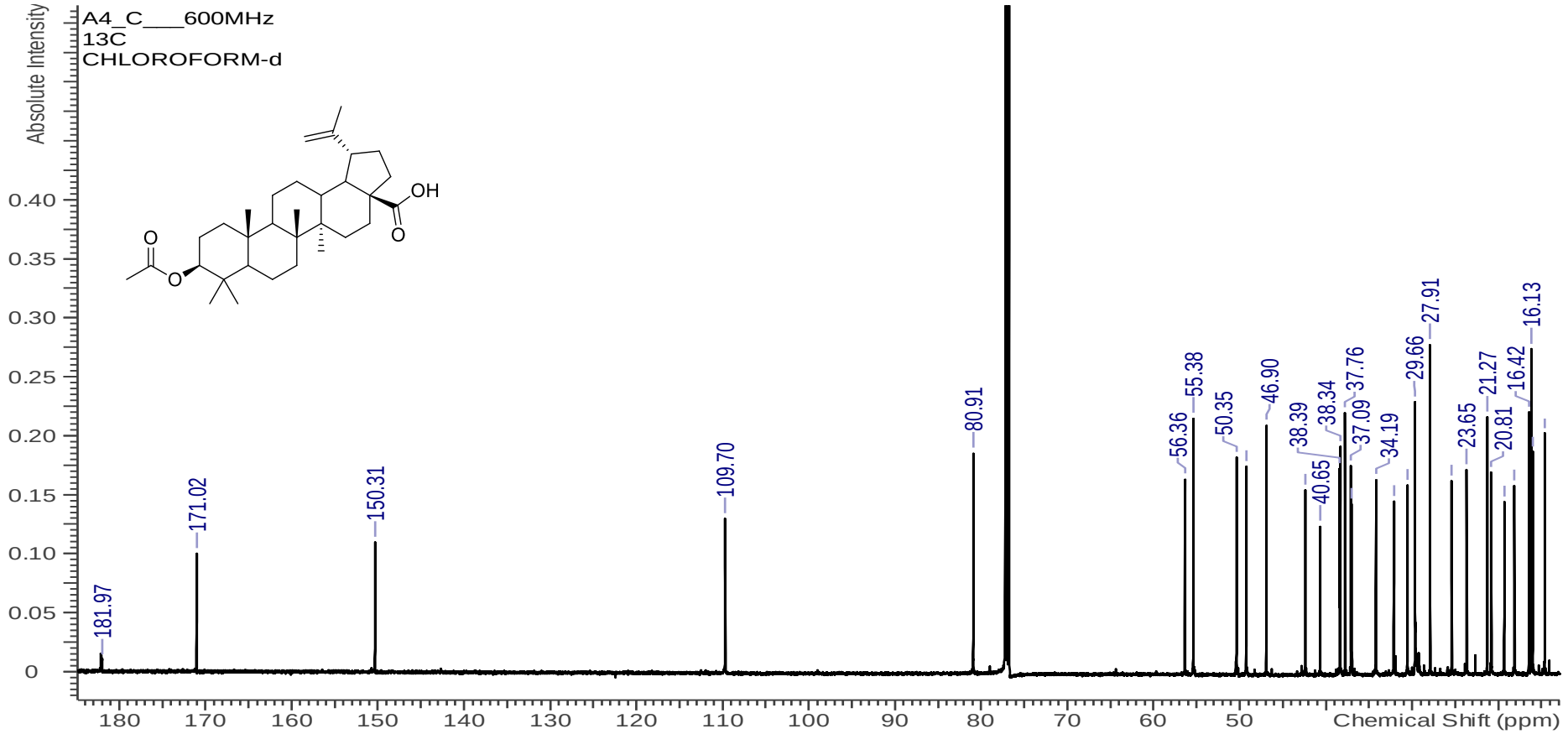

Figure 2.11: ^{13}C-NMR spectrum of BAA (**20**)

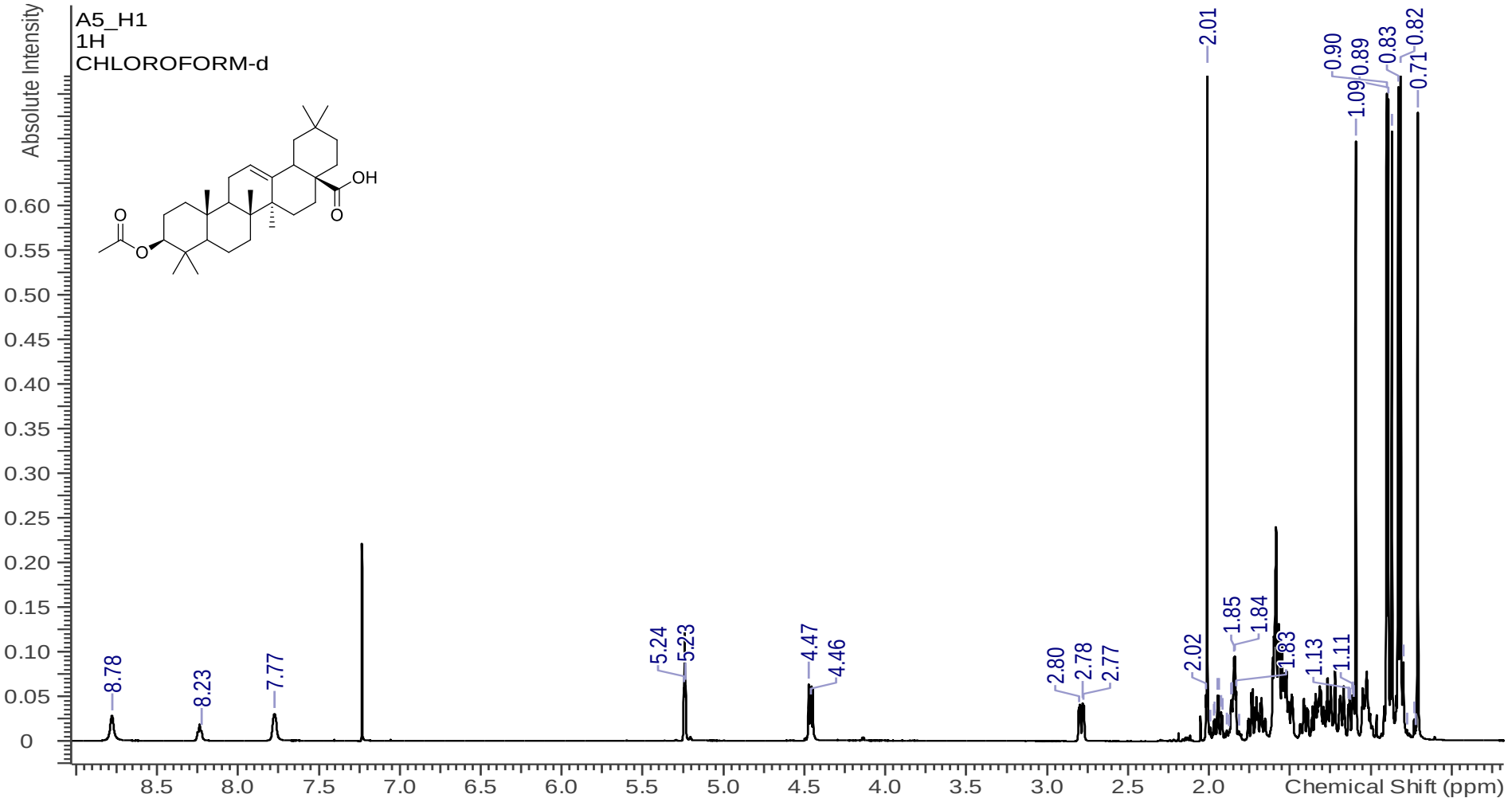

Figure 2.12: ^{1}H-NMR spectrum of OAA (**21**)

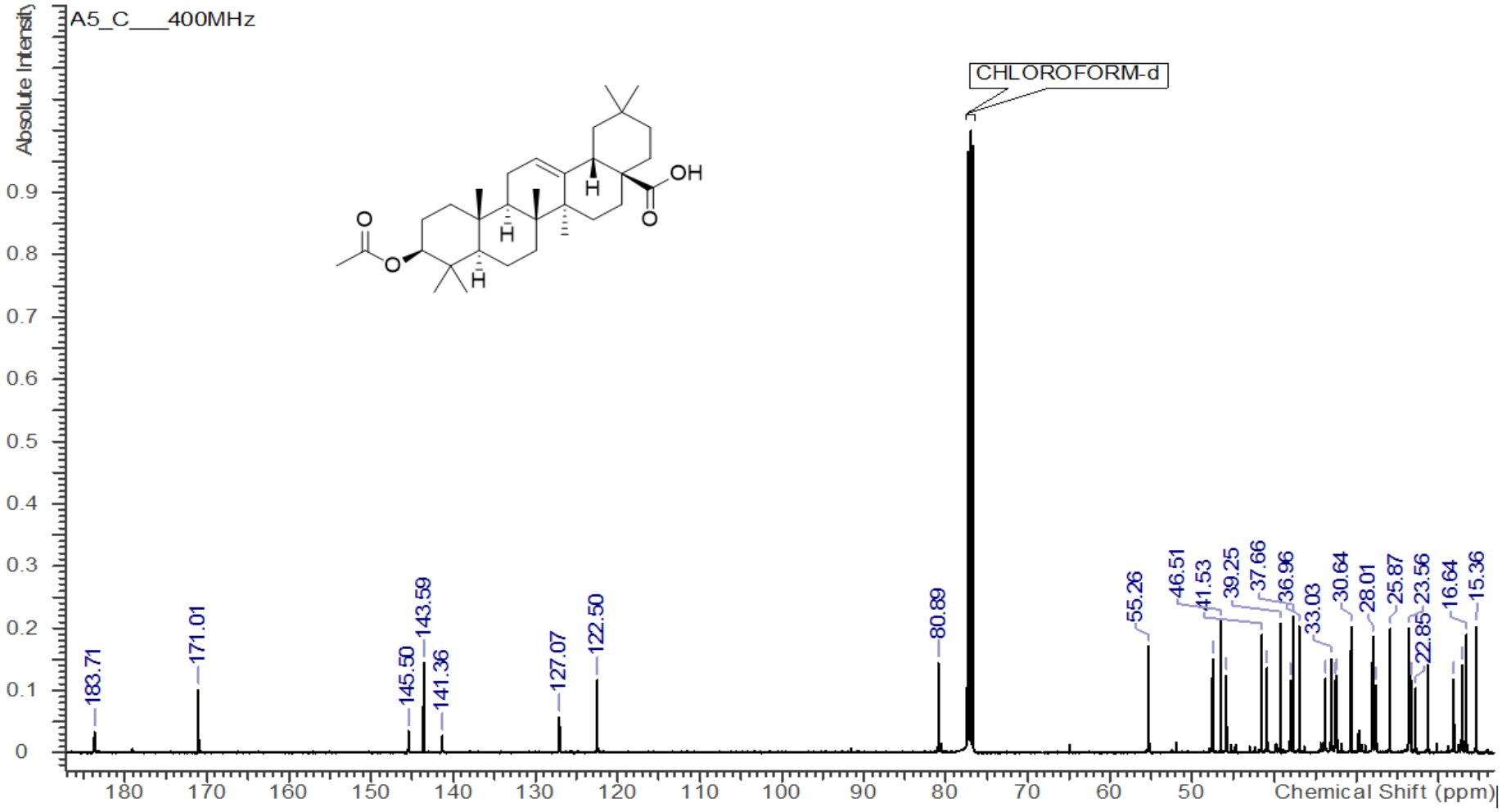

Figure 2.13: ^{13}C-NMR spectrum of OAA (**21**)

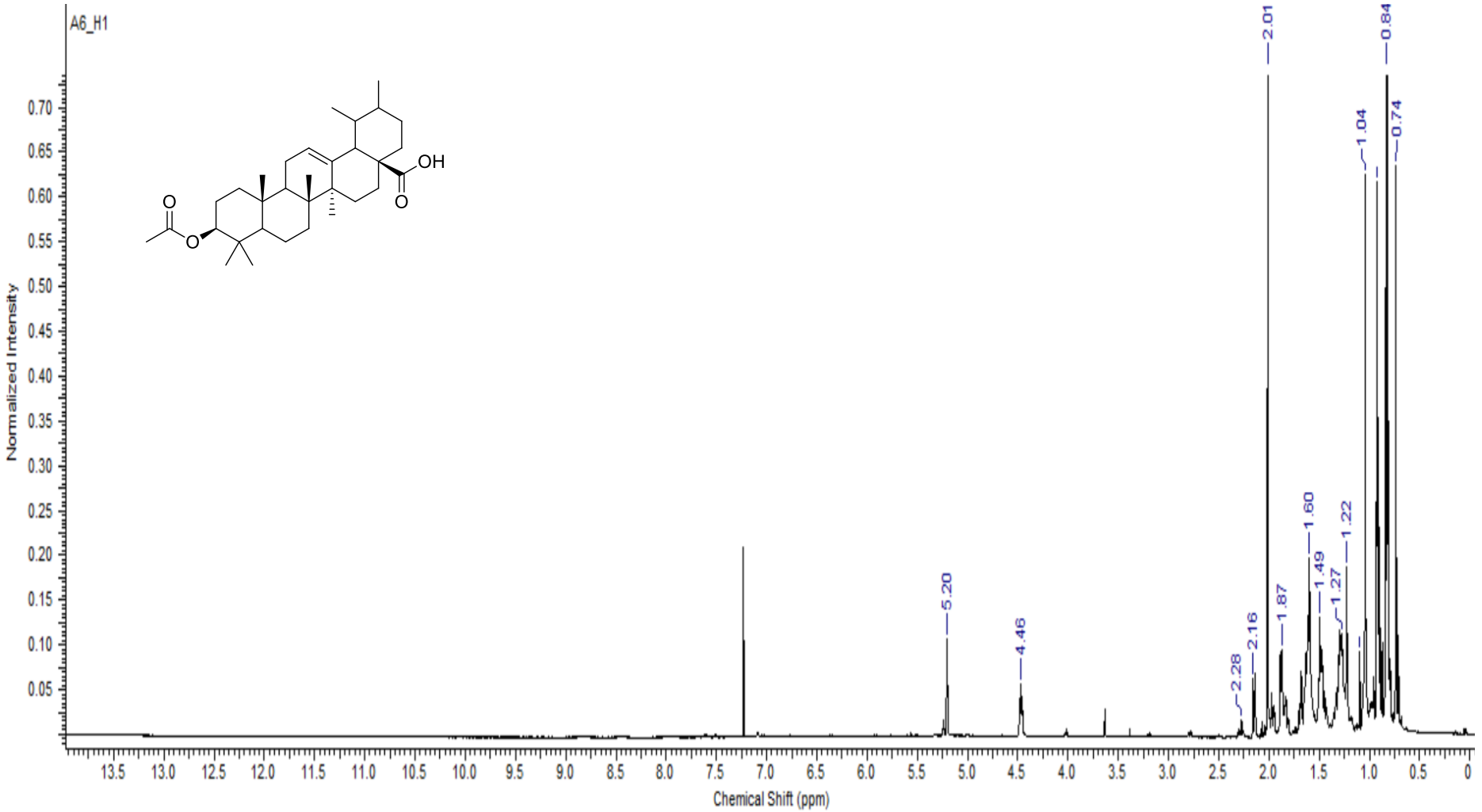

Figure 2.14: ^{1}H-NMR spectrum of UAA (**22**)

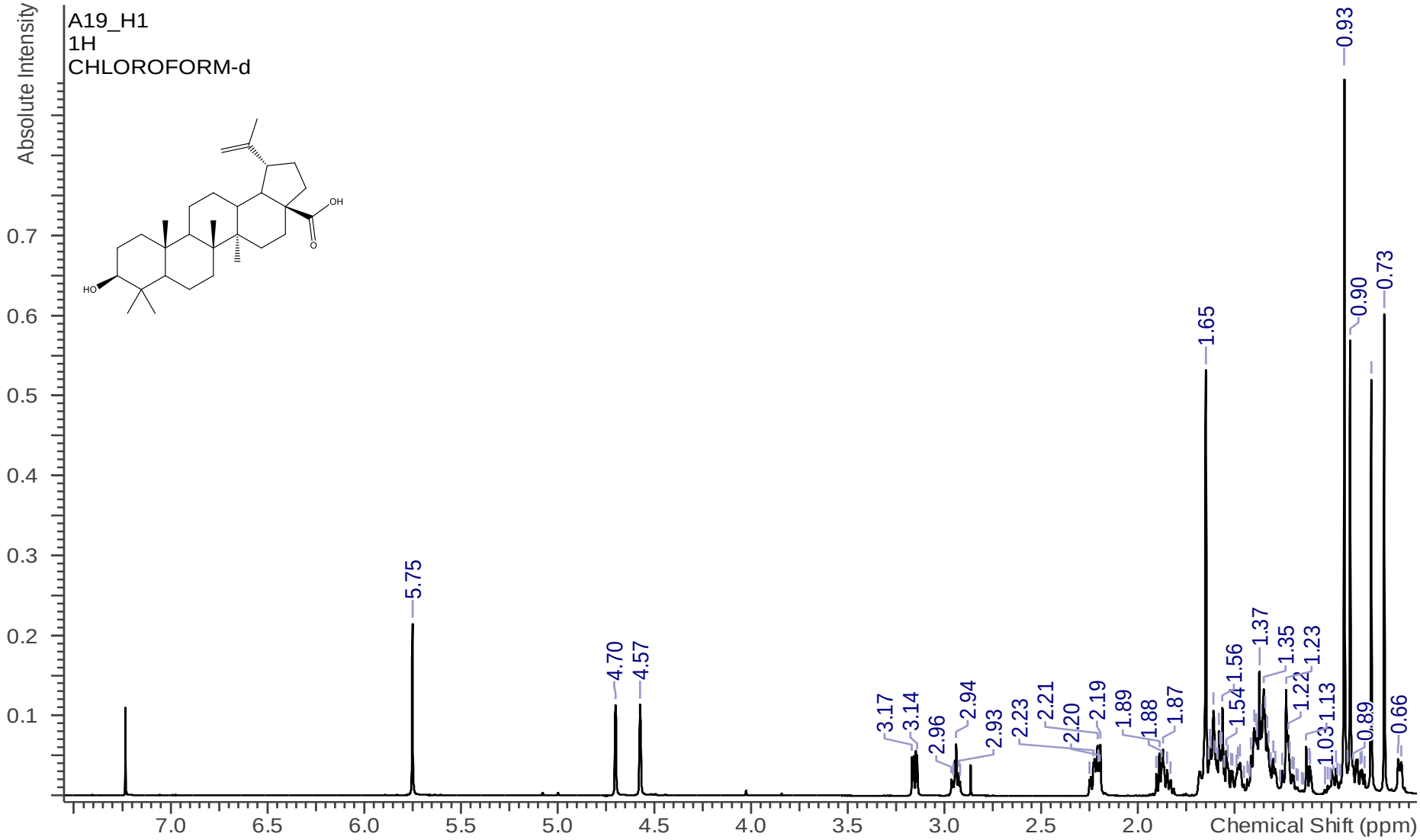

Figure 2.15: ^{1}H-NMR spectrum of compound (**23**)

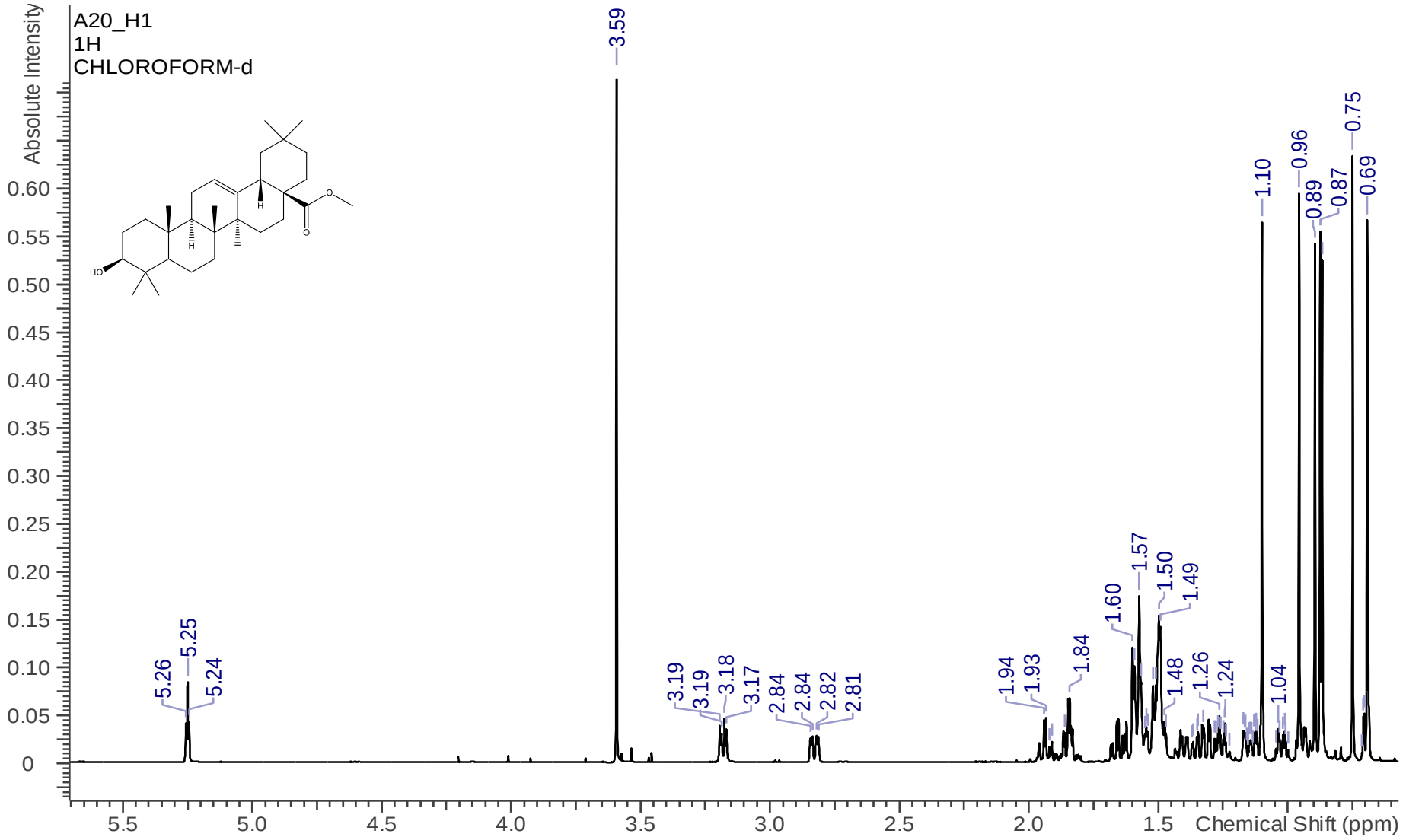

Figure 2.16: ^{1}H-NMR spectrum of methyl oleanolate (**24**)

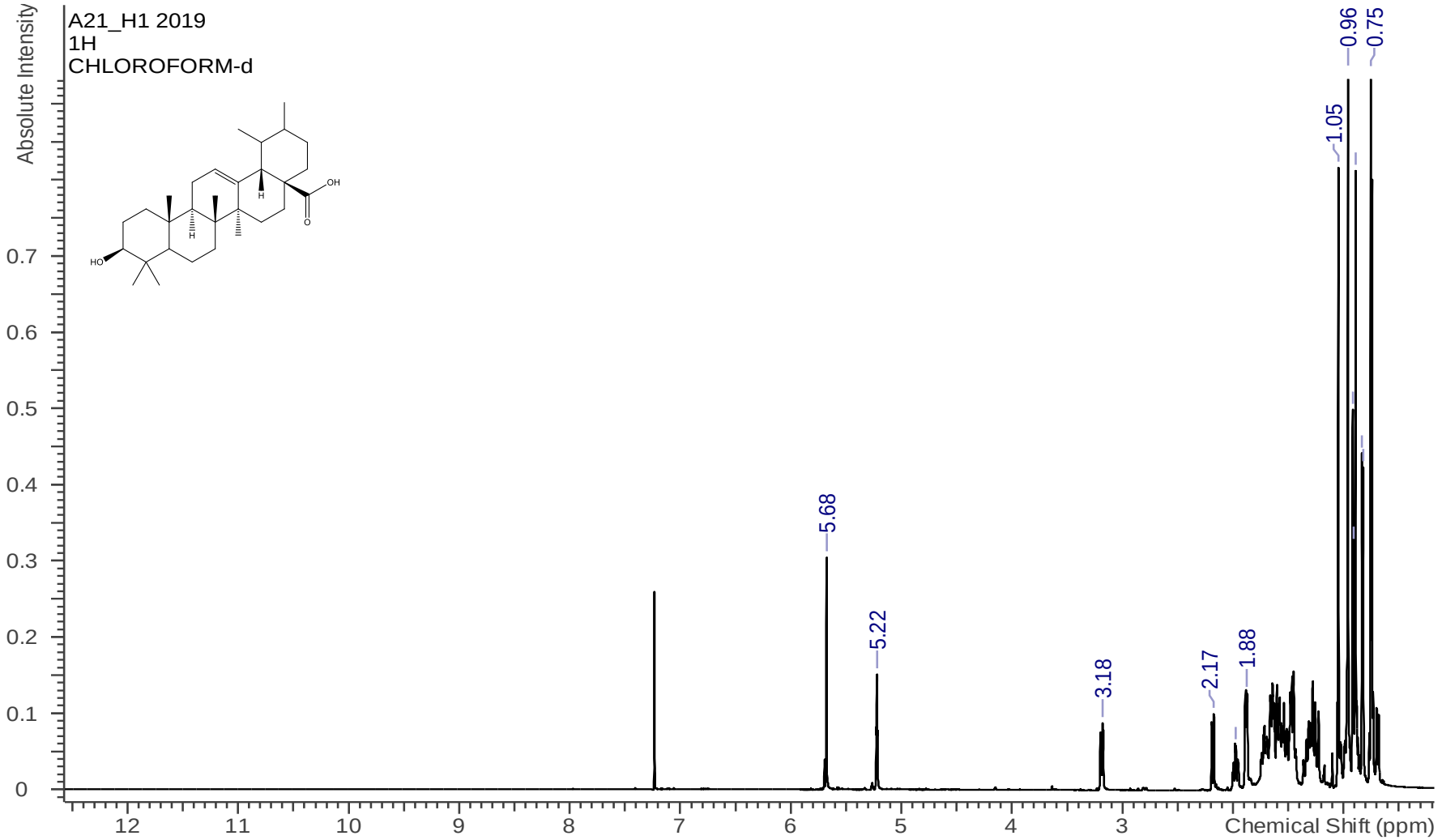

Figure 2.17: ^{1}H-NMR spectrum of Product (**25**)

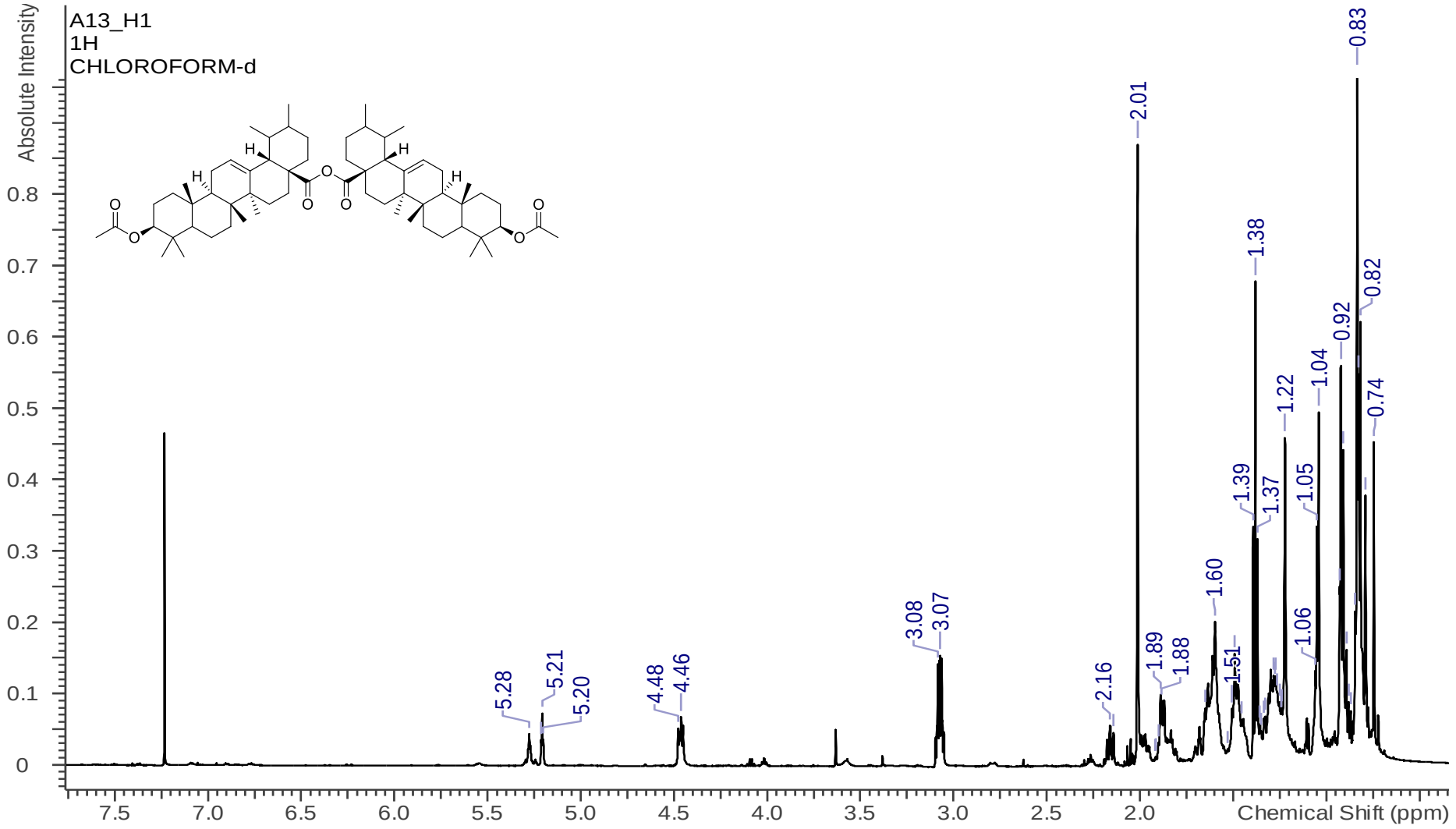

Figure 2.18: ^{1}H-NMR spectrum of Compound A13

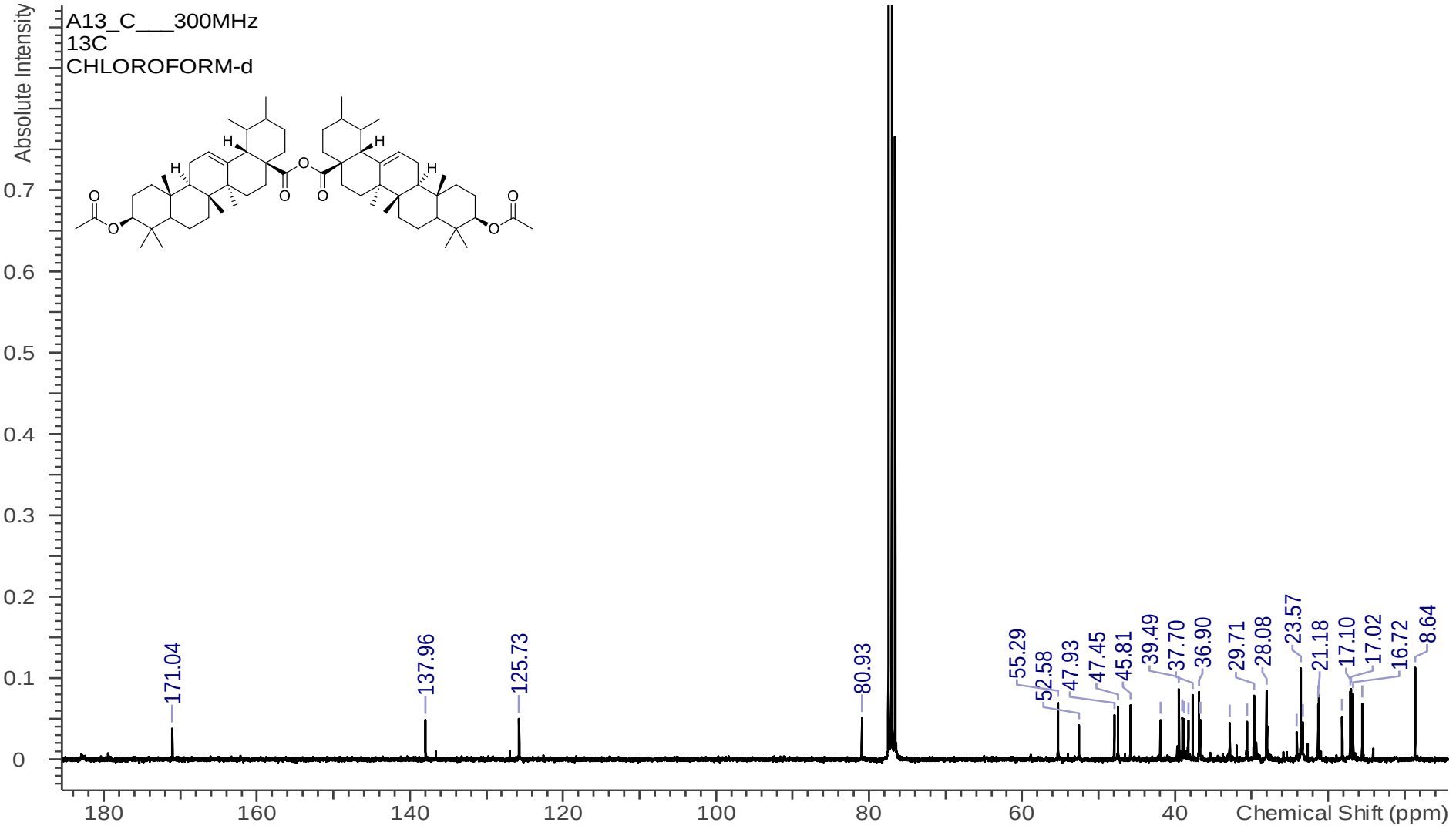

Figure 2.19: ^{13}C-NMR spectrum of Compound A13

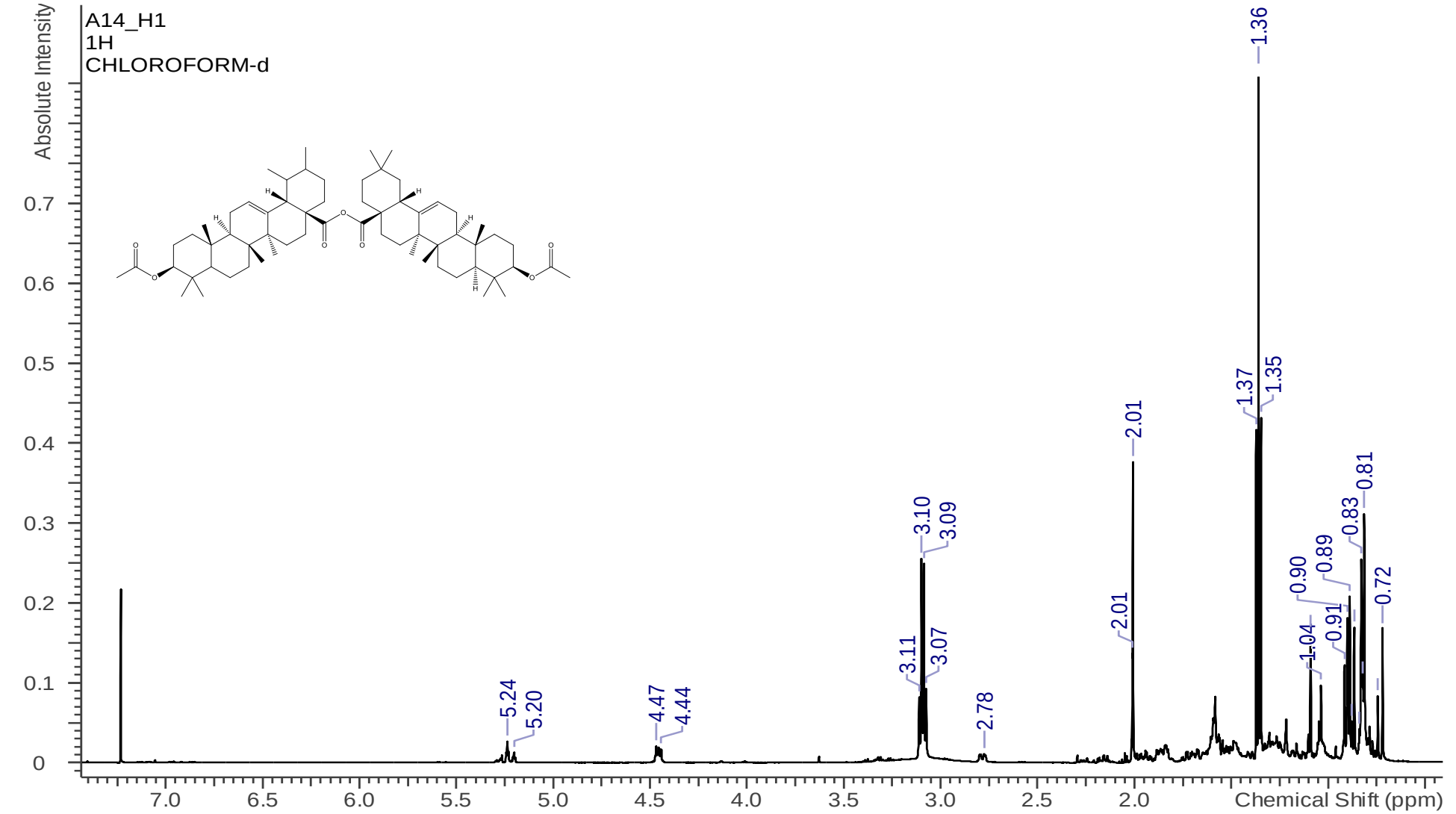

Figure 2.20: ^{1}H-NMR spectrum of Compound A14

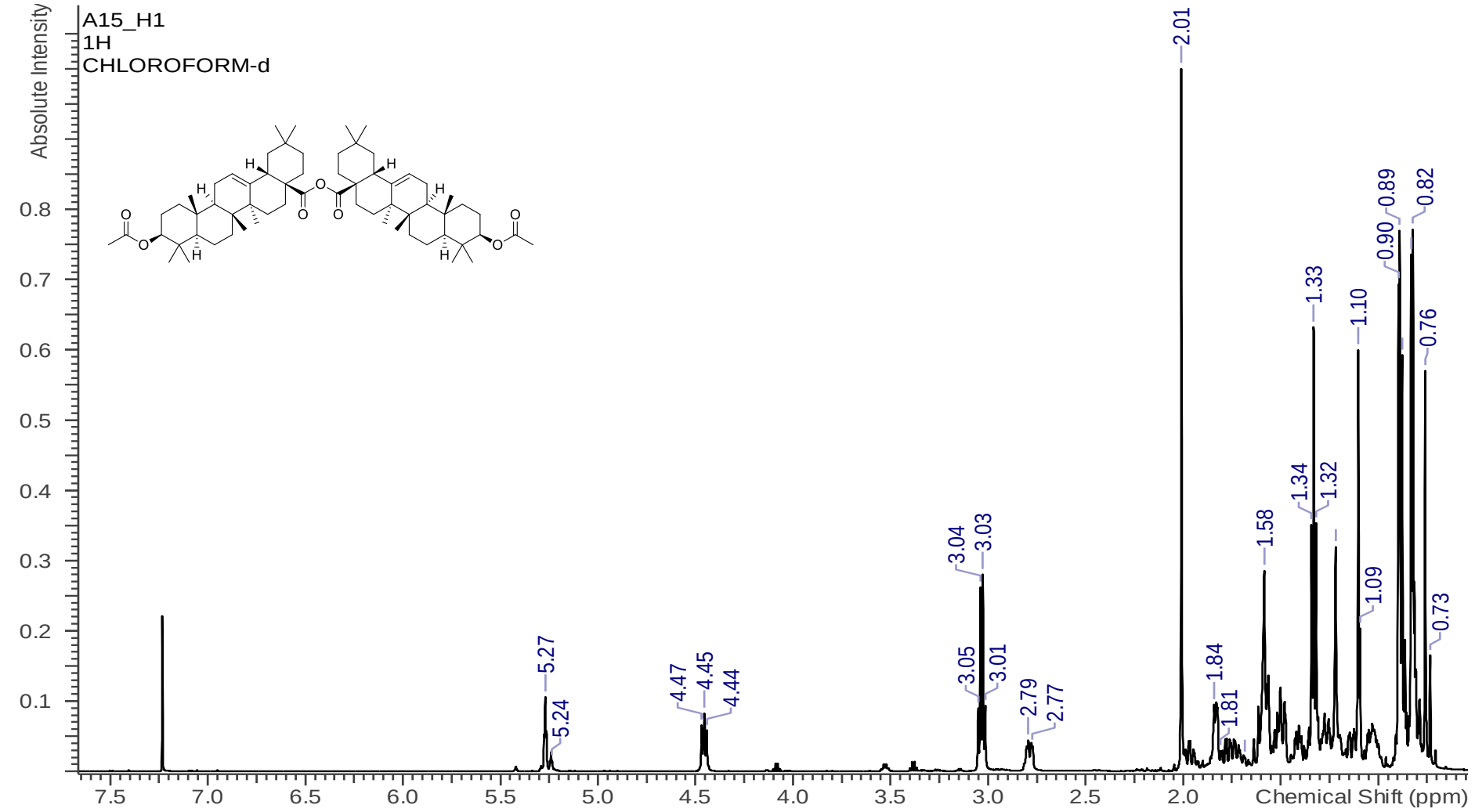

Figure 2.21: ^{1}H-NMR spectrum of Compound A15

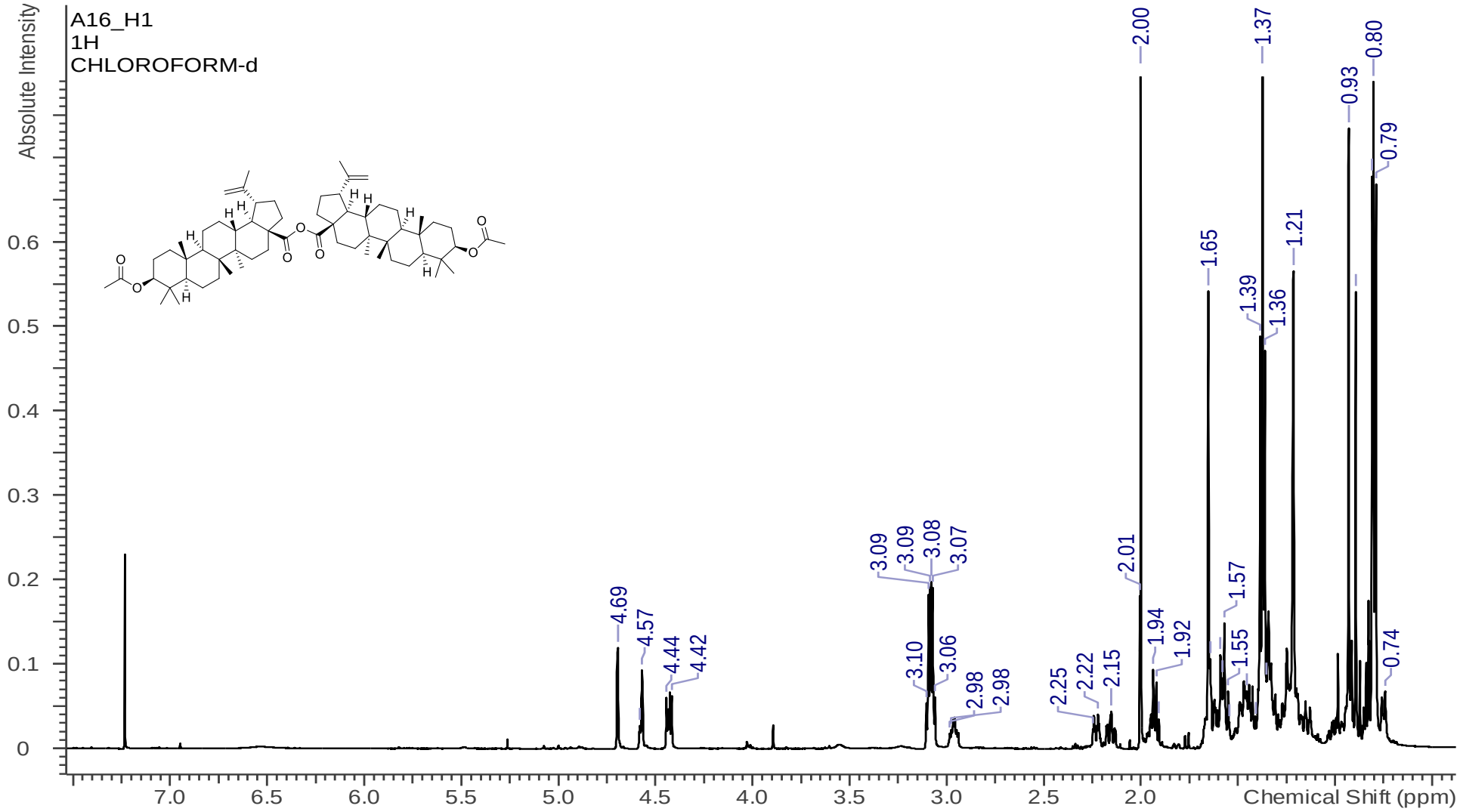

Figure 2.22: ^{1}H-NMR spectrum of Compound A16

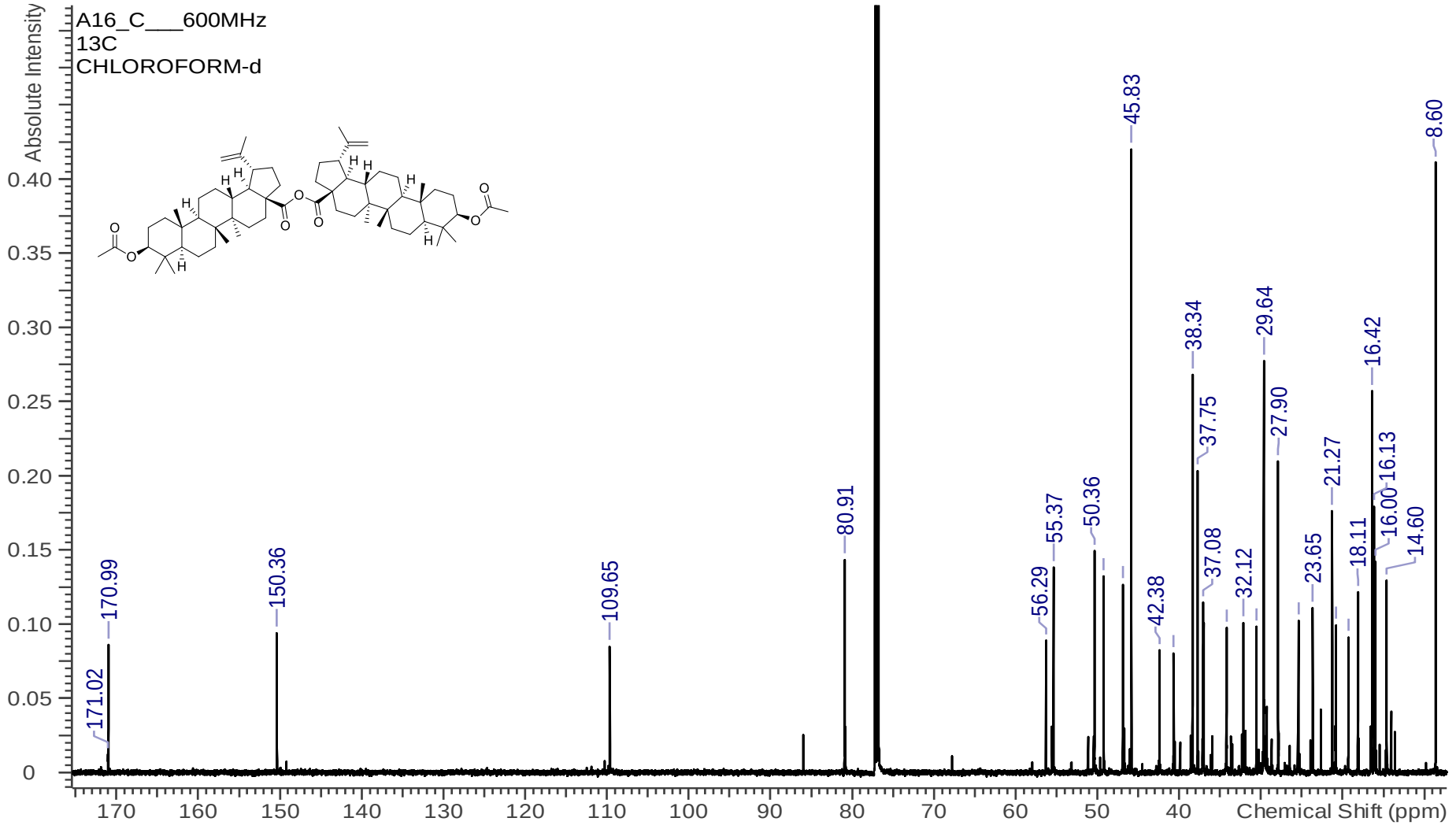

Figure 2.23: ^{13}C-NMR spectrum of Compound A16

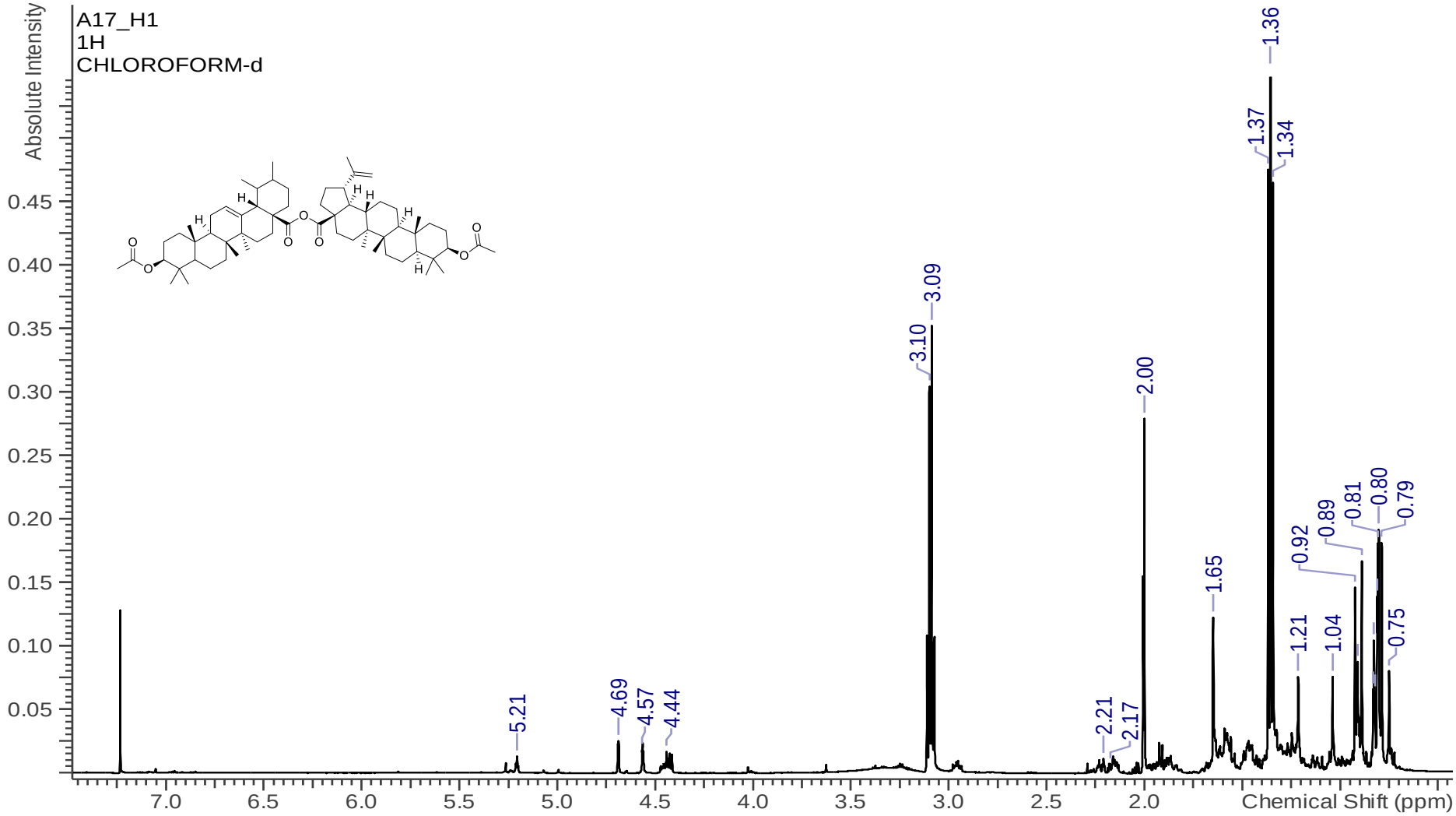

Figure 2.24: ^{1}H-NMR spectrum of Compound A17

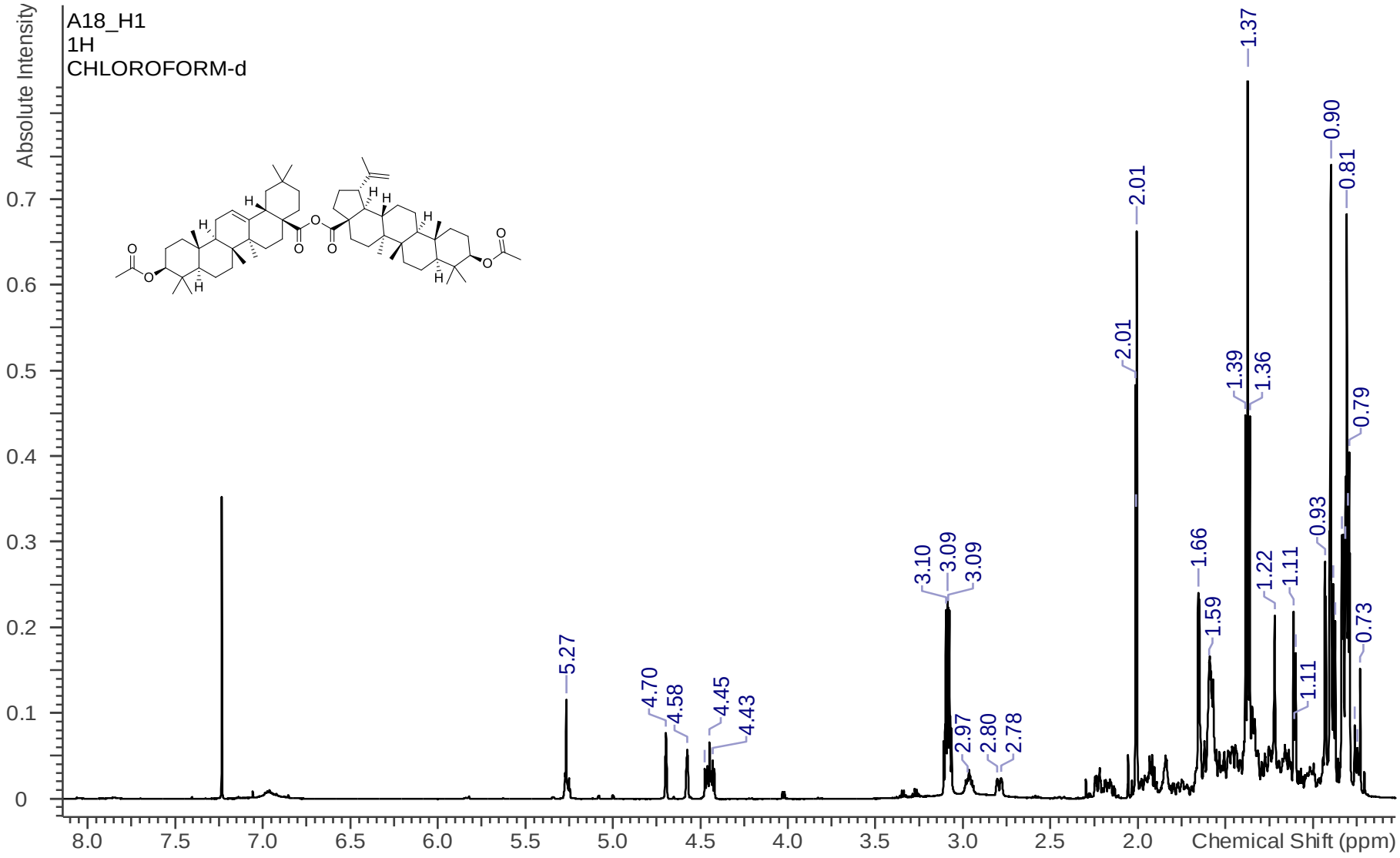

Figure 2.25: ^{1}H-NMR spectrum of Compound A18

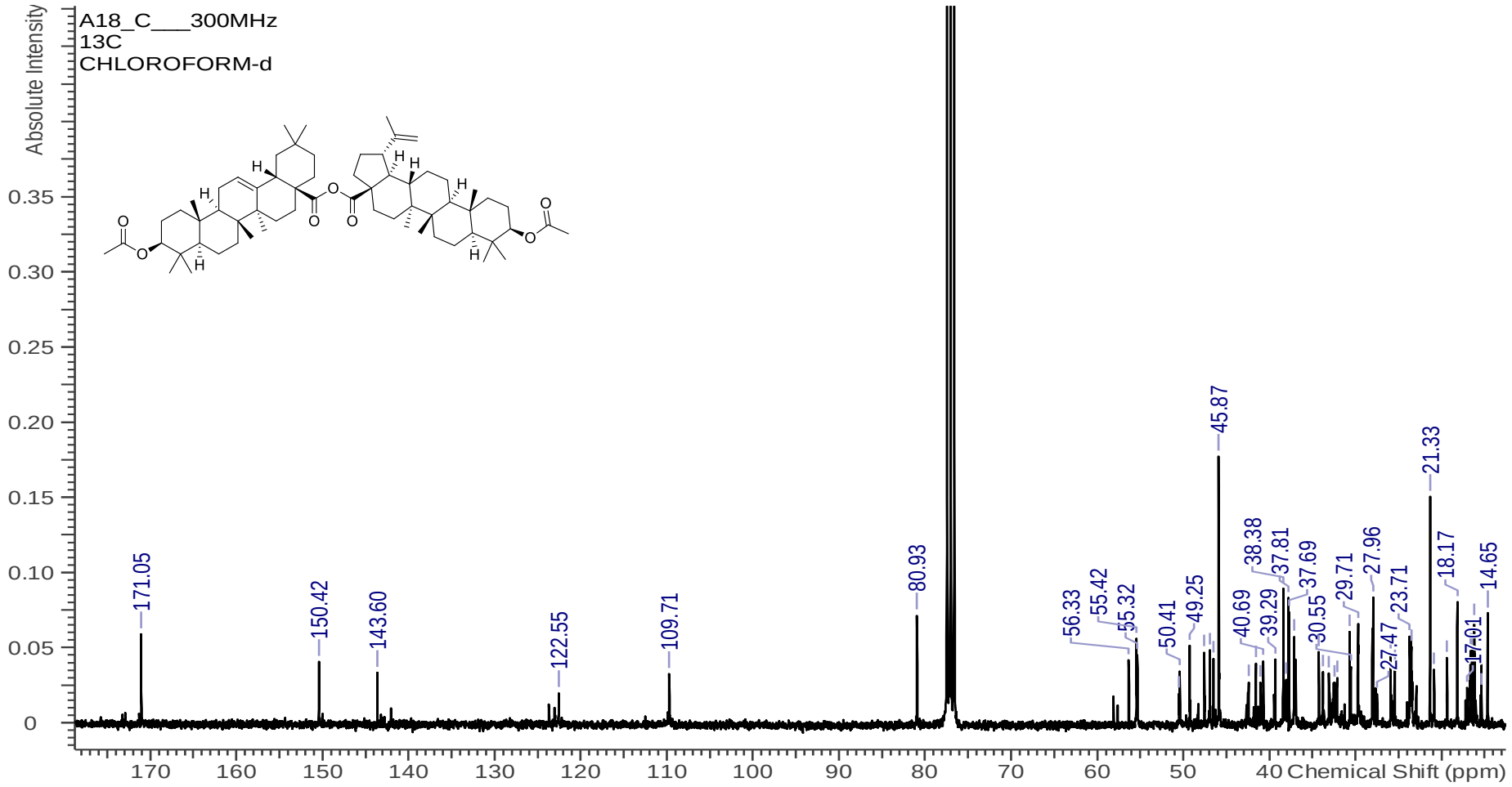

Figure 2.26: ^{13}C-NMR spectrum of Compound A18

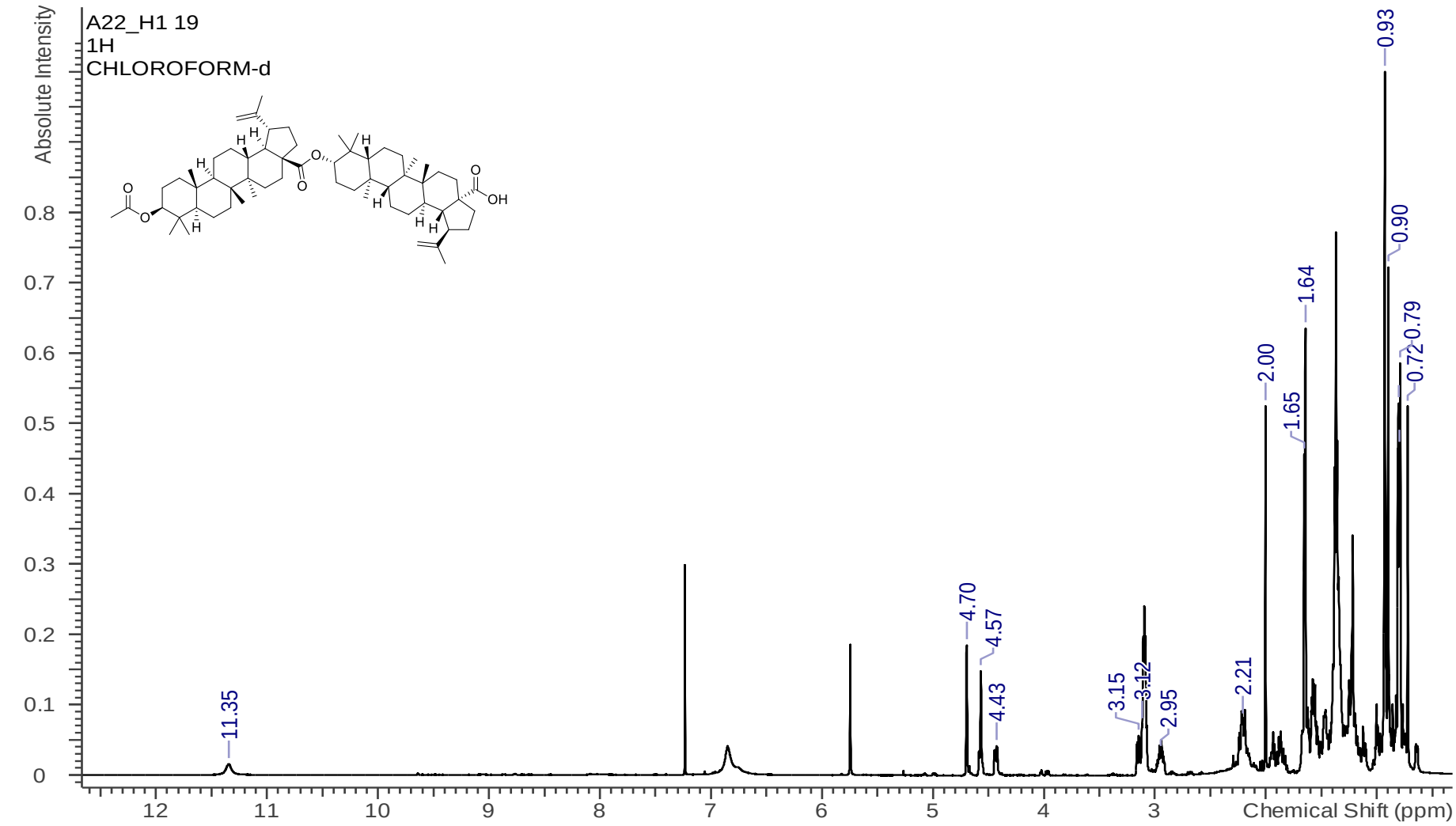

Figure 2.27: ^{1}H-NMR spectrum of Compound A22

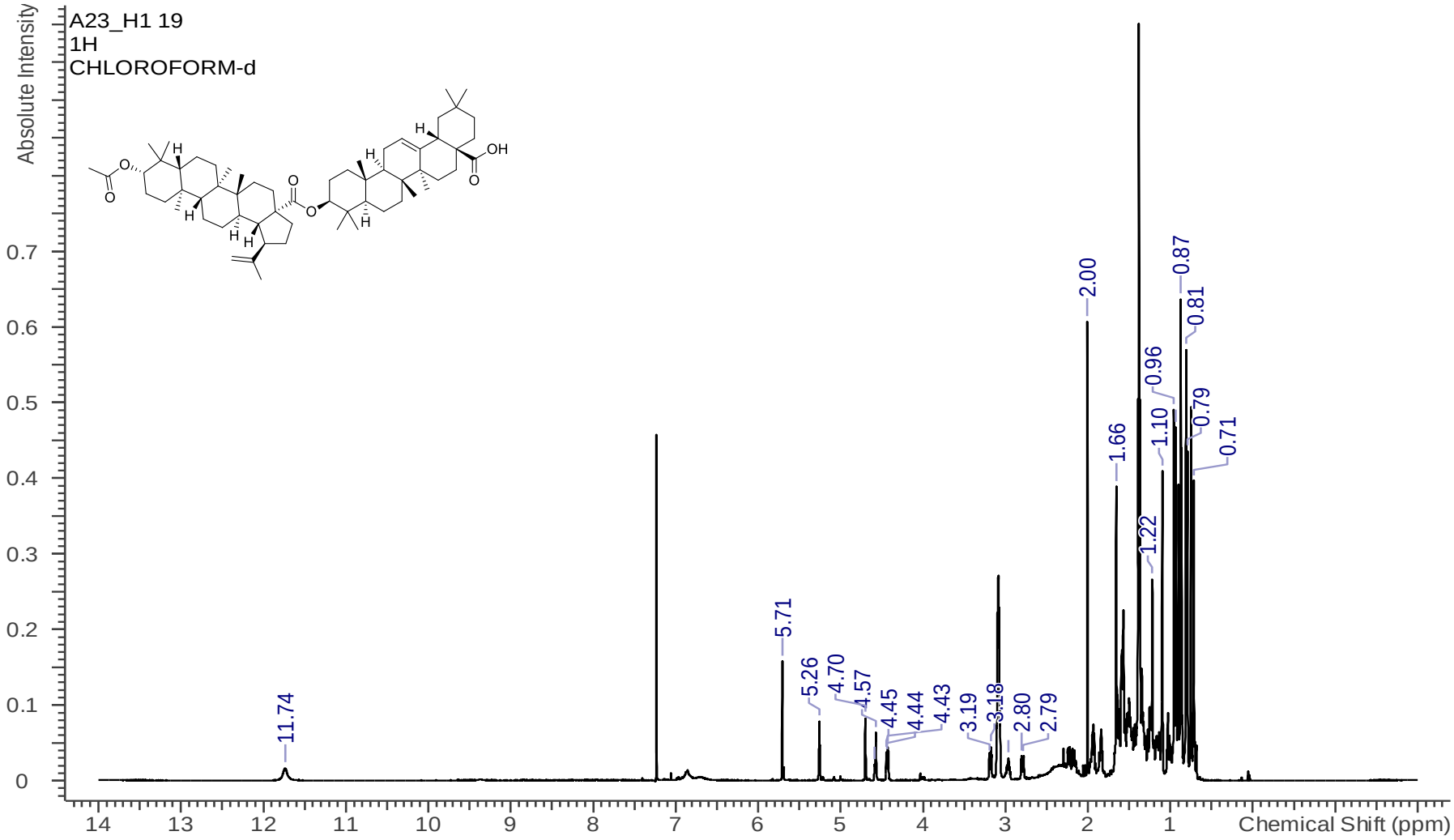

Figure 2.28: ^{1}H-NMR spectrum of Compound A23

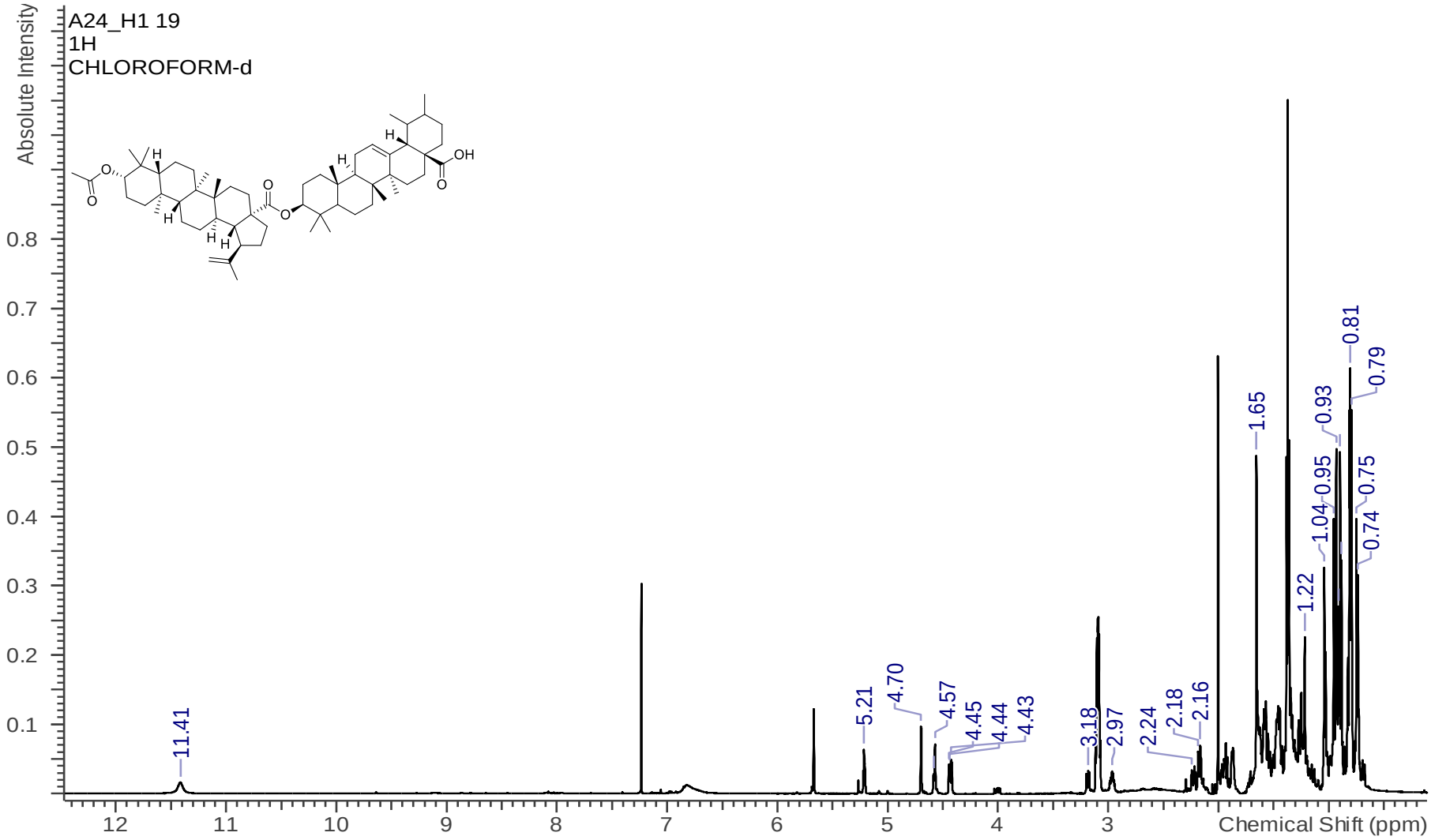

Figure 2.29: ^{1}H-NMR spectrum of Compound A24

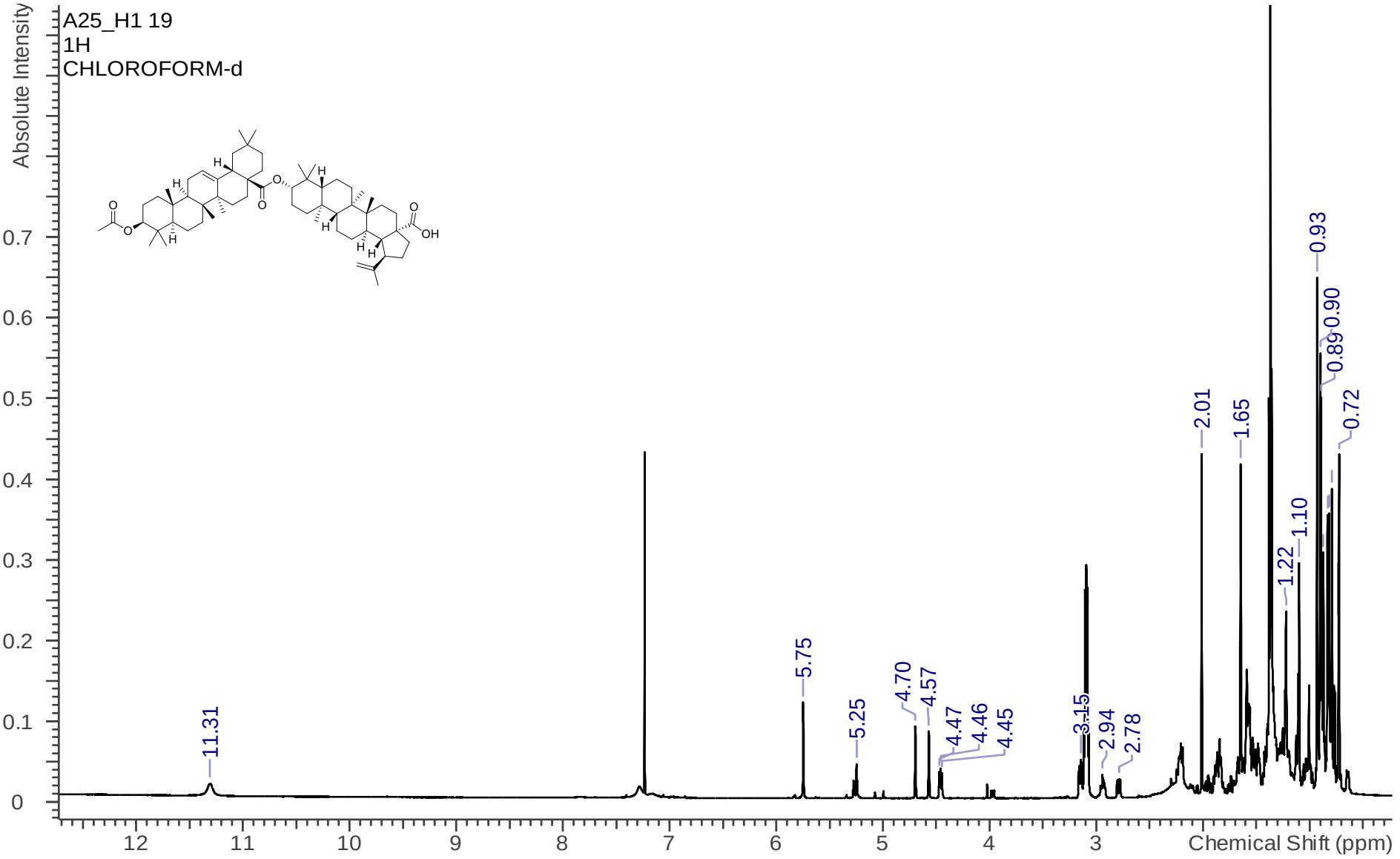

Figure 2.30: ^{1}H-NMR spectrum of Compound A25

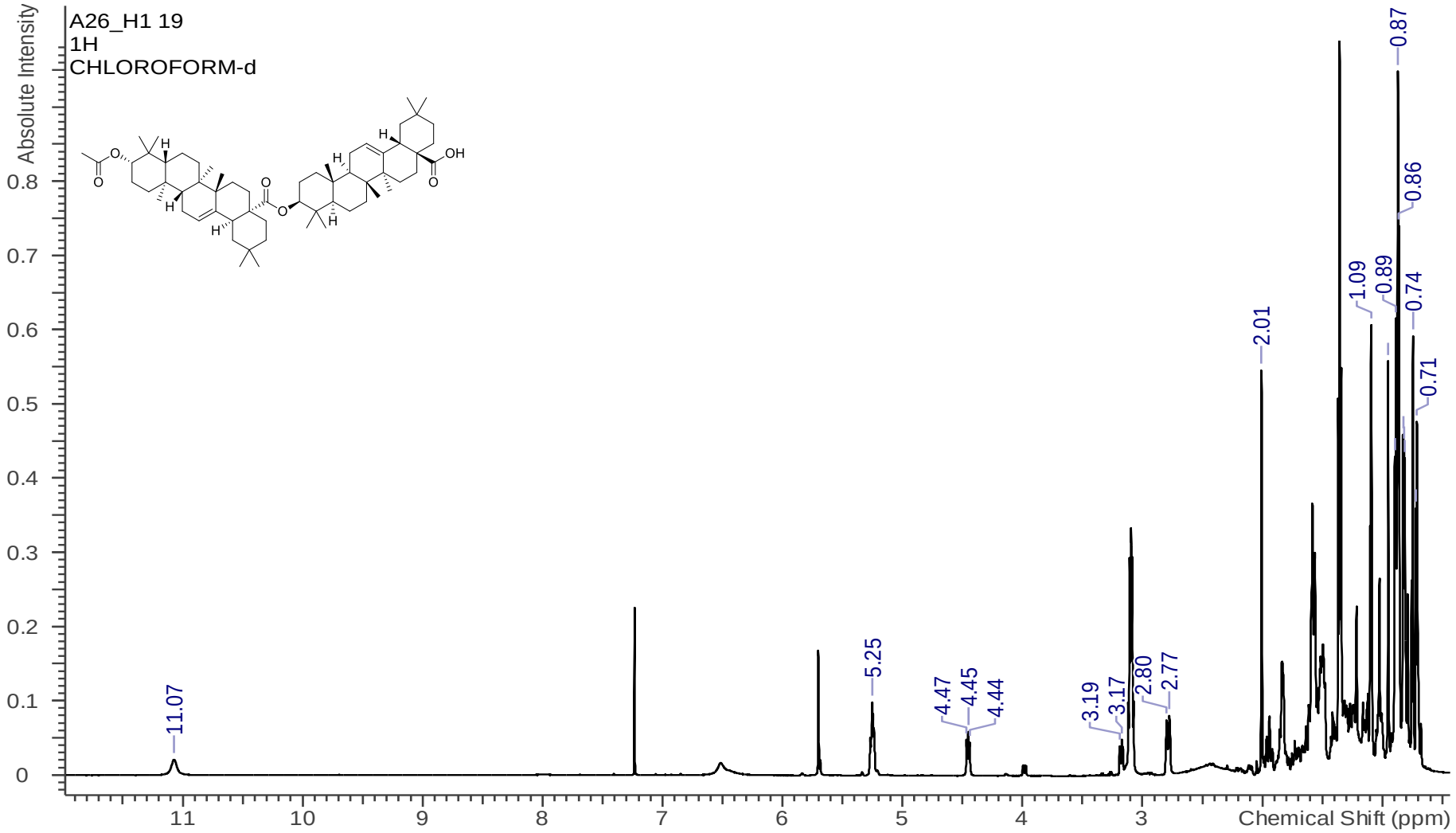

Figure 2.31: ^{1}H-NMR spectrum of Compound A26

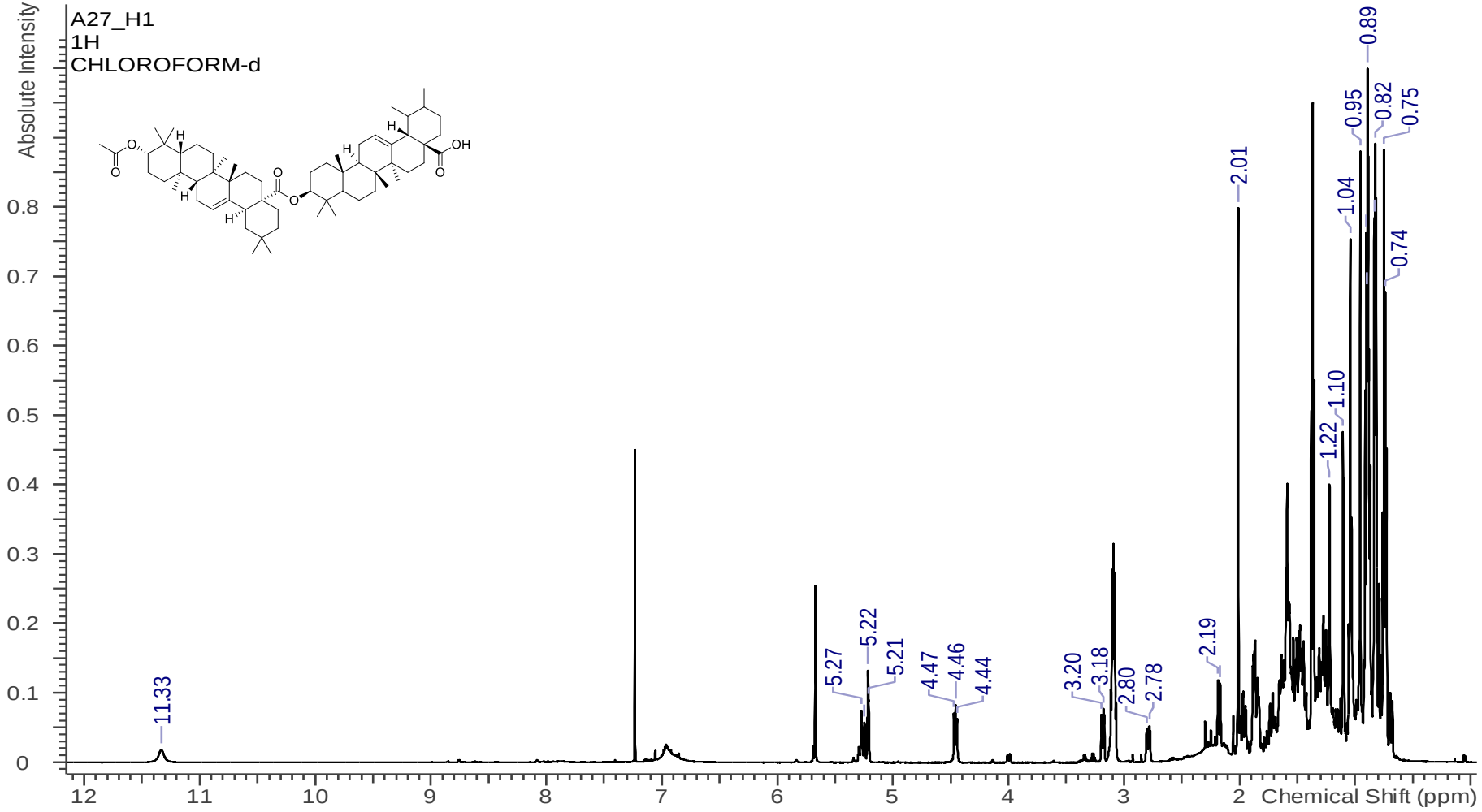

Figure 2.32: ^{1}H-NMR spectrum of Compound A27

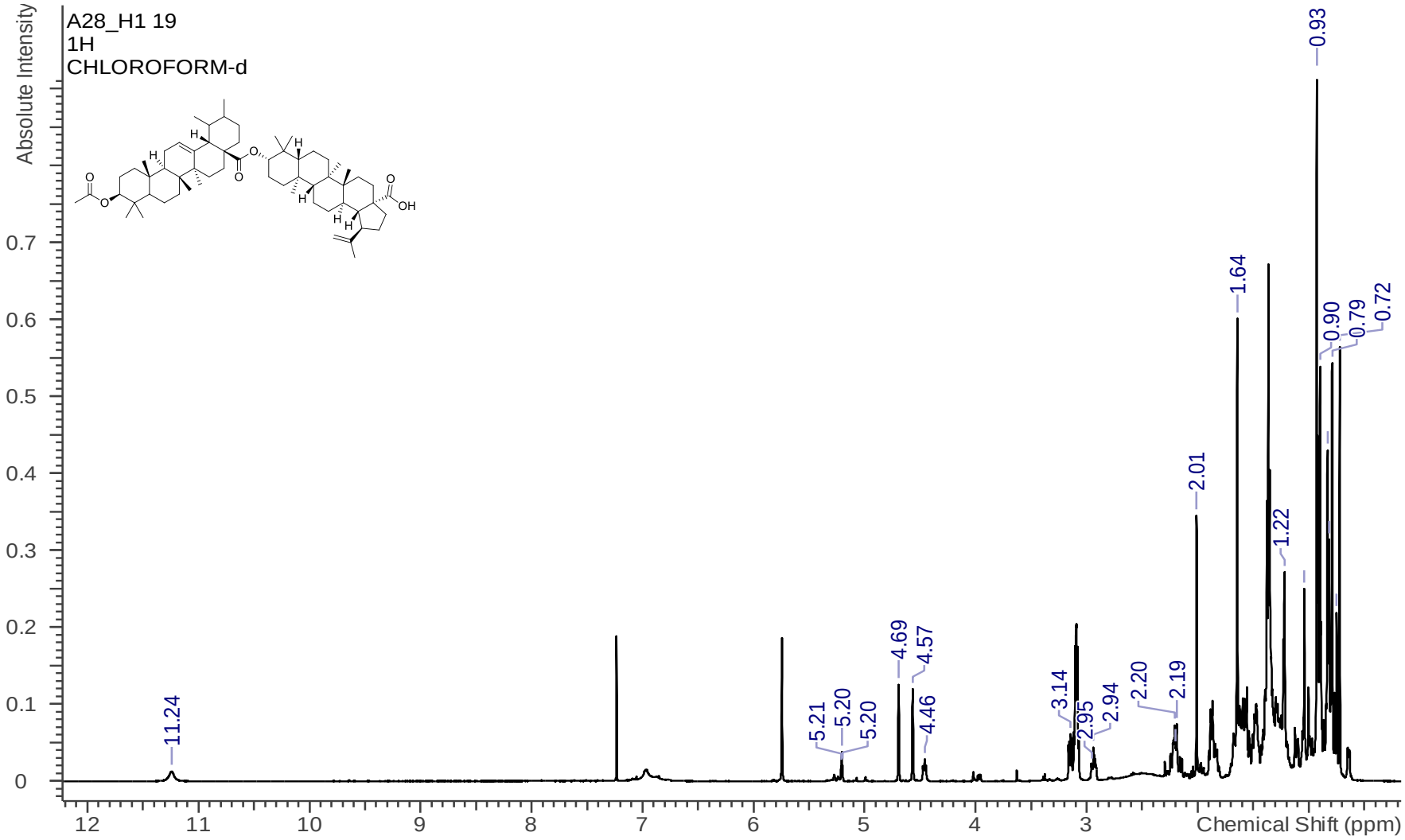

Figure 2.33: ^{1}H-NMR spectrum of Compound A28

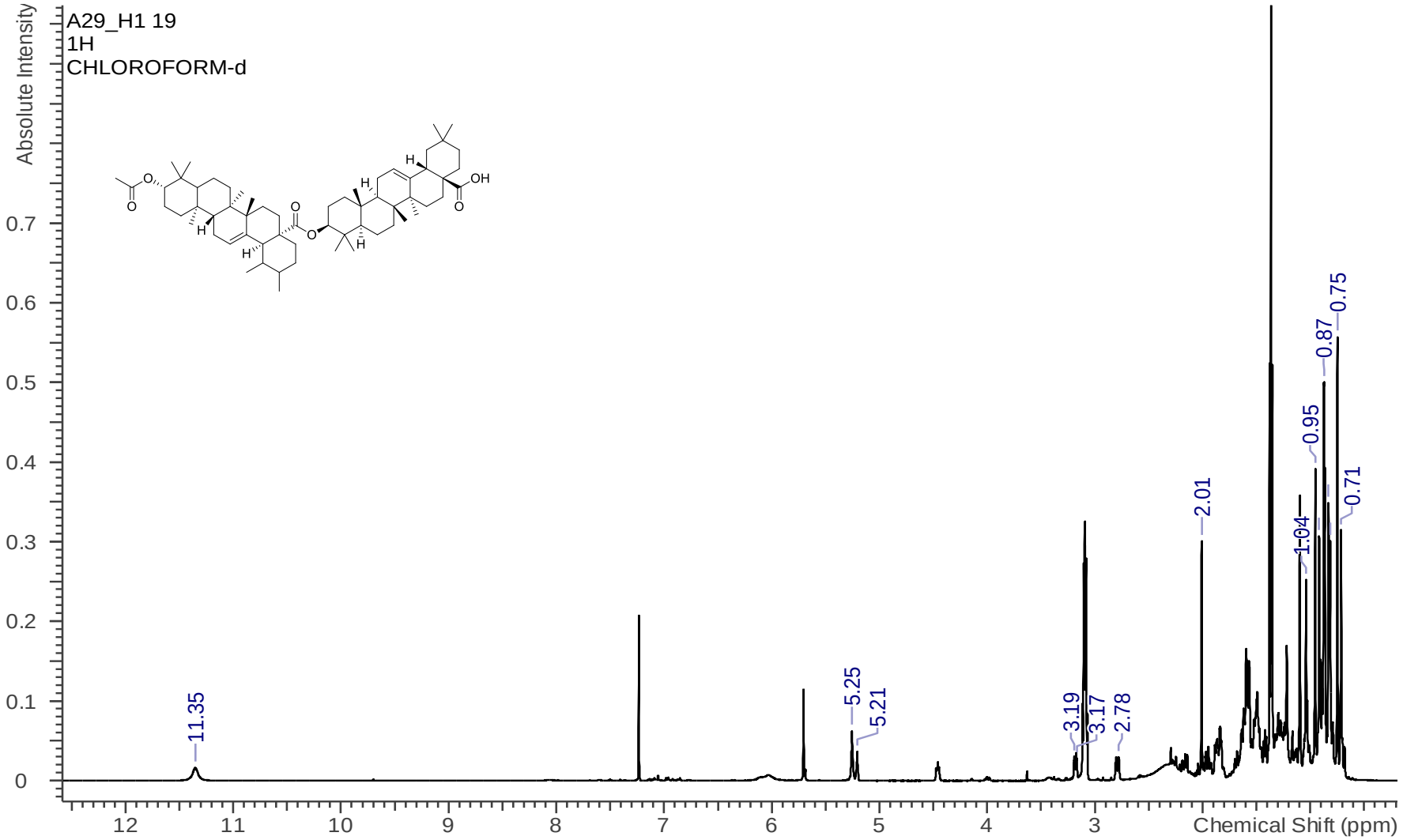

Figure 2.34: ^{1}H-NMR spectrum of Compound A29

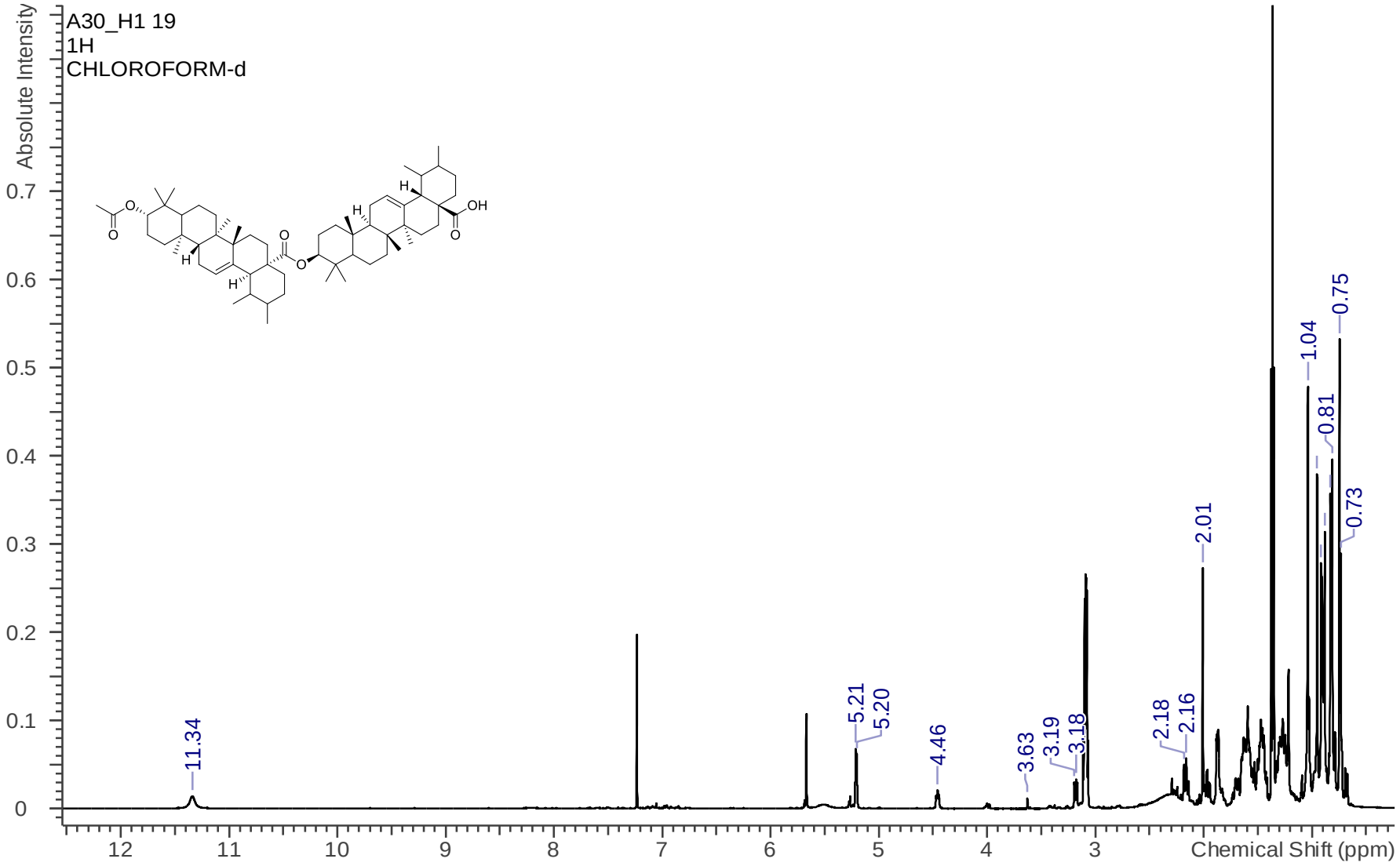

Figure 2.35: ^{1}H-NMR spectrum of Compound A30

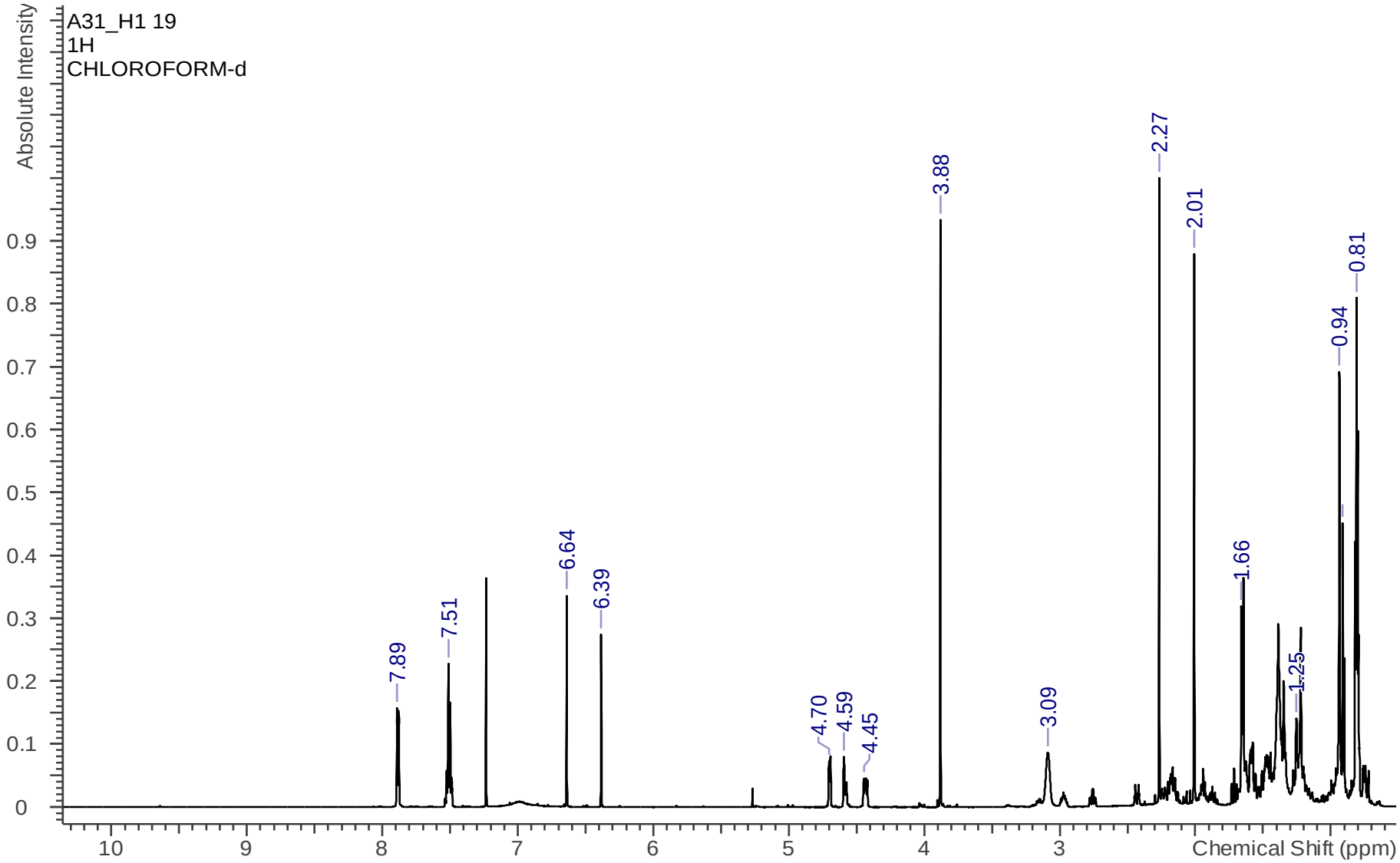

Figure 2.36: ^{1}H-NMR spectrum of Compound A31

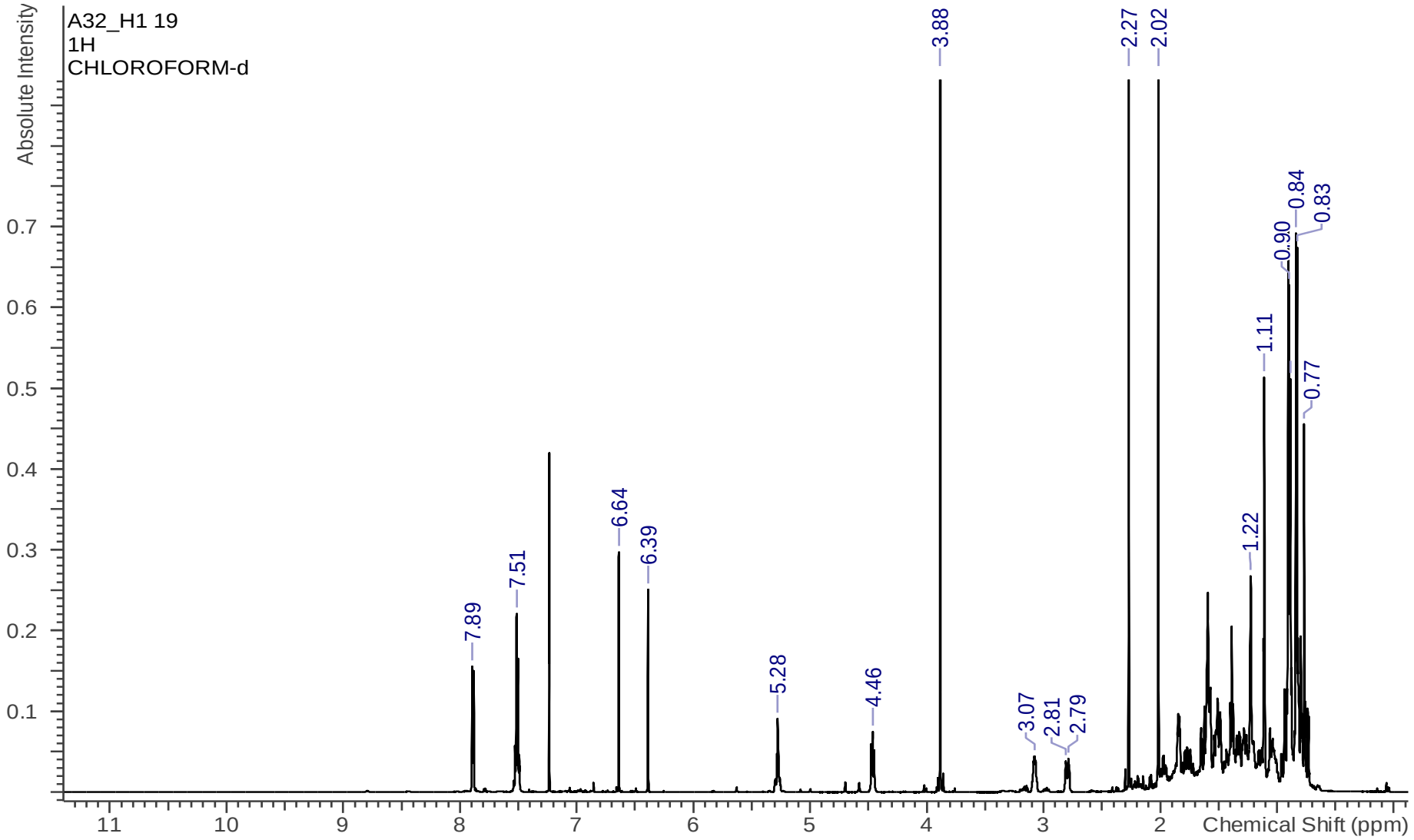

Figure 2.37: ^{1}H-NMR spectrum of Compound A32

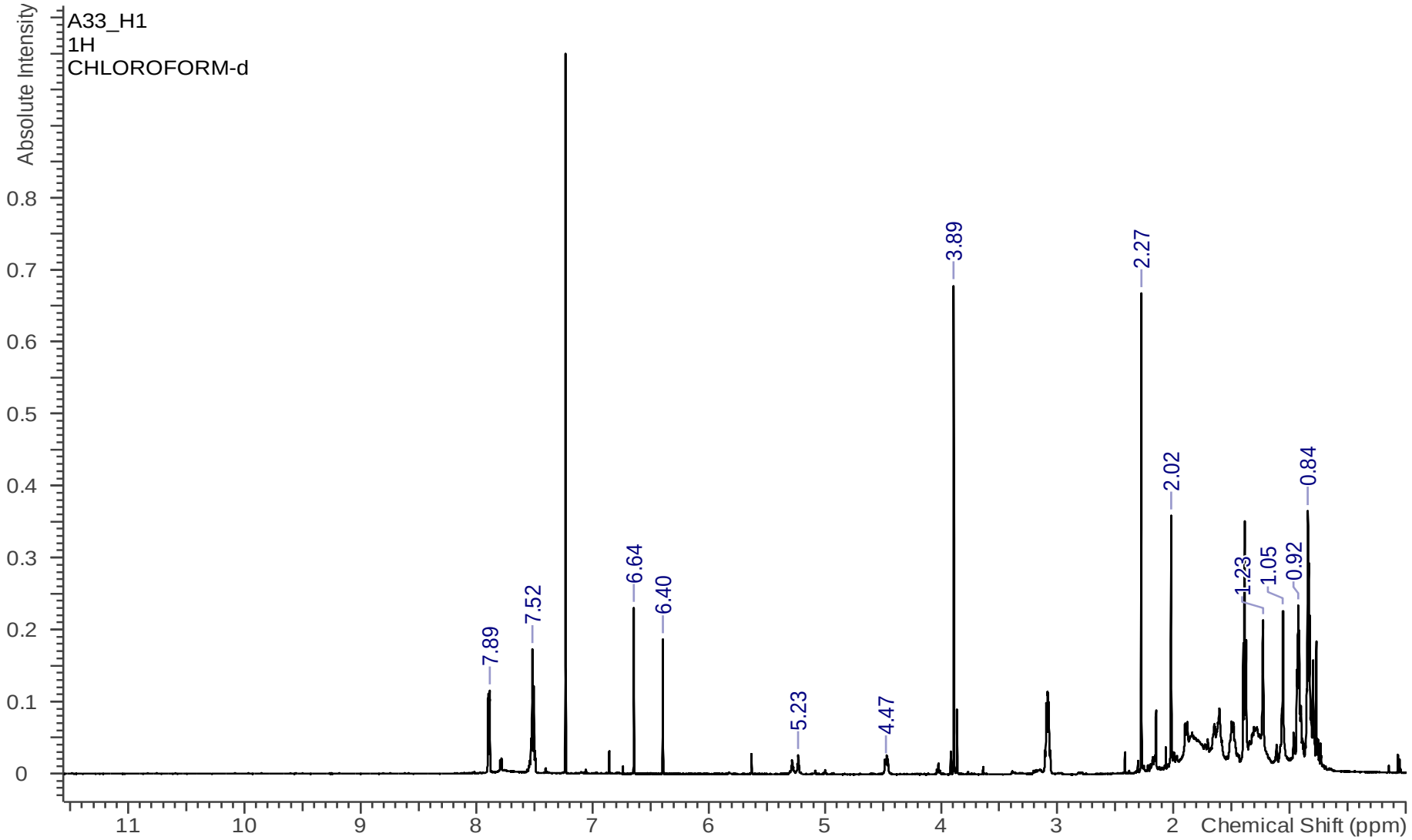

Figure 2.38: ^{1}H-NMR spectrum of Compound A33

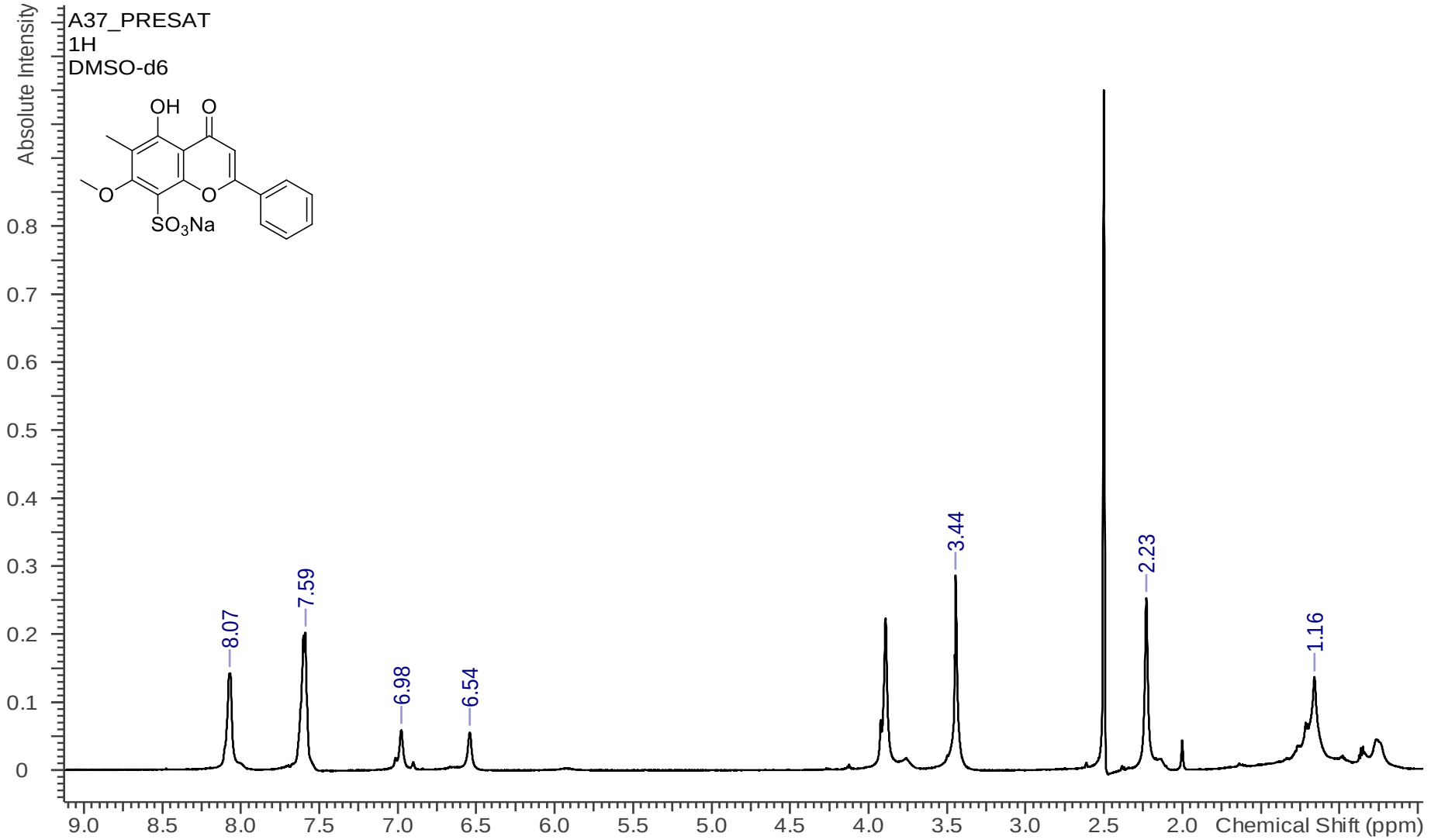

Figure 2.39: ^{1}H-NMR spectrum of Compound A37

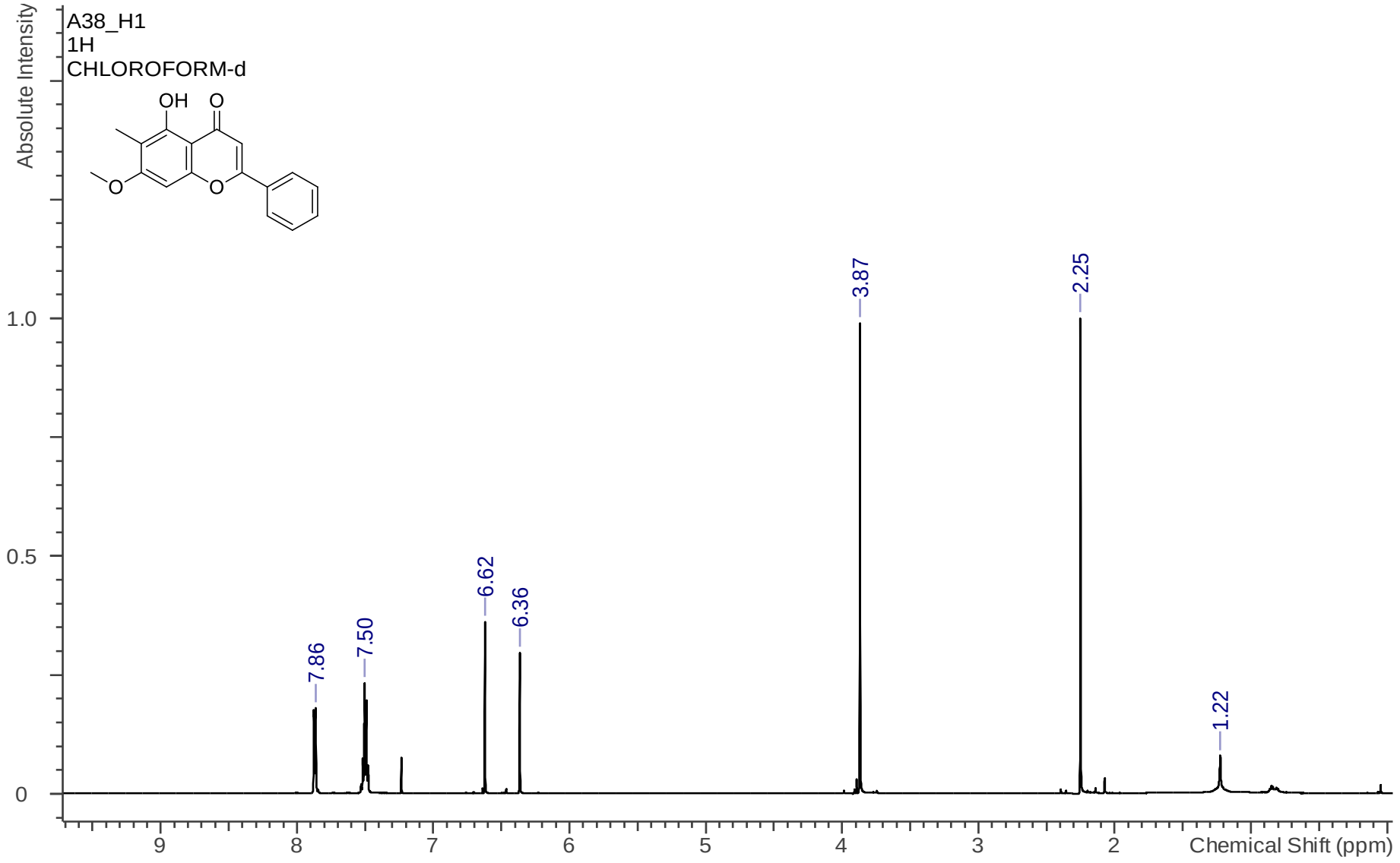

Figure 2.40: ^{1}H-NMR spectrum of Compound A38

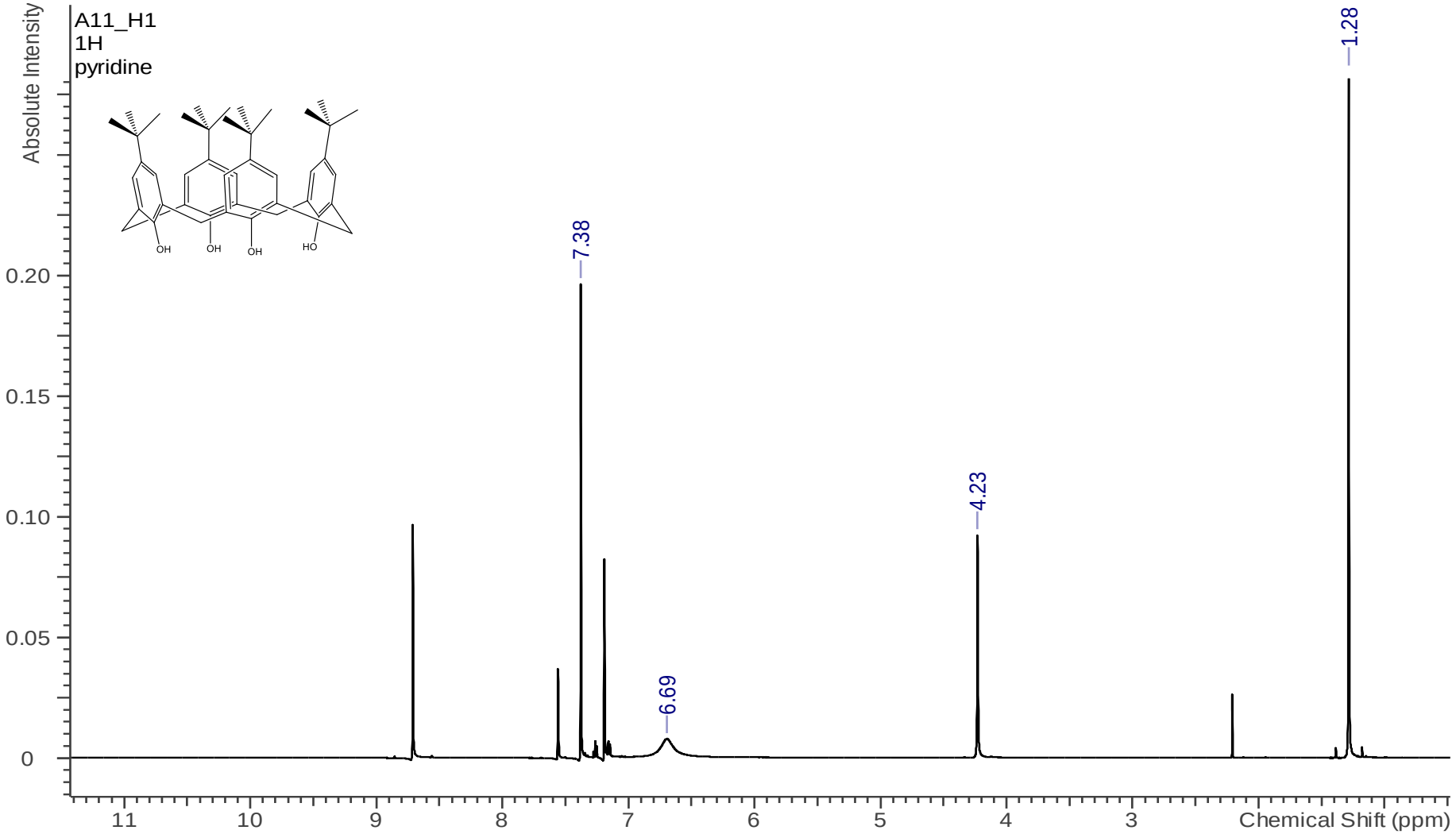

Figure 2.41: ^{1}H-NMR spectrum of p-tertbutylcalix[4]arene (**18**)

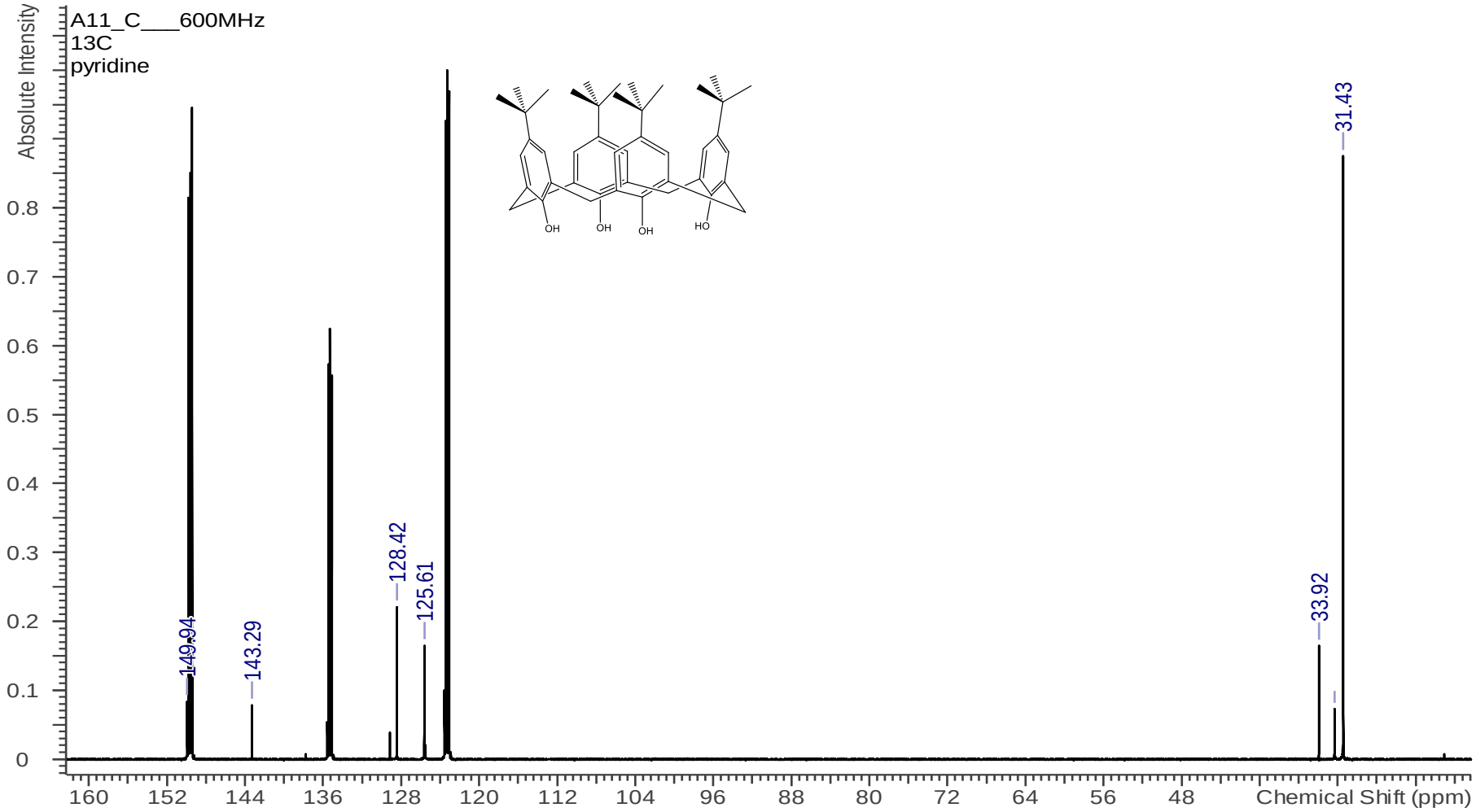

Figure 2.42: ^{1}H-NMR spectrum of p-tertbutylcalix[4]arene (**18**)

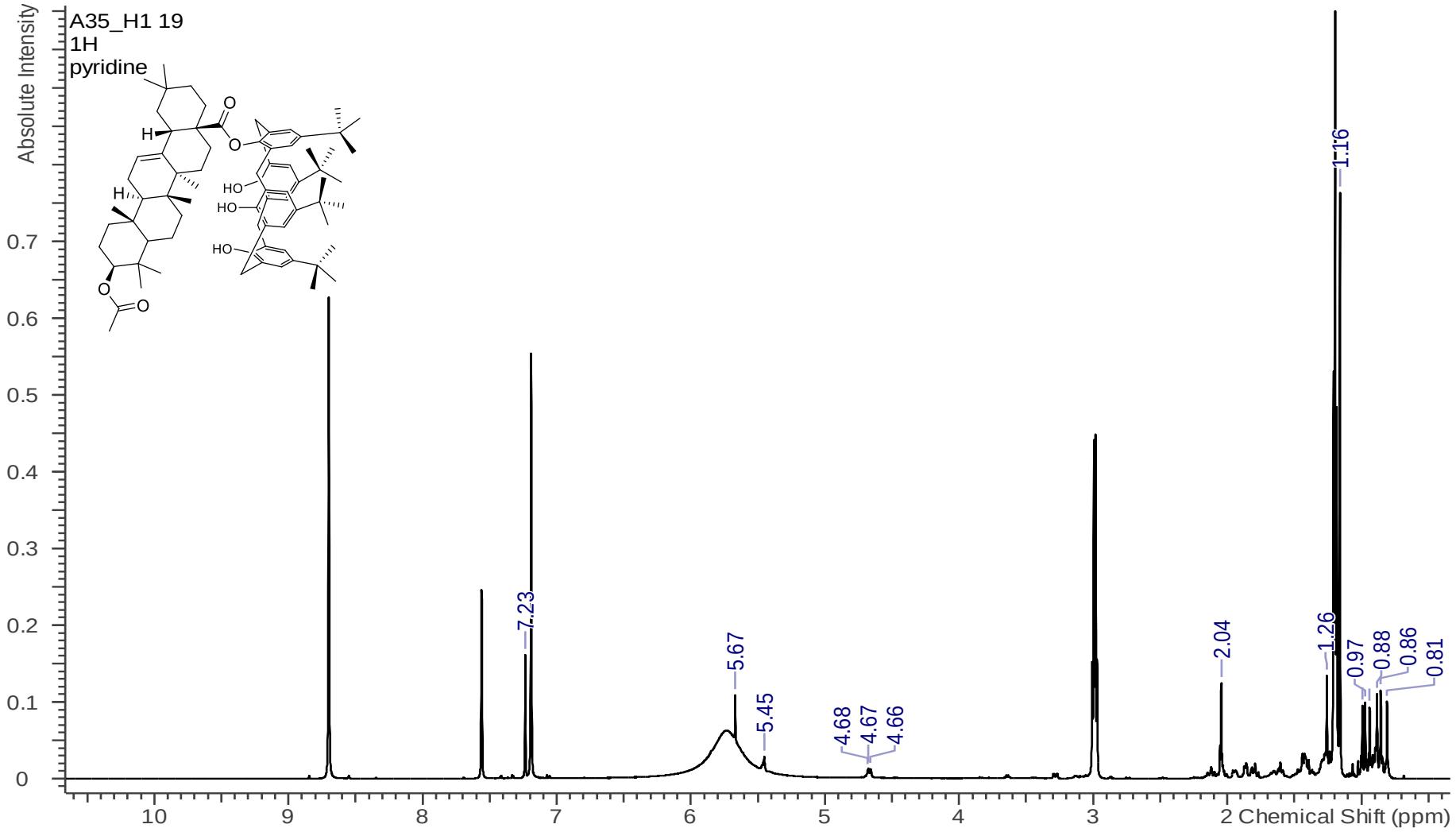

Figure 2.43: ^{1}H-NMR spectrum of Compound A35

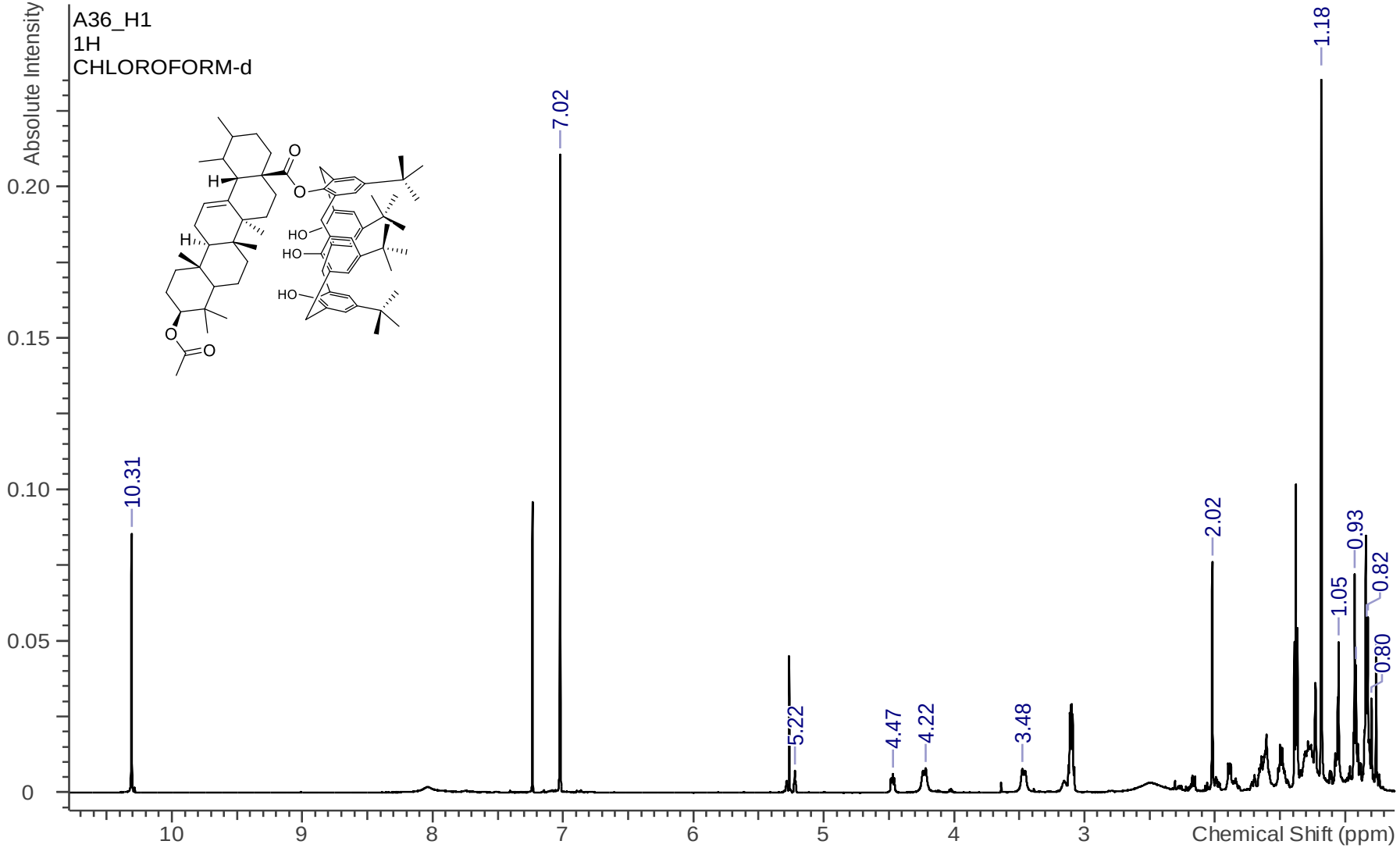

Figure 2.44: ^{1}H-NMR spectrum of Compound A36